SUSITNA-WATANA HYDRO

Clean, reliable energy for the next 100 years.

Report
14-07-REP
v0.0

Susitna-Watana Hydroelectric Project
Probable Maximum Precipitation Study

DRAFT

AEA11-022

Prepared for:
Alaska Energy Authority
813 West Northern Lights Blvd.
Anchorage, AK 99503

Prepared by:
Applied Weather Associates, LLC for MWH
PO Box 175
Monument, CO 80132

March 14, 2014

THIS PAGE INTENTIONALLY LEFT BLANK

The following individuals have been directly responsible for the preparation, review and approval of this Report.

Prepared by: Bill Kappel, Technical Lead

Reviewed by: Ed Tomlinson, Project Manager

Approved by: _____

John Haapala, Lead Hydrologist

Approved by: _____

Brian Sadden, Project Manager

THIS PAGE INTENTIONALLY LEFT BLANK

TABLE OF CONTENTS

List of Attachments

List of Tables

List of Figures

EXECUTIVE SUMMARY

Applied Weather Associates (AWA) has completed a site-specific Probable Maximum Precipitation (SSPMP) study for the Susitna River basin located south of the Alaska Range and north east of Anchorage in Alaska. The purpose of the study was to determine PMP values specific to the watershed, taking into account topography, climate and storm types that affect the region.

The approach used in this study was consistent with those used in the numerous PMP studies that AWA has completed since 1996. This is a storm-based approach similar to the methods and processes employed by the National Weather Service (NWS) in the development of the various Hydrometeorological Reports (HMRs) to the extent the data and current understanding of meteorological processes supports those previous methods. The World Meteorological Organization (WMO) manual for PMP determination (WMO 2009) recommends this storm-based approach when sufficient data are available. This approach identified extreme rainfall events that have occurred over a wide region around southern Alaska from Fairbanks to the Gulf of Alaska west to the Aleutians Island and east to the northern Alaska Panhandle. These storms have meteorological and topographical characteristics similar to extreme rainfall storms that could occur over the Susitna-Watana basin. The largest of these rainfall events were selected for detailed analyses and PMP development.

Nine rainfall events were identified as having similar characteristics to PMP-type events that could potentially occur over the Susitna River basin and could potentially influence the PMP values. Each of these storms were analyzed by AWA for this study using the Storm Precipitation Analysis System (SPAS). Some storms had more than one Depth-Area-Duration (DAD) zone analyzed by SPAS. A total of 13 unique DAD zones were used in the final PMP development for this study.

The general concepts employed to derive the SSPMP values from rainfall maximization, storm transpositioning, and elevation moisture adjustments were consistent with those used in HMR 57 (Hansen et al. 1994) and in the numerous PMP studies completed by AWA (Tomlinson et al. 2006-2013, Kappel et al. 2011-2014). Further, information and processes detailed in Technical Paper 47 (1963), as well as the United States Army Corps of Engineers (USACE) (1975) and Acres (1982) feasibility studies, were used where appropriate. New techniques and databases were used in the study to increase accuracy and reliability, while adhering to the basic approach used in the HMRs and in the WMO Manual. Two updated analysis methodologies were utilized in this study. The first was the use of the Orographic Transposition Factor (OTF), which objectively quantifies the effects of terrain on rainfall enhancement and depletion. This process replaces the NWS K factor/Storm Separation Method (see HMR 57 Section 6 and 8), and allows the unique and highly variable topography at both the in-place storm location and the Susitna River basin to be properly represented in the PMP values and subsequent Probable Maximum Flood (PMF) modeling. The

second was the use of the HYSPLIT trajectory model (Draxler and Rolph 2010), which was used to evaluated the general location of the moisture source regions originating over water. These regions were identified using a NWS reanalysis interface.

New storm maximization factors were computed for each storm of the nine most significant storms using an updated sea surface temperature (SST) climatology and a ship report/satellite SST database (Reynolds et al. 2007 and Kent et al. 2007, NCDC DS 540.0). Each historic extreme rainfall event used for PMP development was maximized, transpositioned, and orographically adjusted to a series grid points covering the entire Susitna River basin using methods consistent with HMR 57 and previous AWA PMP studies when possible and modified to work on a gridded basis. The governing equation used for computation of the SSPMP values for the Susitna River basin is shown in Equation ES.1.

$$PMP_{xhr} = P_{xhr} * IPMF * MTF * OTF \qquad \text{ES.1}$$

where:

PMP_{nhr} is the SSPMP value at the x-hour duration for the 5,131-square mile Susitna River basin (target location);

P_{xhr} is the x-hour 5,131-square mile precipitation observed at the historic in-place storm location (source location);

In-Place Maximization Factor (*IPMF)* is the adjustment factor that increases a storm's maximum amount of atmospheric moisture that could have been present to the storm for rainfall production. It is the ratio of the maximum amount to the actual amount of atmospheric moisture that was available to the storm;

Moisture Transposition Factor (MTF) is the adjustment factor which accounts for the difference in available moisture between the location where the storm occurred and the Susitna-Watana basin;

Orographic Transposition Factor (OTF) is obtained from the results of the comparison of the 24-hour precipitation frequency characteristics between the storm target and source locations. The OTF accounts for differences between orographic effects at the historic in-place storm location and the grid point being evaluated within the Susitna-Watana basin.

A total of 4,767 grid cells, at a resolution of .025° decimal degrees x .025° decimal degrees, were analyzed over the Susitna-Watana basin. The resulting values were analyzed hourly for a total of 216-hours and provided by sub-basin average for use in PMF modeling. These data were distributed spatially the precipitation climatology from NOAA Atlas 14 Volume 7 (Perica et al. 2012). The temporal distribution of the hourly rainfall accumulations followed the temporal pattern

of three historic storms, each with a distinct accumulation pattern. This procedure is preferred compared to moving each storm to the centroid of the basin because it captures the spatial and temporal variability of PMP rainfall as it would occur over the complex terrain of the Susitna-Watana basin. Values were derived for the all-season period, extending from July 1-August 15, with an additional set of seasonality adjustments for use in defining the PMP rainfall from April 1 through October 31.

The last component of the PMP determination process was the development of the meteorological time series used for snowmelt calculations prior to, coincident with, and after the PMP rainfall period. Hourly values for temperatures, dew points, and wind speeds were derived using historic observed conditions during similar rainfall periods. These values were then maximized to represent the expected conditions during the PMP rainfall. Values were derived representing July 1-August 15, with an additional set of seasonality adjustments for use in defining the meteorological time series from April 1 through October 31.

1. INTRODUCTION

This study provides the Site-Specific Probable Maximum Precipitation (SSPMP) values and development procedures for use in the computation of the Probable Maximum Flood (PMF) for the Susitna River basin in the southern Alaska.

1.1 Background

Definitions of probable maximum precipitation (PMP) are found in most of the Hydrometeorological Reports (HMRs) issued by the National Weather Service (NWS). The definition used in the most recently published HMR is "theoretically, the greatest depth of precipitation for a given duration that is physically possible over a given storm area at a particular geographical location at a certain time of the year." (HMR 59, pg. 5). Since the mid-1940s, several government agencies have been developing methods to calculate PMP in various regions of the United States. The NWS (formerly the U.S. Weather Bureau) and the Bureau of Reclamation have been the primary agencies involved in this activity. PMP values from their reports are used to calculate the PMF, which, in turn, is often used for the design of significant hydraulic structures.

The generalized PMP studies currently in use in the conterminous United States include: HMR 49 (1977) for the Colorado River and Great Basin drainage; HMRs 51 (1978), 52 (1982) and 53 (1980) for the U.S. east of the 105th meridian; HMR 55A (1988) for the area between the Continental Divide and the 103rd meridian; HMR 57 (1994) for the Pacific Northwest states west of the Continental Divide; and HMR 58 (1998) and 59 (1999) for the state of California(Figure 1.1). The Susitna-Watana basin is located outside the domain of the HMRs and therefore a SSPMP is required to derive quantifiable and reproducible PMP values.

In addition to these HMRs, numerous Technical Papers and Reports deal with specific subjects concerning precipitation (e.g. NOAA Tech. Report NWS 25 1980 and NOAA Tech. Memorandum NWS HYDRO 45 1995). Topics include maximum observed rainfall amounts, return periods for various rainfall amounts, and specific storm studies. Climatological Atlases (e.g. Technical Paper No. 40 1961; Short Duration Rainfall Frequency Relations for the Western United States 1986; NOAA Atlas 2 1973; NOAA Atlas 14 2002-2014) are available for use in determining precipitation return periods. A number of specialized and regional studies (e.g. Technical Paper 47; Tomlinson 1993; Tomlinson et al. 2002-2013, Kappel et al. 2011-2014) augment generalized PMP reports for specific basins and regions included in the large areas addressed by the various HMRs (Tomlinson and Kappel 2009). TP 47 provides PMP values for Alaska for area sizes up to 400 square miles and durations up to 24 hours.

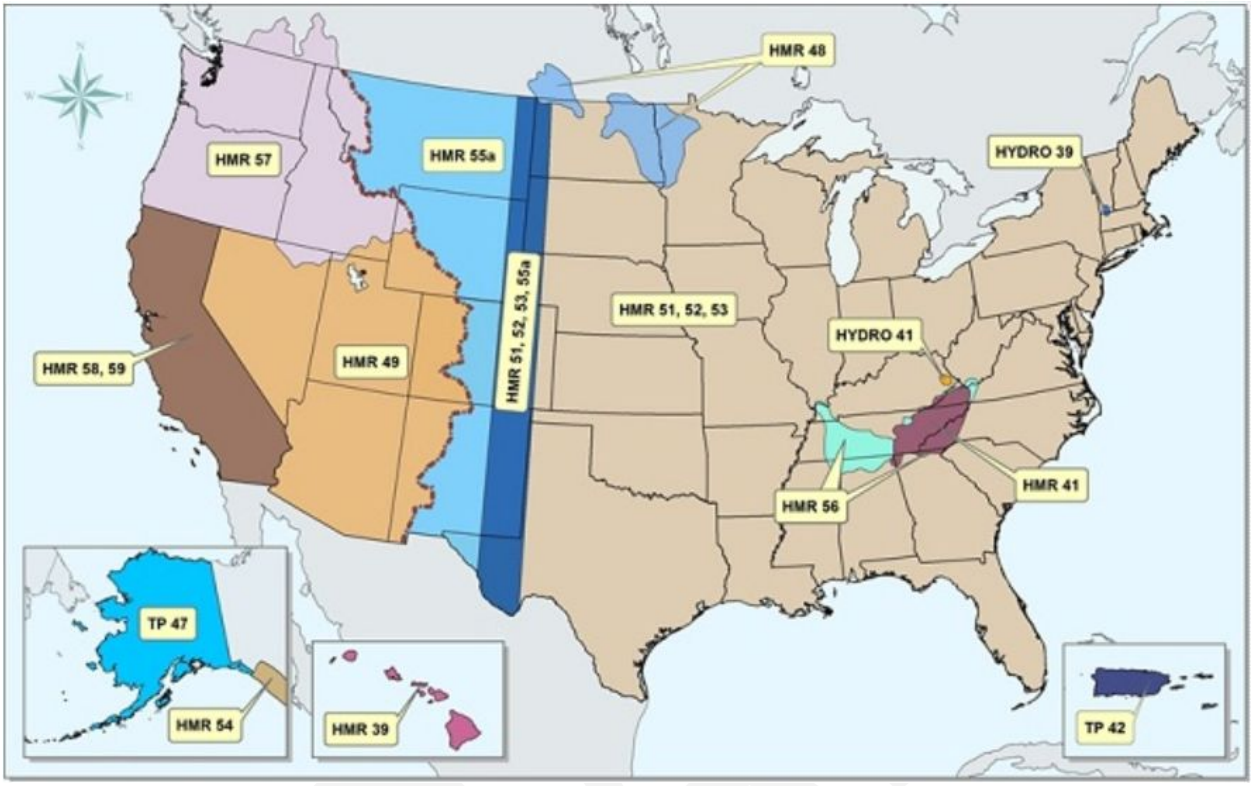

Figure 1.1. Coverage of NWS HMRs as of 2012 (from http://www.nws.noaa.gov/oh/hdsc/studies/pmp.html).

The meteorological and topographical settings within and surrounding the large Susitna River basin create unique effects on precipitation and other meteorological variables that can only be resolved through a detailed analysis specific to the basin. Each of the NWS HMR studies addressing PMP over specific regions also recognized that SSPMP studies could incorporate more site-specific considerations and provide improved PMP estimates. Additionally, by periodically updating storm data and incorporating advances in meteorological concepts, PMP analysts can make improved PMP estimates (HMR 57 Section 14 and Section 15.2 Steps 8-9).

Previous site-specific and regional PMP projects completed by AWA provide examples of PMP studies that explicitly consider the topography of the basins and characteristics of historic extreme rainfall storms over climatologically similar regions surrounding the basins (see Figure 1.2). These site-specific PMP studies have received extensive review and the results have been used in computing the PMF for the watersheds and regions covered. This study follows many of the same procedures used in those studies to determine SSPMP values for the Susitna-Watana basin. These procedures, together with Storm Precipitation Analysis System (SPAS) rainfall analyses[1] are used to compute PMP values using a .025 x .025 decimal degree grid over the Susitna-Watana basin. The grid based approach provides improvements in the spatial evaluation of the historic storm

[1] Appendix D contains a complete description of the SPAS program and its development.

rainfall patterns and how the PMP storm would occur over the highly variable topography unique to the Susitna-Watana basin. In addition, storm specific and generalized temporal distributions can be applied.

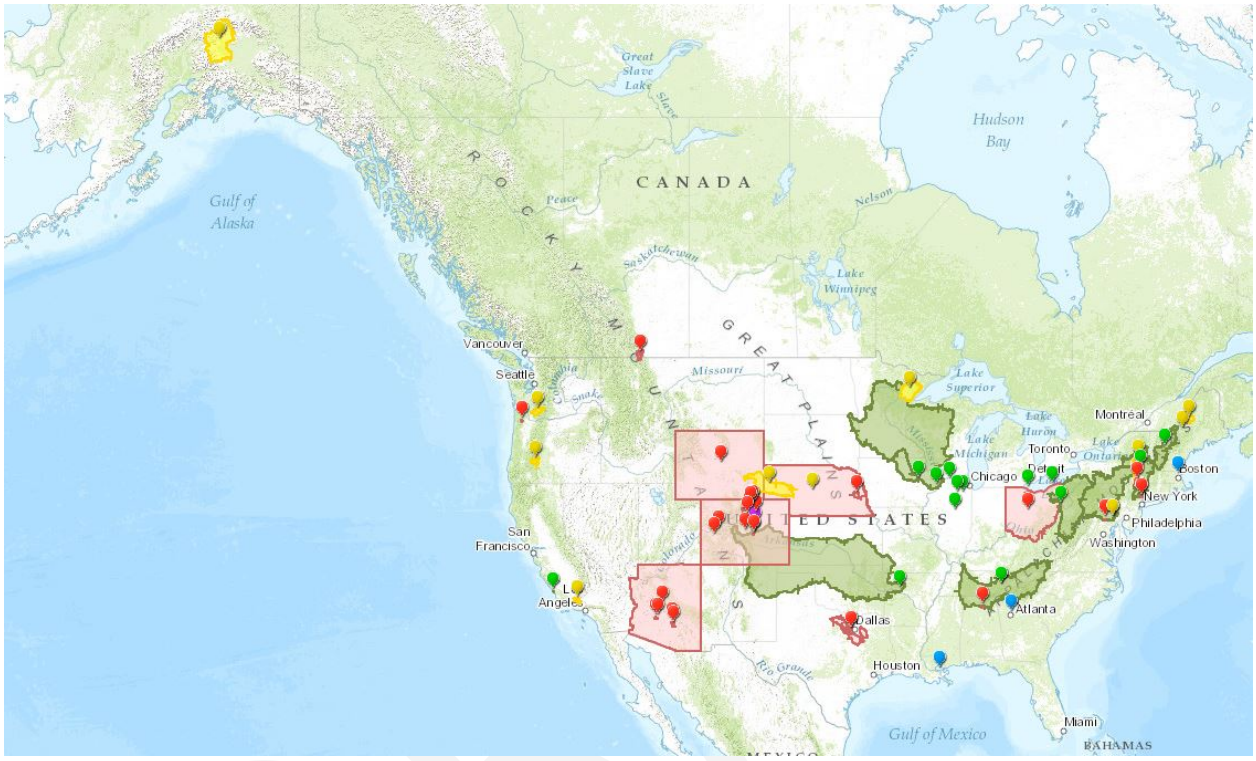

Figure 1.2. Locations of AWA PMP studies as of March 2013.

1.2 Objective

The objective of this study was to perform a site-specific study to determine reliable estimates of PMP values for the Susitna-Watana basin, as well as develop coincident meteorological time series data (temperature, dew point, and wind speed) for use in snow melt calculation. In addition, guidance was provided on the seasonality of both the PMP values and the meteorological time series values because it was critical to provide information on how those values vary beyond the all-season (July-August for PMP) for PMF modeling. This is because it is very likely that the PMF would result at a time when some amount less than the full PMP could accumulate and be augmented by melting snow pack to produce a larger volume of flood runoff versus the time of the year when the full PMP could accumulate but have significantly less snow melt runoff. This all-season PMP would therefore produce a smaller flood volume than the lesser amount of rainfall but higher amount of snow melt. The most reliable methods and data currently available have been used, with new techniques and data used where appropriate.

1.3 Approach

The approach used in this study is consistent with the majority of the procedures that were used in the development of the HMRs, with updated procedures implemented where appropriate. These procedures were applied considering the site-specific characteristics of the Susitna River basin and the unique effects of the topography both in the surrounding region and in the basin. Terrain characteristics are addressed as they specifically affect rainfall patterns, both spatially and in magnitude within the basin. The weather and climate of the region are discussed in Section 2. The process of identifying extreme storms is discussed in Section 3. Procedures used to analyze storms are discussed in Section 4. Adjustments for storm maximization, storm moisture transposition, and orographic transposition are presented in Sections 5, 6, 7 and 8. The meteorological time series and seasonality of PMP development are provided in Section 9. Results are presented in Section 10. Discussions on sensitivities are provided in Section 11 and the recommendations for application are in Section 12.

Procedures used in this study maintained consistency with the general methods used in the HMRs and the previous PMP studies completed by AWA while deviations were incorporated when justified by developments in meteorological analyses and available data. The basic approach identifies major storms that occurred within the region surrounding the Susitna River basin that are PMP storm type (see Section 2.0). This includes the region from central Alaska west to the Bering Strait to the Gulf of Alaska through the Alaska Panhandle (see Section 5.0). The moisture content of each of these storms is increased to a climatological maximum to provide worst case rainfall estimation for each storm at the location where it occurred had all atmospheric process resulting in rainfall production been optimum. The storms are then transpositioned to the Susitna River basin to the extent supportable by similarity of topographic and meteorological conditions. Finally, the largest rainfall amounts from these maximized and transpositioned storms provide the basis for deriving the SSPMP values. Figure 1.3 shows the flow chart of the major steps used in a site-specific storm-based PMP derivation process. Note that the final process used during this study incorporated the use of a grid cell by grid cell delineation and detailed evaluation of orographic effects on rainfall within the basin. The details are included in Equation 1 and Figure 1.4.

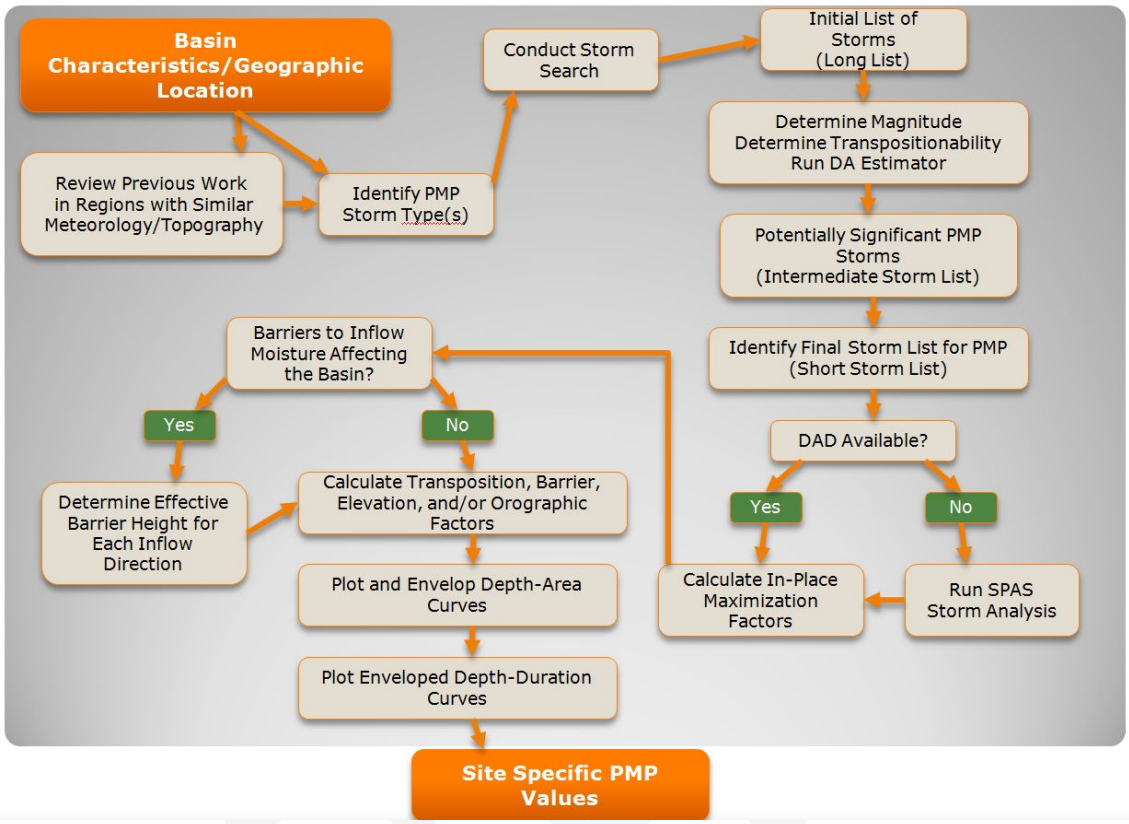

Figure 1.3. Flow chart showing the major steps involved in site-specific PMP development.

For some of the processes used to derive PMP, this study applied standard methods (e.g. WMO 2009 and Hansen et al. 1994), while for others, new techniques were developed. A major advancement utilized during this study was the ability to analyze rainfall and climate data on a gridded basis in a GIS environment. This allowed for in-place maximizations, horizontal moisture transpositioning, and orographic transpositioning using a data grid over the basin. The original SPAS gridded rainfall amounts were analyzed at each storm's in-place location to provide values used for the PMP calculations (see Equation 1.1). The largest of the total adjusted rainfall values at each hour were distributed spatially and temporally over the Susitna-Watana basin. The spatial distribution proved to be very effective in quantifying the unique effects of the highly variable topography on the storm at both the in-place storm location and the Susitna-Watana basin. This process uses the Orographic Transposition Factor (OTF) to quantify the effects of topography on rainfall production and spatial distribution. The OTF is determined by comparing the NOAA Atlas 14 Volume 7 precipitation frequency data (Perica et al. 2012) at the in-place storm location versus the precipitation frequency values at each grid point over the basin. The relationship through a range of precipitation frequency values between the two locations results in a ratio indicating if the in-place storm center location is more or less effective at enhancing rainfall versus the grid point over the basin. The OTF is then combined with the in-place maximization factor and the moisture transposition factor to produce the total adjustment factor for that grid point, for a given storm, for a

given duration. This process is then repeated for all grid points in the basin for all duration analyzed. The assumption in the OTF process is that the NOAA Atlas 14 precipitation frequency values adequately represent the expected effects of topography at a given grid point and by upwind and surrounding topography as reflected in the numerous precipitation events that have occurred at that location and within the region used to produce the precipitation frequency estimates.

This process replaces the use of the NWS Storm Separation Method (SSM). A detailed description of the NWS SSM method can be found in HMR 55A Section 7, with updates to the method in HMR 57 Section 6. The OTF is discussed in Section 6.2 with example results and calculations given in Section 7.3.

Figure 1.4 shows a flow chart of the processes that were used during this study to derive the SSPMP values. Note that most of the processes displayed in Figure 1.3 are included, however the flow chart in Figure 1.4 includes the processes that are unique to this SSPMP study.

The governing equation used for computation of the SSPMP values for the Susitna River basin is:

$$PMP_{xhr} = P_{xhr} * IPMF * MTF * OTF \qquad \text{Equation 1.1}$$

where:

PMP_{xhr} is the SSPMP value at the x-hour duration for the 5,131-square mile Susitna River basin (target location);

P_{xhr} is the x-hour 5,131-square mile precipitation observed at the historic in-place storm location (source location);

In-Place Maximization Factor (*IPMF)* is the adjustment factor determined using the maximum amount of atmospheric moisture that could have been present to the storm for rainfall production;

Moisture Transposition Factor (MTF) is the adjustment factor which accounts for the difference in available moisture between the location where the storm occurred and the Susitna-Watana basin;

Orographic Transposition Factor (OTF) is obtained from the results of the calculation which compares the x-hour precipitation frequency characteristics between the basin grind points and the in-place storm location. The OTF accounts for differences between orographic effects at the historic in-place storm location and the Susitna-Watana basin.

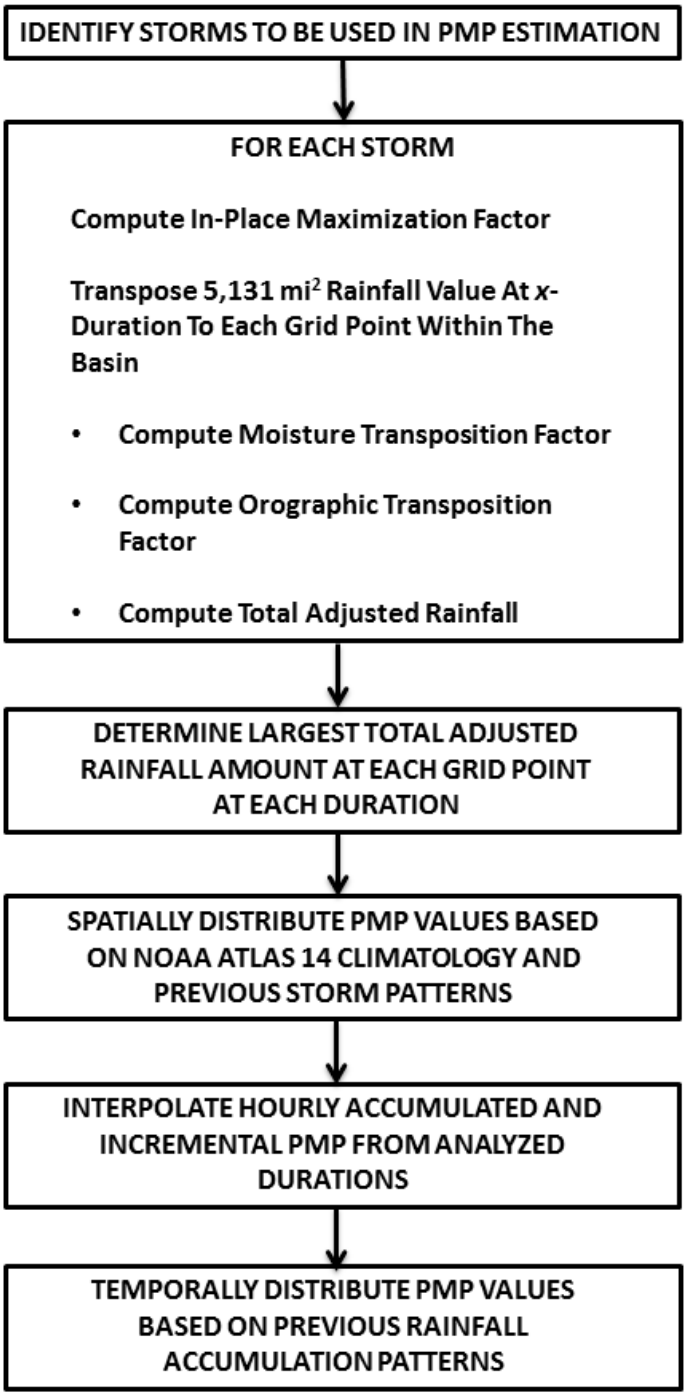

Figure 1.4. Major Components in Computation of Site-Specific PMP for Susitna-Watana Basin.

Advanced computer-based technologies, Weather Service Radar WSR-88D NEXt generation RADar (NEXRAD), and HYbrid Single-Particle Lagrangian Integrated Trajectory (HYSPLIT) model trajectories were used for storm rainfall analyses for all storms used in PMP development. New technology and data were incorporated into the study when they improved reliability. This approach provides the most complete scientific application compatible with the engineering requirements of consistency and reliability for credible PMP estimates.

Storm maximization (also called moisture maximization) analyses have historically used monthly maximum observed 12-hour persisting dew points as published in the *Climatic Atlas of the United States* by the Environmental Data Services, Department of Commerce (1969). However, use of surface based dew points (either persisting or average) is only valid for storms where atmospheric moisture can be quantified using land based, surface dew point observations. In this study, sea surface temperature (SST) values were used in-place of dew point temperatures. SSTs were used in HMRs 57 and 59 as well as several site-specific PMP studies completed by AWA where inflow moisture source regions were located over the Atlantic or Pacific Ocean.

As part of this study, an updated maximum SST climatology was developed, replacing the Marine Climate Atlas of the World (U.S. Navy 1981) used in HMRs 57 and 59. This updated climatology includes monthly mean and +2-sigma maps for the Pacific Ocean from the coastline of the United States to 180°W and from 15°N to the southern Alaska coast. In conjunction with the +2-sigma climatological maps, daily SST maps based on ship and buoy reports used in deriving the storm representative SST values for each storm event (NOAA 2011, Kent et al. 2007, Reynolds et al. 2007, and Worley et al. 2005).

The ESRI ArcGIS, version 10.2 geographic information system (GIS) software environment was used extensively in the study to analyze storms, evaluate climatology data, complete the OTF analyses, delineate the characteristics of the Susitna-Watana basin, identify unique characteristics and terrain features of the region, and produce basin and regional maps.

SPAS provided gridded storm rainfall analyses. The SPAS analyses produced high-resolution gridded maximum rainfall datasets at hourly intervals over the spatial extent for the entire duration of each storm used in this study.

1.4 Basin Location and Description

The Susitna River basin is located in southern Alaska. The area of the drainage basin is approximately 5,131-square miles. The average elevation within the basin is 3,643 feet and varies from 1,456 feet at the proposed dam site to 13,134 feet in the Alaska Range. Figure 1.5 shows the basin location and surrounding topography. Figure 1.6 shows the topography within the basin and the thirty-four major sub-basins.

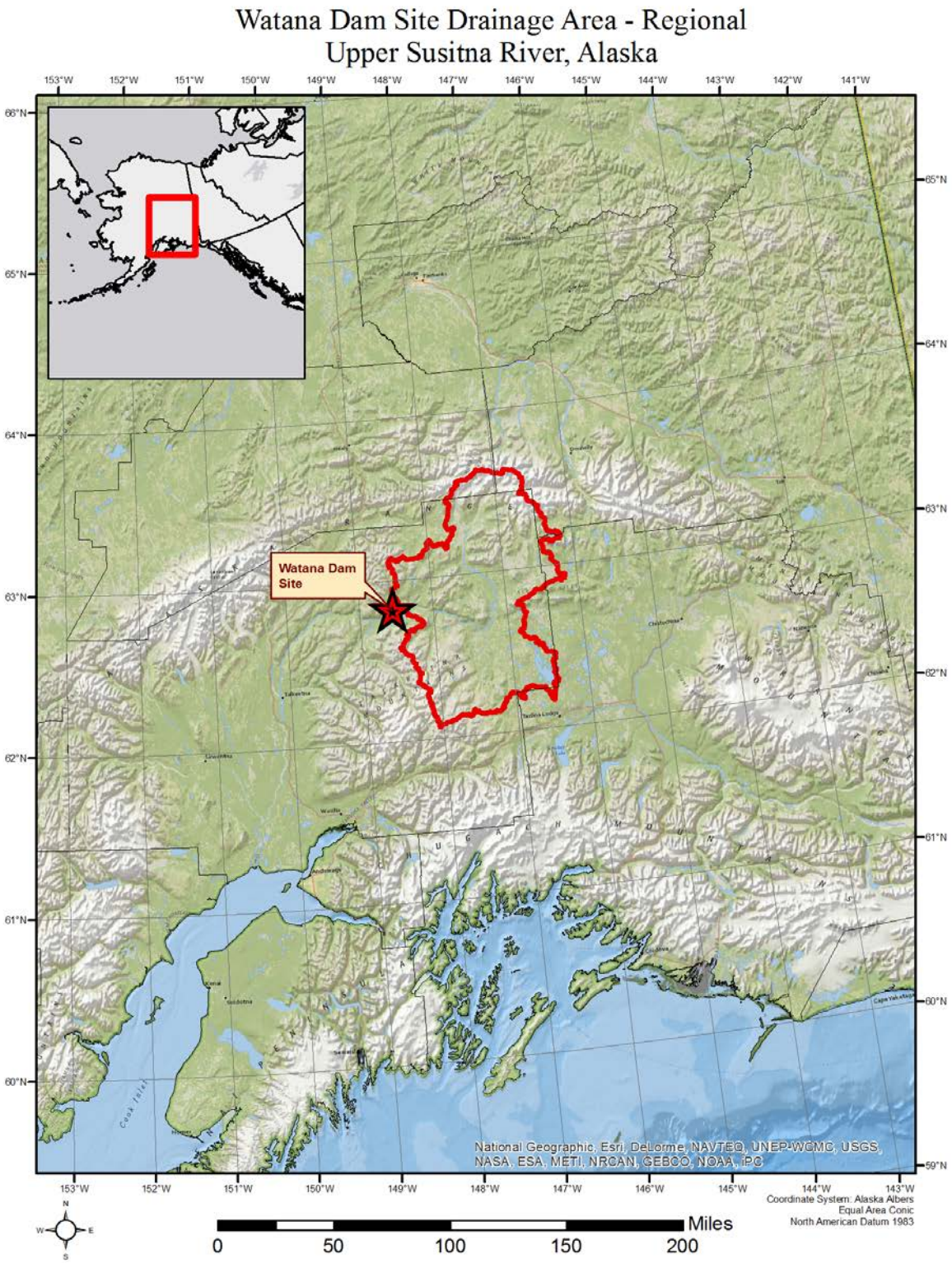

Figure 1.5. Susitna-Watana basin location and surrounding topography.

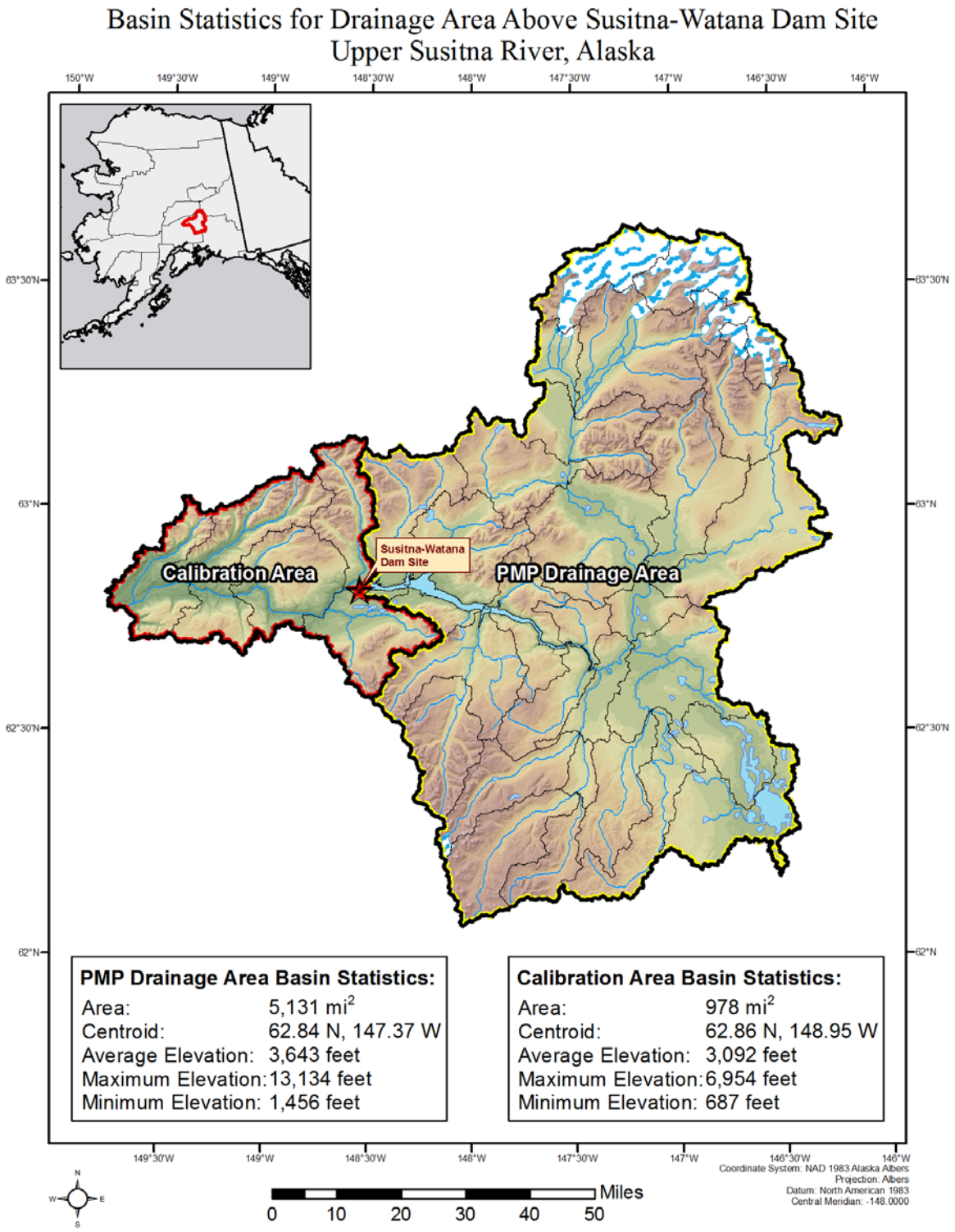

Figure 1.6. Susitna-Watana basin, subbasins, and major hydrologic features.

2. WEATHER AND CLIMATE OF THE SUSITNA-WATANA REGION

2.1 Seasonal Patterns

The weather and climate around the Susitna River basin is known for its extreme seasonality and high variability of weather patterns. Moisture feeding rainfall events in the basin arrives on southerly wind flows, with westerly components sometimes involved. The basin is located between two highly contrasting air mass types. Relatively mild and very moist air masses originated from the Gulf of Alaska and Pacific Ocean contrast with dry and cold Polar air masses from the north. Depending on which air mass is dominating the weather at any given time determines the resulting weather conditions. In addition, the basin is large enough that each of these air masses may be affecting different portions of the basin at the same time. During the months from November through March, temperatures are cold enough that rainfall is rare, and when it occurs it is light enough that flooding is not produced. Starting in April, a rapid transition takes places as warmer temperatures and higher levels of moisture begin to affect the region. Chances for rain increase across the lower elevations closer to the Gulf of Alaska. For most of April and often into May, significant snow pack remains. Over the interior and higher elevations of the basin, significant snow pack often stays well into June. This combination of rain on snow has resulted in some of the largest flood of record for the basin.

The peak season for rainfall occurs from July through early September as the storm track from the Pacific Ocean and Gulf of Alaska intensifies and combines with the highest amount of atmospheric moisture. In rare instances, remnant Tropical Storm moisture becomes entrained in these storms and enhances the rainfall across southern and interior Alaska. An excellent example of this scenario was the Great Fairbanks Flood of August 1967 (see http://en.wikipedia.org/wiki/History_of_Fairbanks,_Alaska). Rare heavy rainfall events, such as the September 2012 and October 1986, provide examples when the rain season is extended beyond expected time frames.

2.2 Orographic Influences

Rainfall in the region of the Susitna River basin is controlled by the orographic effect associated with the steep rise in elevation from sea level to over 12,000 feet south of the basin along the coastal mountains which intercepts most of the moisture moving in from the Gulf of Alaska. However, a major gap in the mountainous terrain occurs through the Cook Inlet and up the Susitna River valley. This allows significant amounts of low level moisture to move into the lower reaches of the Susitna River basin and into the western portions of the basin. In addition, as this moisture encounters the rising elevations of the Alaska Range around Denali as well as the higher elevation at the edge of the basin, it is forced to rise and precipitation enhancement occurs. In combination, all these upwind and along basin higher elevation serve to limit the amount of low-level moisture

reaching into the basin, especially the middle and eastern interior portions. Therefore, average precipitation amounts fall off very quickly within the basin, especially for elevation below 5,000 feet (the majority of the area within the basin). This effect is known as a rainshadow and it is imperative that the PMP value reflect this phenomena. Because of the unique topographic situations both upstream and within the basin, PMP-type rainfall is rare within the basin, but common at upwind locations. Therefore, extensive evaluations were completed to quantify the effects of topography on rainfall spatially and in magnitude, and to provide information on how storms are transpositioned the basin.

The topography within the basin also creates distinct rainfall patterns with extreme variations within the basin. The heaviest precipitation occurs at the western edge of the basin and along the higher elevation of the northern portion of the basin along the Alaska Range. Mean annual precipitation varies from just over 10 inches in the lower elevations of the southeastern portion of the basin to over 60 inches in the Alaska Range in the northeastern portion of the basin (Figure 2.1). At elevations above 5,000 feet, precipitation can be in the form of snow any time of the year.

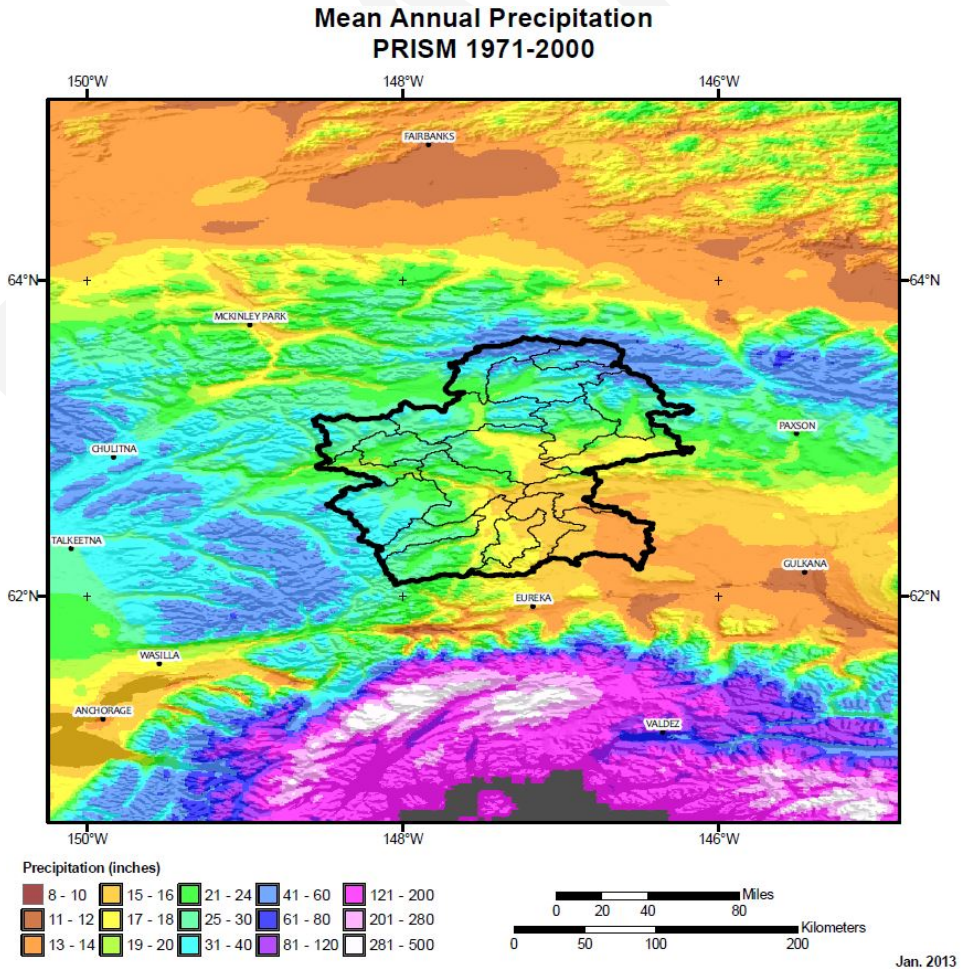

Figure 2.1. Mean annual precipitation based on PRISM 1971-2000 climatology.

2.3 Susitna River basin PMP Storm Type

The region around the basin is directly influenced by strong areas of low pressure (mid-latitude cyclones) moving in from the Pacific Ocean and Gulf of Alaska. These storms, referred to as synoptic storms, often bring with them very active storm dynamics (lift) and high levels of moisture from locations as far south as the subtropics north of Hawaii and points westward. This combination of enhanced lift and moisture often produces widespread heavy rainfall that may last three or more days. When these storms are able to tap into high levels of moisture supplied by the subtropical regions in and around the central Pacific Ocean, extreme rainfalls can occur. This type of scenario is known as an Atmospheric River. On the upslope regions upwind of the Susitna-Watana basin, the storms are further enhanced by orographic processes associated with the steep terrain encountered as they move onshore and are forced to rise over the slopes of the Coastal Range and Alaska Range. As discussed in the previous section, much of this atmospheric moisture rains out on the upwind slopes, thereby eliminating much of the low-level atmospheric moisture by the time it reaches the basin. Therefore, extreme rainfall events are rare in the basin and rainfall amounts are generally less than areas to the west and south of the basin. Synoptic storms cover large areas and produce heavy rains over relatively long periods. This storm type is most common from late June through early October.

2.3.1 Atmospheric Rivers and Mid-Latitude Cyclones

An Atmospheric River is an elongated, narrow, water vapor transport band located in the warm sector of a mid-latitude cyclone, often enhanced by convergence of local moisture (Bao et al. 2006). Atmospheric Rivers contain warm temperatures relative to normal in the surrounding air mass, enhanced water vapor and a strong low-level jet approximately 5,000 above the surface (Zhu and Newell 1998, Neiman et al., 2001, 2008, 2008, 2011, Ralph et al. 2003, 2004, 2005, 2006, 2011). Ralph (2004) demonstrated that more than 90% of the total meridional water vapor flux in the mid-latitudes is attributed to Atmospheric Rivers.

With this type of storm, flooding can be exacerbated antecedent snowpack, especially in the spring season. This scenario is most common between late May and late June after a cooler than normal spring has allowed higher than normal amounts of snowpack to remain over the basin. High levels of moisture and relatively warm temperatures associated with the Atmospheric River events emanating from the subtropical regions of the central Pacific Ocean result in heavy rainfall on a quickly melting snowpack producing increased runoff. These two factors lead to the largest flood events in the region.

2.4 Storm Types Seasonality

The most likely time for a PMP type storm event to occur in the Susitna River basin is from July through early September. However, extreme storms occur as early as May and as late as October.

Figure 2.2 displays the month of occurrence of the individual storm events from the storm search that were considered for PMP development (see Section 3.0). It should be noted that although the heaviest amounts of rainfall occur in the summer months, the higher amounts of snow pack available to combine with the rainfall runoff are likely to produce the largest volumes of flood runoff. Therefore, it is likely that the PMF would result from a combination of rainfall and snowmelt in May or early June.

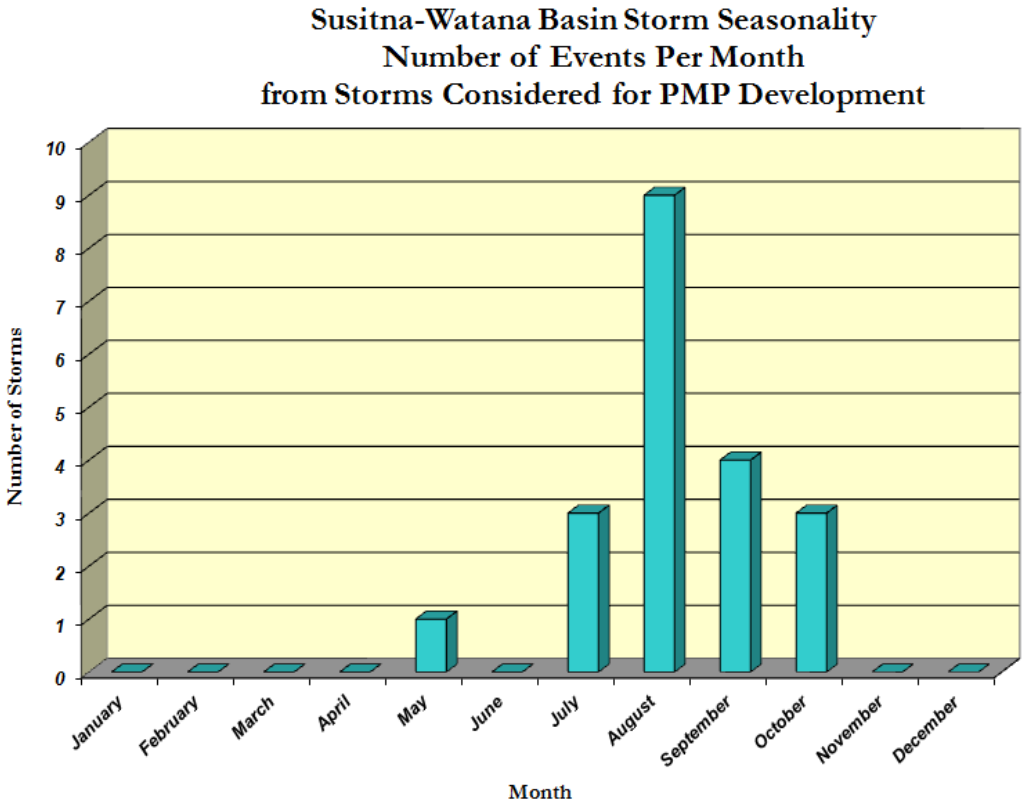

Figure 2.2. Storm seasonality for the Susitna River basin using all storm events from the long storm list.

3. EXTREME STORM IDENTIFICATION

3.1 Storm Search Area

A comprehensive storm search was conducted for this study and included an analysis of all the storms in meteorologically and topographically similar regions to the Susitna-Watana basin. Previous work and documents which discussed and analyzed storm events in the region were also reviewed. These included the reports from the NWS offices in Anchorage and Fairbanks, as well as HMR 57, the Acres (1982) study, and the Harza-Ebasco (1984) PMP work. Nine new storms were identified from the storm search which required full SPAS storm analyses for use in PMP development (Section 4). The primary search area included all geographic locations where extreme rainfall storms similar to those that could occur over the Susitna River basin have been observed. The search area extended from the Alaska Panhandle region (~54°N) to southern interior Alaska (~65°N) and from the Pacific Ocean coastline to northwestern interior Alaska (Figure 3.1). This ensured a large enough area was included in the storm search to capture all significant storms that could potentially influence final PMP values for the basin.

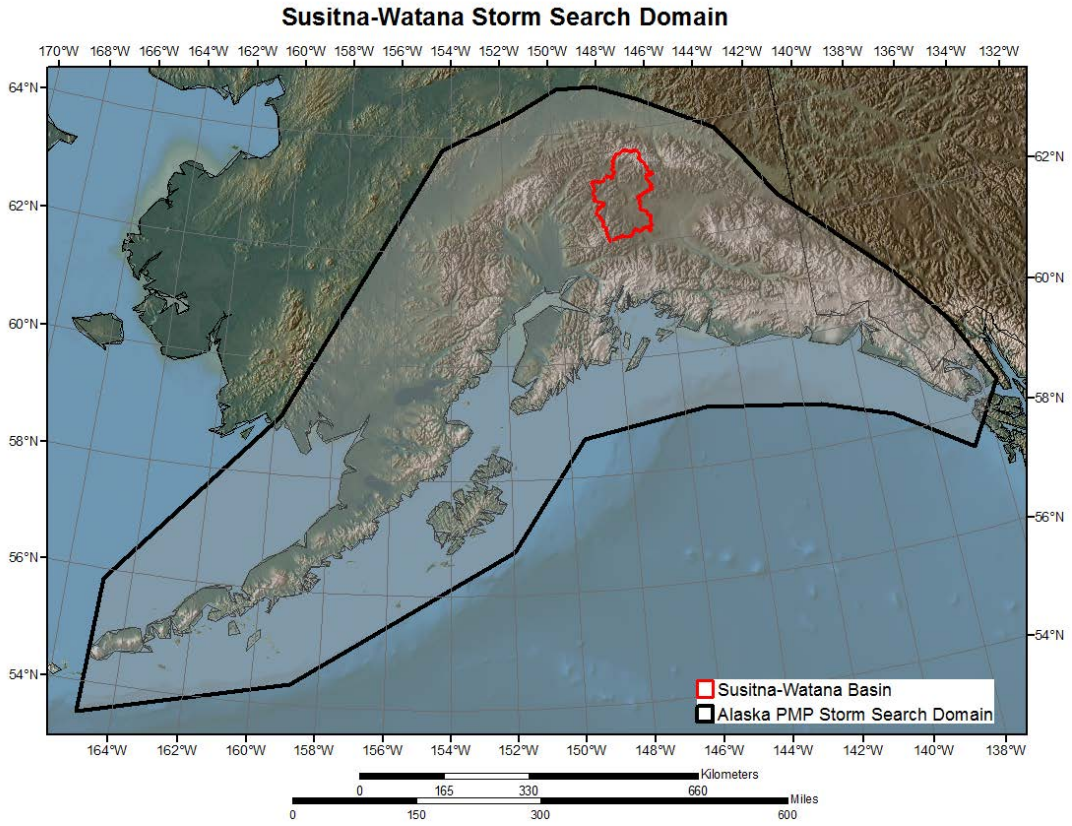

Figure 3.1. Susitna-Watana storm search domain.

3.2 Data Sources

The storm search was conducted using a dataset that included rainfall data from several sources. The primary data sources are listed below:

1. Cooperative Summary of the Day / TD3200 through 2013. These data are published by the National Climatic Data Center (NCDC).
2. Hourly Weather Observations published by NCDC, U.S. Environmental Protection Agency, and Forecast Systems Laboratory (now National Severe Storms Laboratory).
3. NCDC Recovery Disk
4. Hydrometeorological Reports
5. Corps of Engineers Storm Studies
6. Other data published by the Alaska State climate office
7. American Meteorological Society journals
8. Personal communications with various members of the Board of Consultants and others involved in this study
9. Watana and Devil Canyon Sites Probable Maximum Flood Report
10. Susitna Hydroelectric Project v4 Appendix A

3.3 Storm Search Method

The primary search began with identifying hourly and daily stations that have reliable rainfall data within the storm search area described previously. These stations were evaluated to identify the largest 1, 3, and 7 observational-day precipitation totals. Other reference sources such as HMRs and USACE storm reports and USGS flood studies (e.g. Smith 1950, USACE 1975, ACRES 1982, Harza-Ebasco 1984, HMR 42 1966) were reviewed to identify other dates with large rainfall amounts within the storm search domain. The criteria for storms to make the initial list of significant storms (referred to as the long storm list) were events that exceeded the 100-year return frequency value for the specified duration at the storm location.

The resulting long storm list was extensively quality controlled to ensure that only the highest storm rainfall values for each event were selected. Each storm was analyzed to verify its precipitation reports and compare it with rainfall amounts associated with other storms.

These storms values were plotted to ensure they occurred over similar meteorological and topographic regions as the Susitna-Watana drainage basin and could, therefore be used in the next steps of the PMP analysis. Table 3.1 is the long storm list and represents an initial assessment of all the storms found during the initial storm search. Quality control checks eliminated storms with duplicate rainfall centers, rainfall amounts which were accumulations, smaller rainfall centers

associated with the same storm event, and storms that were deemed not transpositionable to the Susitna-Watana basin, etc.

Table 3.1. Long storm list from the storm search. Rainfall values shown are the highest point values in inches over the total storm duration.

Name	ST	Lat	Lon	Year	Mon	Day	Total Rainfall
COAL HARBOR	AK	55.400	-160.817	1900	4	23	10.00
COAL HARBOR	AK	55.400	-160.817	1909	4	3	8.00
CORDOVA WB A	AK	60.500	-145.500	1912	9	26	19.75
CORDOVA WB A	AK	60.500	-145.500	1917	9	9	9.40
CORDOVA WB A	AK	60.500	-145.500	1925	9	20	15.69
CORDOVA WB A	AK	60.500	-145.500	1925	10	6	24.12
CHIGNIK	AK	56.300	-158.400	1927	8	15	14.99
CHIGNIK	AK	56.300	-158.400	1927	9	19	15.43
CHIGNIK	AK	56.300	-158.400	1929	9	8	16.38
CHIGNIK	AK	56.300	-158.400	1930	5	9	18.93
CHIGNIK	AK	56.300	-158.400	1930	5	25	15.78
DENALI NP	AK	63.038	-150.471	1955	8	22	13.75
CORDOVA	AK	60.646	-145.554	1955	8	22	21.67
CAPE SPENCER	AK	58.200	-136.633	1956	11	24	20.93
MT SPURR	AK	61.346	-152.329	1958	7	25	6.62
LITTLE SUSITNA	AK	61.854	-149.229	1959	8	18	13.05
CAPE HINCHINBROOK	AK	60.233	-146.650	1962	4	13	20.50
CAPE HINCHINBROOK	AK	60.233	-146.650	1962	5	9	29.95
CAPE HINCHINBROOK	AK	60.233	-146.650	1962	5	25	13.75
CAPE SPENCER	AK	58.200	-136.633	1966	11	23	15.80
DENALI NP	AK	62.846	-150.513	1967	8	2	12.45
FAIRBANKS	AK	65.521	-147.329	1967	8	2	12.45
HOMER	AK	59.871	-150.563	1967	8	2	12.45
CHIGNIK	AK	56.300	-158.400	1969	6	4	14.81
CAPE HINCHINBROOK	AK	60.233	-146.650	1969	7	24	22.90
CHIGNIK	AK	56.300	-158.400	1969	10	12	14.68
BLACK RAPIDS	AK	63.471	-145.479	1971	8	5	12.17
SUTTON	AK	61.904	-148.863	1971	8	5	11.39
PORTAGE	AK	61.004	-148.663	1971	8	5	12.17
DENALI NP	AK	62.954	-150.079	1980	7	24	7.33
ANGOON PWR	AK	57.499	-134.586	1982	10	12	15.20
DENALI NP	AK	62.829	-151.138	1986	10	8	11.01
SEWARD	AK	60.113	-149.513	1986	10	8	20.80
OUZINKIE	AK	57.933	-152.500	1991	11	1	10.76
WHITTIER	AK	60.713	-148.779	1995	9	19	26.03
SEWARD	AK	60.117	-149.450	1995	9	20	9.81
BIG RIVER LA	AK	60.817	-152.300	1996	3	22	7.50
ELFIN COVE	AK	58.200	-136.667	1996	9	25	8.61
CANNERY CREEK	AK	60.696	-145.688	2003	9	29	23.69
PELICAN	AK	57.950	-136.233	2005	11	17	26.87
BLACK RAPIDS	AK	63.465	-145.685	2006	8	17	16.12
CANNERY CREEK	AK	60.696	-145.688	2006	10	7	23.63
OLD TYONEK	AK	61.260	-151.860	2012	9	15	15.91
KENAI FJORDS NP	AK	59.610	-150.220	2012	9	15	33.96

3.4 Developing the Intermediate List of Extreme Storms

A multiple step process was followed to determine a list of storms considered to be comprehensive enough to ensure that major events were included while eliminating smaller events that would not be significant for determining PMP values at any area size or duration after all adjustments were applied. Initially, all storms previously analyzed during the ACRES 1982, Harza-Ebasco 1984 or by the USACE were moved to the short storm list. The remaining storms were sorted by maximum rainfall amount. This eliminated events based on different locations reporting rainfall amounts associated with the same event. Further analysis was conducted to verify that each storm was transpositionable to the Susitna-Watana basin. Other checks were performed to see whether conditions within the basin during a storm event would have produced snow instead of rain, whether the storm had enough data available to complete an analysis, and whether the storm was within at least 35% of maximum values from other storms. Table 3.2 displays the results of this iterative analysis, including the reason for elimination or inclusion of each storm. In Table 3.2, the columns highlighted with a green header display the various parameters which were analyzed to determine whether a storm could be moved from the long storm list to the intermediate storm list. Each storm was analyzed going from left to right on the table. Once a storm met or did not meet one of the criteria, no further evaluation using the remaining criteria was completed. A notation was entered into the appropriate column associated with a particular selection criterion (i.e. a “yes” or “no”) with all other selection criteria cells associated with a particular storm left blank. The results of this analysis comprised the short storm list as described in the following section.

Table 3.2. Long storm list storm selection criteria used to derive the intermediate storm list.

Name	ST	Lat	Lon	Year	Mon	Day	Total Rainfall	AWA Storm Analysis	Transpositionable to Basin	Snow in the basin	Larger Storm in Similar Location	No Rain in basin or region	Data to Complete Analysis	More than 35% of Max Storm amount (>12.00")
COAL HARBOR	AK	55.400	-160.817	1900	4	23	10.00							No
COAL HARBOR	AK	55.400	-160.817	1909	4	3	8.00							No
CORDOVA WB A	AK	60.500	-145.500	1912	9	26	19.75						No	
CORDOVA WB A	AK	60.500	-145.500	1917	9	9	9.40							No
CORDOVA WB A	AK	60.500	-145.500	1925	9	20	15.69				Yes			
CORDOVA WB A	AK	60.500	-145.500	1925	10	6	24.12						No	
CHIGNIK	AK	56.300	-158.400	1927	8	15	14.99		No			Yes	No	
CHIGNIK	AK	56.300	-158.400	1927	9	19	15.43		No			Yes		
CHIGNIK	AK	56.300	-158.400	1929	9	8	16.38		No				No	
CHIGNIK	AK	56.300	-158.400	1930	5	9	18.93		No				No	
CHIGNIK	AK	56.300	-158.400	1930	5	25	15.78		No			Yes		
DENALI NP	AK	63.038	-150.471	1955	8	22	13.75	Yes						
CORDOVA	AK	60.646	-145.554	1955	8	22	21.67	Yes						
CAPE SPENCER	AK	58.200	-136.633	1956	11	24	20.93		No					
MT SPURR	AK	61.346	-152.329	1958	7	25	6.62	Yes						
LITTLE SUSITNA	AK	61.854	-149.229	1959	8	18	13.05	Yes						
CAPE HINCHINBROOK	AK	60.233	-146.650	1962	4	13	20.50		No	Yes				
CAPE HINCHINBROOK	AK	60.233	-146.650	1962	5	9	29.95		No					
CAPE HINCHINBROOK	AK	60.233	-146.650	1962	5	25	13.75				Yes			
CAPE SPENCER	AK	58.200	-136.633	1966	11	23	15.80		No					
DENALI NP	AK	62.846	-150.513	1967	8	2	12.45	Yes						
FAIRBANKS	AK	65.521	-147.329	1967	8	2	12.45	Yes						
HOMER	AK	59.871	-150.563	1967	8	2	12.45	Yes						
CHIGNIK	AK	56.300	-158.400	1969	6	4	14.81		No			Yes		
CAPE HINCHINBROOK	AK	60.233	-146.650	1969	7	24	22.90		No					
CHIGNIK	AK	56.300	-158.400	1969	10	12	14.68			Yes		Yes		
BLACK RAPIDS	AK	63.471	-145.479	1971	8	5	12.17	Yes						
SUTTON	AK	61.904	-148.863	1971	8	5	11.39	Yes						
PORTAGE	AK	61.004	-148.663	1971	8	5	12.17	Yes						
DENALI NP	AK	62.954	-150.079	1980	7	24	7.33	Yes						
ANGOON PWR	AK	57.499	-134.586	1982	10	12	15.20		No					
DENALI NP	AK	62.829	-151.138	1986	10	8	11.01	Yes						
SEWARD	AK	60.113	-149.513	1986	10	8	20.80	Yes						
OUZINKIE	AK	57.933	-152.500	1991	11	1	10.76			Yes				
WHITTIER	AK	60.713	-148.779	1995	9	19	26.03		No					
SEWARD	AK	60.117	-149.450	1995	9	20	9.81							No
BIG RIVER LA	AK	60.817	-152.300	1996	3	22	7.50							No
ELFIN COVE	AK	58.200	-136.667	1996	9	25	8.61							No
CANNERY CREEK	AK	60.696	-145.688	2003	9	29	23.69		No					
PELICAN	AK	57.950	-136.233	2005	11	17	26.87		No					
BLACK RAPIDS	AK	63.465	-145.685	2006	8	17	16.12	Yes						
CANNERY CREEK	AK	60.696	-145.688	2006	10	7	23.63		No			Yes		
OLD TYONEK	AK	61.260	-151.860	2012	9	15	15.91	Yes						
KENAI FJORDS NP	AK	59.610	-150.220	2012	9	15	33.96	Yes						

3.5 Short Storm List

Each of the storms on the short storm list were evaluated in detail using the SPAS program. Results of these analysis included the development of storm isohyetals and Depth-Area-Duration tables (DADs). Each of these storms was maximized in-place, transpositioned to each grid point comprising the basin. The storm center locations of the various SPAS DAD analyses are plotted for reference in Figure 3.2. Table 3.3 list the final short list of storms.

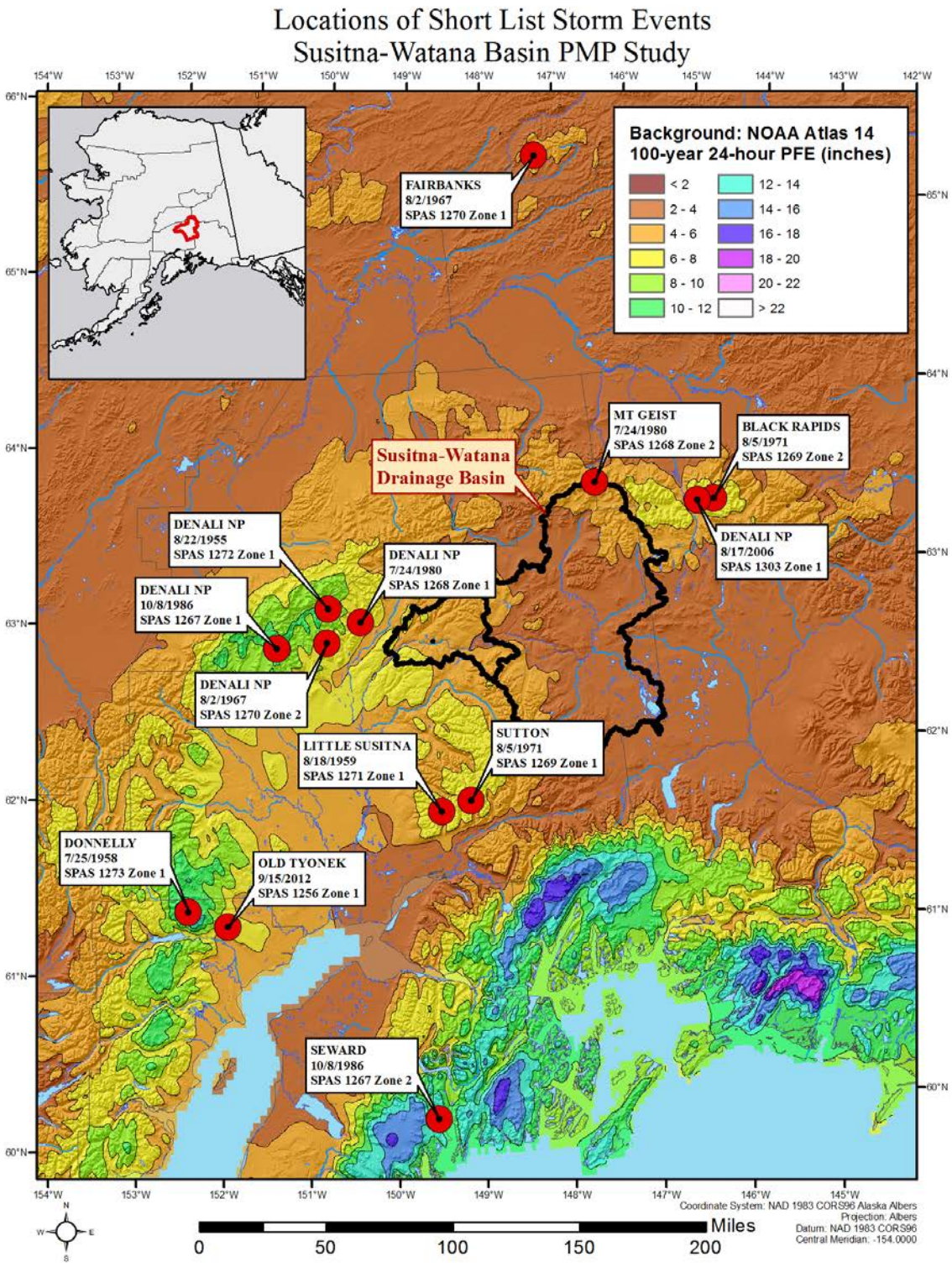

Figure 3.2. Short storm list storm locations

Table 3.3. Susitna-Watana short storm list used in the SSPMP analysis. Rainfall values are the maximum rainfall totals produced the SPAS storm analyses.

Name	ST	Lat	Lon	Year	Mon	Day	Total Rainfall	Precipitation Source
DENALI NP	AK	63.038	-150.471	1955	8	22	13.75	SPAS 1272 Zone 1
MT SPURR	AK	61.346	-152.329	1958	7	25	6.62	SPAS 1273 Zone 1
LITTLE SUSITNA	AK	61.854	-149.229	1959	8	18	13.05	SPAS 1271 Zone 1
DENALI NP	AK	62.846	-150.513	1967	8	2	12.45	SPAS 1270 Zone 2
FAIRBANKS	AK	65.521	-147.329	1967	8	2	12.45	SPAS 1270 Zone 1
BLACK RAPIDS	AK	63.471	-145.479	1971	8	5	12.17	SPAS 1269 Zone 2
SUTTON	AK	61.904	-148.863	1971	8	5	11.39	SPAS 1269 Zone 1
MT GEIST	AK	63.638	-146.971	1980	7	24	5.26	SPAS 1268 Zone 2
DENALI NP	AK	62.954	-150.079	1980	7	24	7.33	SPAS 1268 Zone 1
DENALI NP	AK	62.829	-151.138	1986	10	8	11.01	SPAS 1267 Zone 1
SEWARD	AK	60.113	-149.513	1986	10	8	20.80	SPAS 1267 Zone 2
BLACK RAPIDS	AK	63.465	-145.685	2006	8	17	16.12	SPAS 1303 Zone 1
OLD TYONEK	AK	61.260	-151.860	2012	9	15	15.91	SPAS 1256 Zone 1

4. STORM DEPTH-AREA-DURATION (DAD) ANALYSES

Gridded rainfall values are required for PMP calculations. Therefore, all storms on the short storm list (see Section 3.5) were required to be analyzed using the SPAS program. This program computed the required rainfall values, along with several other products such as mass curves, isohyetal patterns, analysis statistics, and quality control analyses. Detailed results of each of these analyses are included in Appendix C.

There are two main steps in the SPAS DAD analysis: 1) The creation of high-resolution hourly rainfall grids and 2) the computation of Depth-Area (DA) rainfall amounts for various durations. The reliability of the results from step 2) depends on the accuracy of step 1) (Jones 1969, Gou et al 2001, Duchon and Essenberg 2001). Before this process was automated using SPAS, the storm rainfall analyses were very labor intensive and highly subjective. SPAS utilizes a GIS to create spatially-oriented and highly accurate results in an efficient manner. Furthermore, the availability of NEXRAD data allows SPAS to better account for the spatial and temporal variability of storm precipitation for events occurring since the early 1990s. Prior to NEXRAD, the NWS developed and used a method based on Weather Bureau Technical Paper No. 1 (U.S. Weather Bureau 1946). Because this process has been the standard for many years (all DAD produced by the NWS in all the HMRs used this procedure) and holds merit, the SPAS DAD analysis process used in this study attempts to apply the NWS procedure as much as possible. By adopting this approach, some level of consistency between the newly analyzed storms and the hundreds of storms already analyzed by the NWS is achieved. Comparisons between the NWS DAD results and those computed using the SPAS method for two storms (Westfield, MA 1955 and Ritter, IA 1953) produced very similar results (see Appendix D for complete discussion, comparisons, and results).

4.1 Data Collection

The areal extent of a storm's rainfall was evaluated using existing maps and documents along with plots of total storm rainfall. Based on the storm's spatial domain (longitude-latitude box), hourly and daily rainfall data were extracted from our in-house database for specified areas, dates, and times. Rainfall amounts are either observed and recorded each hour (hourly) or once a day (daily). To account for the temporal variability in observation times at daily reporting stations, the extracted hourly data must capture the entire observational period of all daily station reports. For example, if a station takes daily observations at 8:00 AM local time, then the hourly data need to be complete from 8:00 AM local time the day prior. As long as the hourly data are sufficient to capture all of the daily station observations, the hourly variability in the daily observations can be properly addressed.

The daily rainfall database is comprised of data from National Climatic Data Center (NCDC) TD-3206 (pre 1948) and TD-3200 (generally 1948 through present). The hourly rainfall database is

comprised of data from NCDC TD-3240 and NOAAs Meteorological Assimilation Data Ingest System (MADIS). The daily supplemental database is largely comprised of data from "bucket surveys," local rain gauge networks (e.g. ALERT, USGS, etc.) and daily gauges with accumulated data.

4.2 Mass Curves

The most complete rainfall observational dataset available is compiled for each storm. To obtain temporal resolution to the nearest hour in the DAD results, it is necessary to distribute the daily precipitation observations (at daily stations) into hourly values. This process has traditionally been accomplished by anchoring each of the daily stations to a single hourly timer station. However, this may introduce biases and may not correctly represent hourly precipitation at locations between hourly stations. A preferred approach is to anchor the daily station to some set of the nearest hourly stations. This is accomplished using a spatially based approach that is called the spatially based mass curve (SMC) process.

4.3 Hourly or Sub-hourly Precipitation Maps

At this point, SPAS can either operate in its standard mode or in NEXRAD-mode to create high resolution hourly or sub-hourly (for NEXRAD storms) grids. In practice both modes are run when NEXRAD data are available so that a comparison can be made between the methods. Regardless of the mode, the resulting grids serve as the basis for the DAD computations.

4.3.1 Standard SPAS Mode

The standard SPAS mode requires a full listing of all the observed hourly rainfall values, as well as the newly created estimated hourly values from daily and daily supplemental stations. This is done by creating an hourly file that contains the newly created hourly mass curve precipitation data (from the daily and supplemental stations) and the "true" hourly mass curve precipitation. The option of incorporating basemaps was used in this study. If base maps were not used, the individual hourly precipitation values would simply be plotted and interpolated to a raster with an inverse distance weighting (IDW) interpolation routine or some other mathematical scheme using GIS.

4.3.2 NEXRAD Mode

Radar has been in use by meteorologists since the 1960s to estimate rainfall depth. In general, most current radar-derived rainfall techniques rely on an assumed relationship between radar reflectivity and rainfall rate. This relationship is described by the equation (4.1) below:

$$Z = aR^b \qquad \text{Equation 4.1}$$

Where Z is the radar reflectivity, measured in units of dBZ (dBZ stands for decibels of Z), R is the rainfall rate, *a* is the "multiplicative coefficient" and *b* is the "power coefficient". Both *a* and *b* are

related to the drop size distribution (DSD) and the drop number distribution (DND) within a cloud (Martner et al. 2005).

The NWS uses this relationship to estimate rainfall through the use of their network of NEXRAD asites located across the United States. A standard default Z-R algorithm of $Z = 300R^{1.4}$ is the primary algorithm used throughout the country and has proven to produce highly variable results. The variability in the results of Z vs. R is a direct result of differing DSD and DND, and differing air mass characteristics across the United States (Dickens 2003). The DSD and DND are determined by a complex interaction of microphysical processes in a cloud. They fluctuate hourly, daily, seasonally, regionally, and even within the same cloud (see Appendix D for a more detailed description).

Although SPAS uses Equation 4.1 to determine rainfall rates, the *a* and *b* coefficients are explicitly determined for each hour of the storm using a calibration technique. Hourly rain gauge data are used with hourly NEXRAD data in the calibration calculations.

4.4 Depth-Area-Duration Program

The DAD extension of SPAS runs from within a Geographic Resource Analysis Support System (GRASS) GIS environment[2] and utilizes many of the built-in functions for calculation of area sizes and average depths. The following is the general outline of the procedure:

1. Given a duration (e.g. x-hours) and cumulative precipitation, sum up the appropriate hourly or sub-hourly precipitation grids to obtain an x-hour total precipitation grid starting with the first x-hour moving window.

2. Determine x-hour precipitation total and its associated areal coverage. Store these values. Repeat for various lower rainfall thresholds. Store the average rainfall depths and area sizes.

3. The result is a table of depth of precipitation and associated area sizes for each x-hour duration. Summarize the results by moving through each of the area sizes and choosing the maximum precipitation amount. A log-linear plot of these values provides the depth-area curve for the x-hour duration.

4. Based on the log-linear plot of the rainfall depth-area curve for the x-hour duration, determine rainfall amounts for the standard area sizes for the final DAD table. Store these values as the rainfall amounts for the standard sizes for the x-duration period. Determine if the x-hour

[2] Geographic Resource Analysis Support System, commonly referred to as GRASS, this is free Geographic Information System (GIS) software used for geospatial data management and analysis, image processing, graphics/maps production, spatial modeling, and visualization. GRASS is currently used in academic and commercial settings around the world, as well as by many governmental agencies and environmental consulting companies. GRASS is an official project of the Open Source Geospatial Foundation.

duration period is the longest duration period being analyzed. If it is not, analyze the next longest duration period and return to step 1.

5. Construct the final DAD table with the stored rainfall values for each standard area for each duration period.

5. STORM MAXIMIZATION

Storm maximization (also called moisture maximization in the HMRs) is the process of increasing rainfall associated with an observed extreme storm under the potential condition that additional moisture could have been available to the storm and would have increased the rainfall production. This is quantified by increasing the surface dew points (or SSTs for all storms used in this study) to some climatological maximum and calculating the enhanced rainfall amounts that could potentially have been produced (Bolsenga 1965). An additional consideration is usually applied that selects the climatological maximum dew point or SST for a date two weeks towards the climatological maximum warm season from the date that the storm actually occurred. This procedure assumes that the storm could have occurred two weeks earlier or later in the year when maximum dew points or SSTs are higher. Calculations for each storm used in this study are shown in Appendix C.

5.1 New Procedures Used in the Storm Maximization Process

The HYSPLIT trajectory model (Draxler and Rolph 2003, 2010) provides detailed analyses of upwind trajectories of atmospheric moisture that was advected into the storm systems. Using these trajectories, the atmospheric moisture source locations are determined. The procedures followed are similar to the approach used in HMRs 57 and 59. However, by utilizing the HYSPLIT model trajectories, much of the subjectivity is eliminated. Further, details of each evaluation can be explicitly provided and the results are reproducible.

Using SSTs for in-place maximization and storm transpositioning (discussed Section 6) followed the same procedure used with land based surface dew points. Use of the HYSPLIT trajectory model provided a significant improvement in determining the inflow wind vectors originating over the ocean compared to older methods of extrapolating coastal wind observations and estimating moisture advection from synoptic features. This more objective procedure is especially useful for situations where a long distance is involved to reach warmer ocean regions. Timing is not as critical for inflow wind vectors extending over the oceans since SSTs change very slowly with time compared to dew point values over land. Changing wind directions are of greater importance, especially for situations where there is curvature in the wind fields. Any changes in wind curvature and variations in timing are inherently captured in the HYSPLIT trajectories.

5.1.1 HYSPLIT Trajectory Model

The HYSPLIT trajectory model was used during the analysis of each of the rainfall events included on the short storm list when available (1948-present from the National Centers for Environmental Prediction (NCEP) Global Reanalysis fields) (Mesinger et al 2006). Use of a trajectory model provides increased confidence for determining inflow moisture vectors and storm representative SSTs. The HYSPLIT model trajectories have been used to analyze the moisture inflow vectors in

other PMP studies completed by AWA over the past several years. During these analyses, the model trajectory results were verified and the utility explicitly evaluated (e.g. Tomlinson et al. 2006-2011, Kappel et al. 2012-2013).

Instead of subjectively determining the moisture inflow trajectory, the HYSPLIT analysis was used to determine the trajectory of the moisture inflow for various levels in the atmosphere associated with the storm's rainfall production. The HYSPLIT software was run for trajectories at several levels of the lower atmosphere to help determine the moisture source for each storm event. These included 700mb (approximately 10,000 feet), 850mb (approximately 5,000 feet), and storm center location surface elevation[3].

For the majority of the analyses, a combination of all three levels was used to identify the upwind moisture source location. It is important to note that the resulting HYSPLIT model trajectories are only used as a general guide of where to evaluate the moisture source for storms in space and time. The final determination of the storm representative SST and its location is determined following the standard procedures used by AWA in previous PMP studies and as outlined in the HMRs and WMO manuals. Appendix C of this report lists each of the HYSPLIT trajectories used for each storm. As an example, Figures 5.1 show the HYSPLIT trajectories used to determine the inflow moisture vector from the October 1986 rainfall event.

[3] These are standard elevations for atmospheric analysis. Further, the majority of atmospheric moisture available for rainfall production occurs below the 700mb level.

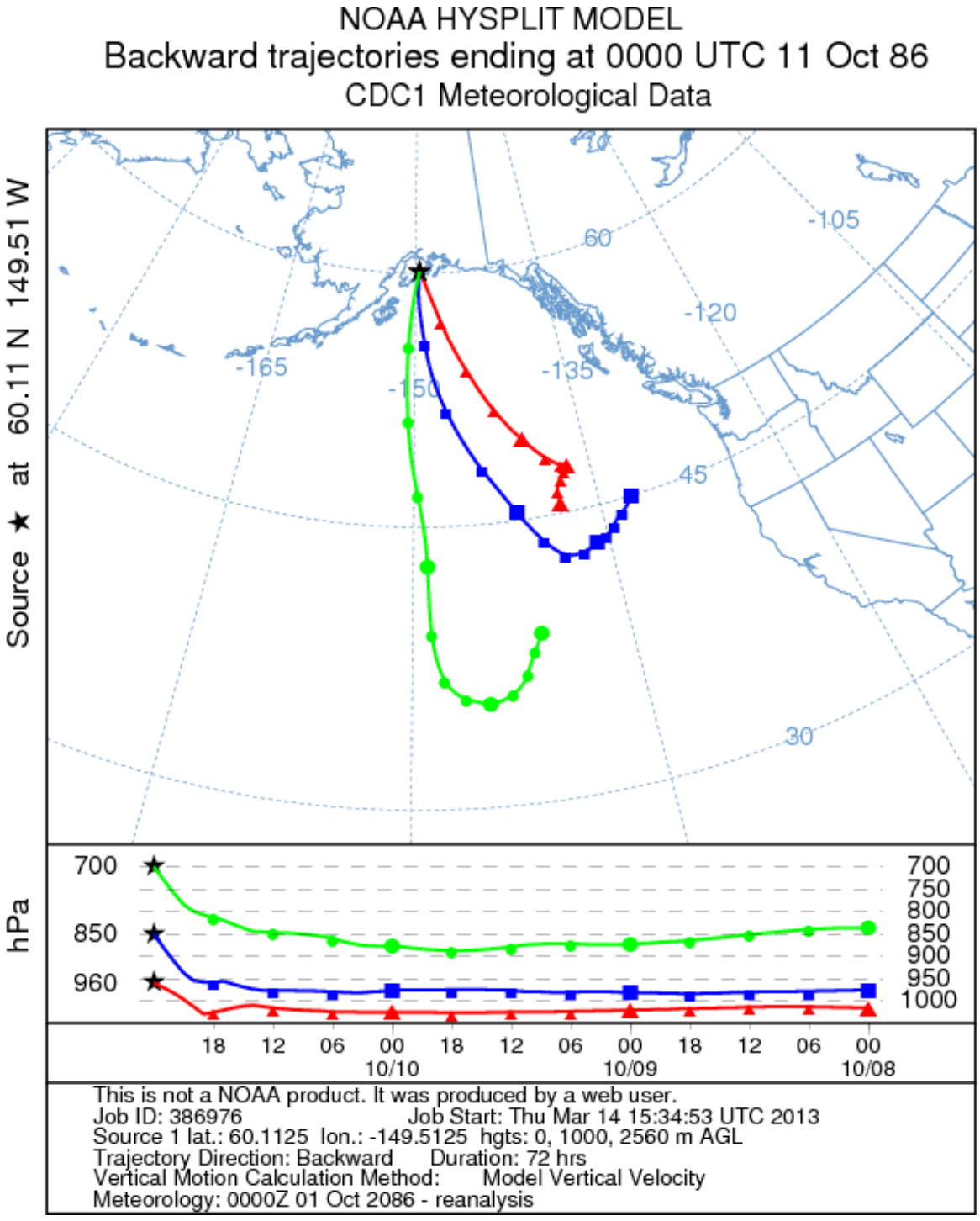

Figure 5.1. Surface (960mb), 850mb, and 700mb HYSPLIT trajectory model results for the October 1986 storm event.

5.1.2 Sea Surface Temperatures (SSTs)

The second data set used in storm analyses contained SSTs derived from the various databases available from NOAA. Daily values were generated from the following sources:

1985 – Present: http://dss.ucar.edu/datasets/ds277.7/
1946 - 1985: http://dss.ucar.edu/datasets/ds195.1/
Prior to 1946: http://dss.ucar.edu/datasets/ds540.0/

Observations were taken from ships, buoys (moored and drifting), automated coastal fixed platforms and drilling rigs, and satellite observations of SSTs (Woodruff et al. 2005). Analyses are archived to the nearest 0.1°F, with a spatial resolution of 1° in both latitude and longitude. For storm analyses, daily SSTs were used to determine the storm representative SST for each storm event on the short storm list. Figure 5.2 is an example daily SST map for the October 1986 storm event.

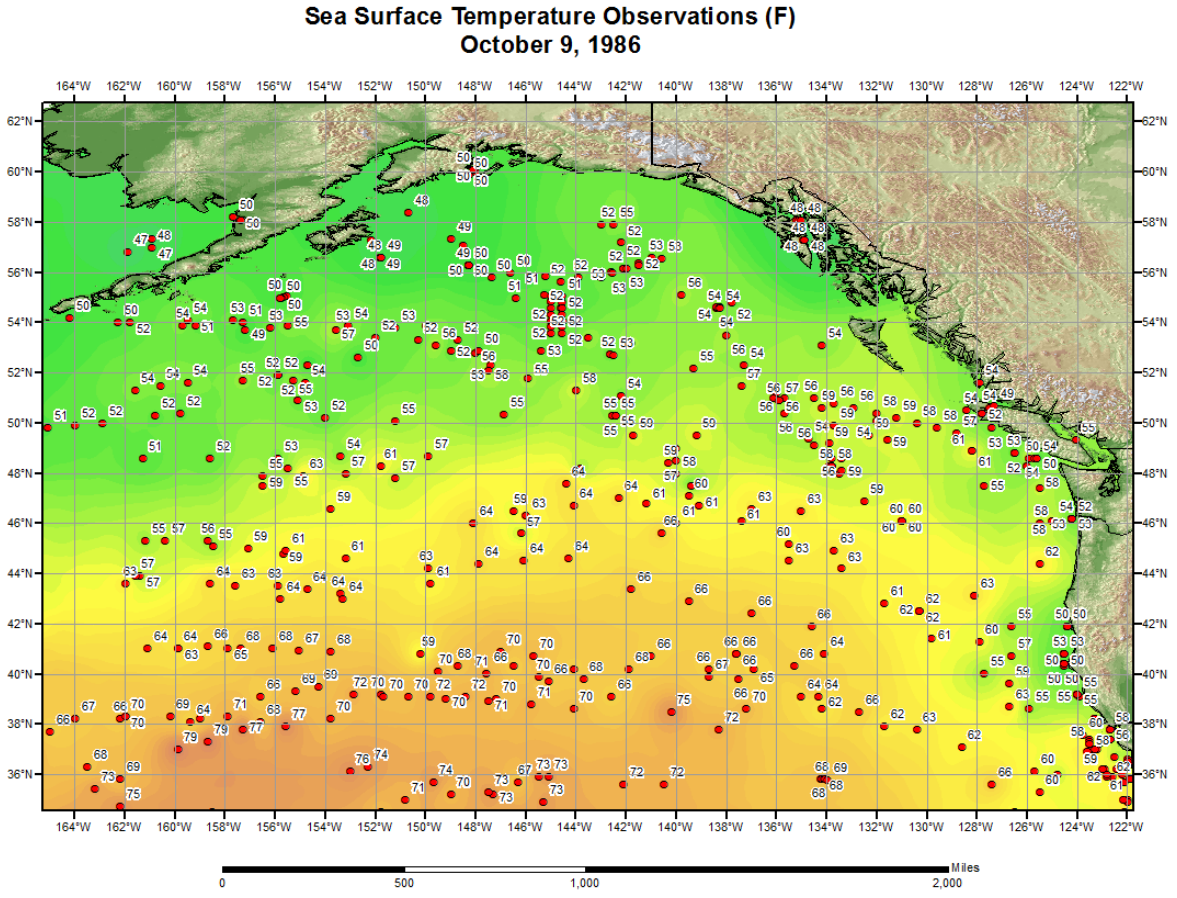

Figure 5.2 **Daily sea surface temperatures for October 9, 1986 over the upwind domain used to determine the storm representative sea surface temperature.**

For computing the maximization factors, a climatology of SSTs was computed for every 1° latitude and longitude, based on data from 1982 through 2012 (from NOAA_OI_SST_V2, http://www.esrl.noaa.gov/psd/) . The standard deviation for each cell was calculated and plus two standard deviations (+2-sigma) were added to the monthly mean SST values for each cell. Monthly maps were produced to provide spatial analyses of the mean plus 2-sigma (two standard deviations warmer than the mean) SSTs. Use of the mean plus 2-sigma SSTs is consistent with the NWS procedure used in HMRs 57 and 59. Figure 5.3 is an example monthly map for October.

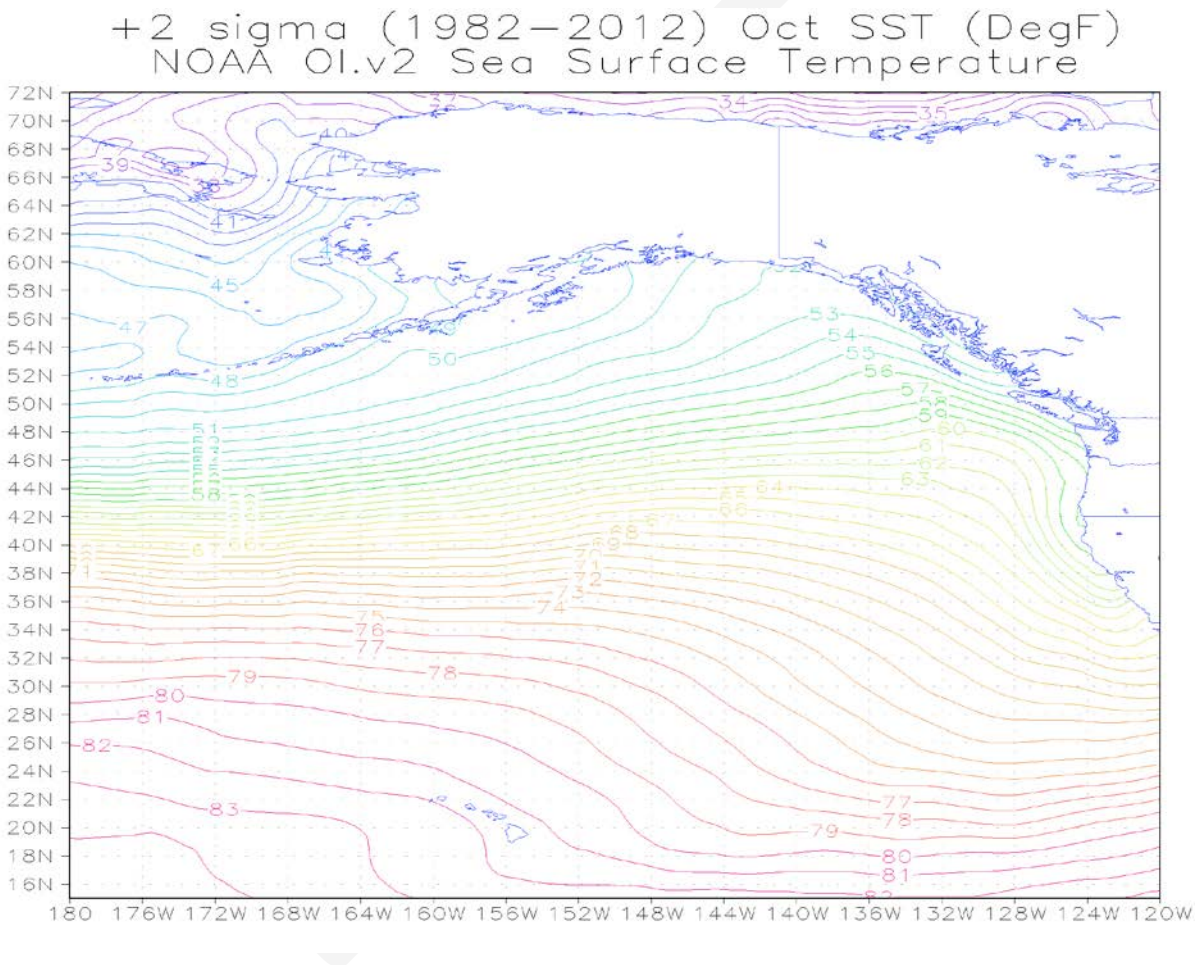

Figure 5.3. +2-sigma sea surface temperature map for October.

5.1.2.1 Use of Sea Surface Temperatures (SSTs)

Dew point observations are not generally available over ocean regions. When the source region of atmospheric moisture feeding an extreme rainfall event originates over the ocean, a substitute for dew points observations is required. The NWS adopted a procedure for using SSTs as surrogates for dew points over the ocean. The value used as the maximum SST in the PMP calculations is determined using the SSTs plus two standard deviations (+2-sigma) warmer than the mean SST.

This provides a value for the maximum SST that has a probability of occurrence of about 0.025, i.e. about the 40-year return frequency value (see Section 5.1.2.1 for more detail).

Following the NWS procedure (e.g. HMR 57) and previous AWA PMP work (Tomlinson et al 2008- 2013, Kappel et al. 2011-2014), storm representative SSTs were substituted for dew points. All storms on the short list were reanalyzed to determine the storm representative SST and the +2-sigma SST. These SST values are then treated the same as dew points and the same process is followed for storm maximization as if the SST values were dew point values taken from land based stations.

Where cold currents affect ocean temperatures adjacent to the coast, use of the cold SSTs is inappropriate to represent the storm atmospheric moisture source region. The procedure that selects a storm representative SST in the region that is the primary source of atmospheric moisture available to the storm is then employed. This procedure requires extending the inflow wind vector over the region of colder SSTs along the immediate coastline and selecting a location over the warmer water of the moisture source region. Daily SSTs are then analyzed over this general region, using HYSPLIT as guidance when available, to determine a homogenous region of SSTs in space and time. Generally, this area should show less than a 1°F temperature change in a 1° latitude x 1° longitude box. This value is the storm representative SST.

For storm maximization, the value for the maximum SST is determined using the mean plus 2-sigma SST for that location for a date two weeks before or after the storm date (which ever provides the climatologically warmer 2-sigma SST values). Storm representative SSTs and the mean plus 2-sigma SSTs are used in the same manner as storm representative dew points and maximum dew points in the maximization and transpositioning procedure.

5.1.2.2 Rationale for Using +2-Sigma SSTs

The NWS states in HMR 57 that the two standard deviations warmer values are approximately equal to a 0.02 probability of occurrence. Specifically, HMR 57 Section 4.3, pp 43-44, states that two standard deviations represent about 98 percent of normally distributed values and this "…places the magnitude of this parameter at about the level of other estimates used in this study, e.g. the 100-year frequency values." For the +2-sigma probability, there is 0.05 out of 1.00 that is not included under the normal distribution curve. The 0.05 is divided between the extremes on the upper and lower ends of the normal distribution curve. Since only the high end (i.e. SST plus two standard deviations warmer) is used, only half of the 0.05 is excluded from under the normal distribution curve, i.e. 0.025. Hence 0.975 or 97.5% is included under the normal distribution curve. Figure 5.4 shows the normal distribution curve with the +1-sigma and +2-sigma values.

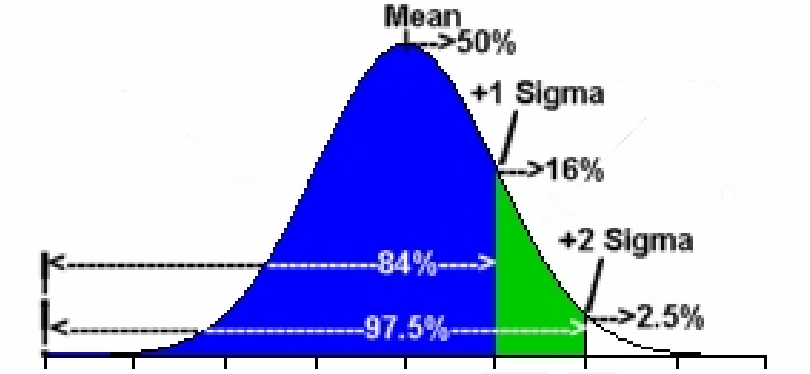

Figure 5.4 Normal distribution curve with +1-sigma and +2-sigma values shown

It appears, for reasons that are not clear in HMR 57, that the NWS increased the value of 0.975 to 0.99 and then concluded that this represents the 100-year frequency value. Therefore, it is important to note that without any adjustments, 0.975 is approximately equal to a 40-year return frequency value.

6. STORM TRANSPOSITIONING

Extreme rain events in meteorologically homogeneous regions surrounding a watershed are a important part of the historical evidence for a basin PMP estimate. Since most basin locations have a limited period of record and number of recording stations for rainfall data collected within the basin boundaries, the number of extreme storms that have been observed over the basin is often limited. This lack of data is especially prevalent for the Susitna River basin because of its remote location. To overcome this, storms that have been observed within similar meteorological and topographic regions are analyzed and adjusted to provide information describing the storm rainfall as if that storm had occurred over the basin being studied. Transfer of a storm from where it occurred to a location that is meteorologically and topographically similar is called storm transpositioning. The underlying assumption is that storms transposed to the basin could occur over the basin under similar meteorological conditions. To properly relocate such storms, it is necessary to address issues of similarity as they relate to meteorological conditions (moisture availability) and topography (difference in elevation and orographic influence) between the in-place storm location and the basin location.

Using ArcGIS, a gridded network was placed over the Susitna-Watana basin. The adopted grid cell resolution for this study is 0.025 x 0.025 decimal degrees in latitude and longitude (90 arc-seconds). The area of the grid cells varies with latitude, averaging approximately 1.4-square miles at the basin location. There are a total of 4,013 grid cells/ grid points within the domain. This universal grid provides a consistent template for the grid cell by grid cell analysis. Figure 6.1 shows the grid over the Susitna-Watana basin.

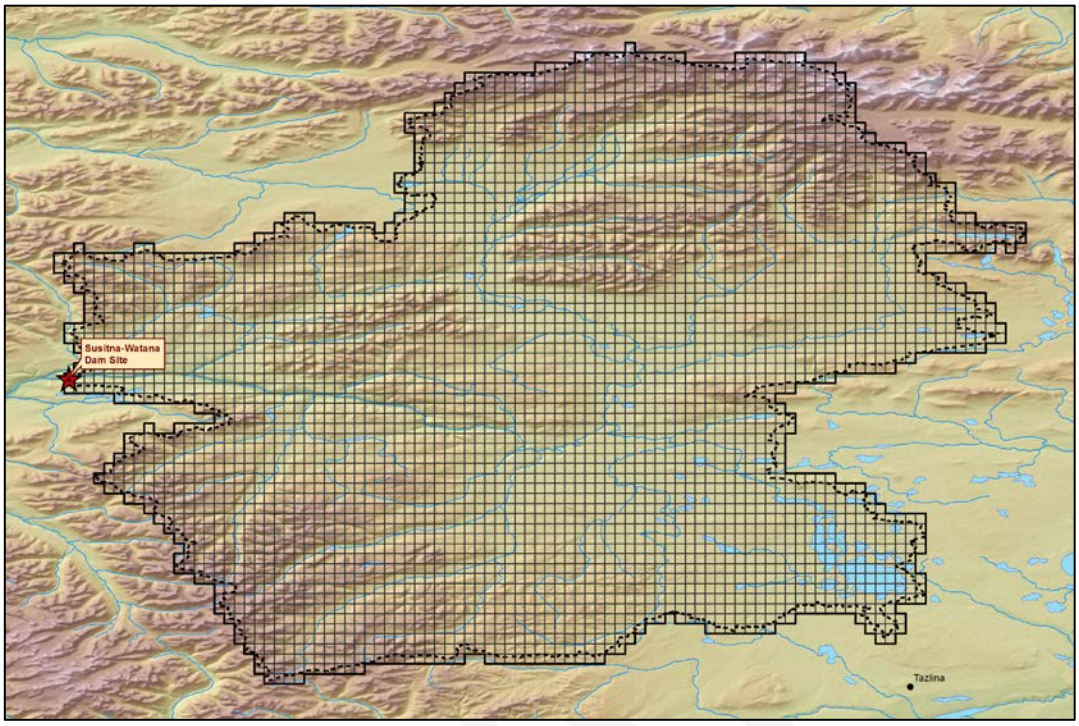

Figure 6.1. The universal 90 arc-second grid network placed over the Susitna-Watana drainage basin.

Each of the short list storms were transposed from the storm center location to each of the 4,013 grid points within the Susitna-Watana basin. The transposition process includes a moisture transposition component and an orographic transposition component. The moisture transposition component closely follows the procedures in HMR 57 and previous AWA studies. The orographic transposition process leverages the NOAA Atlas 14 (Perica et al. 2012) 10 to 1,000-year precipitation frequency values to quantify the differences in extreme rainfall between the historic storm centers and the basin, which is primarily a function of elevation and topography. For moisture transpositioning, only the horizontal difference in available moisture between the storm center and the basin grid points is explicitly accounted for. The vertical component, which accounts for the difference in elevation between the two locations, was not calculated as part of the storm (also called moisture) transposition factor. Instead, this component was accounted for in the derivation of the orographic transposition component: the rainfall values used to derive the ratio at the in-place similar area to the Susitna-Watana basin inherently have the elevation component incorporated. The transposition procedures are defined in the following sections.

6.1 Moisture Transposition

The general procedure for storm maximization has been discussed in Section 5. The same data sets used for maximum SSTs are used in the storm transpositioning procedure. The wind inflow vector connecting the storm location with the storm representative SST location was transpositioned to each grid point within the basin. Figure 6.2 shows an example of inflow vector transpositioning for

the August 1967, Fairbanks, AK storm center. The upwind end of the vector identifies the transposition maximum SST location. The value of the maximum SST at that location provided the transpositioned maximum SST value used to compute the transposition adjustment for relocating the storm to each grid point within the basin. The primary effect of storm transpositioning is to adjust storm rainfall amounts to account for enhanced or reduced atmospheric moisture made available to the storm at the transposed location versus the in-place storm location. The ratio of precipitable water due to available atmospheric moisture (as determined by the SST) at the basin target location to the in-place storm location is expressed as the moisture transposition factor (MTF). Figure 6.2 shows the august +2σ SST as a background grid. The SST grid resolution is 1° x 1° decimal degree; therefore a bilinear interpolation is used to extract the SST value at each grid point with a greater degree of precision.

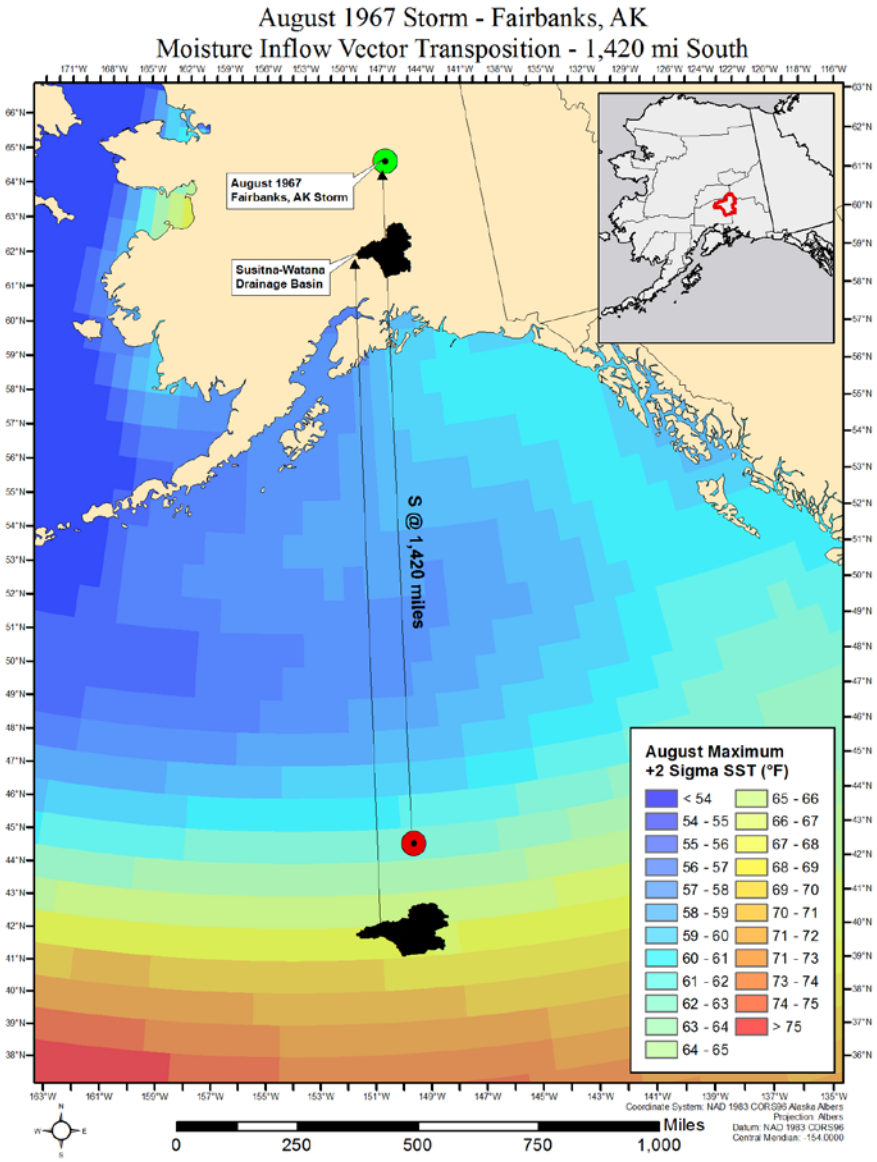

Figure 6.2. An example of inflow wind vector transpositioning for August 1967, Fairbanks storm. The storm representative SST location is ~1,420 miles south of the storm location.

6.2 Orographic Transposition

6.2.1 Topographic Effect on Rainfall

The terrain within the Susitna River basin and the surrounding region is complex, often over relatively short distances (Figure 6.3). When a basin has intervening elevated terrain features that deplete some of the atmospheric moisture available to storms before reaching a basin, these must be taken into account during the storm maximization process. Conversely, when a basin includes terrain which enhances the lift in the atmosphere and increases the conversion of moisture to liquid and ice particles, precipitation processes are enhanced. To account for the enhancements and

reductions of precipitation by terrain features, called orographic effects, explicit evaluations were performed using the OTF calculation. The OTF evaluation of the orographic effect in this study is significantly more objective and reproducible than the HMR procedure.

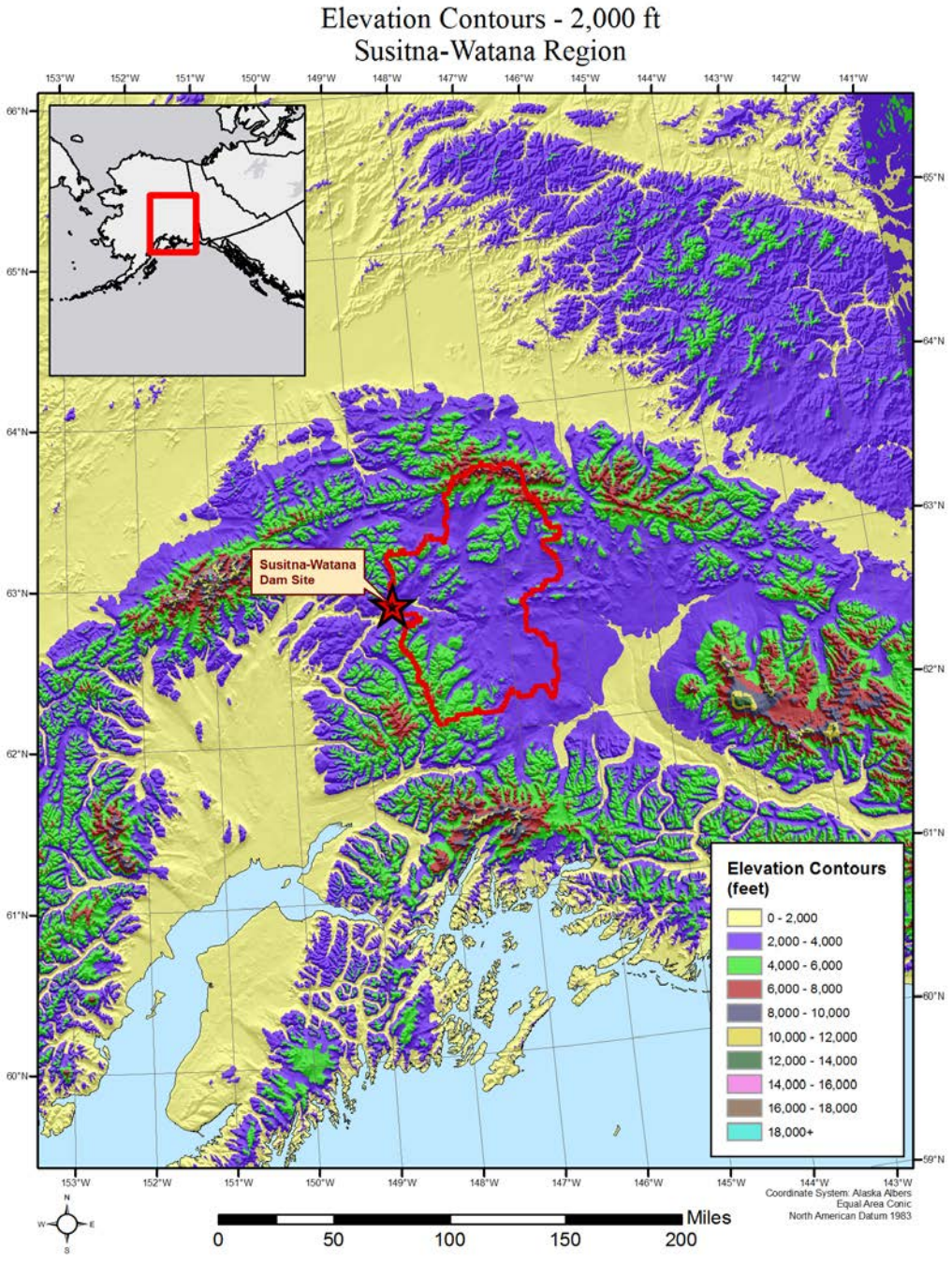

Figure 6.3 2,000-foot elevation contours over the Susitna-Watana region.

Orographic effects on rainfall are explicitly captured in the NOAA Atlas 14 precipitation frequency climatological analyses. Although the orographic effects at a particular location may vary from

storm to storm, the overall effect of the topographic influence is inherent in the climatology of storms that have occurred over various locations, assuming that the climatology is based on storms of the same type being analyzed. The NOAA Atlas 14 analysis should adequately reflect the differences in topographic influences at different locations at durations appropriate to the storm type in similar meteorological and topographical settings.

The procedure used in this study to account for orographic effects assesses the differences between the NOAA Atlas 14 data at the in-place storm location and each grid point within the Susitna-Watana basin. By evaluating the rainfall values for a range of return frequencies at both locations, a relationship between the two locations was established. For this study, precipitation frequency datasets developed as part of NOAA Atlas 14, Volume 7 (Perica et al. 2012) were used to evaluate the orographic effects. Figure 6.4 illustrates the 100-year 24-hour NOAA Atlas 14 precipitation coverage. The spatial distribution clearly exhibits the anchoring of the majority of rainfall to the coastal topography, particularly on the upwind side, while inland regions (such as the Susitna-Watana basin) are under a significant rain shadow effect and experience relatively low rainfall.

The NOAA Atlas 14 precipitation frequency estimates utilize data from the mean annual maximum grids developed using the Oregon State University Climate Group's PRISM system to help spatially distribute the values between data points. PRISM is a peer-reviewed modeling system that combines statistical and geospatial concepts to evaluate gridded rainfall with particular effectiveness in orographic areas (Daly et al. 1994, 1997). NOAA Atlas 14 precipitation frequency estimates implicitly express orographic controls through the adoption of the PRISM system. This study assumes the relationship between precipitation frequency values in areas of similar atmospheric characteristics reveal a quantifiable orographic effect and that terrain influence drives the variability in the relationship between NOAA Atlas 14 values at two distinct point locations.

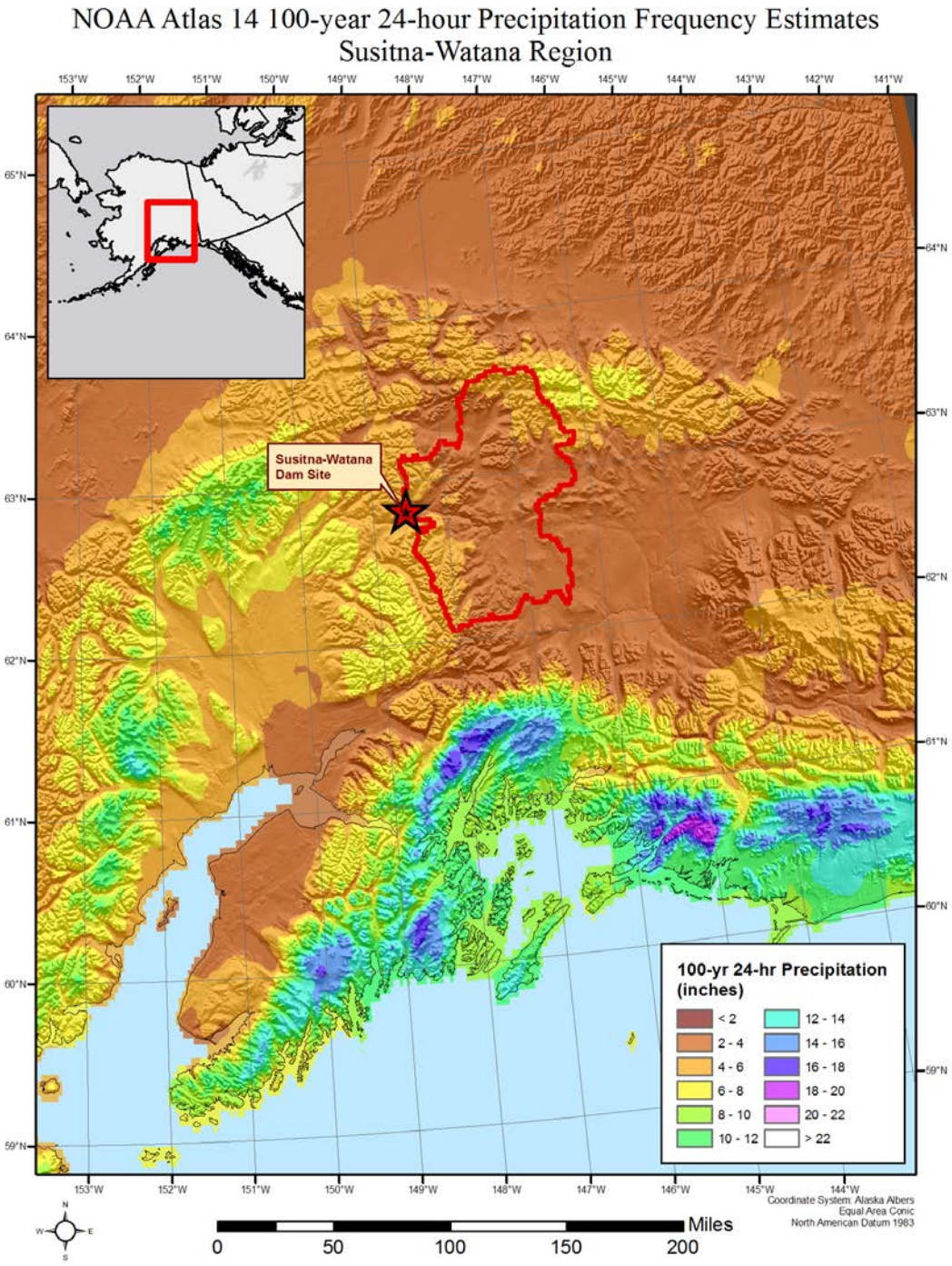

Figure 6.4. 100-year 24-hour NOAA Atlas 14 precipitation over the Susitna-Watana region.

6.2.2 Orographic Transpositioning Procedure

The orographically adjusted rainfall values for a given storm at a target location (grid cell) within the basin are calculated by applying a coefficient of proportionality, determined by the relationship between a NOAA Atlas 14 data series at the source storm location and the corresponding NOAA Atlas 14 values at the target location. For the transposition of a single grid cell at a given duration, the orographic relationship is defined as the linear relationship between the NOAA Atlas 14 values, at that duration, over a range of recurrence intervals. This study evaluates the trend of precipitation frequency estimates through the 10-, 25-, 50-, 100-, 200-, 500-, and 1,000-year average recurrence intervals. The relationship between the target and the source can be expressed as a linear function with P_o as the independent variable and P_i as the dependent variable as shown in Equation 6.1.

$$P_o = mP_i + b \qquad \text{Equation 6.1}$$

where,

P_o	=	orographically adjusted rainfall (target)
P_i	=	in-place rainfall (source)
m	=	proportionality coefficient (slope)
b	=	transposition offset (y-intercept)

Equation 6.1 provides the orographically transpositioned rainfall depth, as a function of the in-place rainfall depth. The in-place rainfall depth used to calculate the orographically transpositioned rainfall use NOAA Atlas 14 values. The 24-hour duration is appropriate for all storms in the short list. To express the orographic effect as a ratio, or OTF, the orographically adjusted rainfall (P_o) is divided by the original source in-place rainfall depth (P_i). It is assumed the orographic effect for a given transposition scenario will remain constant over the durations analyzed. Therefore, the 24-hour OTF is valid for any other duration a storm.

The orographic relationship can be visualized by plotting the average NOAA Atlas 14 depths for the grid point at the source location on the *x*-axis and the NOAA Atlas 14 depths for the grid point at the target location on the *y*-axis, then drawing a best-fit linear trend line among the seven return frequency value points. The trend line describes the general relationship between the NOAA Atlas 14 values at the grid location and the values at the storm location. As an alternative to producing the best-fit linear trendline graphically, linear regression can be used to apply the function mathematically. The mathematical method was applied, in Excel spreadsheets, to efficiently calculate the OTF for each of the basin grid points, for each storm. An example of the determination of the orographic relationship and development of the OTF is given in Section 7.3.

7. PMP CALCULATION PROCEDURES

PMP depths were calculated by comparing the total adjusted rainfall values for all transpositionable storm events for each grid point and taking the largest value, a process comparable to the envelopment of all transpositionable events. In this case, envelopment occurs because the largest PMP depth for a given duration is derived after analyzing all storms for each grid point location, for each duration, over the Susitna-Watana basin.

The adjusted rainfall at a grid point, for a given storm event, was determined by applying a Total Adjustment Factor (TAF) to the SPAS analyzed rainfall depth value corresponding to the basin area size of 5,131 mi^2, at each analyzed duration. The TAF is the product of the three separate storm adjustment factors, the IPMF, the MTF, and the OTF. In-place maximization and moisture transposition are described in Section 6.1. Orographic transposition is described in Section 6.2. These calculations were completed for all transpositionable storm centers, for each of the 4,013 basin grid cells.

An Excel storm adjustment spreadsheet was produced for each of the transpositionable storm centers. These spreadsheets are designed to perform the initial calculation of each of the three adjustment factors, along with the final TAF. The spreadsheet format allows for the large number of data calculations to be performed correctly and consistently in an efficient template format. Information such as the basin NOAA Atlas 14 data, coordinate pairs, grid point elevation values, equations, and the precipitable water lookup table remain constant from storm to storm and remain static within the spreadsheet template. The spreadsheet contains a final adjusted rainfall tab with the adjustment factors, including the TAF, listed for each grid point. A table holding the TAF for each basin grid point was exported to a GIS feature class for each storm. A Python-language scripted GIS tool receives the storm TAF feature classes and the corresponding DAD tables for each of the 13 SPAS DAD zones as input, along with a basin outline feature layer as a model parameter. The tool then calculates and compares the total adjusted rainfall at each grid point within the basin and determines the PMP depth at each duration up to 216-hours. The tool produces gridded PMP datasets for each duration and a point shapefile holding PMP values for all durations.

The following sections describe the procedure for calculating the IPMF, the MTF, the OTF, and the TAF for the creation of the storm adjustment feature classes. The August 1967, Fairbanks, AK event controls PMP at each duration. Examples of calculations using the data from this storm are provided.

7.1 In-Place Maximization Factor

In-place storm maximization is applied to each storm event using the methodology described above. Storm maximization is quantified by applying the IPMF, calculated using Equation 7.2.

$$IPMF = \frac{W_{p,max}}{W_{p,rep}}$$ Equation 7.2

where,

$W_{(p,max)}$ = precipitable water for the maximum +2σ monthly SST
$W_{(p,rep)}$ = precipitable water for the representative SST

EXAMPLE:

Using the storm representative SST temperature and storm center elevation as input, the precipitable water lookup table returns the depth, in inches, used in Equation 7.2. The storm representative SST is 61.0 °F, calculated using the procedures described in Section 5. The storm center elevation is approximated at 7,500 feet at the storm center of 65.52 N, 147.33 W. The storm representative precipitable water value (*Wp, rep*) is calculated:

$$W_{p,rep} = W(@60.0°)_{p,30,000'} - W(@60.0°)_{p,7,500'}$$

$$W_{p,rep} = 1.45" - 0.89"$$

$$\boldsymbol{W_{p,rep} = 0.560"}$$

The temporal transposition date for the August 1967, Fairbanks event is August 15th, therefore the August +2σ SST climatology is appropriate for use to determine the maximum precipitable water. The August climatological maximum +2σ SST at the upwind storm representative location is 62.5°F. The storm location climatological maximum available moisture at the storm in-place elevation of 7,500' ($W_{p,\,max}$) is calculated:

$$W_{p,max} = W(@62.5°)_{p,30,000'} - W(@62.5°)_{p,7,500'}$$

$$W_{p,max} = 1.56" - 0.945$$

$$\boldsymbol{W_{p,max} = 0.615"}$$

The ratio of climatological maximum moisture ($W_{p,max}$) to the in-place storm representative moisture ($W_{p,rep}$) yields the in-place maximization factor using Equation 7.2:

$$IPMF = \frac{0.615}{0.560}$$

$$\boldsymbol{IPMF = 1.10}$$

7.2 Moisture Transposition Factor

The change in available atmospheric moisture between the storm center location and the basin target grid point is quantified using the MTF. This MTF represents the change in available atmospheric moisture due to horizontal distance only and is calculated at the storm center elevation. The change in atmospheric moisture due to vertical displacement is quantified in the OTF, described in the next section. The MTF is calculated as the ratio of moisture for the climatological maximum SST at the target grid cell location to the moisture for the climatological maximum SST at the storm center elevation.

$$MTF = \frac{W_{p,trans}}{W_{p,max}}$$ Equation 7.3

where,

$W_{(p,trans)}$ = maximum precipitable water at the basin grid cell

$W_{(p,max)}$ = maximum precipitable water at the storm center location

EXAMPLE:

The transpositioned climatological maximum available moisture must be determined for each target grid point within the basin domain. There are 4,013 grid cells within the basin domain. Only the first grid cell #1, at 62.075° N, 148.050° W (in the southwest corner of the basin), is discussed in this example. The August climatological maximum SST temperature, at the moisture inflow vector upwind from grid point #1 is 69.0°F. The precipitable water for this SST is adjusted to the in-place storm center elevation of 7,500 feet[4]. The horizontally transpositioned climatological maximum available moisture ($W_{p,\,trans}$) is calculated.

$$W_{p,trans} = W(@69.0°)_{p,30,000'} - W(@69.0°)_{p,7,500'}$$

$$W_{p,trans} = 2.14" - 1.21"$$

$$\boldsymbol{W_{p,trans} = 0.930"}$$

The storm location climatological maximum available moisture ($W_{p,\,max}$) was calculated above for the IPMF:

$$\boldsymbol{W_{p,max} = 0.615"}$$

[4] Note: Although the elevation at grid point #1 is at 6,500 feet, the elevation of the storm center is used to remove the vertical component of the moisture transposition which will be included in the orographic transposition factor.

The MTF is calculated as the ratio of moisture for the climatological maximum SST for the grid cell location ($W_{p,\ trans}$) to the moisture for the climatological maximum SST for the storm center location ($W_{p,\ max}$), from Equation 7.3:

$$MTF = \frac{0.930}{0.615}$$

$$\boldsymbol{MTF = 1.51}$$

7.3 Orographic Transposition Factor

Section 6.2 provides detail on the methods used in this study to define the orographic effect on rainfall. The OTF is calculated by taking the ratio of orographically affected rainfall at the storm in-place location to orographically affected rainfall at the basin grid cell location.

$$OTF = \frac{P_o}{P_i}$$ Equation 7.4

where,

P_o = orographically adjusted rainfall (target)
P_i = SPAS-analyzed in-place rainfall

The orographically adjusted rainfall is determined by applying Equation 7.5 to the SPAS-analyzed rainfall depth. The 24-hour duration was used for P_i to be consistent with the 24-hour duration of the precipitation frequency datasets.

$$P_o = mP_i + b$$ Equation 7.5 (from Equation 6.1)

where,

P_o = orographically adjusted rainfall (target)
P_i = SPAS-analyzed in-place rainfall
m = proportionality coefficient (slope)
b = proportionality variation offset (y-intercept)

EXAMPLE:

Table 7.1 gives an example using NOAA Atlas 14 24-hour values (in inches) at both the storm center grid cell location (source) and a basin grid cell location (target) used to determine the orographic relationship.

Table 7.1. 24-hour NOAA Atlas 14 Precipitation Frequency values at the storm center (source) and grid cell #1 (target) locations.

	10 year	25 year	50 year	100 year	200 year	500 year	1000 year
SOURCE (X-axis)	3.05	3.73	4.27	4.85	5.46	6.32	7.02
TARGET (Y-axis)	2.99	3.65	4.17	4.71	5.28	6.07	6.70

When the NOAA Atlas 14 values are plotted, a best fit trendline can be constructed to provide a visualization of the relationship between the NOAA Atlas 14 values at the source and target locations (Figure 7.1). In this example, the values for the source grid point nearest the Fairbanks, AK (August 1967) storm center are plotted on the *x*-axis while the target values for the first grid point in basin are plotted on the *y*-axis.

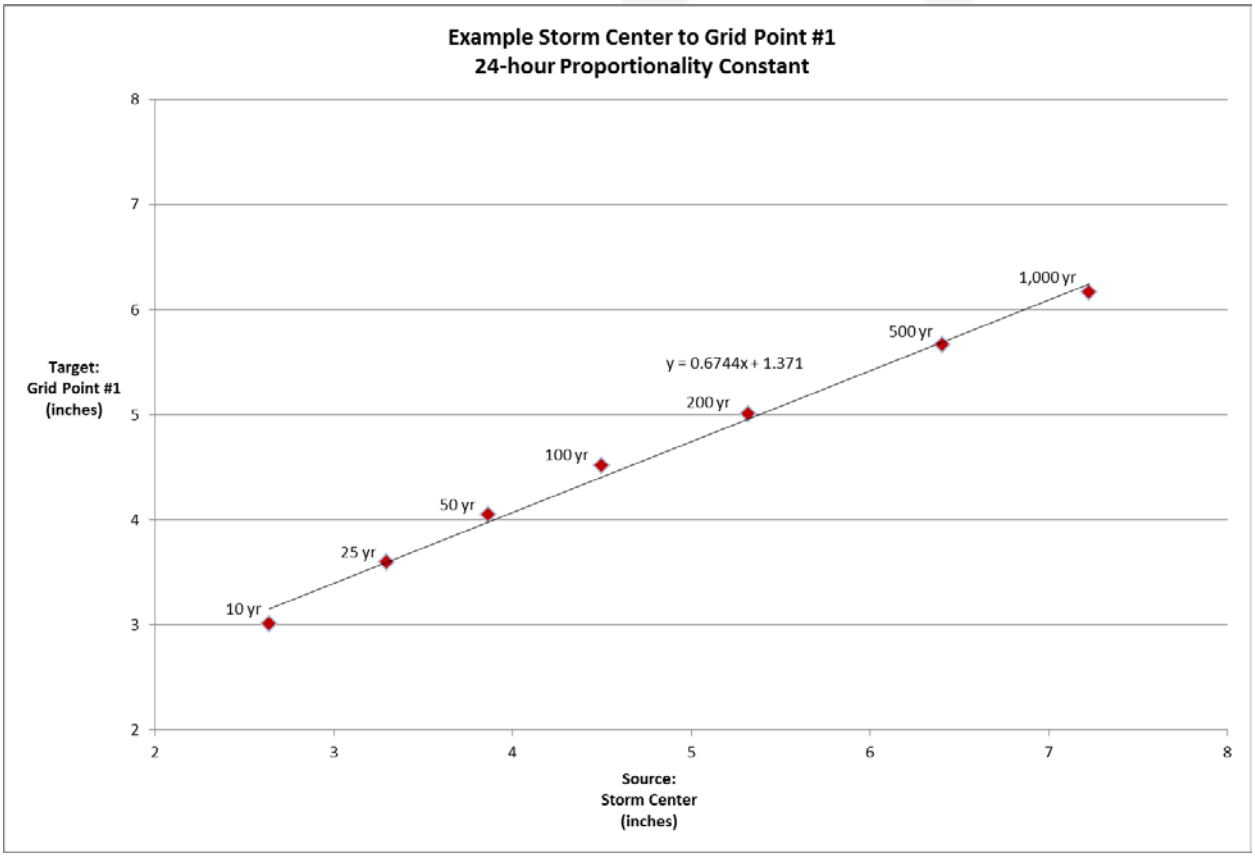

Figure 7.1. Example of NOAA Atlas 14 proportionality between the Fairbanks, 1967 DAD Zone 1 storm center and the Susitna River basin grid cell #1.

The orographically adjusted rainfall at the target location can be determined using the equation of the best fit trendline in slope-intercept form. This linear trendline equation corresponds to equation 7.5.

The slope, *m* is the proportionality coefficient, representing the direct relationship between the source and target cells. The *y*-intercept, *b*, is used to correct for variability in the precipitation frequency estimate recurrence intervals between the source and target locations. The equation for the SPAS 1270_1 24-hour orographically adjusted rainfall transpositioned to grid point #1, based on the linear trendline in Figure 7.5 is:

$$P_o = 0.6744m + 1.371$$

The maximum SPAS analyzed 24-hour point rainfall value of 5.36" is entered as the *Po* value to estimate the target *y*-value, or orographically adjusted rainfall (P_o) of 4.99".

$$P_o = 0.6744(5.36") + 1.371"$$

$$\boldsymbol{P_o = 4.99"}$$

The ratio of the orographically adjusted rainfall (P_o) to the in-place SPAS analyzed 24-hour rainfall (P_i) yields the orographic transposition factor (OTF).

$$OTF = \frac{4.99"}{5.36"}$$

$$\boldsymbol{OTF = 0.93}$$

The OTF to grid cell #1 of the basin is 0.93, or a 7% rainfall reduction from the storm center location due to terrain effects. The OTF is then considered to be a temporal constant for the spatial transposition between that specific source/target grid point pair, for that storm only, and can then be applied to the other durations for the given storm.

7.4 Total Adjusted Rainfall

The TAF is a product of the linear multiplication of the IPMF, MTF, and OTF. The TAF is a combination of the total moisture and terrain influences on the SPAS analyzed rainfall when maximized and transpositioned to the target grid cell.

$$TAF = IPMF * MTF * OTF \qquad \text{Equation 7.7}$$

EXAMPLE:

For grid point #1, the TAF is calculated as shown in Equation 7.7 using the IPMF from Section 7.1, the MTF from Section 7.2, and the OTF from Section 7.3:

$$TAF = 1.10 * 1.51 * 0.93$$

$$TAF = 1.54$$

To calculate the total adjusted rainfall, the TAF is applied to the SPAS analyzed rainfall depth at the basin area size (5,131 mi^2). For the Fairbanks, AK event, the 216-hour SPAS analyzed rainfall depth at the basin size is 8.52". Therefore, the total adjusted rainfall for this storm at grid point #1 is:

$$Total\ Adj.Rainfall_{216-hr} = TAF * Rainfall_{216-hr}$$

$$Total\ Adj.Rainfall_{216-hr} = 1.54 * 8.52"$$

$$Total\ Adj.Rainfall_{216-hr} = 13.12"$$

7.5 Gridded PMP Calculation and Envelopment

The total adjusted rainfall values are computed for each of the 4,013 grid cells in the basin. These calculations are made for a series of index durations sufficient to provide a framework for the temporal distribution of PMP over the basin through a 9-day period. For this study, the index durations are 1-, 6-, 12-, 24-, 48-, 72-, 96-, 120-, 144-, 168-, 192-, and 216-hour durations.

Once the total adjusted rainfall values have been calculated for each of the basin grid cells, the process is repeated for each SPAS DAD zone on the short list. Then the total adjusted rainfall values for all storms at a given grid point are compared and the largest becomes the PMP. When this comparison is made at a grid by grid basis for all storms, the result is an envelopment of adjusted rainfall values. The PMP at each grid point will be derived from whichever storm, after maximization and transposition, produces the largest rainfall. After the total adjusted rainfall had been calculated for all grid points in the basin, for all storms, the Fairbanks, AK event of August 1967 produced the largest depths, at all durations.

The resulting gridded PMP values for each index duration are contained within GIS files in both raster and vector (point) datasets. Due to the large amounts of calculations needed to create the PMP grids, a scripted ArcGIS tool was created using the Python language. The tool performs the following tasks:

1) Calculates the basin size
2) Looks up the SPAS analyzed rainfall depths at the basin size
3) Applies the rainfall depths to the total adjusted rainfall factor for each storm
4) Compares the adjusted rainfall values for all storms to get PMP
5) Outputs the PMP to GIS files
6) Repeats the process for each duration

8. SPATIAL AND TEMPORAL DISTRIBUTION OF PMP

8.1 Spatial Distribution

The spatial distribution of the Susitna-Watana PMP is dependent on a combination of the variation of the gridded OTF and MTF values over the basin. Therefore, the spatial distribution is largely dependent on variation in terrain, which is represented by the 10- through 1,000-year 24-hour NOAA Atlas 14 precipitation frequency spatial distribution over the basin, and to a lesser extent, variation in moisture which is controlled by the gradient of sea surface temperatures at the source location for the controlling storm event.

The variation in available moisture is a smooth gradient with larger values at the southern end of the basin transitioning to smaller values at the northern end. A map of the MTF over the basin (Figure 8.1) illustrates the distribution due to moisture.

As discussed in Section 6.2.1, the topography of the basin and surrounding region is dynamic and varies greatly over the surface of the basin. Therefore, it is expected that the effect of mountainous terrain would be the defining factor in the spatial distribution. The variation of rainfall due to orography, as a result of slope, elevation, and rain shadow effect is inherently represented in the OTF due to it being a function of the NOAA Atlas 14 precipitation frequency relationship between each grid point in the basin and a constant location at the storm center. A map of the OTF over the basin (Figure 8.2) illustrates the spatial distribution due to terrain.

The spatial distribution pattern, due to the variation in terrain and moisture is apparent in the gridded basin PMP maps. Figures 8.3a, 8.3b, and 8.3c show the basin 24-hour, 72-hour, and 216-hour PMP, respectively.

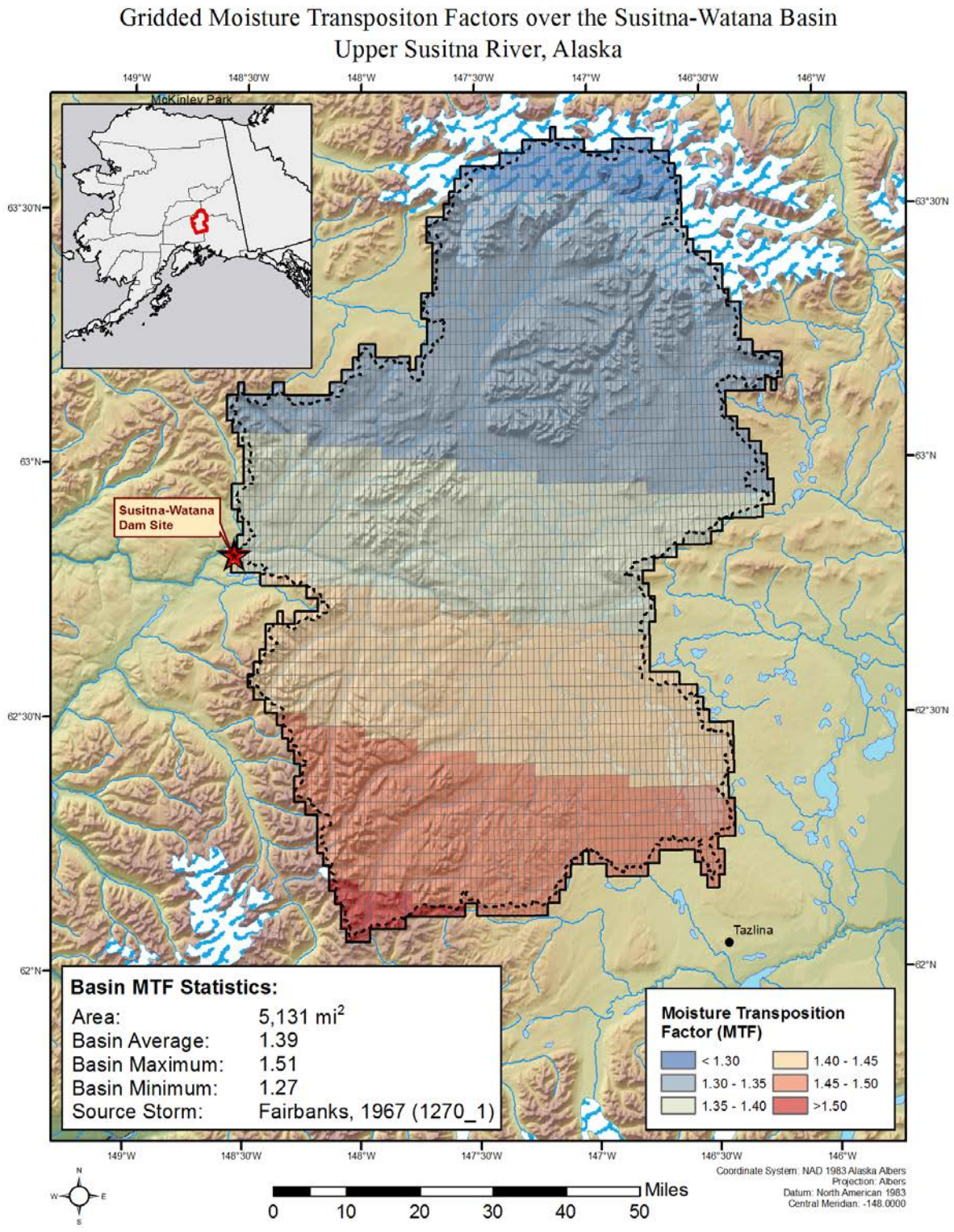

Figure 8.1. Moisture Transposition Factors over the basin.

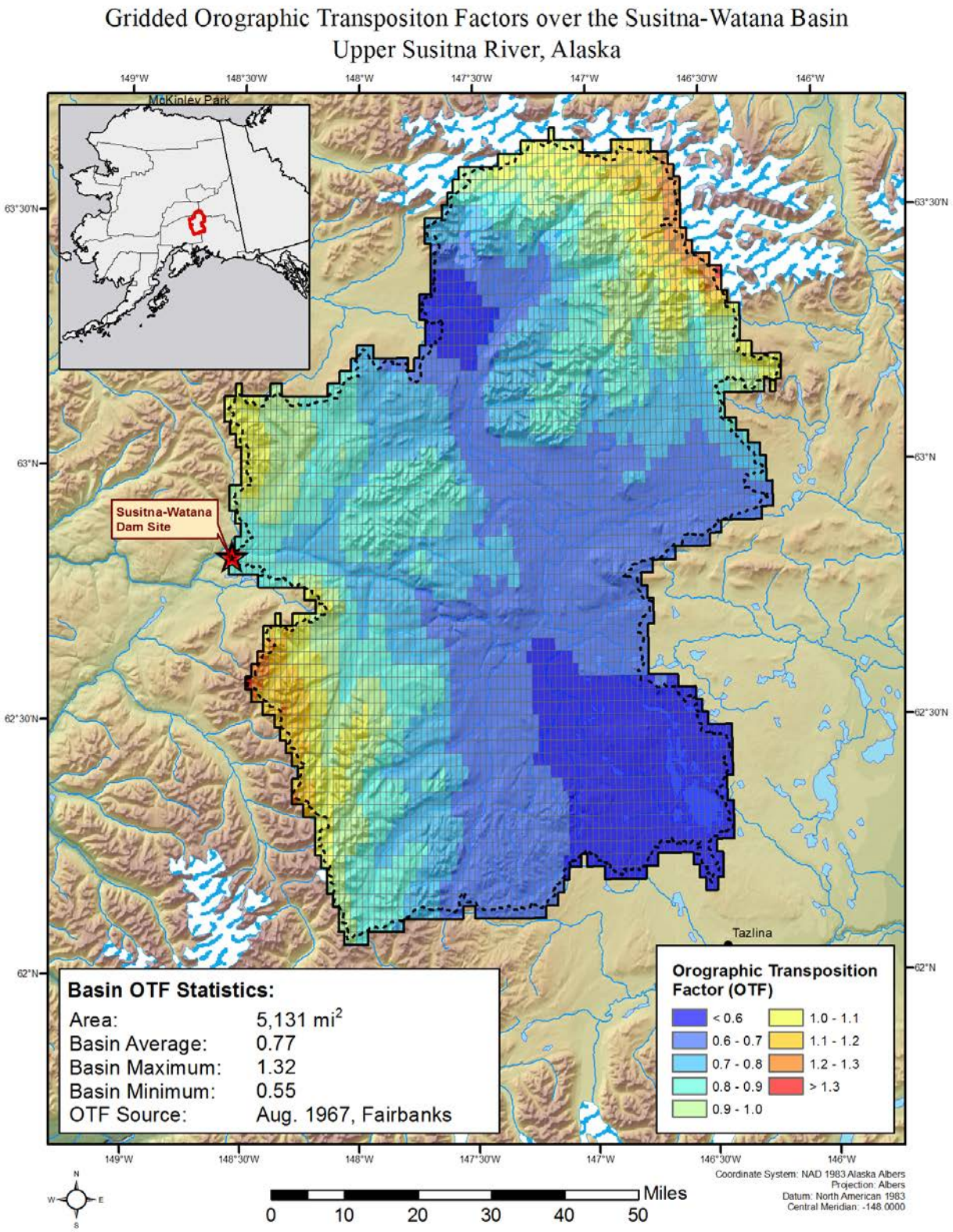

Figure 8.2. Orographic Transposition Factors over the basin

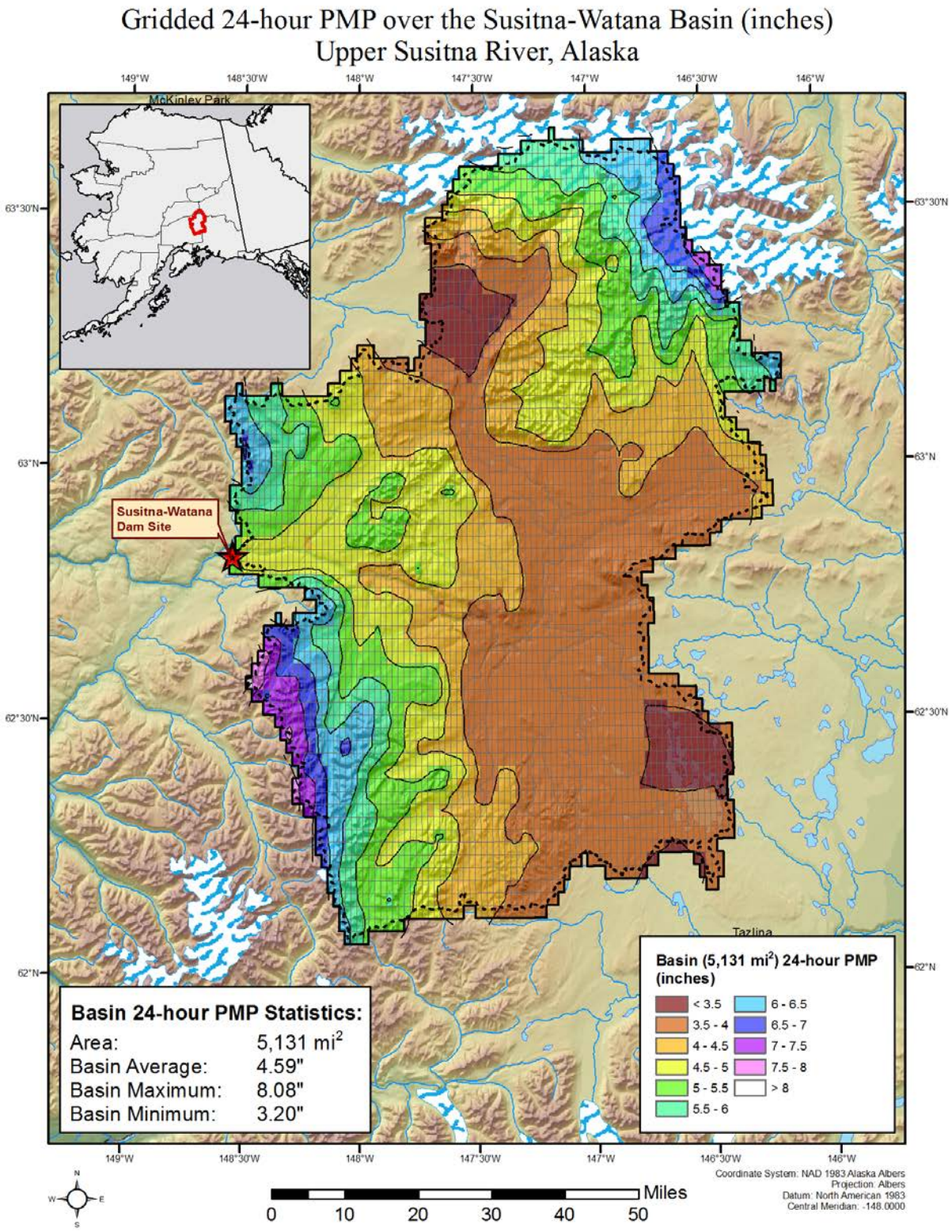

Figure 8.3a. Susitna River basin 24-hour gridded PMP.

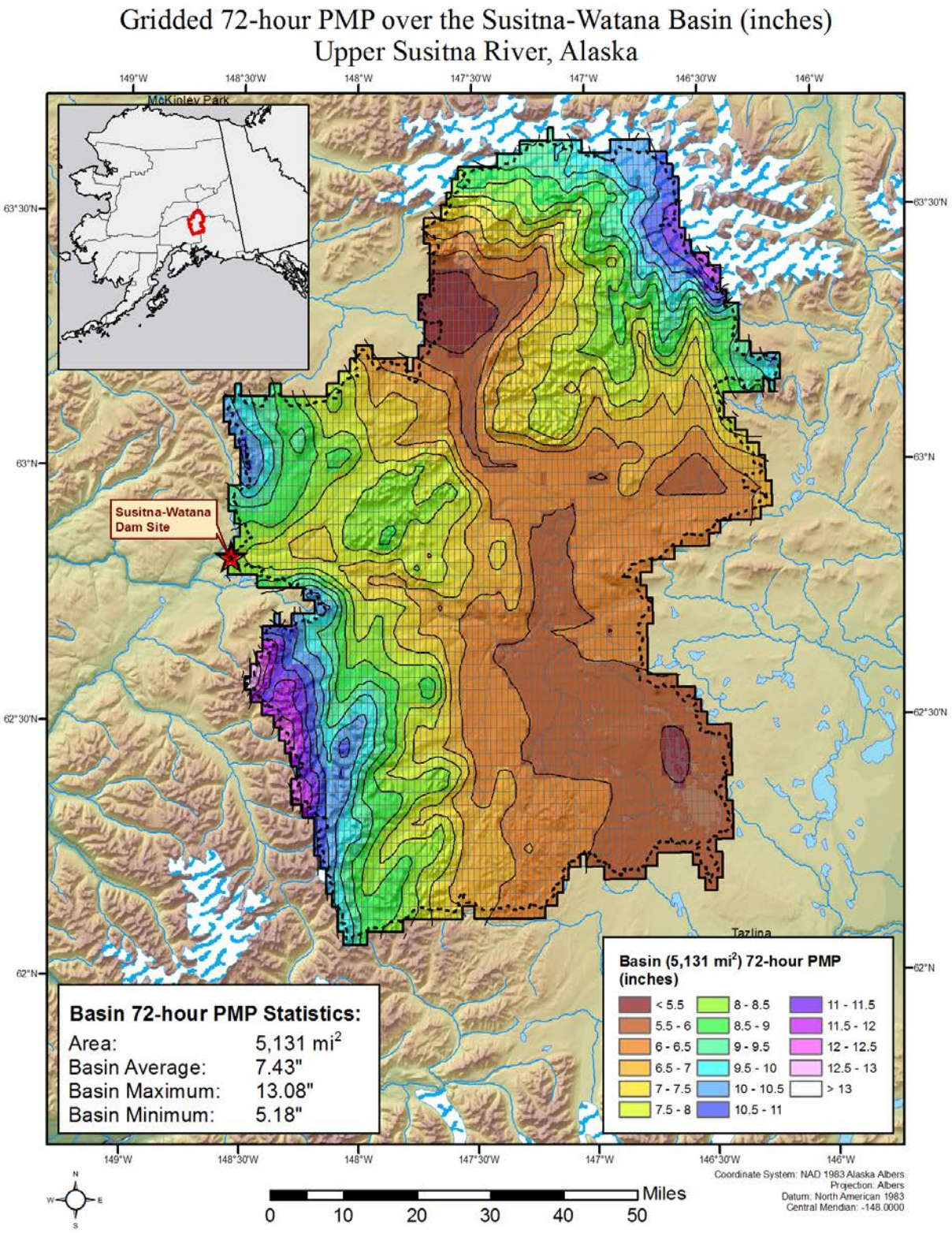

Figure 8.3b. Susitna River basin 72-hour gridded PMP.

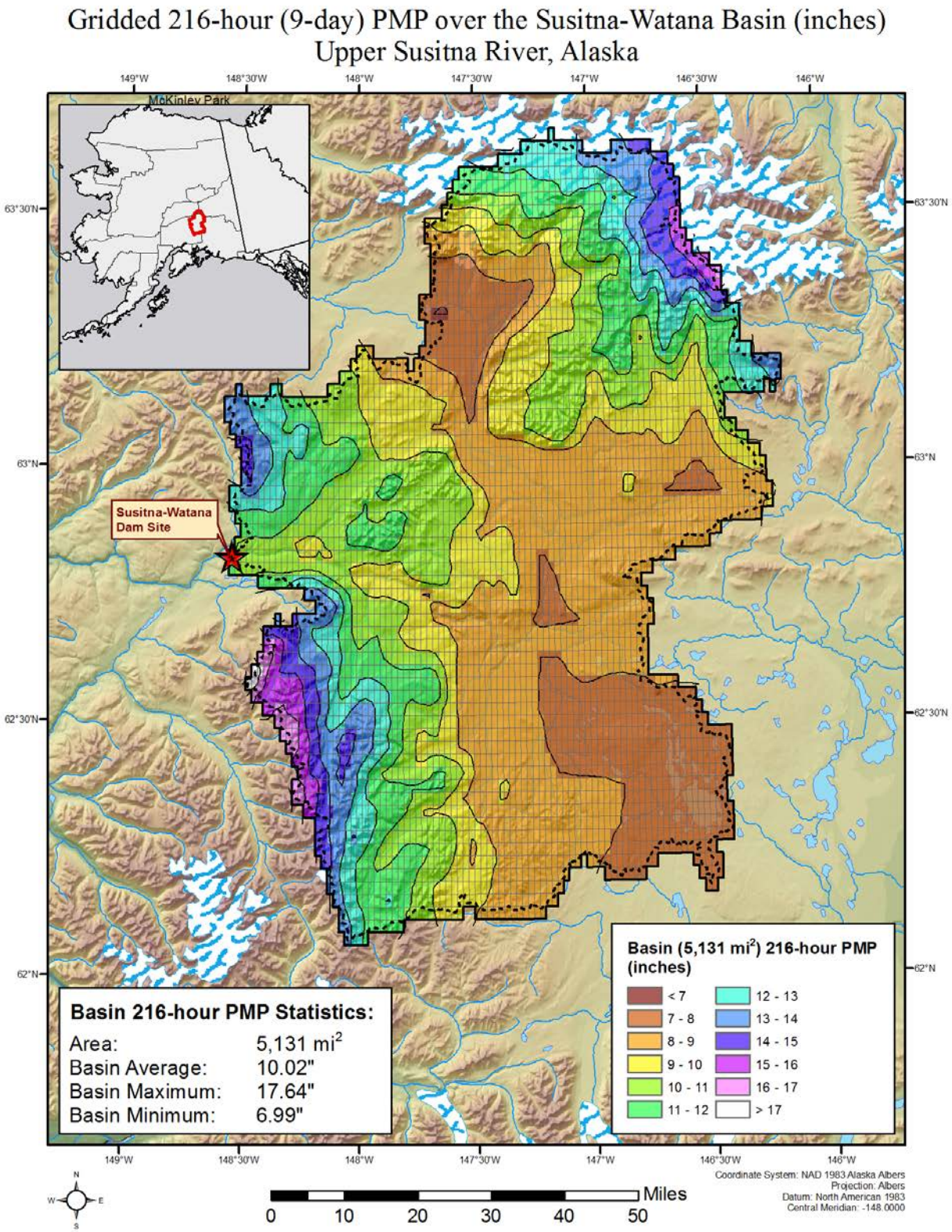

Figure 8.3c. Susitna River basin 216-hour gridded PMP.

8.2 Temporal Distribution

Hourly accumulated PMP depths for each grid point were determined by plotting the basin average PMP values, for each index duration, on a graph. A smooth curve was drawn through each index duration, 1-hour through 216-hour. Using this curve, the PMP accumulations at each hourly interval were estimated. The hourly incremental PMP values could then be calculated from the accumulated PMP values. This process follows the general procedure outlined in HMR 57, however, here it has been scaled up to 1-hour (instead of 6-hour intervals), and extends to a total duration of 216-hour (instead of 72-hours).

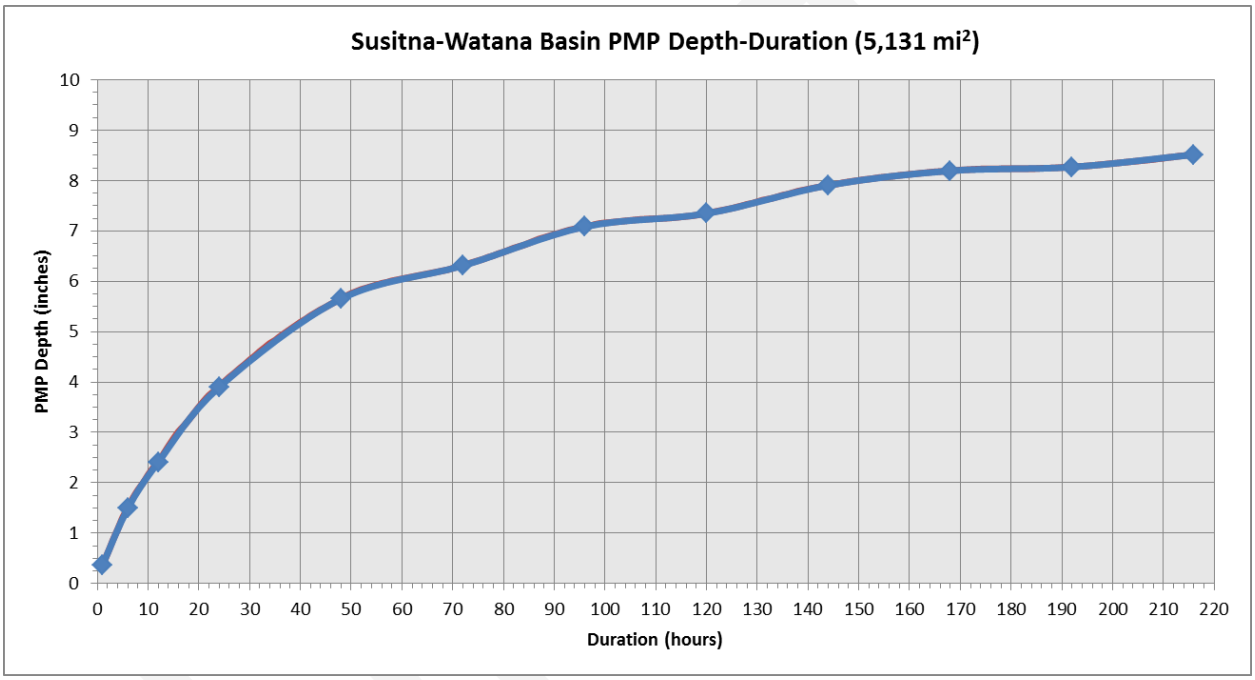

Figure 8.4. Depth-Duration PMP curve used to interpolate accumulated PMP at hourly intervals.

To temporally distribute the gridded PMP values, the incremental depths are re-ordered to mirror the mass curve of three separate storm events: August 1955, Denali N.P. (SPAS 1272) DAD zone 1; August 1967, Fairbanks (SPAS 1270) DAD zone 1; and August 2012, Old Tyonek (SPAS 1256) DAD zone 1.

The temporal distribution pattern for August 1955, Denali N.P. (SPAS 1272) DAD zone 1 applied to the total basin average PMP is shown in Figure 8.5.

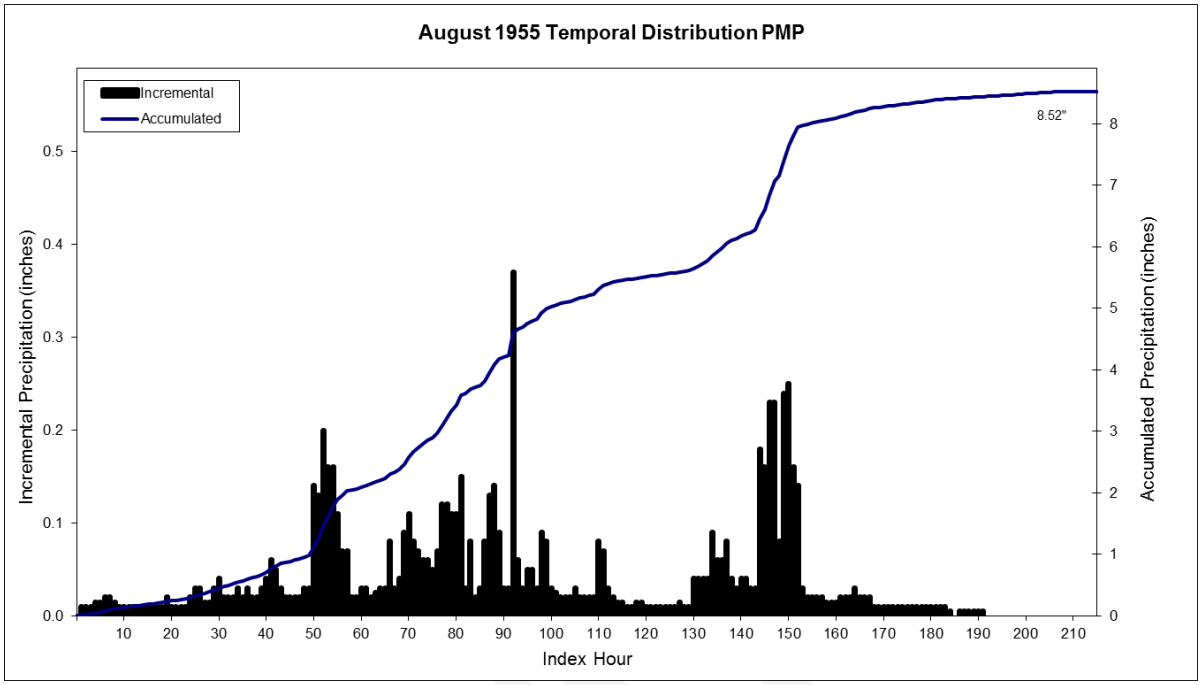

Figure 8.5. August 1955, Denali NP mass curve pattern used for the temporal distribution of the Susitna-Watana PMP.

The temporal distribution pattern for August 1967, Fairbanks (SPAS 1270) DAD zone 1 as applied to the total basin average PMP is shown in Figure 8.6.

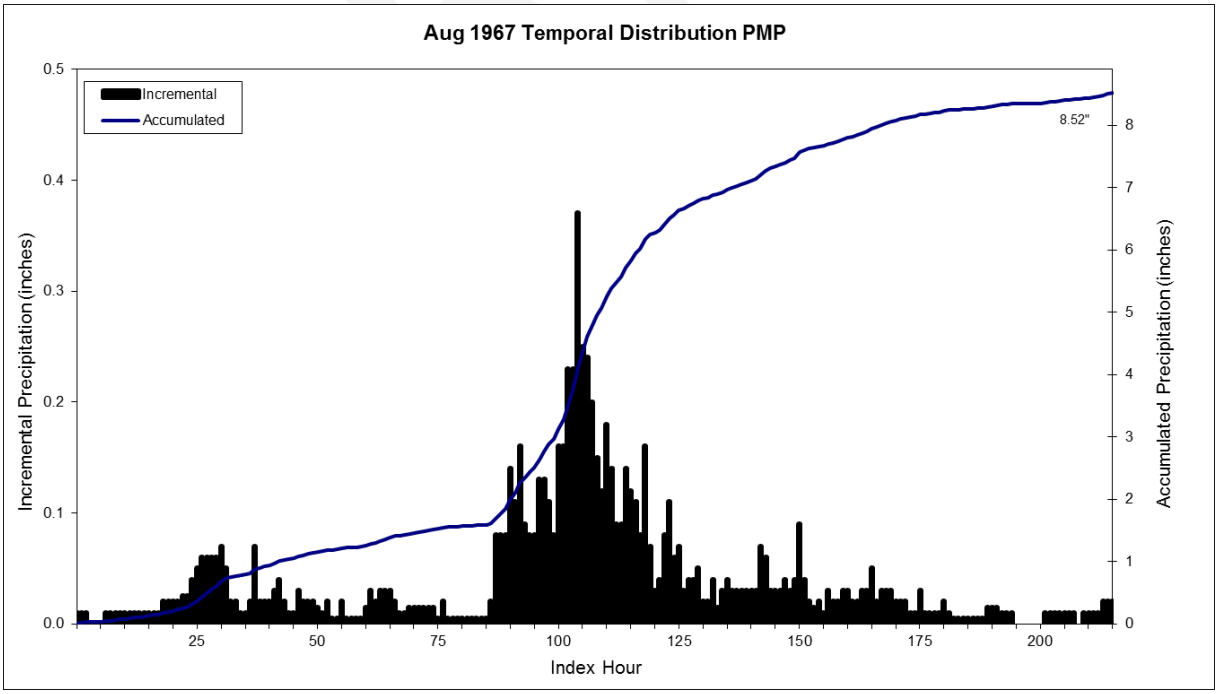

Figure 8.6. August 1967, Fairbanks storm zone 1 mass curve pattern used for the temporal distribution of the Susitna-Watana PMP.

The temporal distribution pattern for August 2012, Old Tyonek (SPAS 1256) DAD zone 1 as applied to the total basin average PMP is shown in Figure 8.7.

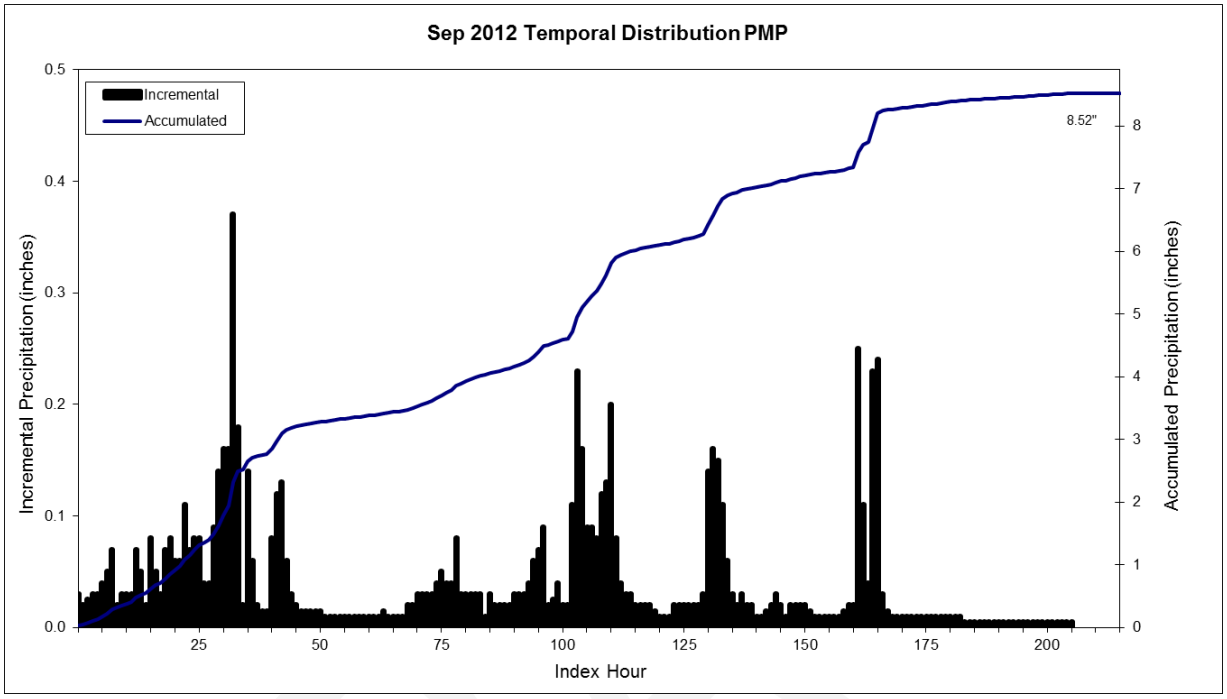

Figure 8.7. August 2012, Old Tyonek storm mass curve pattern used for the temporal distribution of the Susitna-Watana PMP.

9. PMP METEOROLOGICAL TIME SERIES DEVELOPMENT

Hourly meteorological time series were developed for the six calibration events (see Table 12.2.1), over the Susitna River basin in order to aid the hydrologic modeling to best represent expected conditions that would be associated with the PMP rainfall. Meteorological time series parameters have been derived for temperature, dew point temperature and wind speed over the Susitna-Watana basin. The hydrologic model requirements are a single temperature and dew point temperature time series at a given base elevation and wind speed at 1,000-foot increments from 0-feet to 15,000-feet. Temperature lapse rates were estimated using observed surface temperature data for stations in and around the Susitna-Watana basin and Fairbanks radiosonde data.

Vertical wind speed profiles at 1,000-feet increments were derived base on wind speed data from the Fairbanks radiosonde and observed surface wind speed data for stations in and around the Susitna-Watana basin. The radiosonde wind speeds represents free atmospheric winds (unobstructed flow). This free-air data were adjusted to surface wind speeds based on comparisons of anemometer level wind speeds with concurrent free-air wind speeds. The wind speed derivation methodology was based on methods described in HMR 42 (Weather Bureau 1966). HMR 42 measured winds at Gulkana glacier (4,800 feet) and compared to free-air winds at Fairbanks, the study found that average winds on the glacier was 0.60 that of the free-air. In this updated analysis, comparisons were made using both Anchorage and Fairbanks radiosonde data. This analysis showed the Anchorage radiosonde data were not as representative of the surface wind speeds over the basin based on comparisons made to the September 2012 storm event. Instead, the Fairbanks data better represented the timing and magnitude of the observed surface wind speeds.

All six storms were normalized to have a similar index period of 312-hours (see Figure 9.1). For each storm, the index time of the maximum 216-hour accumulated precipitation was determined, this represents the PMP rainfall accumulation window. Then, the 216-hour mid-point was determined by shifting the maximum 216-hour accumulated precipitation index hour 108-hours earlier. Finally, the 108-hour mid-point was used to determine the start and end times of the 216-hour PMP analysis window. The 312-hour window was completed with 24-hours added at the beginning and 72-hours added at the end of the 216-hour PMP window. Hourly temperatures, dew point temperatures, and vertical wind speeds were derived for each of these events for the 312-hour time frame. Figure 9.2 shows the indexed temperature and dew point temperature for the six storm events (base elevation of 2,500 feet).

Once the proper 312-hour window was identified for each of the six storm events, the 312-hour time series data were grouped by month (i.e. all June events grouped together, all August events grouped, and all September events grouped together). For each monthly grouping, an average time series was created based on averaging the individual hourly station meteorological data. Since the

all-season PMP event is more conducive to the rainfall associated with the September and August storm events, an average time series was created based on averaging the September and August storm events time series values. The monthly averaged temperature and dew point temperature profiles for June, August, September and average August/September events are shown in Figure 9.3. The final temperature, dew point temperature and wind speed information were based on the average profiles for August/September (Figure 9.4 and 9.5).

The averaged September and August meteorological time series was selected because it best represents the expected conditions that would be associated with the PMP rainfall. The final PMP temperature and dew point temperature have a base elevation of 2500-ft, the lapse rate used to adjust PMP temperature and dew point temperature to other elevations was -2.63°F per 1,000 feet. The -2.63°F lapse rate was based on the average of all August (1967 and 1971) and September (2012) storm event lapse rates (-2.87°F, -2.85°F, -2.70°F = 2.63°F).

The final vertical wind speed values were based on the average of all August (1967 and 1971) and September (2012) storm events anemometer height wind speeds.

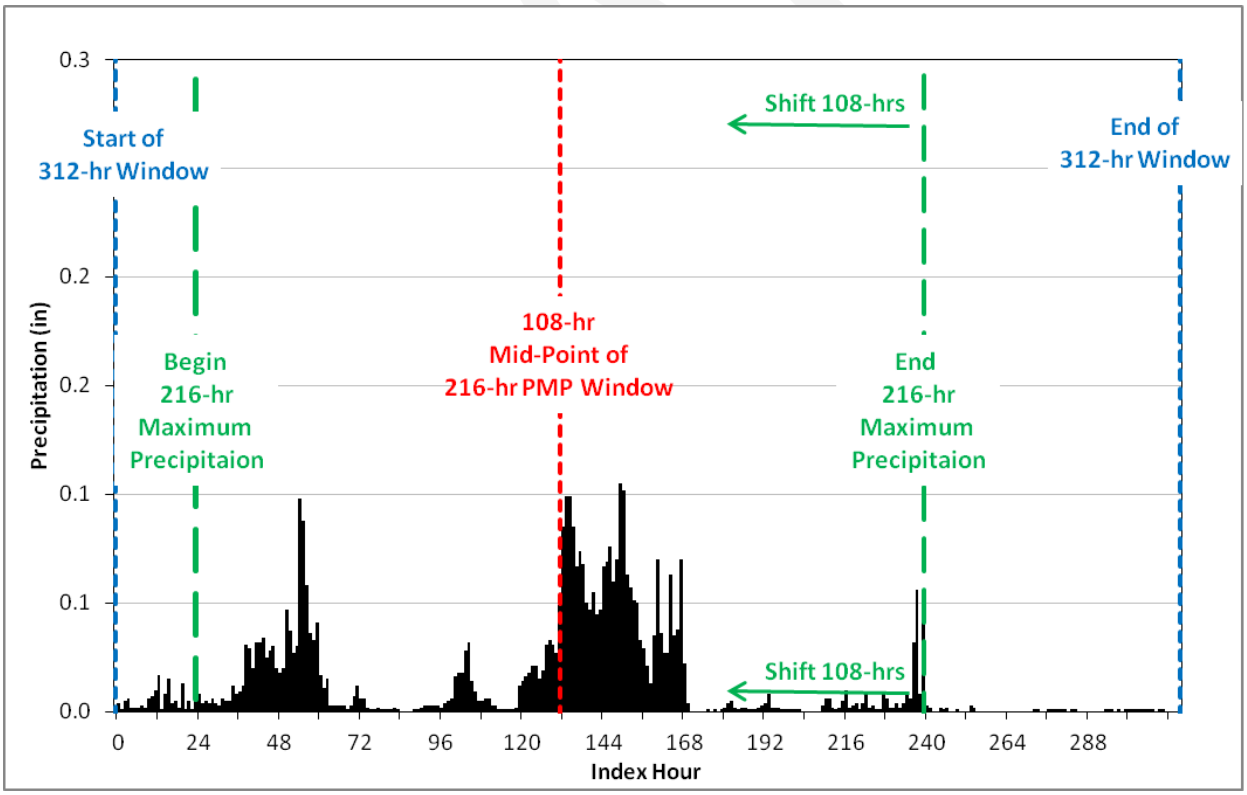

Figure 9.1. Methodology used to create the normalized 312-hour meteorological time series. Maximum 216-hour accumulated precipitation (green line). Mid-point of the 216-hour window basin on the 108-hour shift from the maximum 216-hour accumulation (red line). Start and end point of the 312-hour duration used in this example analysis (blue lines).

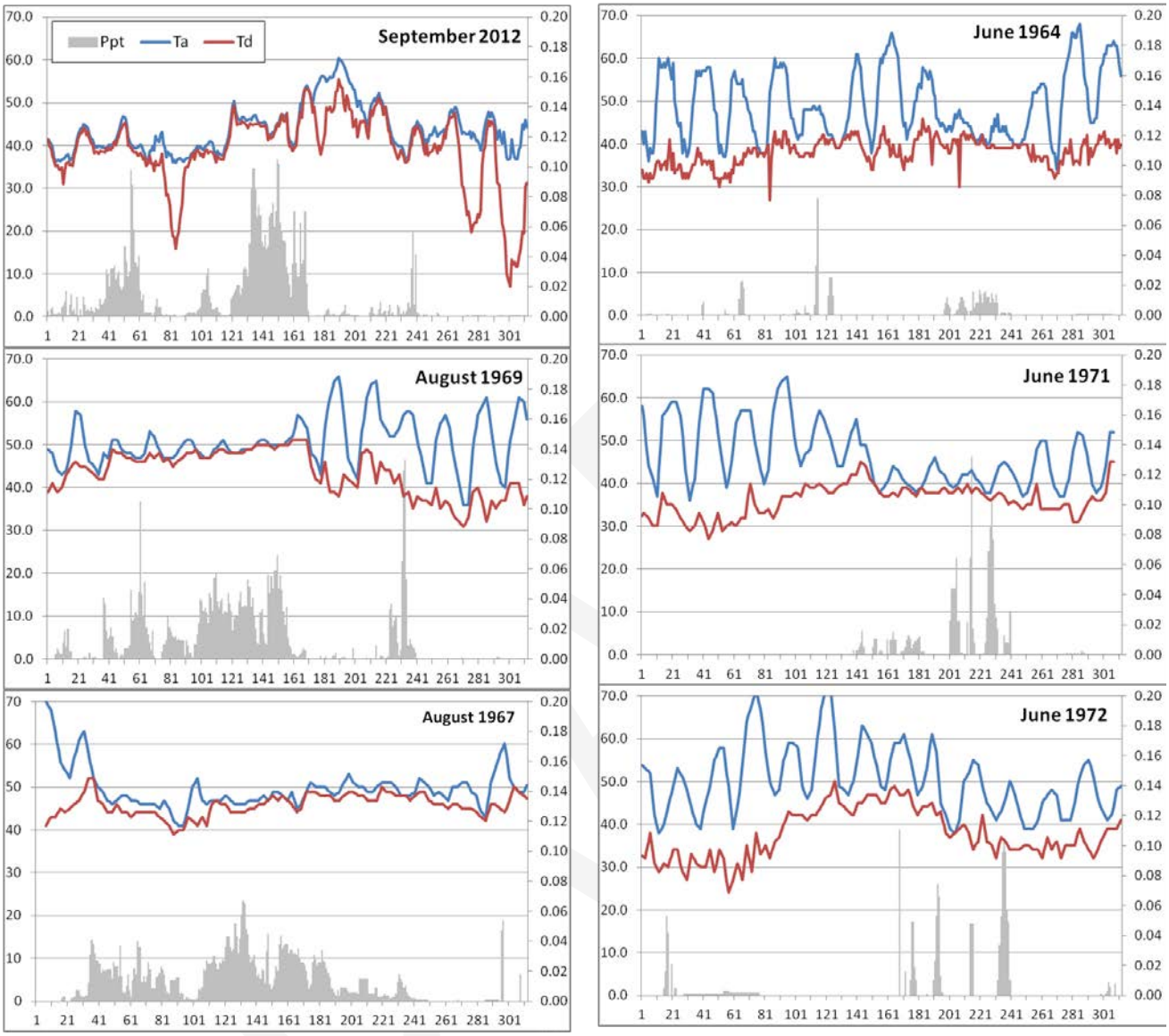

Figure 9.2. Indexed temperature and dew point temperature for the six storm events for a base elevation of 2,500 feet.

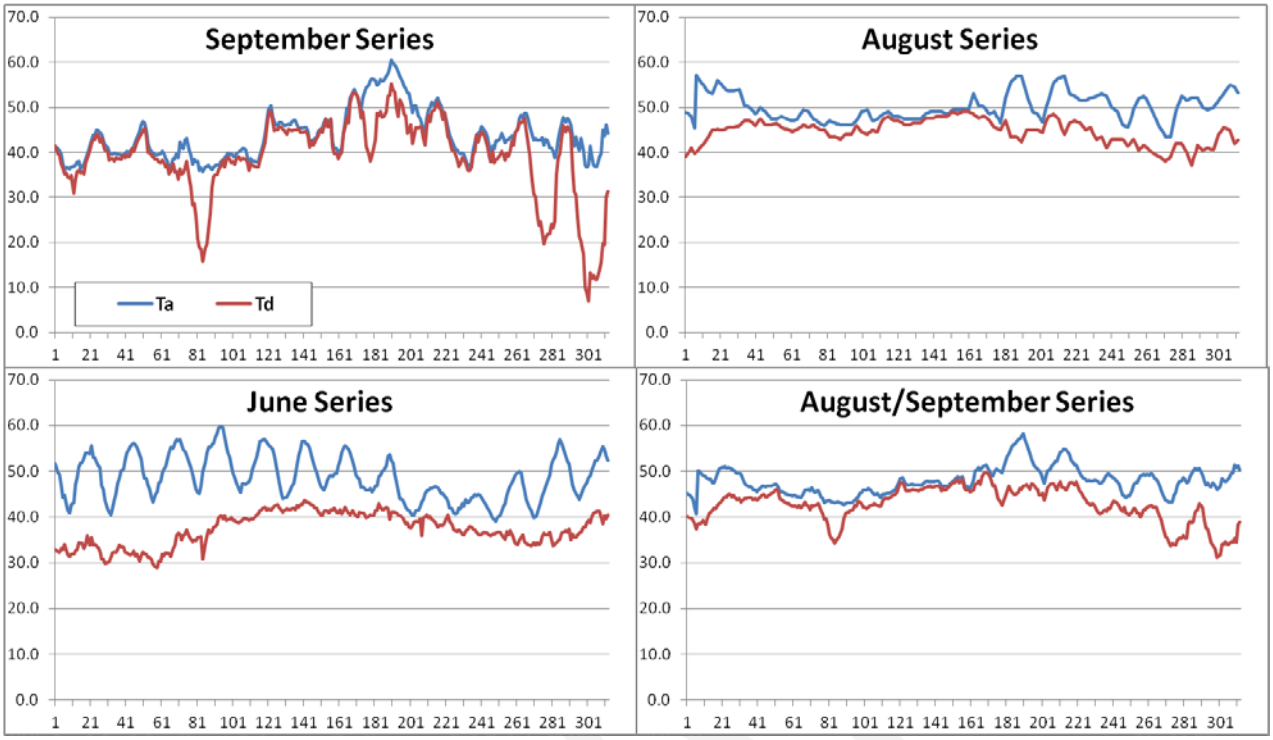

Figure 9.3. Indexed monthly averaged profiles for June, August, September and average August/September for a base elevation of 2,500 feet.

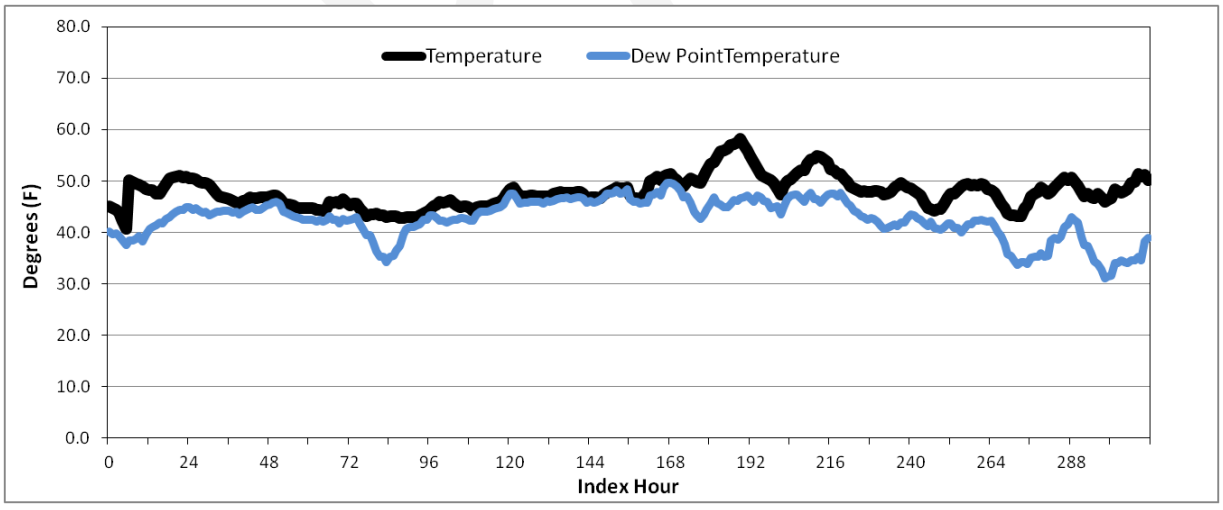

Figure 9.4. PMP non-maximized temperature and dew point temperature data based on the average profiles for August/September for a base elevation of 2,500 feet and lapse rate of -2.63°F per 1,000 feet.

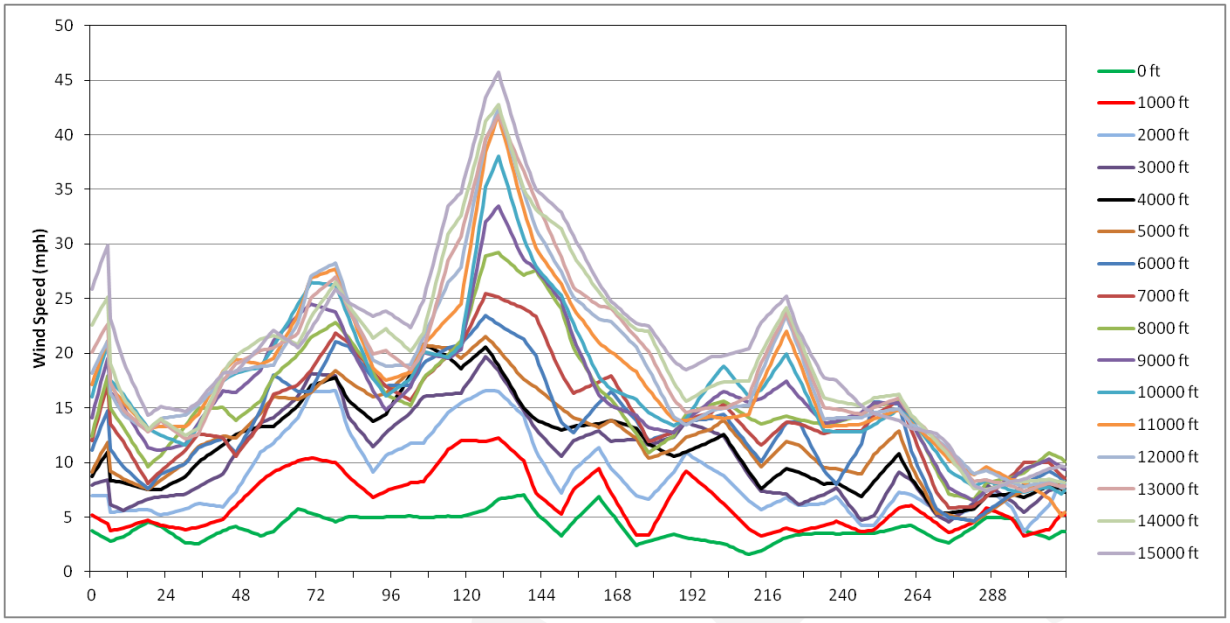

Figure 9.5. Final PMP wind speed values based on the average profiles for August/September for a base elevation of 2,500 feet.

9.1 PMP Temperature Time Series Maximization

The storm representative SST temperature and climatological maximum SST temperature associated with each of the short list storms were analyzed to derive the average difference between the two values in degrees Fahrenheit. The values associated with the storms which control the PMP values were averaged and the resulting value was then applied to each hourly temperature and dew point temperature value. The value derived from this process was 3.0°F. This was the value applied in the maximization process of the temperature and dew point temperature time series used for the snow melt calculations. This was done for all hourly data (in 216-hour window) in order to provide a consistent maximization of the temperature and dew point temperature time series that would be expected to occur during a cool-season PMP rainfall event.

An example of the maximized PMP temperature and dew point temperature data for a PMP event is shown below and the temperature and dew point temperature results displayed in Figure 9.6.

Storm rep SST for = 54.0°F
August 15[5] 2-sigma SST at the storm rep location = 57.0°F
September 15 2-sigma SST at the storm rep location = 56.5°F
Maximization Value = 57.0°F – 54.0°F = 3.0°F

[5] A combination of August and September +2-sigma SST values was used following the procedure of moving a storm two week towards the warmer season for maximization purposes. Because the example event occurred on September 15, the storm is moved to September 1 for storm analysis purposes.

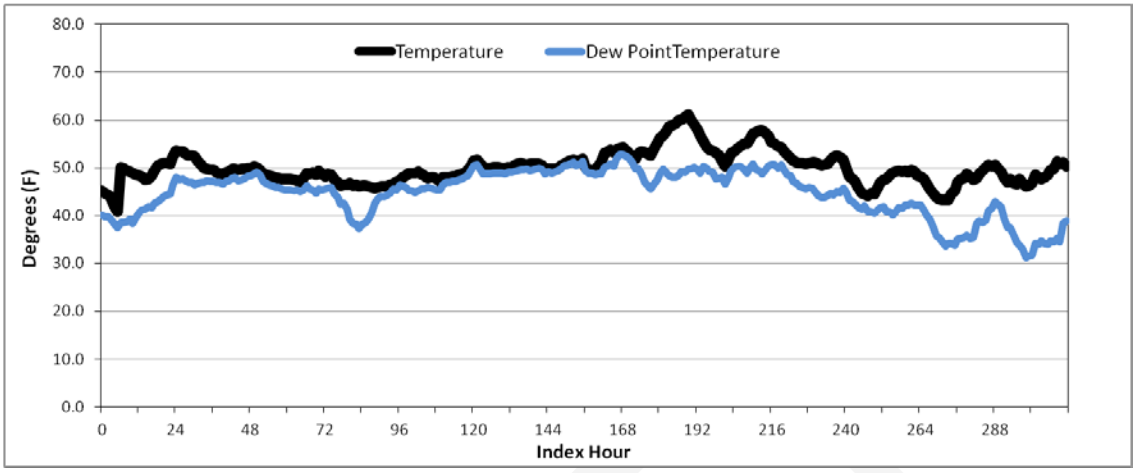

Figure 9.6. Final maximized PMP temperature and dew point temperature data based on the average profiles for August/September for a base elevation of 2,500 feet and lapse rate of -2.63°F per 1,000 feet.

9.2 Seasonality Adjustments for Moving to Other Months

Investigations of the seasonal variation in the Susitna-Watana PMP/PMF required that the maximized PMP temperature, dew point temperature, and wind speed time series values be moved, with appropriate adjustments to the other months when a lesser amount of these values could combine with a great snow melt runoff to produce a larger PMF. Three adjustment factors were determined: i) moving the maximized temperature and dew point temperature time series to other months, ii) moving the wind speed time series to other months, and iii) moving the all-season PMP to other months.

9.2.1 Temperature Seasonality Adjustments

Daily surface climate normal data (1981-2010) were acquired for ten stations (Table 9.1) for a period of April 1 to October 31. For each day, the average temperature was calculated from the ten stations. The average daily temperature for the Susitna-Watana basin, based on ten stations 30-year climate normal is shown in Figure 9.7. The maximum daily average temperature was computed to be 56.6°F. The maximum daily average temperature was used to scale the daily average temperature on a scale of 0.0 to 1.0, with 1.0 equal to 56.6°F. The 1st and 15th of each month scaled daily average temperature were extracted from April to November. The temperatures for July and August were set to 1.00, based on the small changes in temperature and this period represents the all season PMP months. The final seasonality adjustment factors to apply to the all-season PMP temperature and dew point temperature time series are shown in Table 9.2. The adjustment factors should be applied to move the all-season temperature and dew point temperature time series to other months. For example, moving the all-season temperature and dew point temperature from July 15 to May 15 would reduce the time series data by 0.80 (see example below).

July 15 all-season PMP at index hour 1 has a T_a of 45.1°F and T_d of 40.2°F
July 15 to May 15 adjustment = 0.80

May 15 PMP at index hour 1 T_a is 36.1°F and T_d is 32.2°F

Table 9.1 Stations used for temperature and dew point temperature seasonality adjustments.

Station	Elevation (ft)
Anchorage	130
Fairbanks	433
Talkeetna	350
Gulkana	1560
Chulitna River	1355
Paxson	2700
Lake Susitna	2375
Cantwell 2E	2130
Tahneta Pass	2620
Sutton 1W	550

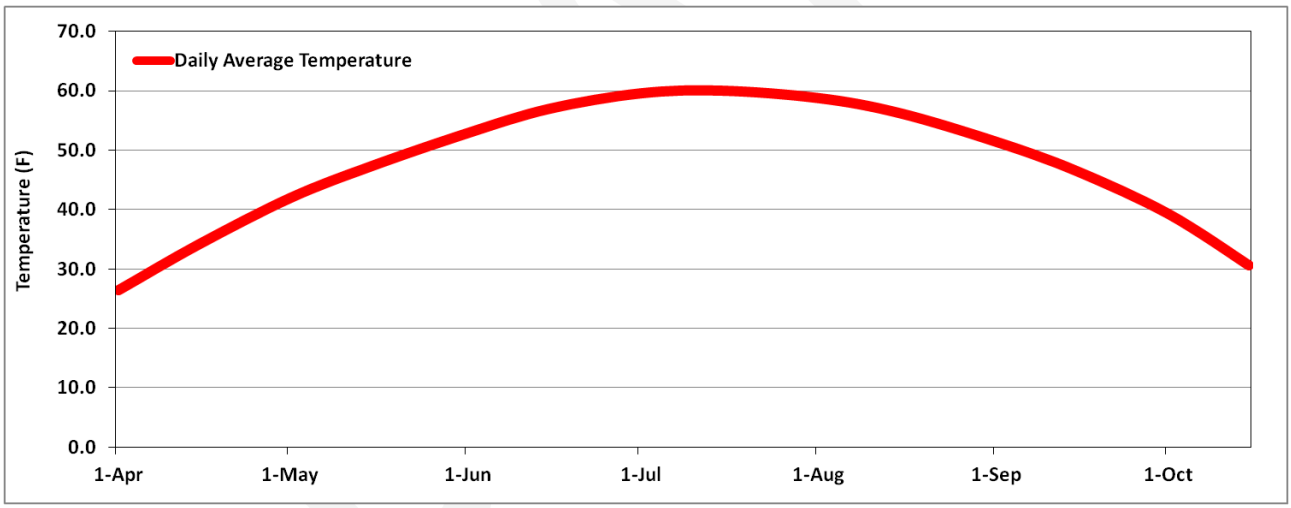

Figure 9.7. Daily average temperature based on ten stations 30-year climate normal around the Susitna-Watana basin.

Table 9.2. Seasonality adjustments to all season PMP temperature and dew point temperature time series.

Ta Td Time Series Seasonality	
Date	Ratio
1-Apr	0.39
15-Apr	0.55
1-May	0.69
15-May	0.80
1-Jun	0.90
15-Jun	0.95
1-Jul	1.00
15-Jul	1.00
1-Aug	1.00
15-Aug	1.00
1-Sep	0.94
15-Sep	0.86
1-Oct	0.77
15-Oct	0.64
1-Nov	0.51

9.2.2 Wind Speed Seasonality Adjustments

Daily average wind speed data was acquired from the Global Historical Climatology Network (GHCN) daily database at four stations (Table 9.3) surrounding the Susitna-Watana basin. The entire period of record for each station was extracted and analyzed. The average daily wind speed for each station was grouped by month, the monthly values were used to identify the monthly average maximum wind speed and average wind speed.

Table 9.3. Stations used for wind speed seasonality adjustments.

Station	Elevation (ft)
Gulkana	1560
Talkeetna	350
Anchorage	433
Fairbanks	500

A final average monthly maximum and average wind speed was calculated based on each of the four stations monthly values. For example, the August average monthly wind speed of 17.2 mph was calculated with the four stations maximum daily wind speed as:

Station		August Wind Speed
Talkeetna	=	14.8
Gulkana	=	23.7
Fairbanks	=	17.0
Anchorage	=	13.2
Average	=	*17.2*

The August average wind speed was computed to be 17.2 mph. The August average wind speed was used to scale the monthly maximum wind speed on a scale of 0.0 to 1.0, with 1.0 equal to 17.2 mph. The final seasonality adjustment factors to apply to the all-season PMP wind speed time series are shown in Table 9.4. The adjustment factors should be applied to the move the all-season wind speed time series to other months. For example, moving the all-season wind speed from August 15 to May 15 would increase the time series data by 1.06 (see example below).

August 15 all-season PMP at index hour 1 and 5000 feet has a Ws of 9.1 mph
August 15 to May 15 adjustment = 1.06
May 15 PMP at index hour 1 and 5000 feet Ws is 9.7 mph

Table 9.4. Seasonality adjustments to all season PMP wind speed time series.

Ws PMP Seasonality	
Month	**Ratio**
15-Jan	-
15-Feb	-
15-Mar	1.45
15-Apr	1.25
15-May	1.06
15-Jun	0.87
15-Jul	0.92
15-Aug	1.00
15-Sep	1.15
15-Oct	1.25
15-Nov	1.28
15-Dec	-

9.2.3 PMP Seasonality Adjustments

Monthly maximum 1-day precipitation data was acquired from the Alaska Climate Research Center for four stations (Table 9.2.5) surrounding the Susitna-Watana basin. Each stations maximum 1-day precipitation was used to scale each stations monthly 1-day maximum precipitation from 0.0 to 1.0. For example, Fairbanks monthly 1-day maximum precipitation was 3.42 inches and occurred in August, the scaled maximum precipitation data at Fairbanks is 1.0 for the month of

August. The average of each four stations monthly scaled maximum precipitation was used to initially identify the PMP seasonality adjustment. The all-season PMP is for the months of July and August, these months had a seasonality adjustment of 1.0. All other months had a reduction based on the average scaled maximum 1-day precipitation. The final PMP seasonality adjustment are shown in Table 9.6.

Table 9.5. Stations used for PMP seasonality adjustments.

Station	Elevation (ft)
Gulkana	1560
Talkeetna	350
Anchorage	433
Fairbanks	500

The adjustment factors should be applied to the move the all-season PMP to other months. For example, moving the all-season PMP from August 15 to May 15 would reduce the PMP magnitude by 0.83 (see example below).

August 15 sub-basin 1 average all-season PMP at 72-hours is 9.95 inches
August 15 to May 15 adjustment = 0.83
May 15 PMP sub-basin 1 72-hour PMP would be 8.26 inches

Table 9.6. Seasonality adjustments to all season PMP.

PMP Seasonality	
Month	**Ratio**
15-Jan	-
15-Feb	-
15-Mar	0.30
15-Apr	0.60
15-May	0.83
15-Jun	0.94
15-Jul	1.00
15-Aug	1.00
15-Sep	0.92
15-Oct	0.80
15-Nov	0.65
15-Dec	-

10. RESULTS

10.1 Site-Specific PMP Values

This study produced site-specific PMP values for use in computing the PMF for the Susitna-Watana basin. Values for durations from 1- through 216-hours have been computed for each grid cell within the basin. After all adjustments were applied to all the storms on the short storm list, the Fairbanks August, 1967 storm event resulted in the largest values at all area sizes and all durations. The spatial and temporal patterns associated with the three storms from the storm list with different temporal patterns were then used to distribute the PMP rainfall. Finally, the gridded hourly PMP values were averaged by sub-basin.

Results of this analysis are displayed in Tables 10.1a-c, one for each of the temporal distributions applied. These include the all-season PMP values for each sub-basin as a sub-basin average amount at the x-duration. The total basin (5,131 mi^2) is also included and used for comparisons to previous work in the region.

Table 10.1a. Site-specific PMP values for Susitna-Watana basin using the August, 1967 storm temporal distribution.

Sub-basin	Drainage Area (sq.mi.)	All Season 1-hr PMP (inches)	All Season 6-hr PMP (inches)	All Season 24-hr PMP (inches)	All Season 72-hr PMP (inches)	All Season 216-hr PMP (inches)
1	52.6	0.60	2.47	6.09	9.95	13.83
2	226.4	0.50	2.04	5.02	8.21	11.41
3	295.4	0.37	1.53	3.77	6.16	8.56
4	149.3	0.56	2.31	5.69	9.31	12.93
5	354.0	0.44	1.79	4.43	7.24	10.06
6	153.4	0.48	1.97	4.86	7.94	11.03
7	67.5	0.32	1.31	3.23	5.29	7.35
8	189.9	0.39	1.60	3.94	6.44	8.95
9	187.7	0.41	1.69	4.18	6.83	9.50
10	326.8	0.39	1.61	3.98	6.51	9.04
11	273.5	0.41	1.67	4.12	6.73	9.35
12	74.7	0.36	1.46	3.61	5.90	8.21
13	222.5	0.34	1.39	3.44	5.62	7.81
14	135.1	0.33	1.36	3.35	5.48	7.62
15	185.1	0.36	1.50	3.69	6.03	8.38
16	164.3	0.37	1.51	3.73	6.10	8.48
17	253.2	0.35	1.45	3.57	5.84	8.12
18	100.0	0.43	1.78	4.39	7.18	9.98
19	202.2	0.50	2.04	5.04	8.24	11.45
20	36.3	0.37	1.53	3.77	6.16	8.56
21	162.7	0.50	2.06	5.07	8.29	11.52
22	92.0	0.36	1.47	3.63	5.93	8.25
23	174.2	0.41	1.70	4.19	6.86	9.53
24	157.4	0.43	1.78	4.38	7.17	9.96
25	184.0	0.61	2.52	6.23	10.18	14.15
26	222.9	0.54	2.23	5.50	8.99	12.49
27	269.6	0.47	1.94	4.78	7.81	10.85
28	218.5	0.52	2.13	5.26	8.60	11.96
29	36.8	0.43	1.75	4.31	7.05	9.80
Total/Avg.	5168.2	0.43	1.78	4.40	7.19	10.00

Table 10.1b. Site-specific PMP values for Susitna-Watana basin using the August, 1955 storm temporal distribution.

Sub-basin	Drainage Area (sq.mi.)	All Season 1-hr PMP (inches)	All Season 6-hr PMP (inches)	All Season 24-hr PMP (inches)	All Season 72-hr PMP (inches)	All Season 216-hr PMP (inches)
1	52.6	0.60	1.93	3.83	7.64	13.83
2	226.4	0.50	1.59	3.16	6.31	11.41
3	295.4	0.37	1.20	2.37	4.73	8.56
4	149.3	0.56	1.81	3.58	7.15	12.93
5	354.0	0.44	1.40	2.79	5.56	10.06
6	153.4	0.48	1.54	3.06	6.10	11.03
7	67.5	0.32	1.03	2.04	4.06	7.35
8	189.9	0.39	1.25	2.48	4.95	8.95
9	187.7	0.41	1.33	2.63	5.25	9.50
10	326.8	0.39	1.26	2.51	5.00	9.04
11	273.5	0.41	1.31	2.59	5.17	9.35
12	74.7	0.36	1.15	2.27	4.54	8.21
13	222.5	0.34	1.09	2.16	4.32	7.81
14	135.1	0.33	1.06	2.11	4.21	7.62
15	185.1	0.36	1.17	2.32	4.63	8.38
16	164.3	0.37	1.18	2.35	4.69	8.48
17	253.2	0.35	1.13	2.25	4.49	8.12
18	100.0	0.43	1.39	2.77	5.52	9.98
19	202.2	0.50	1.60	3.17	6.33	11.45
20	36.3	0.37	1.20	2.37	4.73	8.56
21	162.7	0.50	1.61	3.19	6.37	11.52
22	92.0	0.36	1.15	2.28	4.56	8.25
23	174.2	0.41	1.33	2.64	5.27	9.53
24	157.4	0.43	1.39	2.76	5.51	9.96
25	184.0	0.61	1.98	3.92	7.82	14.15
26	222.9	0.54	1.74	3.46	6.91	12.49
27	269.6	0.47	1.52	3.01	6.00	10.85
28	218.5	0.52	1.67	3.31	6.61	11.96
29	36.8	0.43	1.37	2.72	5.42	9.80
Total/Avg.	5168.2	0.43	1.40	2.77	5.53	10.00

Table 10.1c. Site-specific PMP values for Susitna-Watana basin using the September, 2012 storm temporal distribution.

Sub-basin	Drainage Area (sq.mi.)	All Season 1-hr PMP (inches)	All Season 6-hr PMP (inches)	All Season 24-hr PMP (inches)	All Season 72-hr PMP (inches)	All Season 216-hr PMP (inches)
1	52.6	0.60	1.79	3.77	6.40	13.83
2	226.4	0.50	1.47	3.11	5.28	11.41
3	295.4	0.37	1.11	2.33	3.96	8.56
4	149.3	0.56	1.67	3.52	5.99	12.93
5	354.0	0.44	1.30	2.74	4.66	10.06
6	153.4	0.48	1.42	3.00	5.11	11.03
7	67.5	0.32	0.95	2.00	3.40	7.35
8	189.9	0.39	1.16	2.44	4.15	8.95
9	187.7	0.41	1.23	2.59	4.40	9.50
10	326.8	0.39	1.17	2.46	4.19	9.04
11	273.5	0.41	1.21	2.55	4.33	9.35
12	74.7	0.36	1.06	2.23	3.80	8.21
13	222.5	0.34	1.01	2.13	3.62	7.81
14	135.1	0.33	0.98	2.07	3.53	7.62
15	185.1	0.36	1.08	2.28	3.88	8.38
16	164.3	0.37	1.09	2.31	3.93	8.48
17	253.2	0.35	1.05	2.21	3.76	8.12
18	100.0	0.43	1.29	2.72	4.62	9.98
19	202.2	0.50	1.48	3.12	5.30	11.45
20	36.3	0.37	1.11	2.33	3.96	8.56
21	162.7	0.50	1.49	3.14	5.34	11.52
22	92.0	0.36	1.06	2.25	3.82	8.25
23	174.2	0.41	1.23	2.59	4.41	9.53
24	157.4	0.43	1.29	2.71	4.61	9.96
25	184.0	0.61	1.83	3.85	6.55	14.15
26	222.9	0.54	1.61	3.40	5.78	12.49
27	269.6	0.47	1.40	2.96	5.03	10.85
28	218.5	0.52	1.54	3.26	5.54	11.96
29	36.8	0.43	1.27	2.67	4.54	9.80
Total/Avg.	5168.2	0.43	1.29	2.72	4.63	10.00

10.2 PMP Comparison with Previous Studies

There have been previous studies investigating PMP over the Upper Susitna drainage basin: the Susitna Hydroelectric Project Feasibility Report (Acres 1982) and the Harza-Ebasco Susitna Joint Venture (1984). The PMP calculation procedures and tools employed in this study have significantly evolved since the publication of these PMP studies. However, the generalized approach of storm maximization and transposition is similar. Furthermore, despite the occurrence and analysis of recent precipitation events that have occurred since these studies, the August 1967 (the Great Fairbanks Flood) event remains the controlling storm for PMP.

The Harza-Ebasco study reported an all-season basin average 72-hour PMP of 6.85" for 5,180 mi^2. A seasonality factor of 0.93 was applied to June 15th and a factor of 0.73 was applied to May 15th. The 72-hour PMP from the Harza-Ebasco study is summarized in Table 10.2.

Table 10.2. Harza-Ebasco 1984 Susitna 72-hour Basin PMP and spring season adjustments.

Season	72-hour PMP: Harza-Ebasco	
	Factor	PMP
All-season	1.00	6.85
15-Jun	0.93	6.37
15-May	0.73	5.00

The Acres study reported an all-season basin average 72-hour PMP of 5.90" for 5,180 mi^2. A seasonality factor of 0.70 was applied to June 15th. The Acres study did not seasonally adjust PMP to May. At the 216-hour duration, a basin average PMP of 12.54" was reported. The 72-hour PMP from the Acres study is summarized in Table 10.3 and the 216-hour PMP is summarized in Table 10.4.

Table 10.3. Acres 1982 Susitna 72-hour Basin PMP and spring season adjustments.

Season	72-hour PMP: Acres	
	Factor	PMP
All-season	1.00	5.90
15-Jun	0.70	4.13
15-May	N/A	N/A

Table 10.4. Acres 1982 Susitna 216-hour Basin PMP and spring season adjustments.

Season	216-hour PMP: Acres	
	Factor	PMP
All-season	1.00	12.54
15-Jun	0.70	8.90
15-May	N/A	N/A

The gridded basin average 72-hour PMP provided by AWA in this study is 7.43" for 5,132 mi^2, before the application of the various storm-based temporal distribution patterns. A seasonality factor of 0.94 was applied to June 15th and a seasonality factor of 0.83 was applied to May 15th. At the 216-hour duration, a basin average PMP of 12.54" was calculated. The 72-hour PMP from this study is summarized in Table 10.5 and the 216-hour PMP is summarized in Table 10.6

Table 10.5. AWA Susitna-Watana 72-hour Basin PMP and spring season adjustments

Season	72-hour PMP: AWA	
	Factor	PMP
All-season	1.00	7.43
15-Jun	0.94	6.98
15-May	0.83	6.17

Table 10.6. AWA Susitna-Watana 216-hour Basin PMP and spring season adjustments

Season	216-hour PMP: AWA	
	Factor	PMP
All-season	1.00	10.02
15-Jun	0.94	9.42
15-May	0.83	8.32

The ratio of AWA PMP to the Acres (72-hour and 216-hour) and Harza-Ebasco (216-hour) is shown in Table 10.7.

Table 10.7. Ratios of AWA PMP to the Acres and Harza-Ebasco studies.

Season	Ratio of AWA PMP to:		
	Acres (72hr)	Acres (216hr)	Harza-Eb.
All-season	1.26	0.80	1.08
15-Jun	1.69	1.06	1.10
15-May	N/A	N/A	1.23

Generally, the AWA PMP magnitudes are somewhat larger than previous estimates, particularly for the Acres study at 72-hours. There are numerous factors contributing to the differences stemming from both the source data and methods applied. There are several methodologies and data sets employed by the AWA PMP study that differ from previous studies and may contribute to differences in PMP. These include; high spatial and temporal resolution SPAS analyses for each storm and the resulting DAD tables and mass curves, updated storm maximization using SST data, improved geospatial technologies that allow for improved analysis of source moisture and storm maximization, gridded analysis of moisture and orographic transposition over the basin, availability of NOAA Atlas 14 values, and improved temperature-time series and seasonality relations. It is also likely that there are differences in the basin boundary delineation.

10.3 Comparison of PMP with NOAA Atlas 14

NOAA Atlas 14 Volume 7 provides gridded partial duration and annual maximum precipitation data over Alaska. In addition to return frequency analysis, these data can provide an accurate representation of the relationship between historical rainfall and terrain. PMP values were compared with 100-year rainfall values as a general check for reasonableness. The ratio of the PMP to the 24-hour 100-year return period rainfall amounts is generally expected to range between two and four, with values as low as 1.7 and as high as 5.5 found in HMRs 57 and 59 (Hansen et al.. 1994, Corrigan et al. 1999). In HMR 59 it is stated "…*the comparison indicates that larger ratios are in lower elevations where short-duration, convective precipitation dominates, and smaller ratios in higher elevations where general storm, long duration precipitation is prevalent*". Therefore, it would be reasonable to expect the ratios for the Susitna River basin to be in the low end of the range.

A gridded basin comparison was made between the 24-hour AWA PMP values and the 24-hour NOAA Atlas 14 precipitation frequency datasets. The NOAA Atlas 14 precipitation depths are considered point values and have no areal reduction applied. For this reason, the 24-hour basin PMP was calculated with the minimum SPAS resolution (0.20 mi^2) to approximate point values, instead of the basin size of 5,131 mi^2. The ratio of 24-hour PMP to NOAA Atlas 14 precipitation was calculated for the 100-year return period. Table 10.8 shows the basin average NOAA Atlas 14 precipitation for 10-year through 1,000-year events. The 100-year basin average is 3.65" over 24-hours. The basin average 0.20 mi^2 PMP is 6.34" for a 24-hour period (Table 10.8). This indicates a factor of 1.74 times the 100-year NOAA Atlas 14 depth (Table 10.9). The largest ratio for all of the 4,013 grid points was 1.86 and the smallest ratio was 1.58, indicating a fairly low amount of variation over the basin.

Table 10.8. Gridded basin average 24-hour NOAA Atlas 14 precipitation for the 10-1,000 year return periods. Gridded basin average 24-hour point PMP.

	10-year	25-year	50-year	**100-year**	200-year	500-year	1,000-year
24-hr Precip. Frequency (NOAA Atlas 14)	2.37	2.85	3.24	**3.65**	4.11	4.73	5.19
Gridded Basin Average 24-hour PMP (0.2sqmi)				6.34			

Table 10.9. Ratio of 24-hour PMP to 100-year NOAA Atlas 14 precipitation.

Average Basin Ratio (24hr PMP:NOAA Atlas 14 100-yr)	**1.74**
Max. Basin Ratio (24hr PMP:NOAA Atlas 14 100-yr)	1.86
Min. Basin Ratio (24hr PMP:NOAA Atlas 14 100-yr)	1.58

It should also be noted that the 24-hour basin average 1,000-year rainfall is 5.19", putting the basin average PMP of 6.34" well above the 1,000 return frequency.

11. DISCUSSION OF PMP PARAMETERS

In the process of deriving SSPMP values, various assumptions were made and specific procedures were used which could be derived from a range of possible alternatives. Therefore, it is important to understand how the assumptions made could potentially affect certain aspects of the SSPMP calculations. Assumptions related to a saturated atmospheric column from the surface through 30,000 feet during the storm maximization and transposition process and that the storms analyzed are at maximum storm efficiency are discussed.

11.1 Assumptions

11.1.1 Saturated Storm Atmospheres

The atmospheric air masses that provide moisture to both the historic storms and the PMP storm are assumed to be saturated through the entire depth of the atmosphere and to contain the maximum moisture possible based on the surface dew point. This assumes moist pseudo-adiabatic temperature profiles for both the historic storms and the PMP storm. Limited evaluation of this assumption in the EPRI Michigan/Wisconsin PMP study (Tomlinson 1993) and the Blenheim Gilboa (Tomlinson et al. 2008) study indicated that historic storm atmospheric profiles are generally not entirely saturated and contain somewhat less precipitable water than is assumed in the PMP procedure. It follows that the PMP storm (if it were to occur) would also have somewhat less precipitable water available than the assumed saturated PMP atmosphere would contain. What is used in the PMP procedure is the *ratio* of precipitable water associated with each storm. If the precipitable water values for each storm are both slightly overestimated, the ratio of these values will be essentially unchanged. For example, consider the case where instead of a historic storm with a storm representative dew point of 70^{o} F degrees having 2.25 inches of precipitable water assuming a saturated atmosphere, it actually had 90% of that value or about 2.02 inches. The PMP procedure assumes the same type of storm with similar atmospheric characteristics for the maximized storm but with a higher dew point, say 76^{o} F degrees. The maximized storm, having similar atmospheric conditions, would have about 2.69 inches of precipitable water instead of the 2.99 inches associated with a saturated atmosphere with a dew point of 76^{o} F degrees. The maximization factor computed using the assumed saturated atmospheric values would be 2.99/2.25 = 1.33. If both storms were about 90% saturated instead, the maximization factor would be 2.69/2.02 = 1.33. Therefore potential inaccuracy of assuming saturated atmospheres (whereas the atmospheres may be somewhat less than saturated) should have a minimal impact on storm maximization and subsequent PMP calculations.

11.1.2 Maximum Storm Efficiency

The assumption is made that if a sufficient period of record is available for rainfall observations, at least a few storms would have been observed that attained or came close to attaining the maximum

efficiency possible in nature for converting atmospheric moisture to rainfall for regions with similar climates and topography. The further assumption is made that if additional atmospheric moisture had been available, the storm would have maintained the same efficiency for converting atmospheric moisture to rainfall. The ratio of the maximized rainfall amounts to the actual rainfall amounts would be the same as the ratio of the precipitable water in the atmospheres associated with each storm.

There are two issues to be considered. First is the assumption that a storm has occurred that has a rainfall efficiency close to the maximum possible. Unfortunately, state-of-the-science in meteorology does not support a theoretical evaluation of storm efficiency. However, if the period of record is considered (generally over 100 years), along with the extended geographic region with transpositionable storms, it is accepted that there should have been at least one storm with dynamics that approach the maximum efficiency for rainfall production.

The other issue is the assumption that storm efficiency does not change if additional atmospheric moisture is available. Storm dynamics could potentially become more efficient or possibly less efficient depending on the interaction of cloud microphysical processes with the storm dynamics. Offsetting effects could indeed lead to the storm efficiency remaining essentially unchanged. For the present, the assumption of no change in storm efficiency is accepted.

11.2 Parameters

This discussion applies to both dew points and SSTs although only SSTs will be addressed in this sections as SSTs are used as substitutes for land based dew points for all storms in this study for inflow vectors that originate over ocean regions and have the same sensitivity considerations.

The maximization factor depends on the determination of storm representative SSTs, along with maximum historical SST values. The magnitude of the maximization factor varies depending on the values used for the storm representative SST and the maximum SST. Holding all other variables constant, the maximization factor is smaller for higher storm representative SSTs as well as for lower maximum SST values. Likewise, larger maximization factors result from the use of lower storm representative SSTs and/or higher maximum SSTs. The magnitude of the change in the maximization factor varies dependent on the SST values. For the range of SST values used in most PMP studies, the maximization factor for a particular storm will change about 5% for every 1^{o} F difference between the storm representative and maximum SST values. The same sensitivity applies to the transposition factor, with about a 5% change for every 1^{o}F change in either the in-place maximum SST or the transposition maximum SST.

For example, consider the following case:

Storm representative SST: 75^{o}F Precipitable water: 2.85”

Maximum SST: 79 ^{o} F Precipitable water: 3.44"
Maximization factor = 3.44"/2.85" = 1.21

If the storm representative SST were 74 ^{o} F with precipitable water of 2.73",
Maximization factor = 3.44"/2.73" = 1.26 (an increase of approximately 4%)

If the maximum SST were 78 ^{o} F with precipitable water of 3.29",
Maximization factor = 3.29"/2.85" = 1.15 (a decrease of approximately 5%)

12. RECOMMENDATIONS FOR APPLICATION

12.1 Site-Specific PMP Applications

Site-specific PMP values have been computed that provide rainfall amounts for use in computing the PMF. The study addressed several issues that could potentially affect the magnitude of the PMP storm over the Susitna-Watana basin.

The HMRs use a procedure for locating the largest amounts of rainfall associated with the PMP storm, such that the largest volume of rain falls within the watershed boundaries, either using the 100-year 24-hour isopercental analysis or using a significant storm over the basin and the judgment of the user (HMR 57 Section 15.2, Step 9). As the authors of HMR 57 explicitly state in that section of the report, "It is left to a future study to resolve the issue of how to distribute general storm PMP…" This study has directly addressed this issue by using the gridded approach and developing spatial and temporal patterns based on the largest historic storm events that have occurred over the basin. Further, the temperature time series developed for this study explicitly addresses the antecedent and within-storm temperature profile that would be expected during a PMP storm over the basin, thereby eliminating much of the subjectivity employed in previous HMRs (e.g. HMR 57 Section 15.2 Step 10). These updated applications, based on actual data specific to the storms which affect this basin, allows the PMP rainfall to be distributed in a pattern that is physically possible based on the unique topography and climate of the basin. It is recommended that the use of the gridded approach to spatially distribute the PMP rainfall at each duration at each grid point be used to derive the PMF as presented in this report for the Susitna-Watana basin.

The storm search and selection of storms for the short list emphasized storms with the largest rainfall values that occurred over areas that are both meteorologically and topographically similar to the Susitna-Watana drainage basin. Results of this study should not be used for watersheds where meteorological and/or topographical parameters are different from the Susitna-Watana drainage basin without further evaluation.

12.2 Calibration Storm Events

AWA utilized the SPAS to analyze rainfall over the Susitna-Watana basin. Six storm events were selected for calibration of the PMF hydrologic model (Table 12.1). AWA analyzed a sufficiently large storm domain that included sufficient hourly rain gauge observations to calibrate the NEXRAD data if available over larger domain that included the Susitna-Watana region. Quality controlled NEXRAD data was acquired from Weather Decisions Technologies, Inc. Non-radar events utilized climatological basemaps to aid in the spatial distribution of precipitation.

Table 12.1. Six storm events were selected for hydrologic model calibration.

Hydrologic Calibration Events Selected		
SPAS #	Date	Radar
1256	Sep-12	Yes
1269	Aug-71	No
1270	Aug-67	No
6008	Jun-64	No
6009	Jun-71	No
6010	Jun-72	No

The rainfall analysis results were provided on a 1/3mi^2 grid with a temporal frequency of 60-minutes. In addition to the rainfall grids, clipped to the Susitna-Watana drainage, sub-basin average rainfall statistics were provided for all 34 sub-basins. Note, the calibration analysis included six extra sub-basins for calibration purposes to include the region immediately downstream of the dam site to the Gold Creek USGS gage.

12.2.1 September 14-30, 2012 Precipitation

The hourly precipitation grids derived from the SPAS 1256 analysis were used in conjunction with SPAS-Lite 6007 as the basis for the Susitna-Watana calibration. SPAS-Lite 6007 was utilized to fill in a longer duration than what was analyzed for SPAS 1256, the calibration period is referenced as SPAS 1256. The SPAS 1256 analysis encompassed the 34 sub-basins of Susitna-Watana. The SPAS 1256 hourly grids were clipped to each of the Susitna-Watana sub-basins, the sub-basin average statistics were calculated and added to an Excel spreadsheet used for hydrologic calibration. The calibration deliverables are based on the SPAS hourly precipitation data for 9/14-30/2012. In general, between 0.80 and 10.30 inches of rain fell across the Susitna-Watana drainage (Figure 12.1 - 12.3).

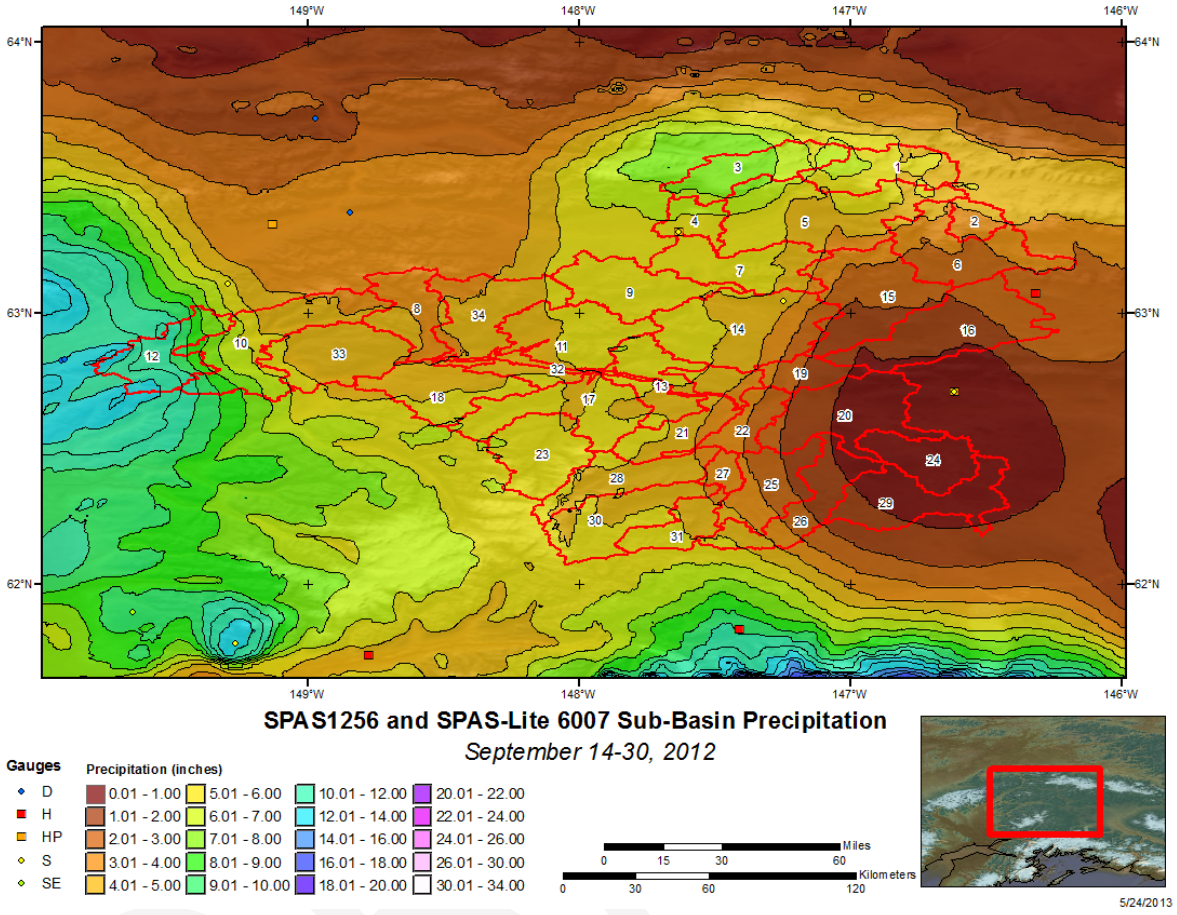

Figure 12.1. Total storm rainfall for SPAS 1256 across Susitna-Watana drainage.

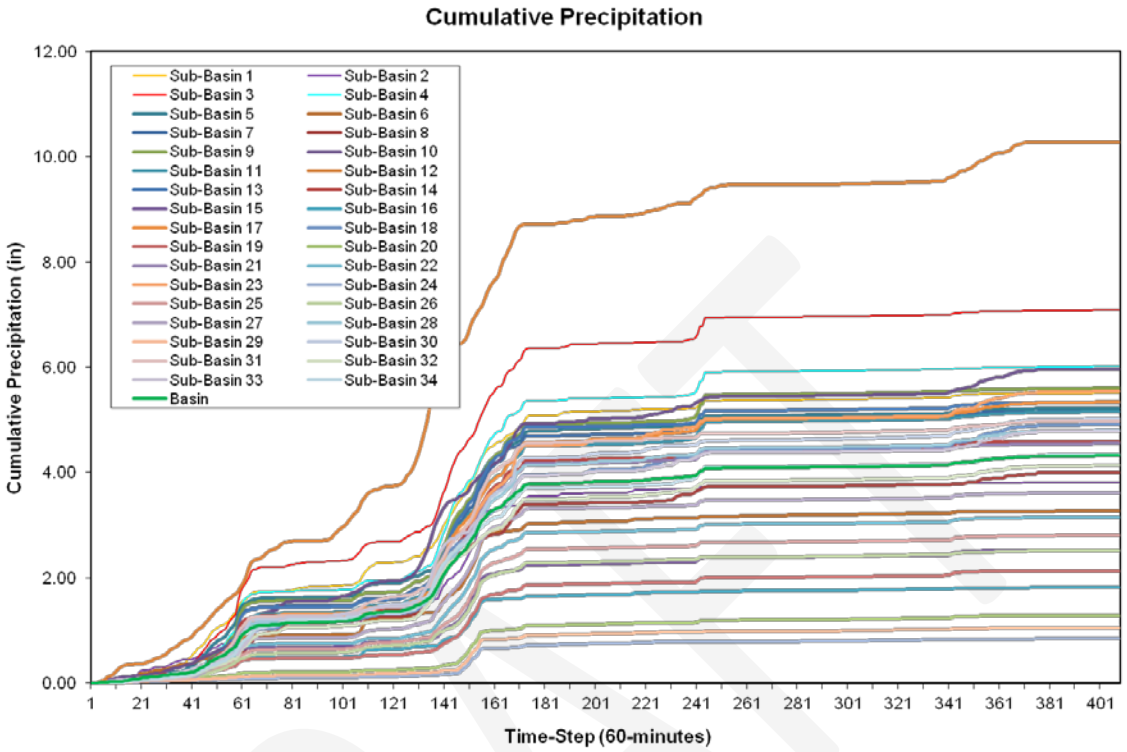

Figure 12.2. Susitna-Watana sub-basin average accumulated rainfall SPAS 1256.

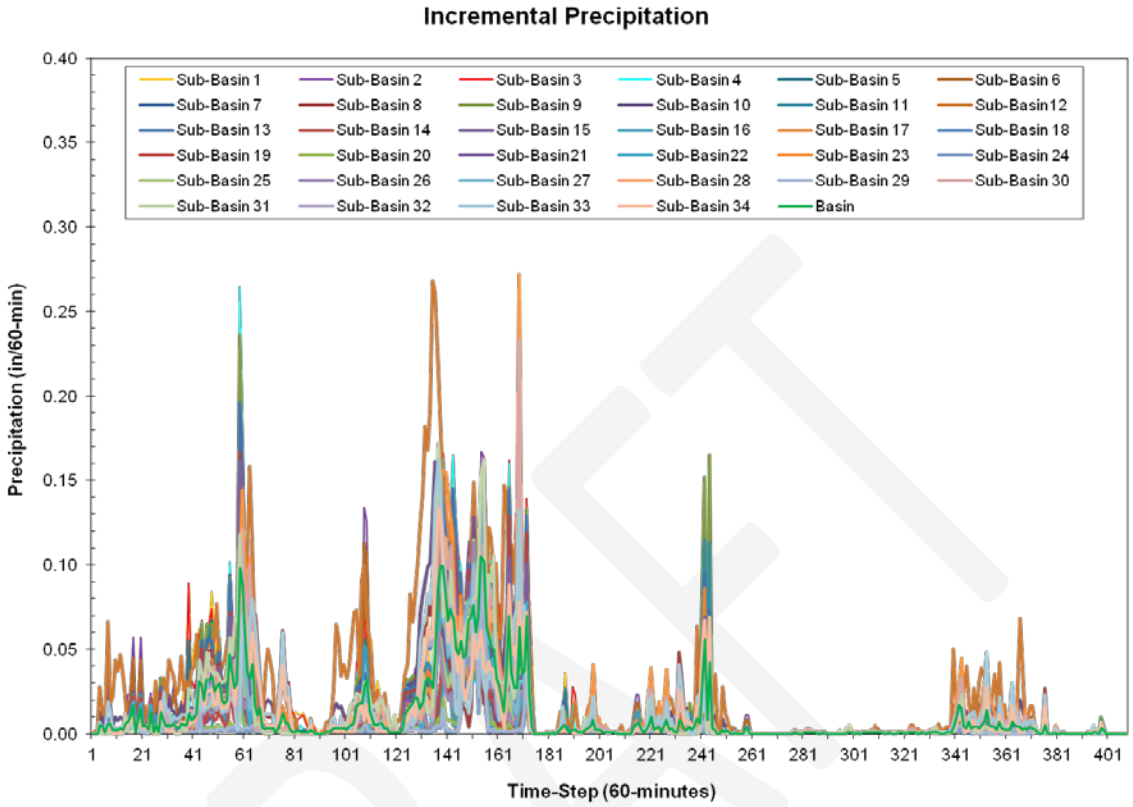

Figure 12.3. Susitna-Watana sub-basin average incremental rainfall SPAS 1256.

12.2.2 August 14-17, 1971 Precipitation

The hourly precipitation grids derived from the SPAS 1269 analysis were used in conjunction with SPAS-Lite 6001 as the basis for the Susitna-Watana calibration. SPAS-Lite 6001 was utilized to fill in a longer duration than what was analyzed for SPAS 1269, the calibration period is referenced as SPAS 1269. The SPAS 1269 analysis encompassed the 34 sub-basins of Susitna-Watana. The SPAS 1269 hourly grids were clipped to each of the Susitna-Watana sub-basins, the sub-basin average statistics were calculated and added to an Excel spreadsheet used for hydrologic calibration. The calibration deliverables are based on the SPAS hourly precipitation data for 8/4-17/1971. In general, between 1.50 and 5.80 inches of rain fell across the Susitna-Watana drainage (Figure 12.4 - 12.6).

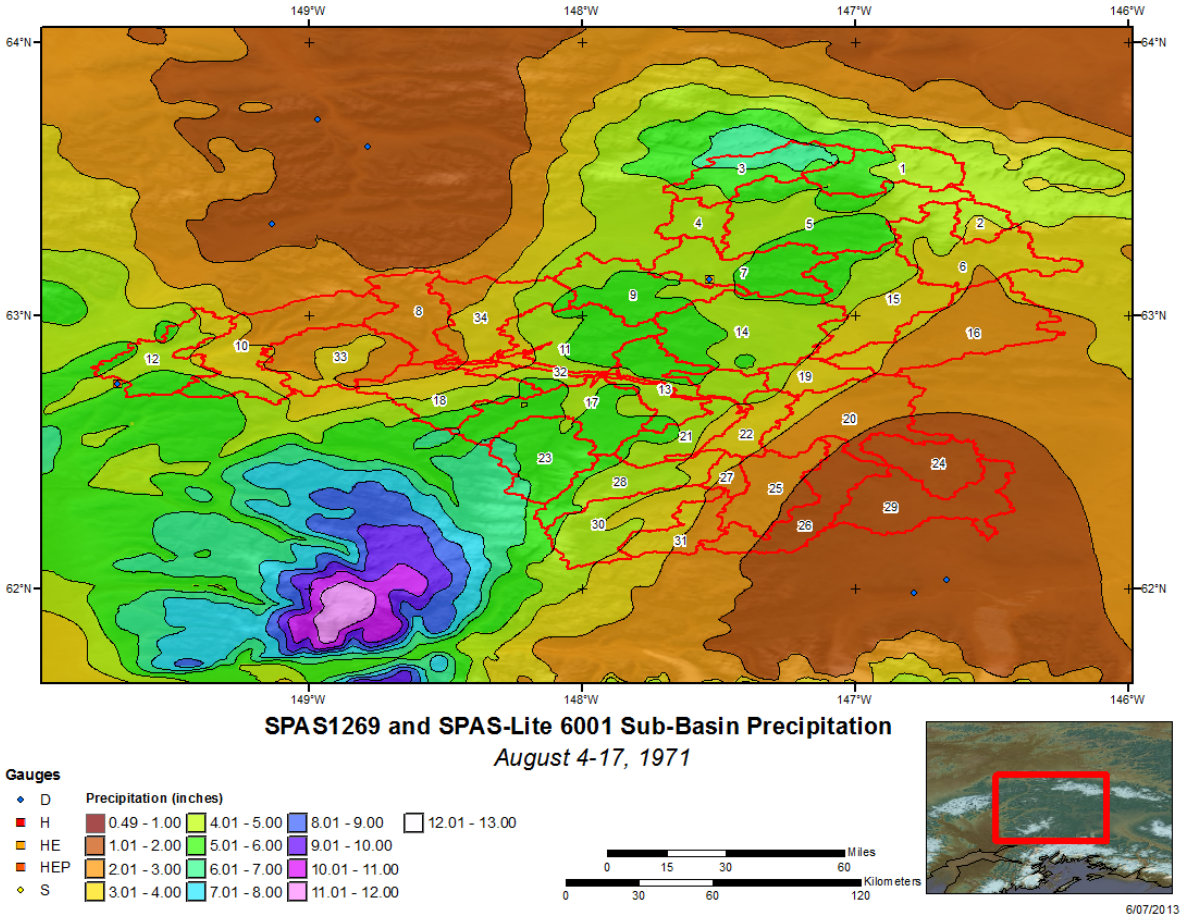

Figure 12.4. Total storm rainfall for SPAS 1269 across Susitna-Watana drainage.

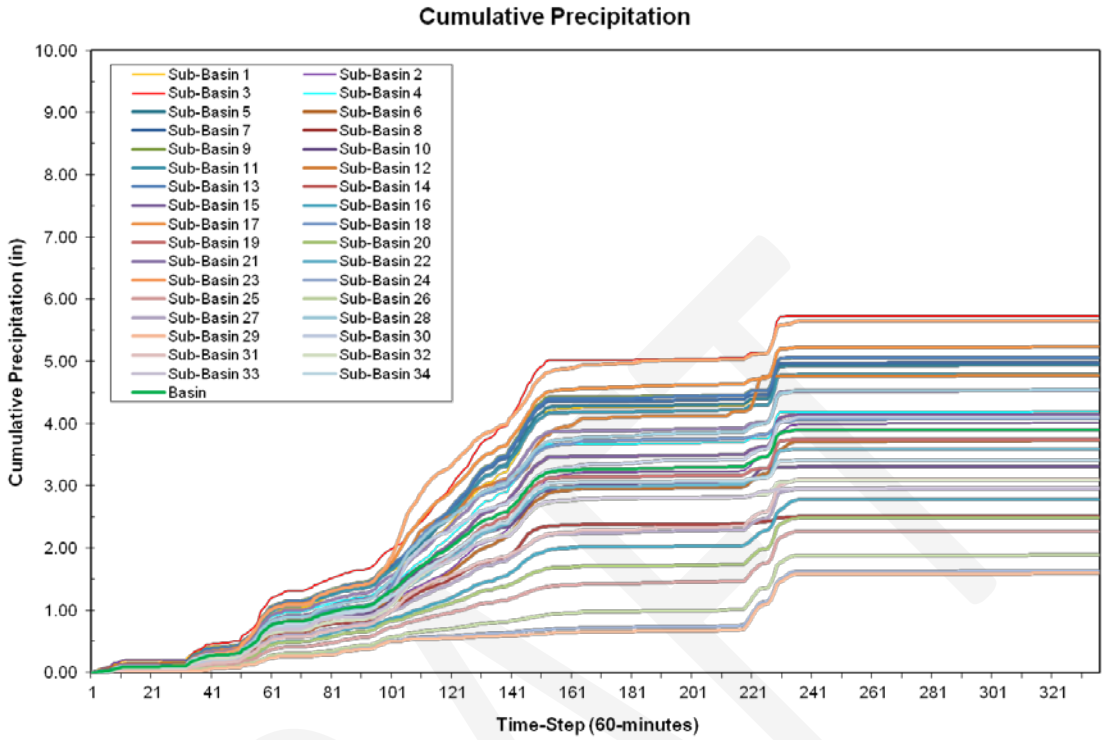

Figure 12.5. Susitna-Watana sub-basin average accumulated rainfall SPAS 1269.

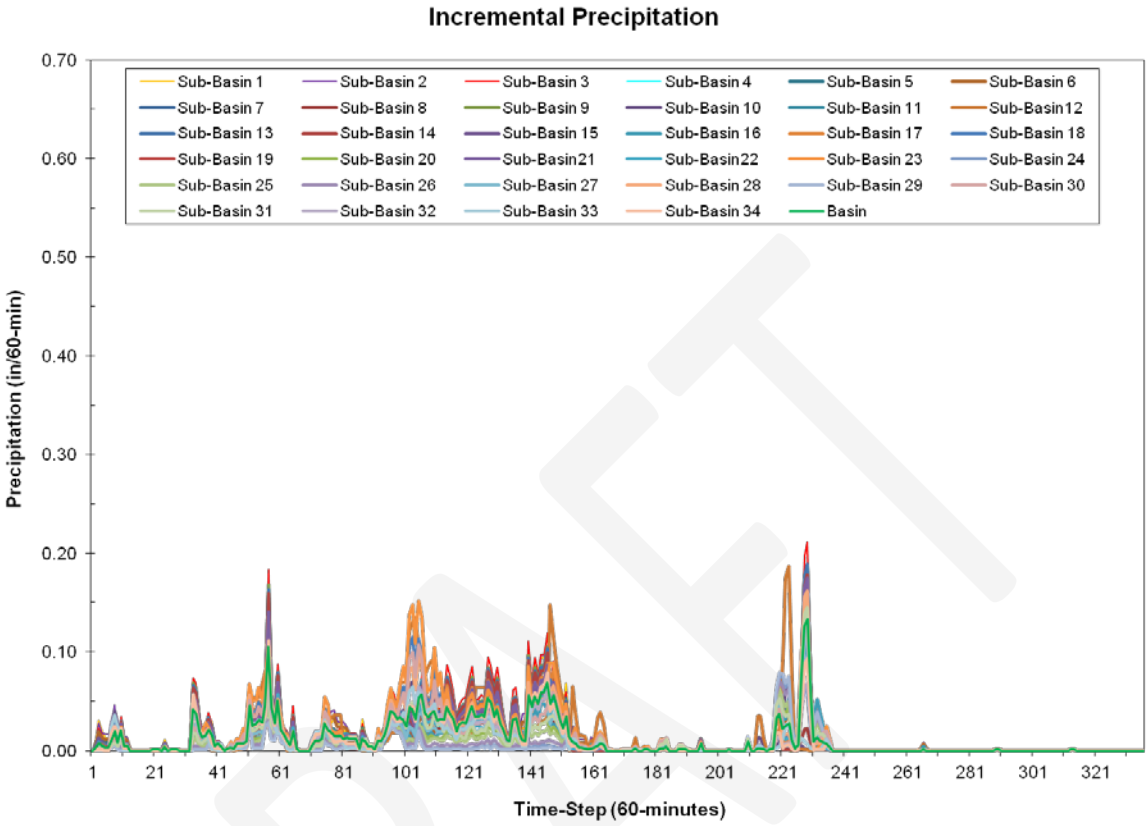

Figure 12.6. Susitna-Watana sub-basin average incremental rainfall SPAS 1269.

12.2.3 August 8-21, 1967 Precipitation

The hourly precipitation grids derived from the SPAS 1270 analysis were used in conjunction with SPAS-Lite 6002 as the basis for the Susitna-Watana calibration. SPAS-Lite 6002 was utilized to fill in a longer duration than what was analyzed for SPAS 1270, the calibration period is referenced as SPAS 1270. The SPAS 1270 analysis encompassed the 34 sub-basins of Susitna-Watana. The SPAS 1270 hourly grids were clipped to each of the Susitna-Watana sub-basins, the sub-basin average statistics were calculated and added to an Excel spreadsheet used for hydrologic calibration. The calibration deliverables are based on the SPAS hourly precipitation data for 8/8-21/1967. In general, between 0.50 and 7.20 inches of rain fell across the Susitna-Watana drainage (Figure 12.7 - 12.9).

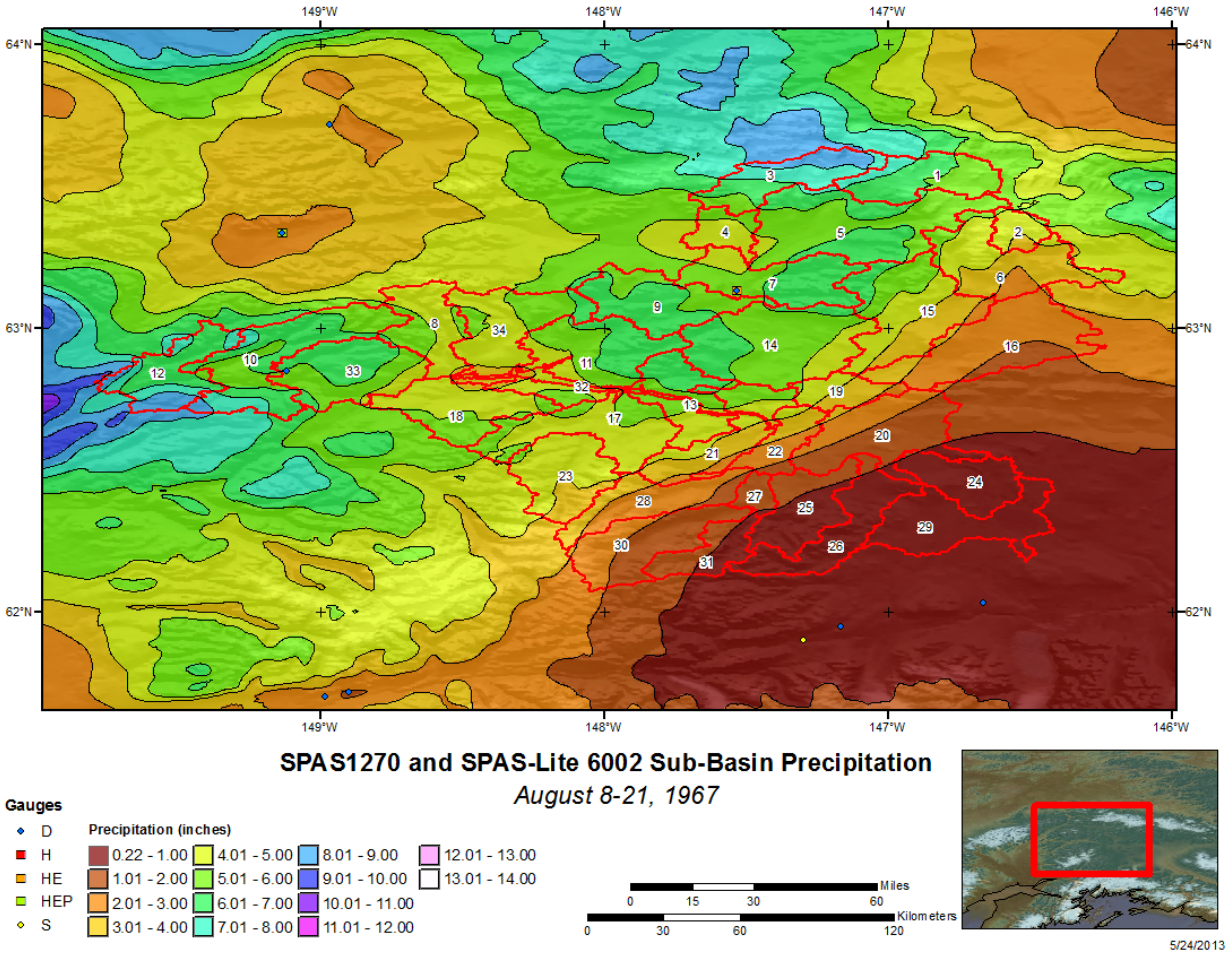

Figure 12.7. Total storm rainfall for SPAS 1270 across Susitna-Watana drainage.

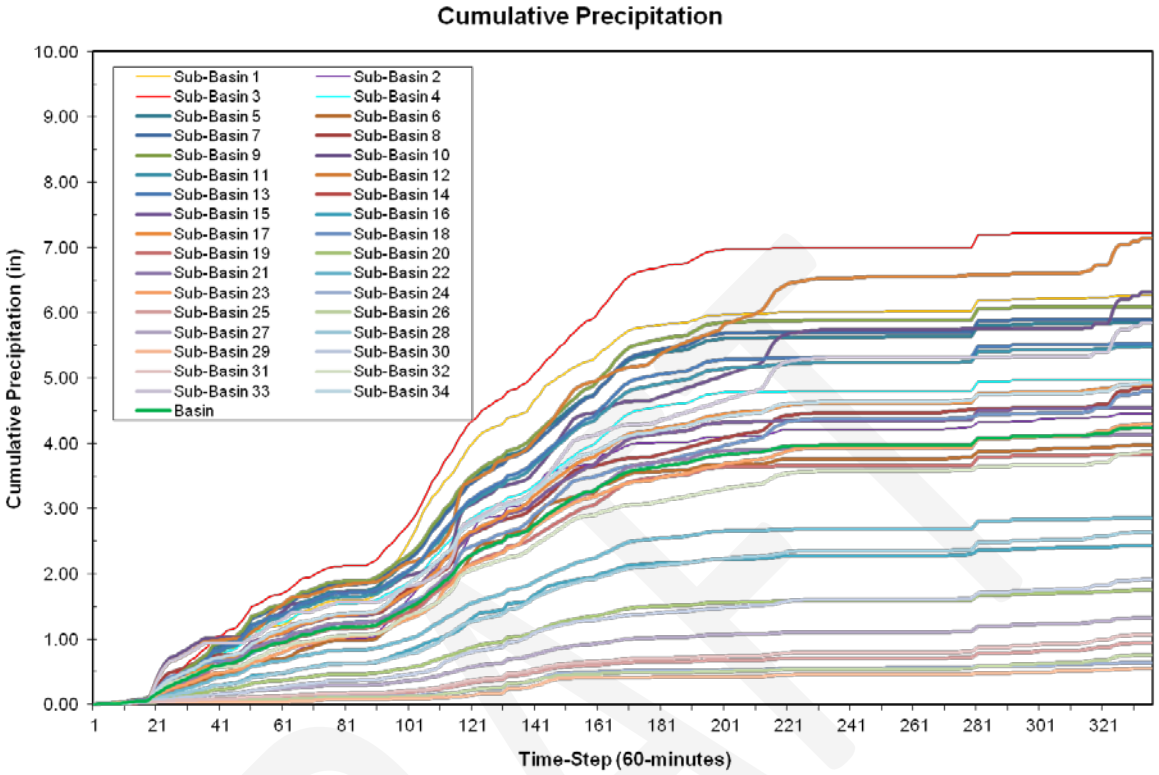

Figure 12.8. Susitna-Watana sub-basin average accumulated rainfall SPAS 1270.

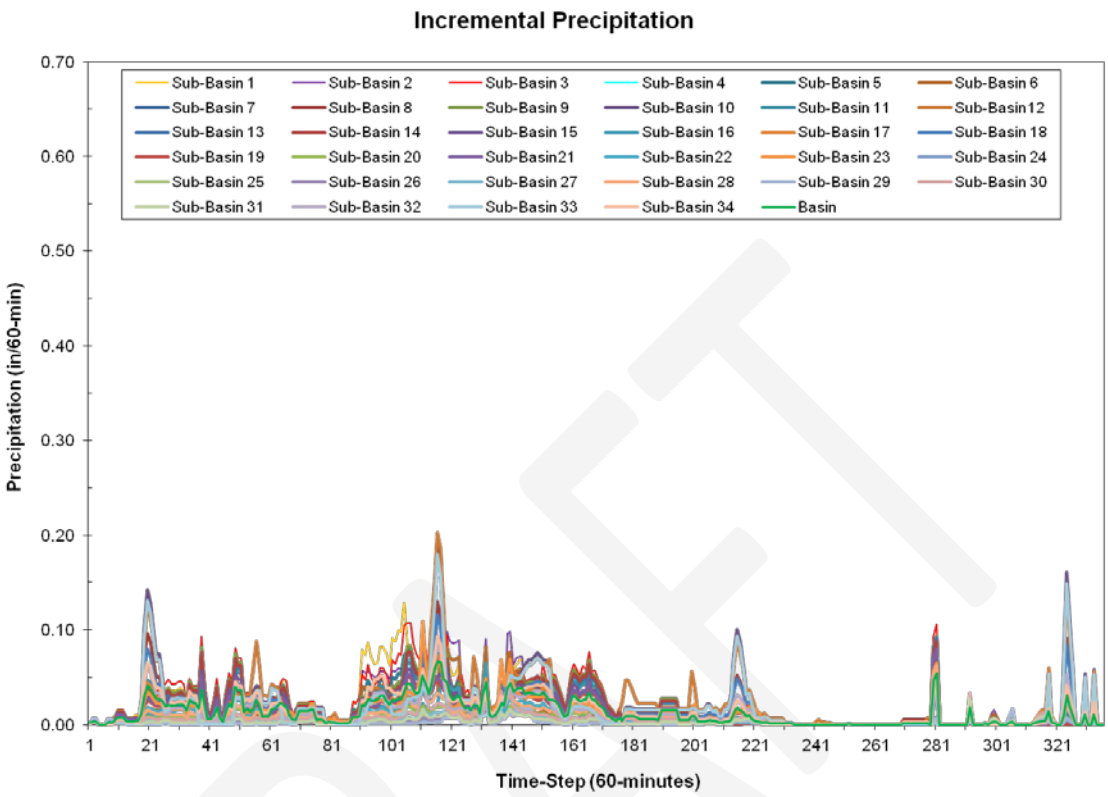

Figure 12.9. Susitna-Watana sub-basin average incremental rainfall SPAS 1270.

12.2.4 May 27, 1964 - June 13, 1964 Precipitation

The hourly precipitation grids derived from the SPAS-Lite 6008 analysis were used as the basis for the Susitna-Watana basin calibration. The SPAS-Lite 6008 analysis encompassed the 34 sub-basins of Susitna-Watana. The SPAS-Lite 6008 hourly grids were clipped to each of the Susitna-Watana sub-basins, the sub-basin average statistics were calculated and added to an Excel spreadsheet used for hydrologic calibration. The calibration deliverables are based on the SPAS hourly precipitation data for 5/27/1964 - 6/13/1964. In general, between 0.20 and 1.50 inches of rain fell across the Susitna-Watana drainage (Figure 12.10 - 12.12).

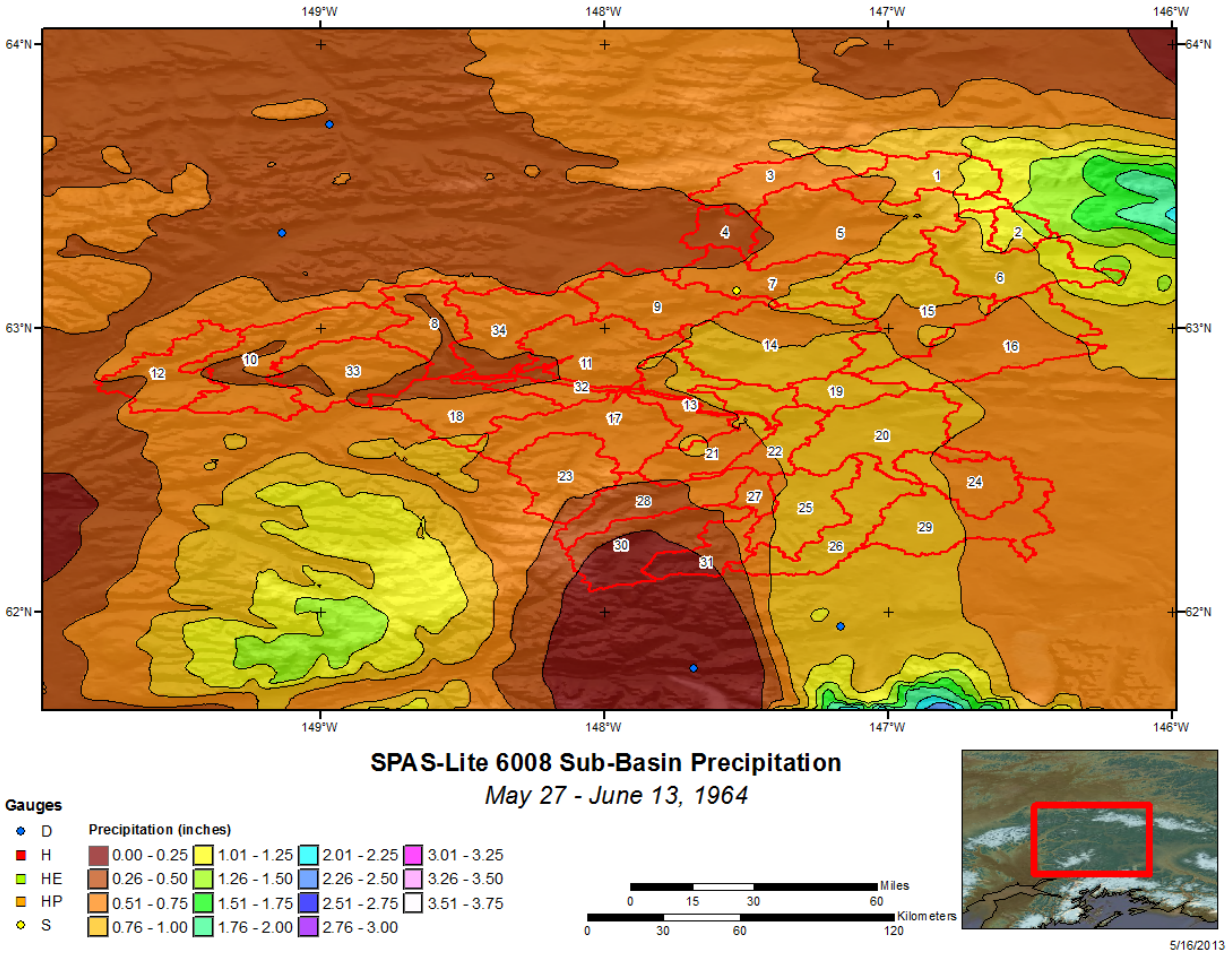

Figure 12.10. Total storm rainfall for SPAS 6008 across Susitna-Watana drainage.

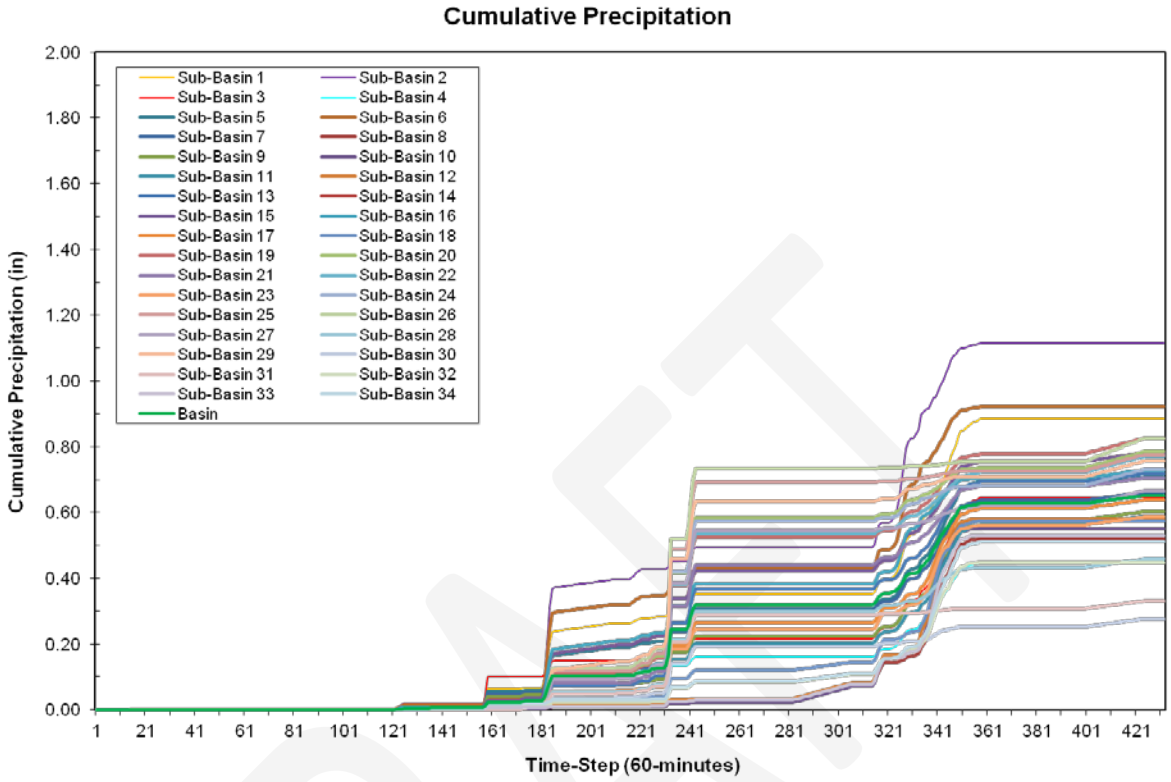

Figure 12.11. Susitna-Watana sub-basin average accumulated rainfall SPAS 6008.

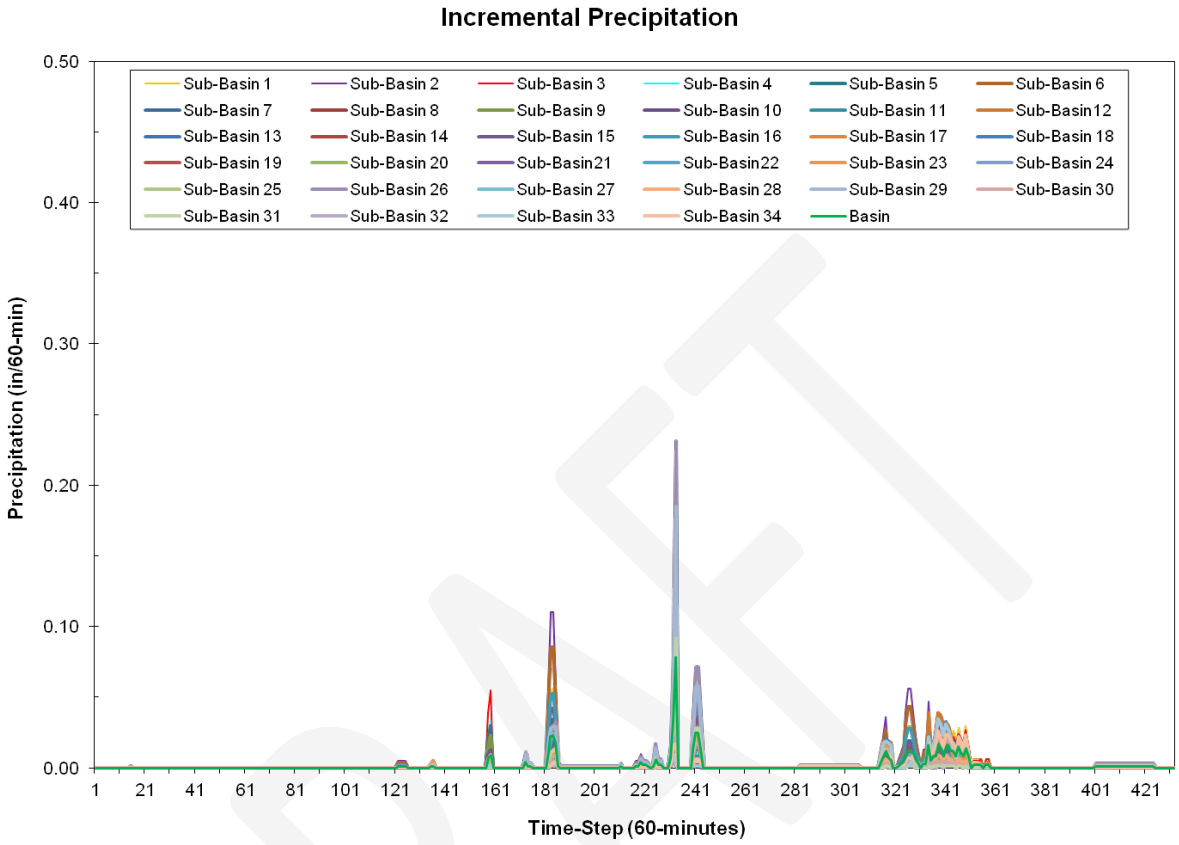

Figure 12.12. Susitna-Watana sub-basin average incremental rainfall SPAS 6008.

12.2.5 June 3-17, 1971 Precipitation

The hourly precipitation grids derived from the SPAS-Lite 6009 analysis were used as the basis for the Susitna-Watana basin calibration. The SPAS-Lite 6009 analysis encompassed the 34 sub-basins of Susitna-Watana. The SPAS-Lite 6009 hourly grids were clipped to each of the Susitna-Watana sub-basins, the sub-basin average statistics were calculated and added to an Excel spreadsheet used for hydrologic calibration. The calibration deliverables are based on the SPAS hourly precipitation data for 6/3-17/1971. In general, between 0.20 and 1.30 inches of rain fell across the Susitna-Watana drainage (Figure 12.13 - 12.15).

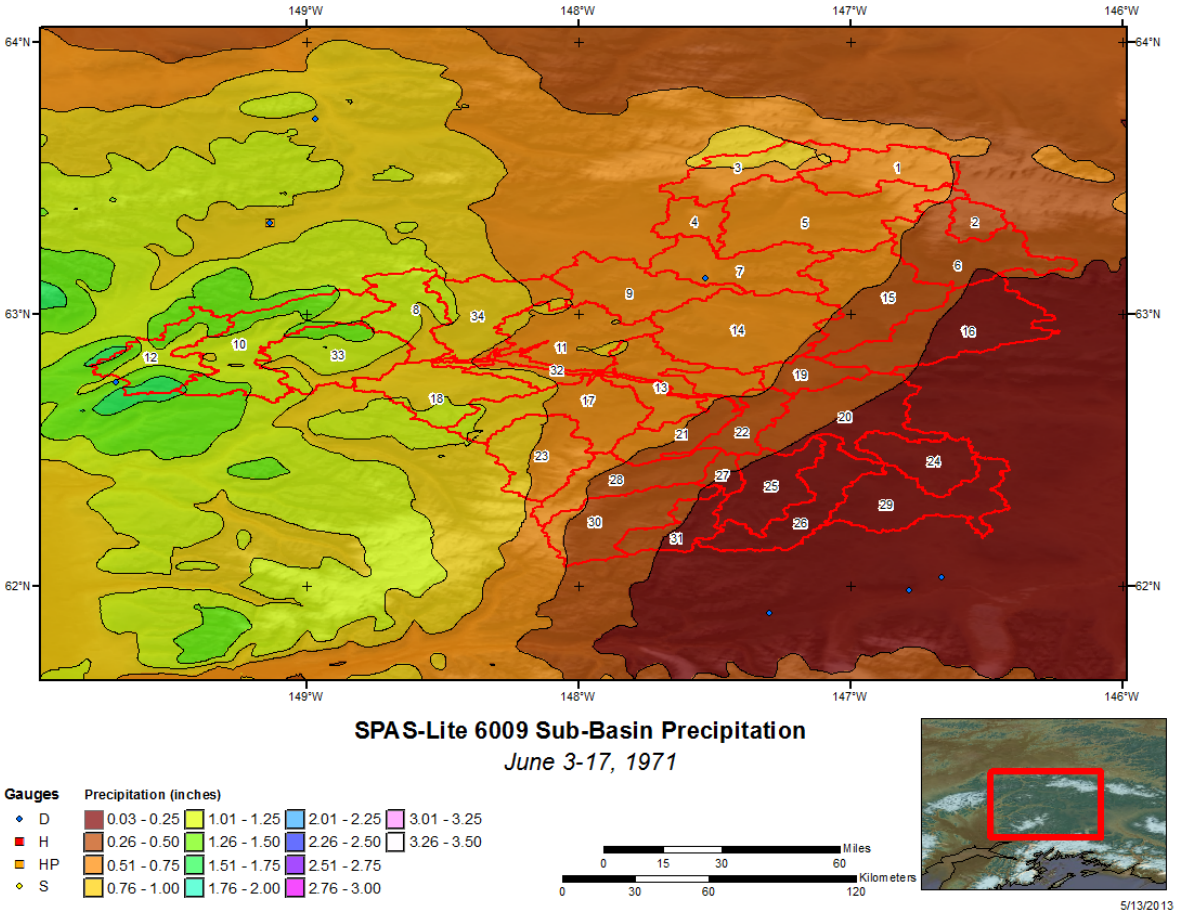

Figure 12.13. Total storm rainfall for SPAS 6009 across Susitna-Watana drainage.

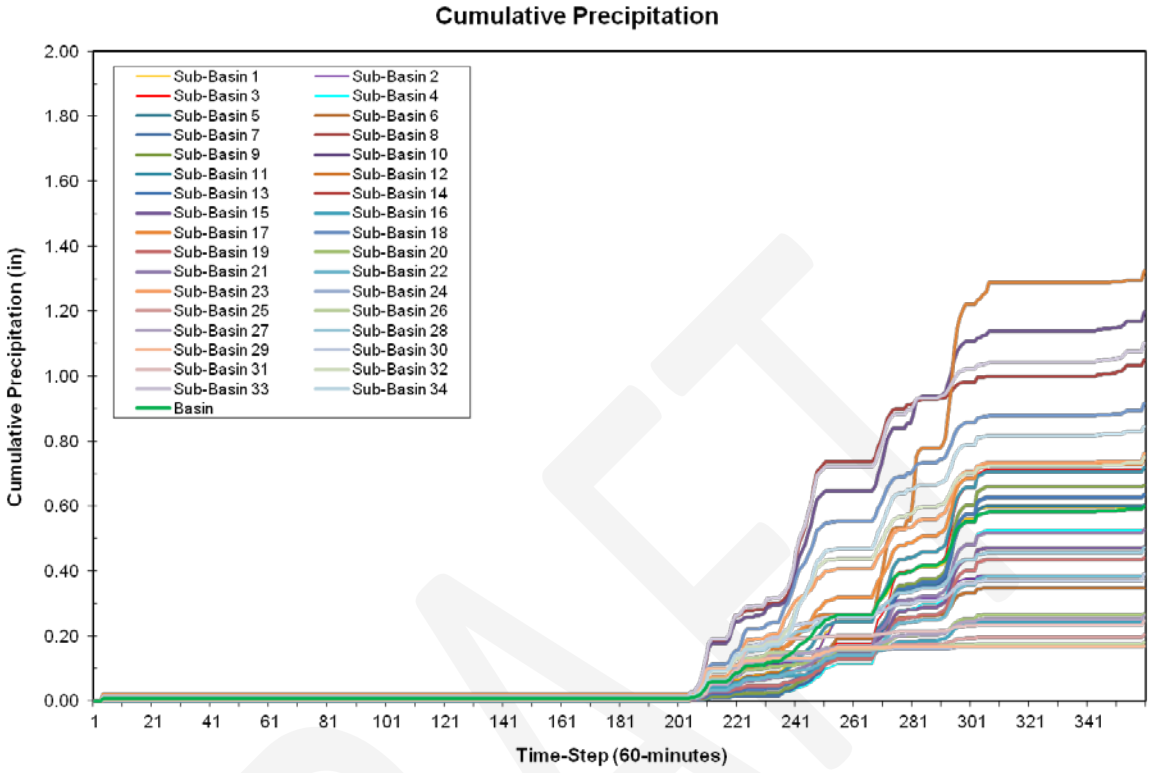

Figure 12.14. Susitna-Watana sub-basin average accumulated rainfall SPAS 6009.

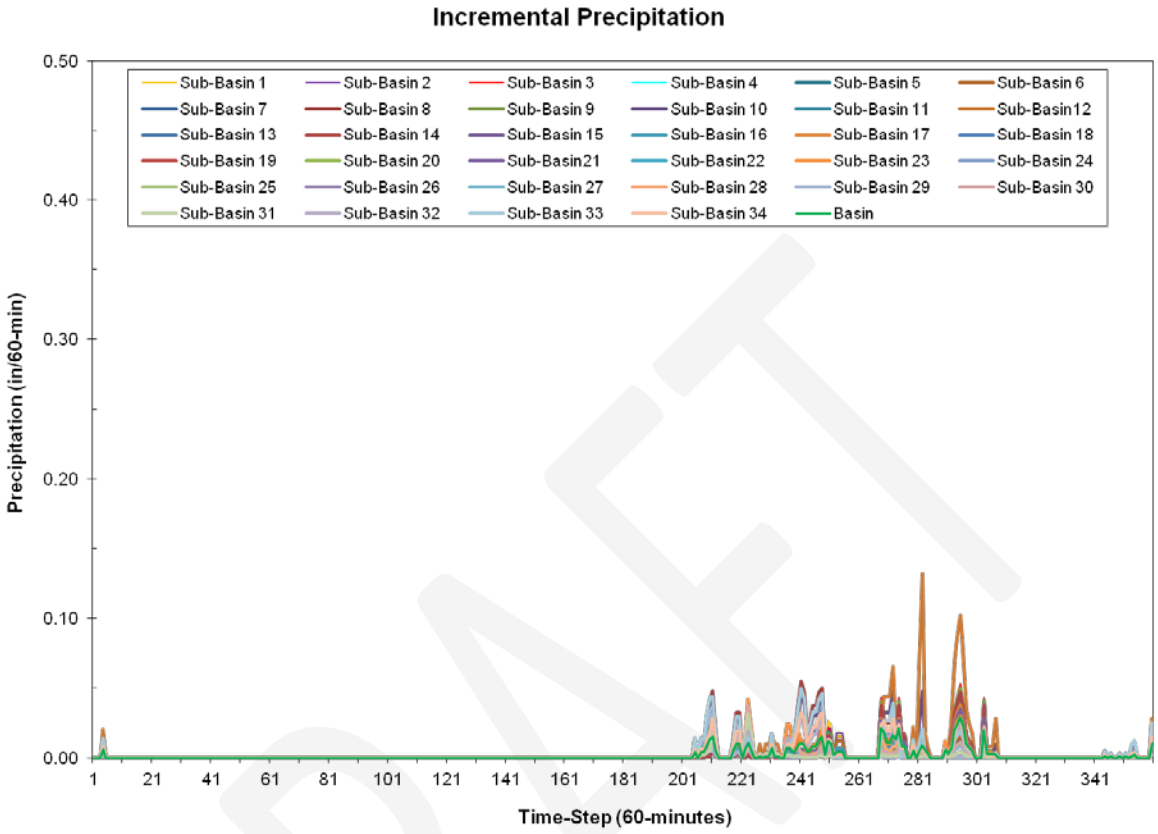

Figure 12.15. Susitna-Watana sub-basin average incremental rainfall SPAS 6009.

12.2.6 June 7-22, 1972 Precipitation

The hourly precipitation grids derived from the SPAS-Lite 6010 analysis were used as the basis for the Susitna-Watana basin calibration. The SPAS-Lite 6010 analysis encompassed the 34 sub-basins of Susitna-Watana. The SPAS-Lite 6010 hourly grids were clipped to each of the Susitna-Watana sub-basins, the sub-basin average statistics were calculated and added to an Excel spreadsheet used for hydrologic calibration. The calibration deliverables are based on the SPAS hourly precipitation data for 6/7-22/1972. In general, between 0.50 and 1.50 inches of rain fell across the Susitna-Watana drainage (Figure 12.16 - 12.18).

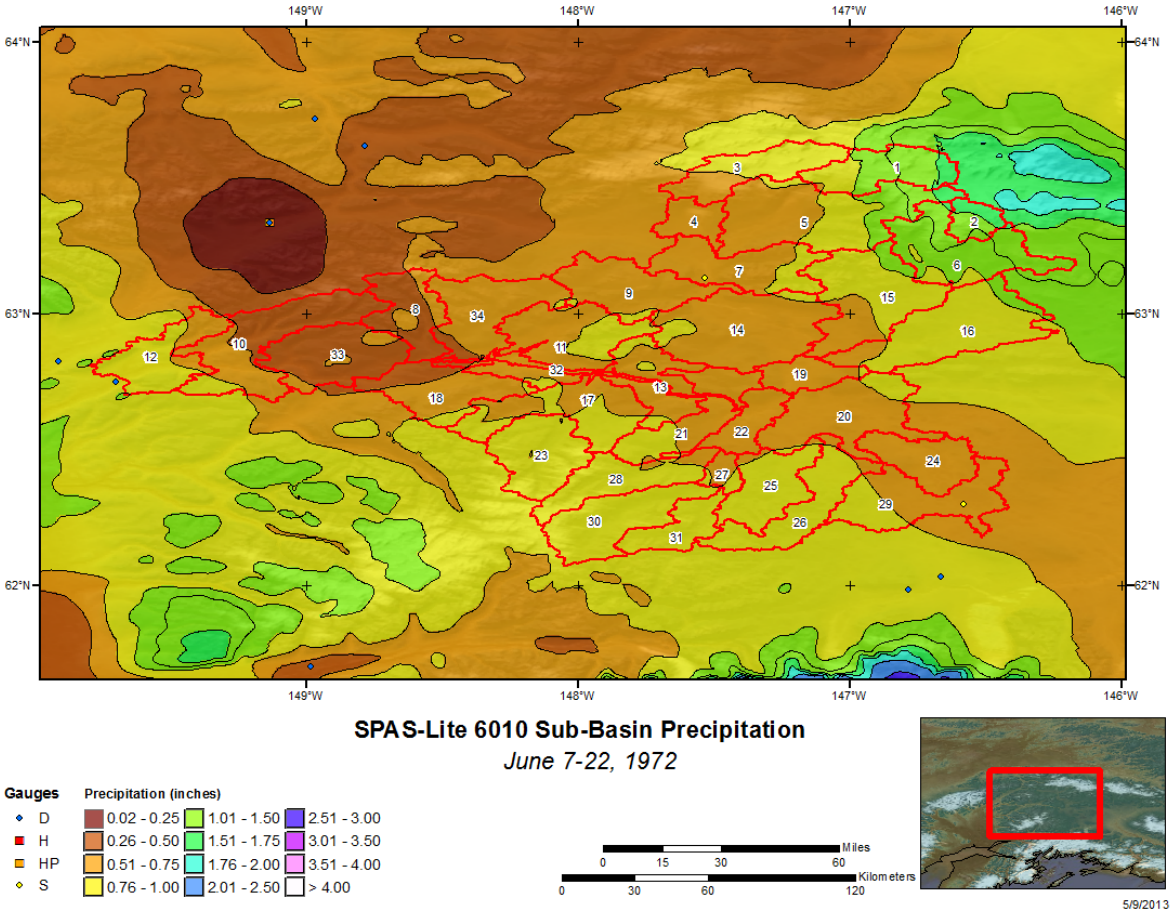

Figure 12.16. Total storm rainfall for SPAS 6010 across Susitna-Watana drainage.

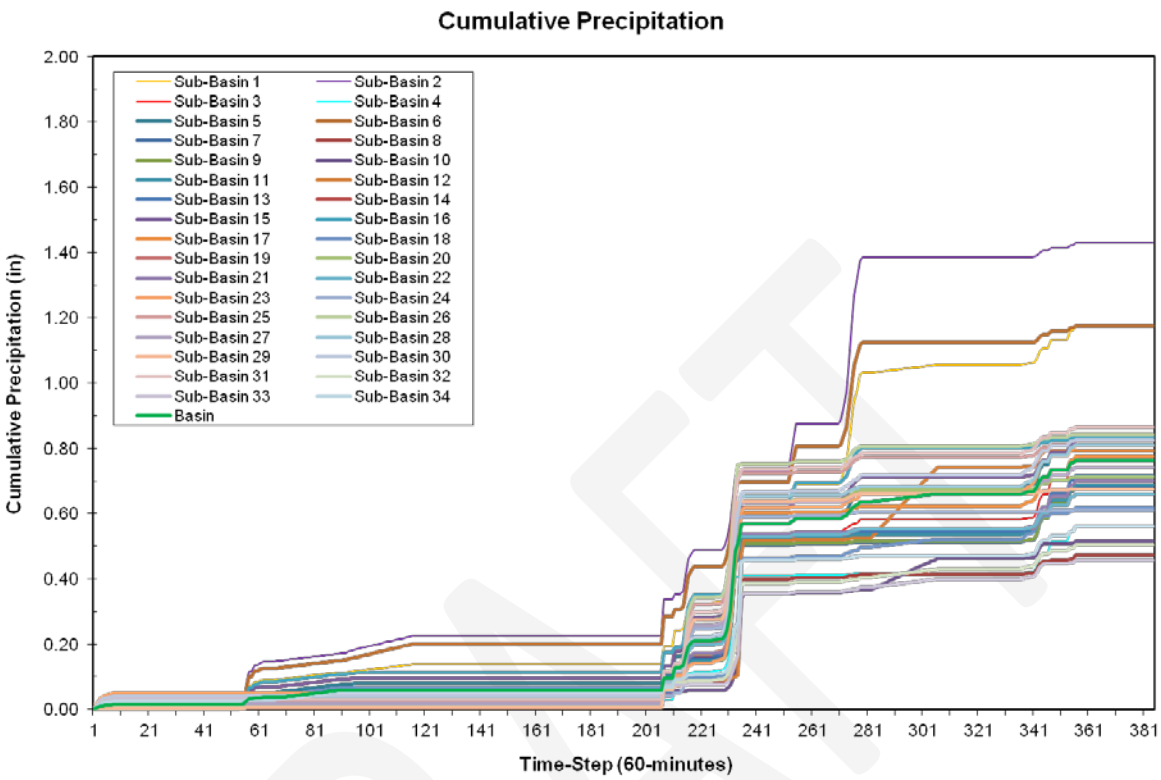

Figure 12.17. Susitna-Watana sub-basin average accumulated rainfall SPAS 6010.

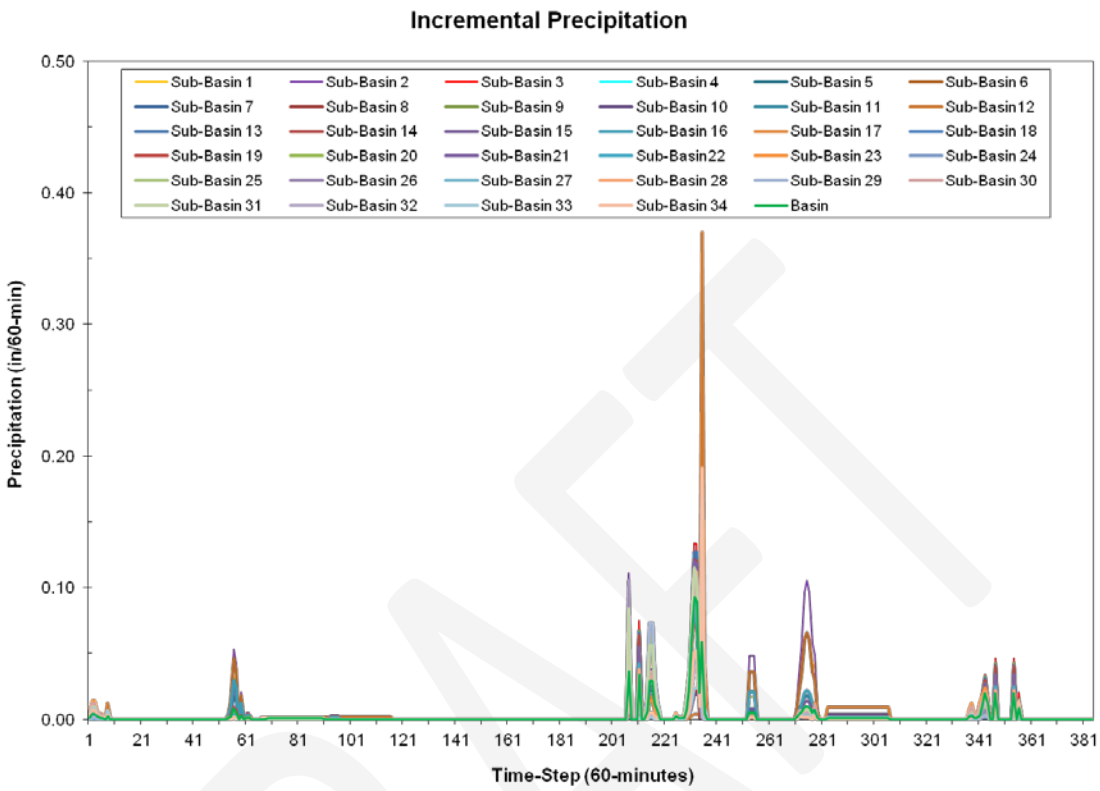

Figure 12.18. Susitna-Watana sub-basin average incremental rainfall SPAS 6010.

12.3 Meteorological Time Series for Calibration Events

Hourly meteorological time series were developed for the six calibration events (see Table 12. 1). The meteorological time series parameters derived were temperature, dew point temperature and wind speed over the Susitna-Watana basin. The hydrologic model requirements were a single temperature and dew point temperature time series at a given base elevation and wind speed at 1000-feet increments from 0-feet to 15000-feet. Temperature lapse rates were estimated using observed surface temperature data for stations in and around the Susitna River basin and the Fairbanks and Anchorage radiosonde data.

Vertical wind speed profiles at 1000-feet increments were derived base on wind speed data from the Fairbanks radiosonde data and observed surface wind speed data for stations in and around the Susitna-Watana basin. The radiosonde wind speed represents free atmospheric wind (unobstructed flow). The free-air data were adjusted to surface wind speeds elevations based on comparisons of anemometer level wind speeds with concurrent free-air wind speeds. The wind speed derivation methodology was based on methods described in HMR 42 (Weather Bureau 1966). HMR 42 measured winds at Gulkana glacier (4800 feet) and compared to free-air winds at Fairbanks, the study found that average wind on the glacier to be 0.60 that of the free-air. In this updated analysis,

comparisons were made using both Anchorage and Fairbanks radiosonde data. This analysis showed the Anchorage radiosonde data were not as representative of the surface wind speeds over the basin based on comparisons made to the September 2012 storm event. Instead, the Fairbanks data better represented the timing and magnitude of the observed surface wind speeds.

12.3.1 September 14-30, 2012 Meteorological Time Series

Temperature lapse rates were estimated using observed surface temperature data for stations in and around the Susitna-Watana basin. Lapse rates were derived each hour using observed surface data at two locations. Station based lapse rates were calculated between: i) Independence Mine and Talkeetna, ii) PAZK and Talkeetna, iii) PAZK and Renee, and iv) Monahan Flats and McKinley. The hourly lapse rates were used to calculate an average lapse rate for the entire calibration period and an average lapse rate based on when rain was occurring during the calibration event (Table 12.2).

Station data were also used to derive an average station based lapse rate for each hour of the storm event. The stations used for this analysis were PAZK, PANC, Blair Lakes, Dunkle Hills, Eielson VC, Paxson, Renee, Toklat, Independence Mine, Monahan Flat, Susitna VH, Tokositna Valley, Fairbanks, Ft Greeley, Gulkana, Mckinley NP, Palmer, and Talkeetna. The station average lapse rate was derived using linear regression between temperature and elevation. Based on the hourly station data linear relationship, a lapse rate (regression slope) was calculated for each hour of the analysis period. The average of the station based lapse rates (based on linear regression) was compared to individual station (station 1 @ X elevation compared to station 2 @ X elevation) based lapse rates discussed above (Table 12.2).

Vertical temperature at 1000-foot increments from 0-feet to 6000-feet were derived base on temperature data from the Fairbanks radiosonde. The Fairbanks radiosonde lapse rate data were used to calculate an average lapse rate for the entire calibration period (Table 12.2). The radiosonde wind speed represents free atmospheric winds, unobstructed flow, the free-air data were adjusted to surface wind speeds based on comparisons of anemometer level wind speeds with concurrent free-air wind speeds. Surface wind speeds were compared at six locations with varying elevations across the Susitna River basin to the Fairbanks free-air wind speeds. The average free-air adjustment for the six stations was 0.620 with a maximum of 0.968 and a minimum of 0.385 (Table 12.3). In order to convert free-air wind speed data to anemometer level wind speeds the adjustment/ratio is applied to the free-air data. For example, at 1000-foot elevation free-air wind speed is 45-mph would be 30-mph at the anemometer level (45-mph * 0.666 = 30-mph). The radiosonde data are measured every 12-hours (0-UTC and 12-UTC), the 12-hour data were interpolated to hourly data using the bounding hourly data and a linear relationship.

Table 12.2. Station based and radiosonde based lapse rates for September 14-30, 2012.

Station Comparisons	Hourly Average	Hourly Rainfall Average	FAI Radiosonde
Indep. Mine vs. Talkeetna	-2.50	-1.98	-
PAZK vs. Talkeetna	-2.17	-1.69	-
PAZK vs. Renee	-3.10	-3.64	-
Monahan Flat vs. McKinley	-1.73	-2.53	-
All Stations	-2.40	-2.38	-
Average	-2.38	-2.44	-2.43

Table 12.3. Fairbanks radiosonde free-air wind speed conversion ratio to anemometer height wind speed for September 14-30, 2012.

Station	Elevation (ft)	FAI Radiosonde Ratio
Gulkana	1500	0.968
McKinley	1500	0.471
Talkeetna	500	0.769
PAZK	3500	0.385
Renee	2500	0.623
Eielson	3500	0.505
	Average	*0.620*
	Maximum	0.968
	Minimum	0.385

The final temperature and dew point temperature series were based on surface data at Monahan Flats, AK with a base elevation of 2700-foot (Figure 12.19). The Monahan Flats station data were selected because it was within the Susitna River basin and provided a complete and representative profile of temperature and dew point temperature. The lapse rate used to adjust temperature and dew point temperature to other elevations was -2.40°F. The -2.40°F lapse rate was based on the average of all station comparisons. The final vertical wind speed data were based on Fairbanks free-air wind speeds with an adjustment ratio of 0.620 applied to represent anemometer level wind speeds (Figure 12.20).

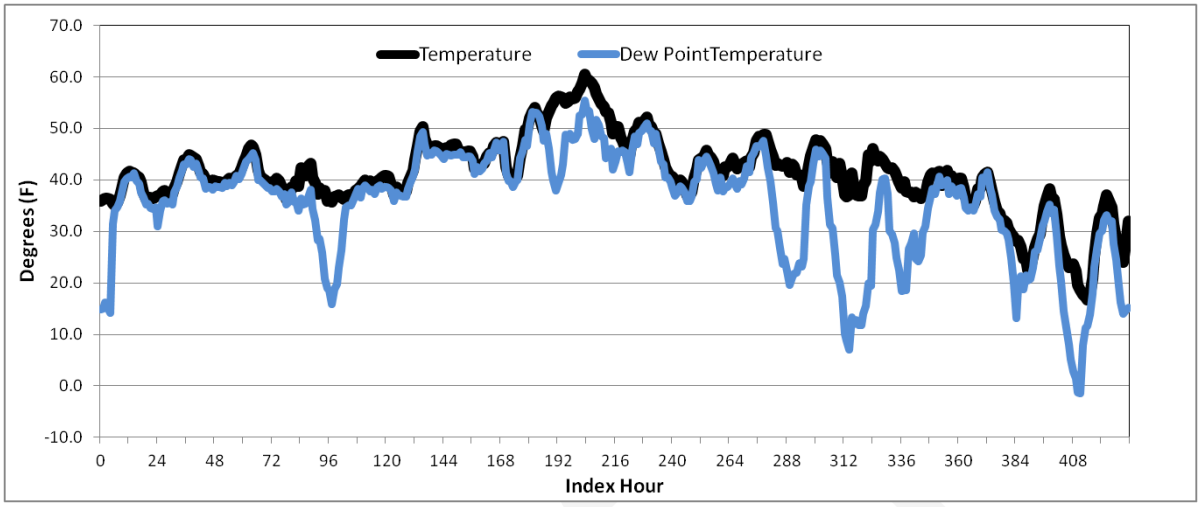

Figure 12.19. Temperature and dew point time series based on surface data at Summit, AK with a base elevation of 2400-ft and lapse rate of -2.40°F for September 14-30, 2012.

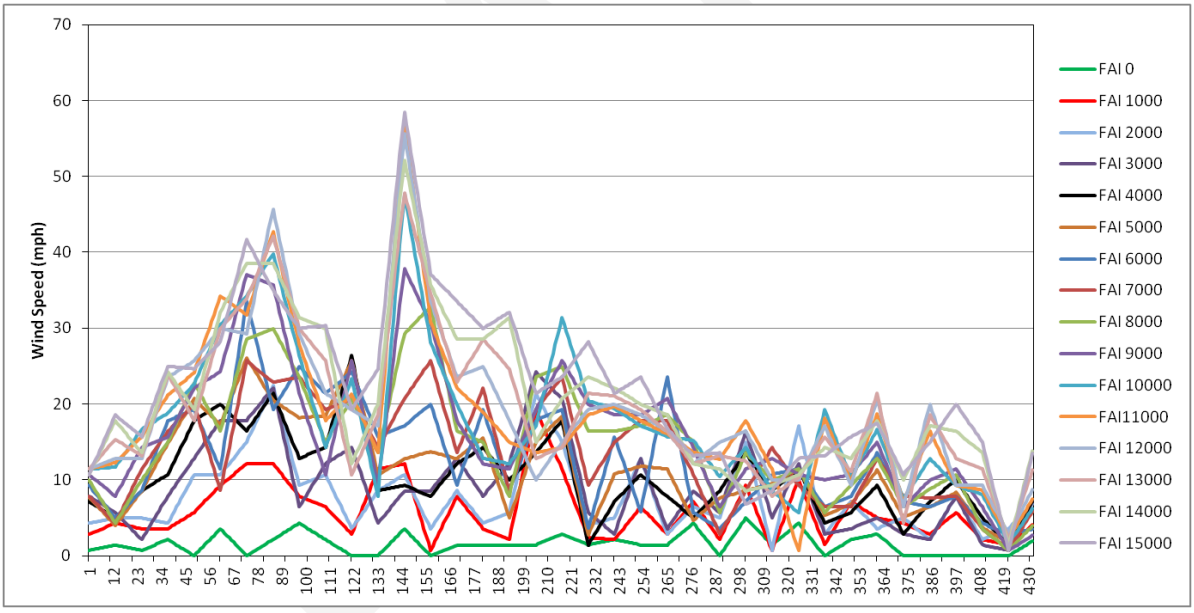

Figure 12.20. Wind speed data based on Fairbanks free-air wind speeds with an adjustment ratio of 0.62 applied to represent anemometer level wind speeds for September 14-30, 2012.

12.3.2 August 4-17, 1971 Meteorological Time Series

Temperature lapse rates were estimated using observed surface temperature data for stations in and around the Susitna-Watana basin. Lapse rates were derived each hour using observed surface data at two locations. Station based lapse rates were calculated between: i) Talkeetna and Summit, ii) Anchorage and Gulkana, iii) Ft Greeley and Summit, and iv) Ft Greeley and Fairbanks. The hourly

lapse rates were used to calculate an average lapse rate for the entire calibration period and an average lapse rate based on when rain was occurring during the calibration event (Table 12.4).

Station data were also used to derive an average station based lapse rate for each hour of the storm event. The stations used for this analysis were PANC, Anchorage, Fairbanks, Ft Greeley, Gulkana, Summit, and Talkeetna. The station average lapse rate was derived using linear regression between temperature and elevation. Based on the hourly station data linear relationship, a lapse rate (regression slope) was calculated for each hour of the analysis period. The average of the station based lapse rates (based on linear regression) was compared to individual station (station 1 @ X elevation compared to station 2 @ X elevation) based lapse rates discussed above (Table 12.4).

Vertical temperature at 1000-foot increments from 0-feet to 6000-feet were derived base on temperature data from the Fairbanks radiosonde. The Fairbanks radiosonde lapse rate data were used to calculate an average lapse rate for the entire calibration period (Table 12.4).

Table 12.4. Station based and radiosonde based lapse rates for August 4-17,1971.

Station Comparisons	Hourly Average	Hourly Rainfall Average	FAI Radiosonde
Talkeetna vs. Summit	-3.31	-2.62	-
Anchorage vs. Gulkana	-0.86	0.17	-
Ft Greely vs. Summit	-3.34	-5.15	-
Ft Greely vs. Fairbanks	-2.47	-2.18	-
All Stations	-2.27	-2.11	-
Average*	-2.85	-3.01	-3.40

* Comparison excludes Anchorage vs. Gulkana lapse rate

The radiosonde wind speed represents free atmospheric winds, unobstructed flow, the free-air data were adjusted to surface wind speeds elevations based on comparisons of anemometer level wind speeds with concurrent free-air wind speeds. Surface wind speeds were compared at six locations with varying elevations across the Susitna River basin to the Fairbanks free-air wind speeds (Table 12.5). The average free-air adjustment for the six stations was 0.666 with a maximum of 0.895 and a minimum of 0.390. In order to convert free-air wind speed data to anemometer level wind speeds the adjustment/ratio is applied to the free-air data. For example, at 1000-foot elevation free-air wind speed is 45-mph would be 30-mph at the anemometer level (45-mph * 0.666 = 30-mph). The radiosonde data are measured every 12-hours (0-UTC and 12-UTC), the 12-hour data were interpolated to hourly data using the bounding hourly data and a linear relationship.

Table 12.5. Fairbanks radiosonde free-air wind speed conversion ratio to anemometer height wind speed for August 4-17, 1971.

Station	Elevation (ft)	FAI Radiosonde Ratio
Gulkana	1500	0.768
Summit	2500	0.608
Talkeetna	500	0.390
Anchorage	0	0.869
Ft Greely	1500	0.468
Fairbanks	500	0.895
	Average	*0.666*
	Maximum	0.895
	Minimum	0.390

The final temperature and dew point temperature series were based on surface data at Summit, AK with a base elevation of 2400-foot (Figure 12.21). The Summit station data were selected because it was in close proximity to the Susitna River basin and provided a complete and representative profile of temperature and dew point temperature. The lapse rate used to adjust temperature and dew point temperature to other elevations was -2.85°F. The -2.85°F lapse rate was based on the average of all station comparison except the Anchorage and Gulkana comparison. The final vertical wind speed data were based on Fairbanks free-air wind speeds with an adjustment ratio of 0.666 applied to represent anemometer level wind speeds (Figure 12.22).

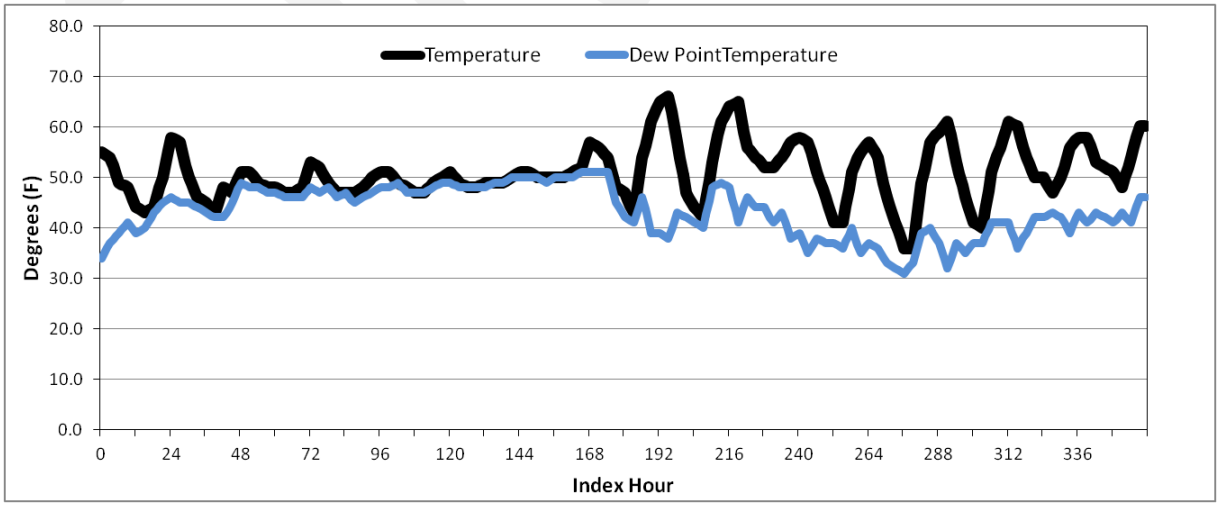

Figure 12.21. Temperature and dew point temperature series based on surface data at Summit, AK with a base elevation of 2400-ft and lapse rate of -2.85°F for August 4-17, 1971.

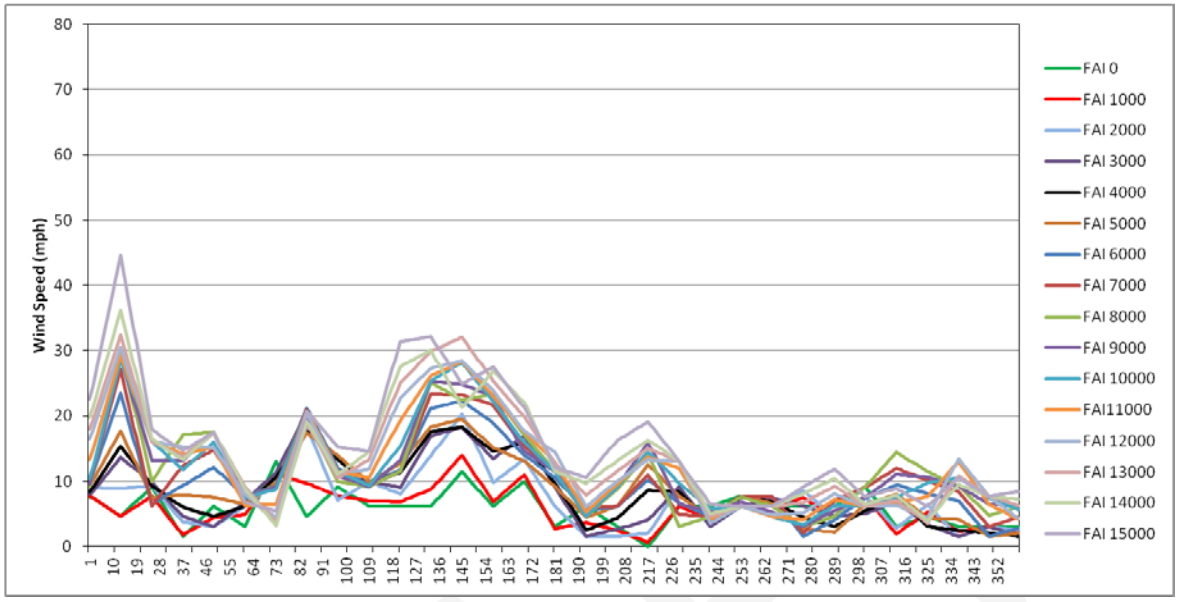

Figure 12.22. Wind speed data based on Fairbanks free-air wind speeds with an adjustment ratio of 0.666 applied to represent anemometer level wind speeds for August 4-17,1971.

12.3.3 August 8-21, 1967 Meteorological Time Series

Temperature lapse rates were estimated using observed surface temperature data for stations in and around the Susitna-Watana basin. Lapse rates were derived each hour using observed surface data at two locations. Station based lapse rates were calculated between: i) Talkeetna and Summit, ii) Anchorage and Gulkana, iii) Ft Greeley and Summit, and iv) Ft Greeley and Fairbanks. The hourly lapse rates were used to calculate an average lapse rate for the entire calibration period and an average lapse rate based on when rain was occurring during the calibration event (Table 12.6).

Station data were also used to derive an average station based lapse rate for each hour of the storm event. The stations used for this analysis were KINR, Anchorage, Cordova, Fairbanks, Ft Greeley, Gulkana, Nenana, Summit, and Talkeetna. The station average lapse rate was derived using linear regression between temperature and elevation. Based on the hourly station data linear relationship, a lapse rate (regression slope) was calculated for each hour of the analysis period. The average of the station based lapse rates (based on linear regression) was compared to individual station (station 1 @ X elevation compared to station 2 @ X elevation) based lapse rates discussed above (Table 12.6).

Vertical temperature at 1000-foot increments from 0-feet to 6000-feet were derived base on temperature data from the Fairbanks radiosonde. The Fairbanks radiosonde lapse rate data were used to calculate an average lapse rate for the entire calibration period (Table 12.6).

Table 12.6. Station based and radiosonde based lapse rates for August 8-21, 1967.

Station Comparisons	Hourly Average	Hourly Rainfall Average	FAI Radiosonde
Talkeetna vs. Summit	-3.51	-3.83	-
Anchorage vs. Gulkana	-1.72	-2.13	-
Ft Greely vs. Summit	-7.33	-7.22	-
Ft Greely vs. Fairbanks	0.46	0.17	-
All Stations	-1.39	-1.35	-
Average*	-2.70	-2.87	-3.25

* -2.87 was used based on testing lapse rate at Summit to Anchorage and Nenana

The radiosonde wind speed represents free atmospheric winds, unobstructed flow, the free-air data were adjusted to surface wind speeds elevations based on comparisons of anemometer level wind speeds with concurrent free-air wind speeds. Surface wind speeds were compared at six locations with varying elevations across the Susitna River basin to the Fairbanks free-air wind speeds (Table 12.7). The average free-air adjustment for the six stations was 0.610 with a maximum of 0.813 and a minimum of 0.337. In order to convert free-air wind speed data to anemometer level wind speeds the adjustment/ratio is applied to the free-air data. For example, at 1000-ft elevation free-air wind speed is 45-mph would be 30-mph at the anemometer level (45-mph * 0.620 = 27.5-mph). The radiosonde data are measured every 12-hours (0-UTC and 12-UTC), the 12-hour data were interpolated to hourly data using the bounding hourly data and a linear relationship.

Table 12.7. Fairbanks radiosonde free-air wind speed conversion ratio to anemometer height wind speed for August 8-21, 1967.

Station	Elevation (ft)	FAI Radiosonde Ratio
Gulkana	1500	0.813
Summit	2500	0.643
Talkeetna	500	0.662
Cordova	0	0.337
Ft Greely	1500	0.411
Fairbanks	500	0.519
	Average*	*0.610*
	Maximum	0.813
	Minimum	0.337

* Average excludes Cordova

The final temperature and dew point temperature series were based on surface data at Summit, AK with a base elevation of 2400-foot (Figure 12.23). The Summit station data were selected because it was in close proximity to the Susitna River basin and provided a complete and representative profile of temperature and dew point temperature. The lapse rate used to adjust temperature and dew point temperature to other elevations was -2.87°F. The final vertical wind speed data were based on Fairbanks free-air wind speeds with an adjustment ratio of 0.610 applied to represent anemometer level wind speeds (Figure 12.24).

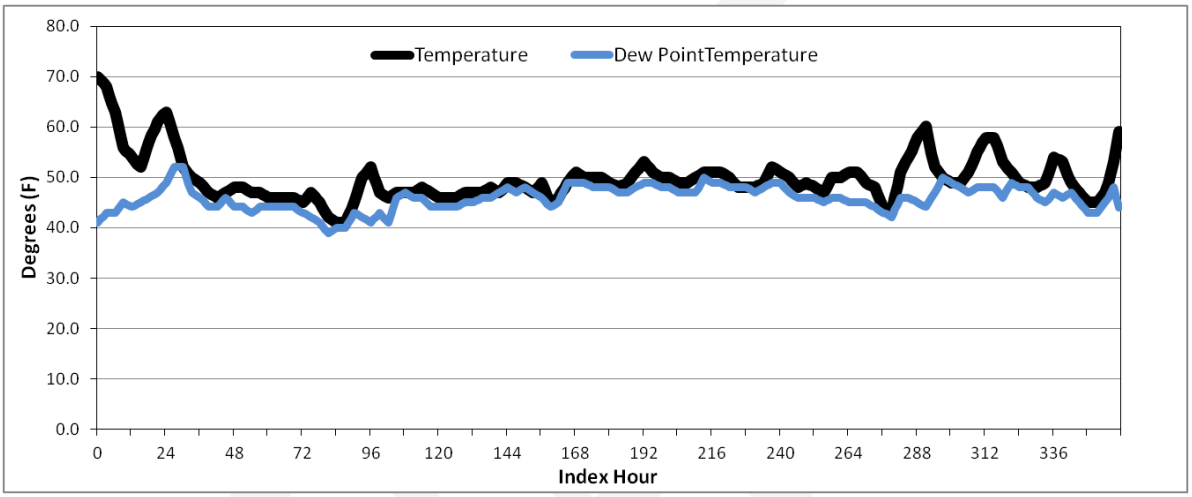

Figure 12.23. Temperature and dew point temperature series based on surface data at Summit, AK with a base elevation of 2400-ft and lapse rate of -2.87°F for August 8-21, 1967.

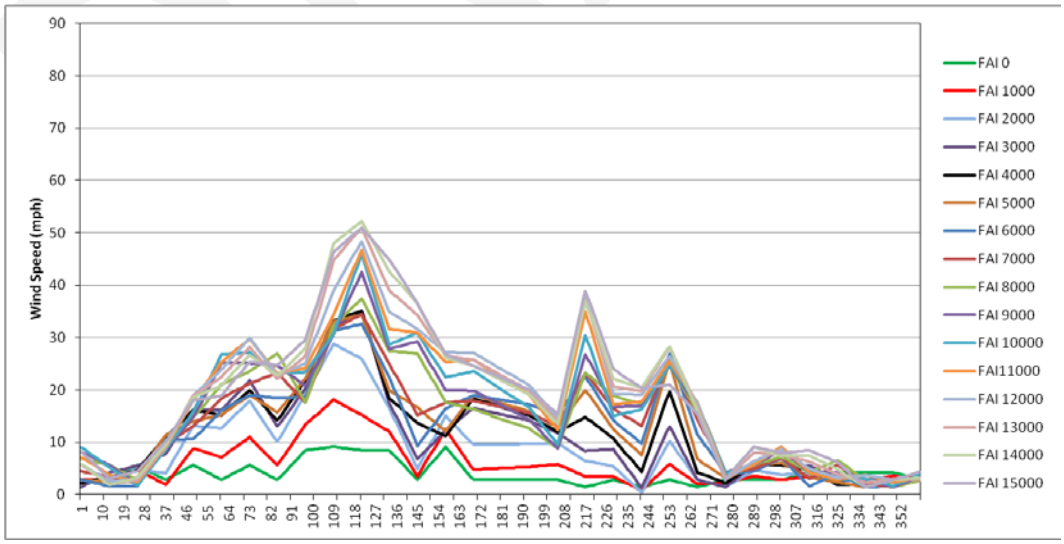

Figure 12.24. Wind speed data based on Fairbanks free-air wind speeds with an adjustment ratio of 0.610 applied to represent anemometer level wind speeds for August 8-21, 1967.

12.3.4 May 27, 1964 - June 13, 1964 Meteorological Time Series

Temperature lapse rates were estimated using observed surface temperature data for stations in and around the Susitna-Watana basin. Lapse rates were derived each hour using observed surface data at two locations. Station based lapse rates were calculated between: i) Talkeetna and Summit, ii) Anchorage and Gulkana, iii) Ft Greeley and Summit, and iv) Ft Greeley and Fairbanks. The hourly lapse rates were used to calculate an average lapse rate for the entire calibration period and an average lapse rate based on when rain was occurring during the calibration event (Table 12.8).

Station data were also used to derive an average station based lapse rate for each hour of the storm event. The stations used for this analysis were PANC, Anchorage, Fairbanks, Ft Greeley, Gulkana, Summit, and Talkeetna. The station average lapse rate was derived using linear regression between temperature and elevation. Based on the hourly station data linear relationship, a lapse rate (regression slope) was calculated for each hour of the analysis period. The average of the station based lapse rates (based on linear regression) was compared to individual station (station 1 @ X elevation compared to station 2 @ X elevation) based lapse rates discussed above (Table 12.8).

Vertical temperature at 1000-foot increments from 0-feet to 6000-feet were derived base on temperature data from the Fairbanks radiosonde. The Fairbanks radiosonde lapse rate data were used to calculate an average lapse rate for the entire calibration period (Table 12.8).

Table 12.8 Station based and radiosonde based lapse rates for May 27 - June 13, 1964.

Station Comparisons	Hourly Average	Hourly Rainfall Average	FAI Radiosonde
Talkeetna vs. Summit	-4.17	-4.09	-
Anchorage vs. Gulkana	0.02	1.35	-
Ft Greely vs. Summit	-5.93	-7.36	-
Ft Greely vs. Fairbanks	-1.18	-0.27	-
All Stations	-3.01	-2.08	-
Average*	-3.57	-3.45	-3.54

* Comparison excludes Anchorage vs. Gulkana lapse rate

The radiosonde wind speed represents free atmospheric winds, unobstructed flow, the free-air data were adjusted to surface wind speeds elevations based on comparisons of anemometer level wind speeds with concurrent free-air wind speeds. Surface wind speeds were compared at six locations with varying elevations across the Susitna River basin to the Fairbanks free-air wind speeds (Table 12.9). The average free-air adjustment for the six stations was 0.614 with a maximum of 0.839 and a minimum of 0.448. In order to convert free-air wind speed data to anemometer level wind speeds the adjustment/ratio is applied to the free-air data. For example, at 1000-ft elevation

free-air wind speed is 45-mph would be 30-mph at the anemometer level (45-mph * 0.614 = 27.6-mph). The radiosonde data are measured every 12-hours (0-UTC and 12-UTC), the 12-hour data were interpolated to hourly data using the bounding hourly data and a linear relationship.

Table 12.9. Fairbanks radiosonde free-air wind speed conversion ratio to anemometer height wind speed for May 27 – June 13, 1964.

Station	Elevation (ft)	FAI Radiosonde Ratio
Gulkana	1500	0.571
Summit	2500	0.615
Talkeetna	500	0.448
Anchorage	0	0.839
Ft Greely	1500	0.525
Fairbanks	500	0.685
	Average	*0.614*
	Maximum	0.839
	Minimum	0.448

The final temperature and dew point temperature series were based on surface data at Summit, AK with a base elevation of 2400-feet (Figure 12.25). The Summit station data were selected because it was in close proximity to the Susitna River basin and provided a complete and representative profile of temperature and dew point temperature. The lapse rate used to adjust temperature and dew point temperature to other elevations was -3.57°F. The -3.57°F lapse rate was based on the average of all station comparison except the Anchorage and Gulkana comparison. The final vertical wind speed data were based on Fairbanks free-air wind speeds with an adjustment ratio of 0.614 applied to represent anemometer level wind speeds (Figure 12.26).

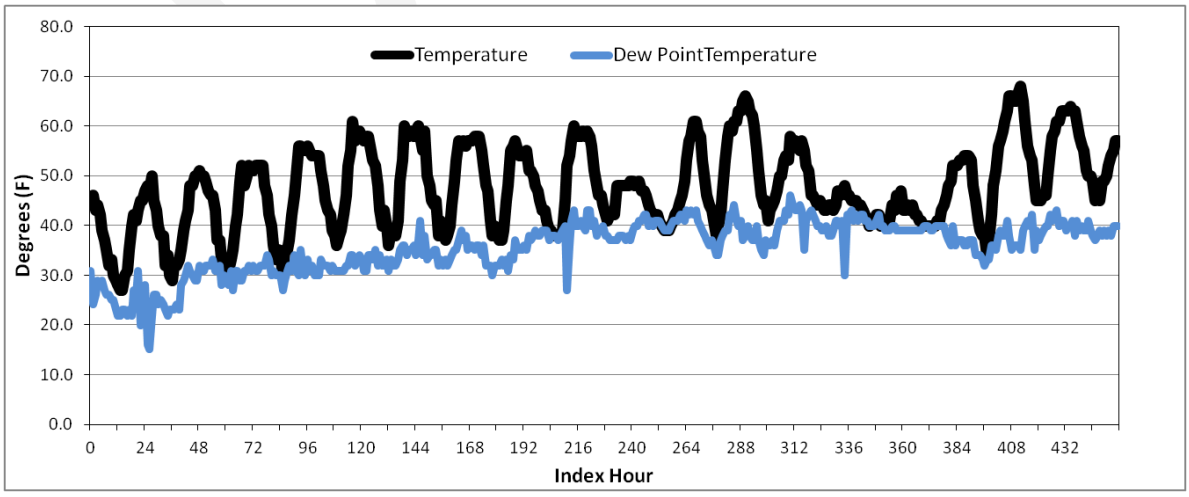

Figure 12.25. Temperature and dew point temperature series based on surface data at Summit, AK with a base elevation of 2400-ft and lapse rate of -3.57°F for May 27 - June 13, 1964.

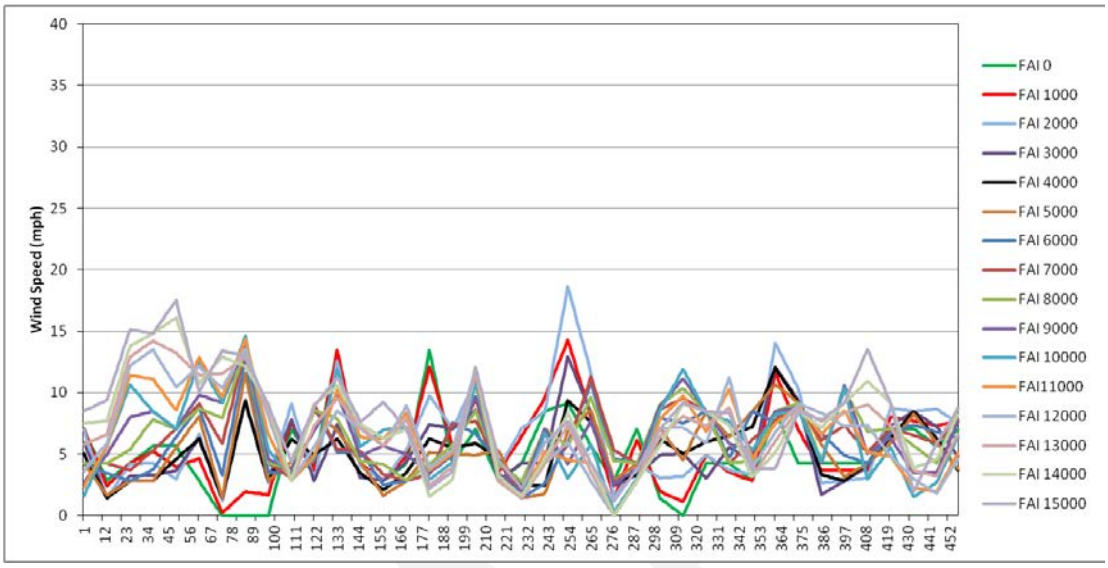

Figure 12.26. Wind speed data based on Fairbanks free-air wind speeds with an adjustment ratio of 0.614 applied to represent anemometer level wind speeds for May 27 - June 13, 1964.

12.3.5 June 3-17, 1971 Meteorological Time Series

Temperature lapse rates were estimated using observed surface temperature data for stations in and around the Susitna-Watana basin. Lapse rates were derived each hour using observed surface data at two locations. Station based lapse rates were calculated between: i) Talkeetna and Summit, ii) Anchorage and Gulkana, iii) Ft Greeley and Summit, and iv) Ft Greeley and Fairbanks. The hourly lapse rates were used to calculate an average lapse rate for the entire calibration period and an average lapse rate based on when rain was occurring during the calibration event (Table 12.10).

Station data were also used to derive an average station based lapse rate for each hour of the storm event. The stations used for this analysis were PANC, Anchorage, Fairbanks, Ft Greeley, Gulkana, Summit, and Talkeetna. The station average lapse rate was derived using linear regression between temperature and elevation. Based on the hourly station data linear relationship, a lapse rate (regression slope) was calculated for each hour of the analysis period. The average of the station based lapse rates (based on linear regression) was compared to individual station (station 1 @ X elevation compared to station 2 @ X elevation) based lapse rates discussed above (Table 12.10).

Vertical temperature at 1000-foot increments from 0-feet to 6000-feet were derived base on temperature data from the Fairbanks radiosonde. The Fairbanks radiosonde lapse rate data were used to calculate an average lapse rate for the entire calibration period (Table 12.10).

Table 12.10. Station based and radiosonde based lapse rates for June 3-17, 1971.

Station Comparisons	Hourly Average	Hourly Rainfall Average	FAI Radiosonde
Talkeetna vs. Summit	-3.89	-3.44	-
Anchorage vs. Gulkana	1.99	0.92	-
Ft Greely vs. Summit	-12.35	-11.15	-
Ft Greely vs. Fairbanks	-3.39	-2.83	-
All Stations	-2.05	-2.49	-
Average*	-3.11	-2.92	-3.76

* Comparison excludes Anchorage vs. Gulkana lapse rate

* Comparison excludes Ft Greeley vs. Summit lapse rate

The radiosonde wind speed represents free atmospheric winds, unobstructed flow, the free-air data were adjusted to surface wind speeds elevations based on comparisons of anemometer level wind speeds with concurrent free-air wind speeds. Surface wind speeds were compared at six locations with varying elevations across the Susitna River basin to the Fairbanks free-air wind speeds (Table 12.11). The average free-air adjustment for the six stations was 0.785 with a maximum of 0.946 and a minimum of 0.493. In order to convert free-air wind speed data to anemometer level wind speeds the adjustment/ratio is applied to the free-air data. For example, at 1000-ft elevation free-air wind speed is 45-mph would be 30-mph at the anemometer level (45-mph * 0.785 = 35.3-mph). The radiosonde data are measured every 12-hours (0-UTC and 12-UTC), the 12-hour data were interpolated to hourly data using the bounding hourly data and a linear relationship.

Table 12.11. Fairbanks radiosonde free-air wind speed conversion ratio to anemometer height wind speed for June 3-17, 1971.

Station	Elevation (ft)	FAI Radiosonde Ratio
Gulkana	1500	0.895
Summit	2500	0.719
Talkeetna	500	0.493
Anchorage	0	0.909
Ft Greely	1500	0.910
Fairbanks	500	0.946
	Average*	*0.785*
	Maximum	0.946
	Minimum	0.493

* Average excludes Anchorage

The final temperature and dew point temperature series were based on surface data at Summit, AK with a base elevation of 2400-feet (Figure 12.28). The Summit station data were selected because it was in close proximity to the Susitna River basin and provided a complete and representative profile of temperature and dew point temperature. The lapse rate used to adjust temperature and dew point temperature to other elevations was -2.90°F. The -2.90°F lapse rate was based on the average of all station comparison except the Anchorage and Gulkana comparison and Ft Greeley and Summit comparison. The final vertical wind speed data were based on Fairbanks free-air wind speeds with an adjustment ratio of 0.785 applied to represent anemometer level wind speeds (Figure 12.28).

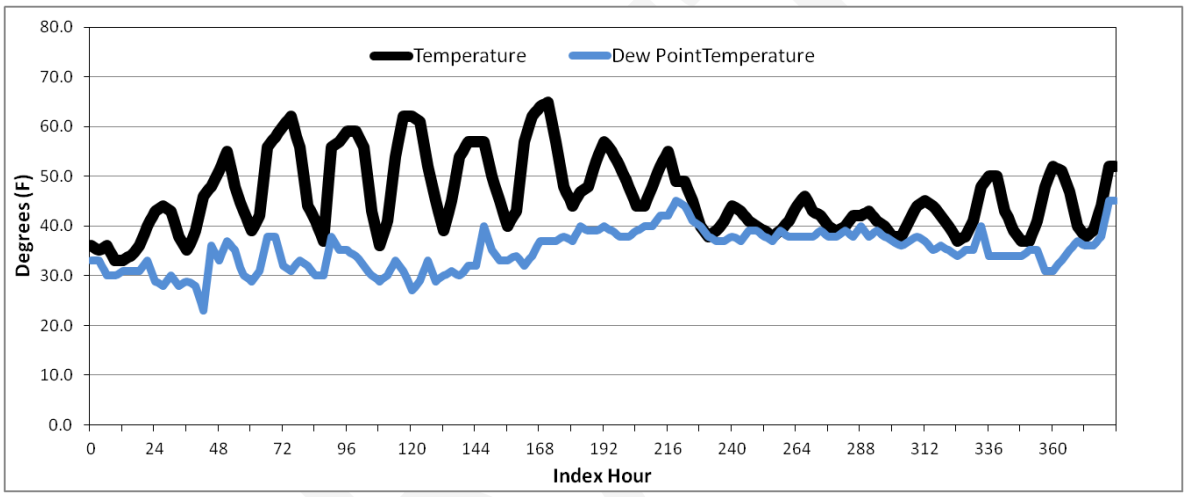

Figure 12.27. Temperature and dew point temperature series based on surface data at Summit, AK with a base elevation of 2400-ft and lapse rate of -2.90°F for June 3-17, 1971.

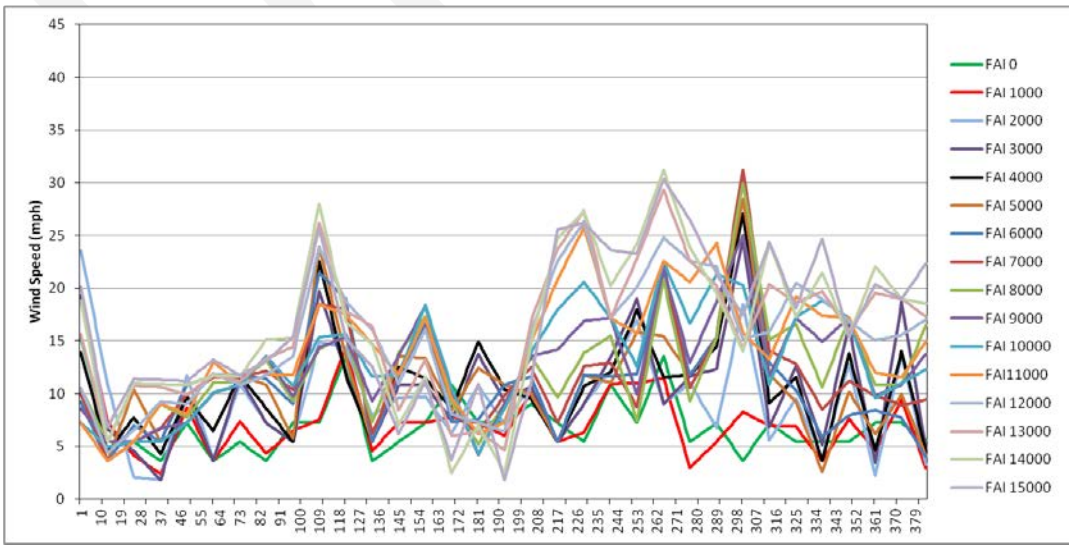

Figure 12.28. Wind speed data based on Fairbanks free-air wind speeds with an adjustment ratio of 0.785 applied to represent anemometer level wind speeds for June 3-17, 1971.

12.3.6 June 7-22, 1972 Meteorological Time Series

Temperature lapse rates were estimated using observed surface temperature data for stations in and around the Susitna-Watana basin. Lapse rates were derived each hour using observed surface data at two locations. Station based lapse rates were calculated between: i) Talkeetna and Summit, ii) Anchorage and Gulkana, iii) Ft Greeley and Summit, and iv) Ft Greeley and Fairbanks. The hourly lapse rates were used to calculate an average lapse rate for the entire calibration period and an average lapse rate based on when rain was occurring during the calibration event (Table 12.12).

Station data were also used to derive an average station based lapse rate for each hour of the storm event. The stations used for this analysis were PANC, Anchorage, Fairbanks, Ft Greeley, Gulkana, Summit, and Talkeetna. The station average lapse rate was derived using linear regression between temperature and elevation. Based on the hourly station data linear relationship, a lapse rate (regression slope) was calculated for each hour of the analysis period. The average of the station based lapse rates (based on linear regression) was compared to individual station (station 1 @ X elevation compared to station 2 @ X elevation) based lapse rates discussed above (Table 12.12).

Vertical temperature at 1000-foot increments from 0-feet to 6000-feet were derived base on temperature data from the Fairbanks radiosonde. The Fairbanks radiosonde lapse rate data were used to calculate an average lapse rate for the entire calibration period (Table 12.12).

Table 12.12. Station based and radiosonde based lapse rates for June 7-22, 1972.

Station Comparisons	Hourly Average	Hourly Rainfall Average	FAI Radiosonde
Talkeetna vs. Summit	-3.20	-2.16	-
Anchorage vs. Gulkana	1.06	0.84	-
Ft Greely vs. Summit	-5.19	-6.53	-
Ft Greely vs. Fairbanks	-1.36	-2.13	-
All Stations	-1.65	-1.30	-
Average*	-2.85	-3.03	-3.52

* Comparison excludes Anchorage vs. Gulkana lapse rate

The radiosonde wind speed represents free atmospheric winds, unobstructed flow, the free-air data were adjusted to surface wind speeds elevations based on comparisons of anemometer level wind speeds with concurrent free-air wind speeds. Surface wind speeds were compared at six locations with varying elevations across the Susitna River basin to the Fairbanks free-air wind speeds (Table 12.13). The average free-air adjustment for the six stations was 0.887 with a maximum of

0.979 and a minimum of 0.748. In order to convert free-air wind speed data to anemometer level wind speeds the adjustment/ratio is applied to the free-air data. For example, at 1000-ft elevation free-air wind speed is 45-mph would be 30-mph at the anemometer level (45-mph * 0.887 = 39.9-mph). The radiosonde data are measured every 12-hours (0-UTC and 12-UTC), the 12-hour data were interpolated to hourly data using the bounding hourly data and a linear relationship.

Table 12.13. Fairbanks radiosonde free-air wind speed conversion ratio to anemometer height wind speed for June 7-22, 1972.

Station	Elevation (ft)	FAI Radiosonde Ratio
Gulkana	1500	0.979
Summit	2500	0.914
Talkeetna	500	0.886
Anchorage	0	0.929
Ft Greely	1500	0.748
Fairbanks	500	0.868
	Average	*0.887*
	Maximum	0.979
	Minimum	0.748

The final temperature and dew point temperature series were based on surface data at Summit, AK with a base elevation of 2400-feet (Figure 12.29). The Summit station data were selected because it was in close proximity to the Susitna River basin and provided a complete and representative profile of temperature and dew point temperature. The lapse rate used to adjust temperature and dew point temperature to other elevations was -2.85°F. The -2.85°F lapse rate was based on the average of all station comparison except the Anchorage and Gulkana comparison. The final vertical wind speed data were based on Fairbanks free-air wind speeds with an adjustment ratio of 0.887 applied to represent anemometer level wind speeds (Figure 12.30).

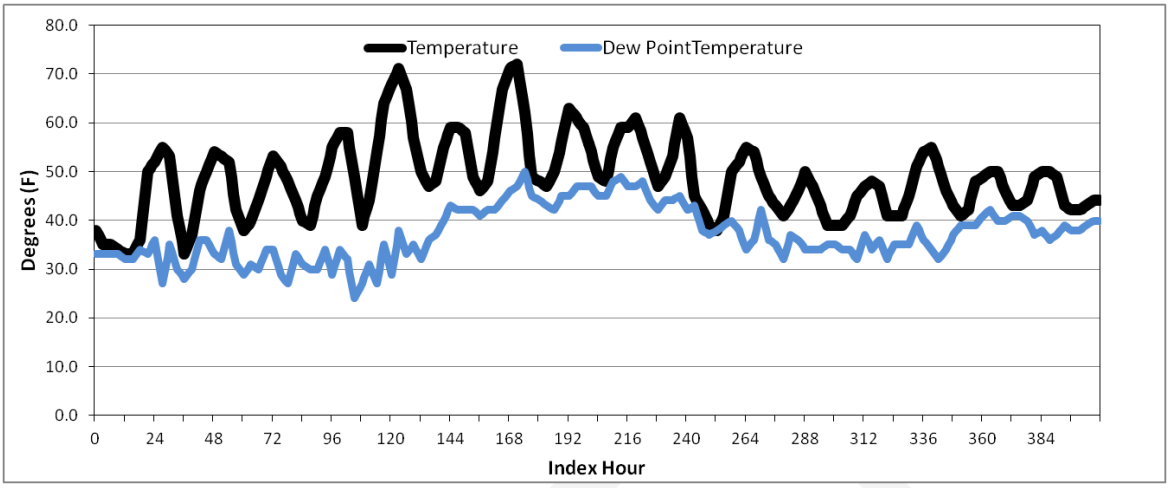

Figure 12.29. Temperature and dew point temperature series based on surface data at Summit, AK with a base elevation of 2400-ft and lapse rate of -2.85°F for June 7-22, 1972.

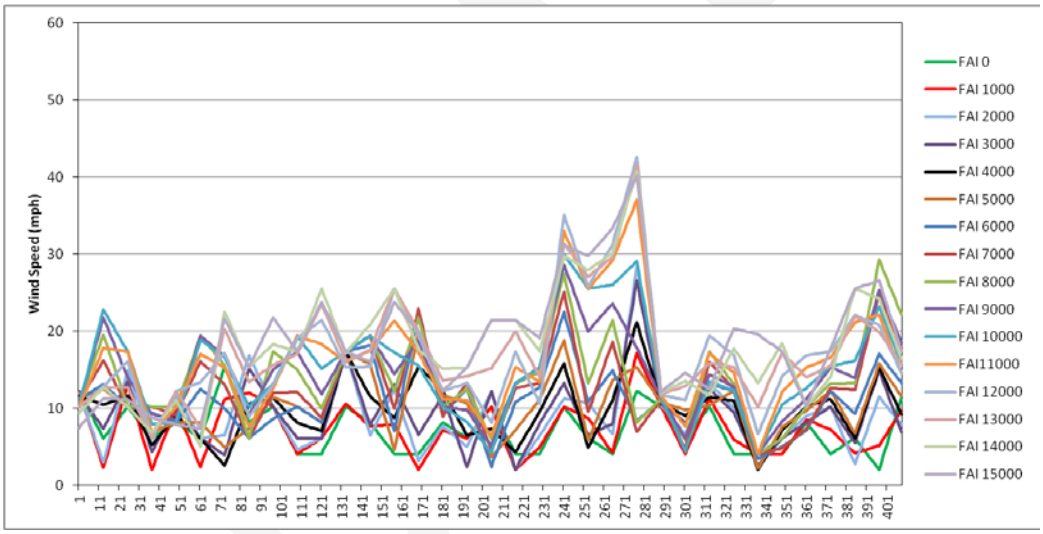

Figure 12.30. Wind speed data based on Fairbanks free-air wind speeds with an adjustment ratio of 0.887 applied to represent anemometer level wind speeds for June 7-22, 1972.

GLOSSARY

Adiabat: Curve of thermodynamic change taking place without addition or subtraction of heat. On an adiabatic chart or pseudo-adiabatic diagram, a line showing pressure and temperature changes undergone by air rising or condensation of its water vapor; a line, thus, of constant potential temperature.

Adiabatic: Referring to the process described by adiabat.

Advection: The process of transfer (of an air mass property) by virtue of motion. In particular cases, advection may be confined to either the horizontal or vertical components of the motion. However, the term is often used to signify horizontal transfer only.

Air mass: Extensive body of air approximating horizontal homogeneity, identified as to source region and subsequent modifications.

Barrier: A mountain range that partially blocks the flow of warm humid air from a source of moisture to the basin under study.

Basin centroid: The point at the exact center of the drainage basin as determined through geographical information systems calculations using the basin outline.

Cold front: Front where relatively colder air displaces warmer air.

Convergence: Horizontal shrinking and vertical stretching of a volume of air, accompanied by net inflow horizontally and internal upward motion.

Cyclone: A distribution of atmospheric pressure in which there is a low central pressure relative to the surroundings. On large-scale weather charts, cyclones are characterized by a system of closed constant pressure lines (isobars), generally approximately circular or oval in form, enclosing a central low-pressure area. Cyclonic circulation is counterclockwise in the northern hemisphere and clockwise in the southern. (That is, the sense of rotation about the local vertical is the same as that of the earth's rotation.)

dBZ: It is a meteorological measure of equivalent reflectivity (Z) of a radar signal reflected off a remote object. The reference level for Z is 1 $mm^6\ m^{-3}$, which is equal to 1 μm^3. It is related to the number of drops per unit volume and the sixth power of drop diameter.

Depth-Area curve: Curve showing, for a given duration, the relation of maximum average depth to size of area within a storm or storms.

Depth-Area-Duration: The precipitation values derived from Depth-Area and Depth-Duration curves at each time and area size increment analyzed for a PMP evaluation.

Depth-Area-Duration values: The combination of depth-area and duration-depth relations. Also called depth-duration-area.

Decimal Degrees: Latitude and longitude geographic coordinates as decimal fractions and are used in many Geographic Information Systems (GIS). Decimal degrees are an alternative to using degrees, minutes, and seconds. As with latitude and longitude, the values are bounded by ±90° and ±180° each. Positive latitudes are north of the equator, negative latitudes are south of the equator. Positive longitudes are east of Prime Meridian, negative longitudes are west of the Prime Meridian. Latitude and longitude are usually expressed in that sequence, latitude before longitude.

Depth-Duration curve: Curve showing, for a given area size, the relation of maximum average depth of precipitation to duration periods within a storm or storms.

Dew point: The temperature to which a given parcel of air must be cooled at constant pressure and constant water vapor content for saturation to occur.

Envelopment: A process for selecting the largest value from any set of data. In estimating PMP, the maximum and transposed rainfall data are plotted on graph paper, and a smooth curve is drawn through the largest values.

Front: The interface or transition zone between two air masses of different parameters. The parameters describing the air masses are temperature and dew point.

General storm: A storm event, that produces precipitation over areas in excess of 500-square miles, has a duration longer than 6 hours, and is associated with a major synoptic weather feature.

HYSPLIT: HYbrid Single-Particle Lagrangian Integrated Trajectory. A complete system for computing parcel trajectories to complex dispersion and deposition simulations using either puff or particle approaches. Gridded meteorological data, on one of three conformal (Polar, Lambert, or Mercator latitude-longitude grid) map projections, are required at regular time intervals. Calculations may be performed sequentially or concurrently on multiple meteorological grids, usually specified from fine to coarse resolution.

In-Place Maximization Factor: The adjustment factor representing the maximum amount of atmospheric moisture that could have been present to the storm for rainfall production

Isohyets: Lines of equal value of precipitation for a given time interval.

Isohyetal Pattern: The pattern formed by the isohyets of an individual storm.

Jet Stream: A strong, narrow current concentrated along a quasi-horizontal axis (with respect to the earth's surface) in the upper troposphere or in the lower stratosphere, characterized by strong vertical and lateral wind shears. Along this axis it features at least one velocity maximum (jet streak). Typical jet streams are thousands of kilometers long, hundreds of kilometers wide, and several kilometers deep. Vertical wind shears are on the order of 10 to 20 mph per kilometer of altitude and lateral winds shears are on the order of 10 mph per 100 kilometer of horizontal distance.

Mass curve: Curve of cumulative values of precipitation through time.

Mid-latitude frontal system: An assemblage of fronts as they appear on a synoptic chart north of the tropics and south of the polar latitudes. This term is used for a continuous front and its characteristics along its entire extent, its variations of intensity, and any frontal cyclones along it.

Moisture Transposition Factor: The adjustment factor which accounts for the difference in available moisture between the location where the storm occurred and the Susitna River basin

Observational day: The 24-hour time period between daily observation times for two consecutive days at cooperative stations, e.g., 6:00PM to 6:00PM.

One-hundred year rainfall event: The point rainfall amount that has a one-percent probability of occurrence in any year. Also referred to as the rainfall amount that on the average occurs once in a hundred years or has a 1 percent chance of occurring in any single year.

Orographic Rainfall: Rainfall enhancement resulting mainly from the forced lifting of moisture-laden air masses by elevated terrain, when combined with unstable atmospheric conditions often results in heavy (high intensity, long duration) rainfall at rates higher than what would be experienced if the elevated terrain were not present.

Orographic Transposition Factor: A factor obtained from the results of the proportionality constant calculation which compares the 24-hour precipitation frequency characteristics between the storm target and source locations

Polar front: A semi-permanent, semi-continuous front that separates tropical air masses from polar air masses.

Precipitable water: The total atmospheric water vapor contained in a vertical column of unit cross-sectional area extending between any two specified levels in the atmosphere; commonly expressed in terms of the height to which the liquid water would stand if the vapor were completely condensed and collected in a vessel of the same unit cross-section. The total precipitable water in the atmosphere at a location is that contained in a column or unit cross-section extending from the

earth's surface all the way to the "top" of the atmosphere. The 30,000 foot level (approximately 300mb) is considered the top of the atmosphere in this study.

Persisting dew point: The dew point value at a station that has been equaled or exceeded throughout a specific period of time. Commonly durations of 12 or 24 hours are used, though other durations may be used at times.

Probable Maximum Precipitation (PMP): Theoretically, the greatest depth of precipitation for a given duration that is physically possible over a given size storm area at a particular geographic location at a certain time of the year.

Pseudo-adiabat: Line on thermodynamic diagram showing the pressure and temperature changes undergone by saturated air rising in the atmosphere, without ice-crystal formation and without exchange of heat with its environment, other than that involved in removal of any liquid water formed by condensation.

Pseudo-adiabatic: Referring to the process described by the pseudo-adiabat.

Rainshadow: The region, on the lee side of a mountain or mountain range, where the precipitation is noticeably less than on the windward side.

PMP storm pattern: The isohyetal pattern that encloses the PMP area, plus the isohyets of residual precipitation outside the PMP portion of the pattern.

Saturation: Upper limit of water-vapor content in a given space; solely a function of temperature.

Short list of storms: The short list of storms is the final list of storms used to derive the site-specific PMP values for the basin. The list represents the most extreme historic storms of record that are considered to be PMP-type storm events.

Spatial distribution: The geographic distribution of precipitation over a drainage according to an idealized storm pattern of the PMP for the storm area.

Storm maximization: The process of adjusting observed precipitation amounts upward based upon the hypothesis of increased moisture inflow to the storm. (Also referred to as “moisture maximization” in HMR 57)

Storm transposition: The hypothetical transfer, or relocation of storms, from the location where they occurred to other areas where they could occur. The transfer and the mathematical adjustment of storm rainfall amounts from the storm site to another location is termed "explicit transposition." The areal, durational, and regional smoothing done to obtain comprehensive individual drainage estimates and generalized PMP studies is termed "implicit transposition" (WMO, 1986).

Synoptic: Showing the distribution of meteorological elements over an area at a given time, e.g., a synoptic chart. Use in this report also means a weather system that is large enough to be a major feature on large-scale maps (e.g., of the continental U.S.).

Temporal distribution: The time order in which incremental PMP amounts are arranged within a PMP storm.

Tropical Storm: A cyclone of tropical origin that derives its energy from the ocean surface.

Transposition limits: The outer boundaries of the region surrounding an actual storm location that has similar, but not identical, climatic and topographic characteristics throughout. The storm can be transpositioned within the transposition limits with only relatively minor modifications to the observed storm rainfall amounts.

Acronyms and Abbreviations used in this report

ALERT: Automated Local Evaluation in Real Time

AWA: Applied Weather Associates, LLC

DA: Depth-Area

DAD: Depth-Area-Duration

.dbf: Database file extension

DD: Depth-Duration

dd: decimal degrees

DEM: Digital elevation model

DND: drop number distribution

DSD: drop size distribution

EPRI: Electric Power Research Institute

F: Fahrenheit

FERC: Federal Energy Regulatory Commission

GIS: Geographical Information System

GRASS: Geographic Resource Analysis Support System

HMR: Hydrometeorological Report

HYSPLIT: Hybrid Single Particle Lagrangian Integrated Trajectory Model

IPMF: In-Place Maximization Factor

mb: millibar

mph: Mile per hour

MTF: Moisture Transposition Factor

NCAR: National Center for Atmospheric Research

NCDC: National Climatic Data Center

NCEP: National Centers for Environmental Prediction

NESDIS: National Environmental Satellite, Data, and Information Service

NEXRAD: National Weather Service 88-D Next Generation Radar

NOAA: National Oceanic and Atmospheric Administration

NWS: National Weather Service

PMF: Probable Maximum Flood

OTF: Orographic Transposition Factor

PMP: Probable Maximum Precipitation

PW: Precipitable water

QC: Quality control

R: Rainfall rate

RAWS: Remote Automated Weather Station

SNOTEL: Snow Telemetry station

SPAS: Storm Precipitation and Analysis System

SPP: Storm Precipitation Period

SSPMP: Site-specific Probable Maximum Precipitation

SST: Sea Surface Temperature

USACE: US Army Corps of Engineers

USGS: United States Geological Survey

WMO: World Meteorological Organization

Z: Radar reflectivity, measured in units of dBZ

REFERENCES

American Meteorological Society, 1996: *Glossary of Weather and Climate*, Boston, Ma., 272 pp.

Bao, J.W., S.A. Michelson, P.J. Neiman, F.M. Ralph, and J.M. Wilczak, 2006: Interpretation of Enhanced Integrated Water Vapor Bands Associated with Extratropical Cyclones: Their Formation and Connection to Tropical Moisture. *Mon. Wea. Rev.*, **134**, 1063–1080.

Bolsenga, S.J., 1965: The Relationship between Total Atmospheric Water Vapor and Surface Dewpoint on a Mean Daily and Hourly Basis, *J. Appl. Meteor.*, **4**, 430–432.

Bonnin, G.M., Todd, D., Lin, B., Parzybok, T., Yekta, M., and D. Riley, 2011: Precipitation-Frequency Atlas of the United States, NOAA Atlas 14, Volumes 1 through 6, NOAA, National Weather Service, Silver Spring, Maryland. http://hdsc.nws.noaa.gov/hdsc/pfds/

Corps of Engineers, U.S. Army, 1945-1973: Storm Rainfall in the United States, Depth-Area-Duration Data. Office of Chief of Engineers, Washington, D.C.

Corrigan, P., D.D. Fenn, D.R. Kluck, and J.L. Vogel, 1999: Probable Maximum Precipitation for California, *Hydrometeorological Report Number 59*, National Weather Service, National Oceanic and Atmospheric Administration, U. S. Department of Commerce, Silver Spring, Md, 392 pp.

Daly, C., R.P. Neilson, and D.L. Phillips, 1994: A Statistical-Topographic Model for Mapping Climatological Precipitation over Mountainous Terrain. *J. Appl. Meteor.*, **33**, 140–158.

Daly, C., G. Taylor, and W. Gibson, 1997: The PRISM Approach to Mapping Precipitation and Temperature, 10th Conf. on Applied Climatology, Reno, NV, Amer. Meteor. Soc., 10-12.

Draxler, R.R. and Rolph, G.D., 2003: HYSPLIT (HYbrid Single-Particle Lagrangian Integrated Trajectory) Model access via NOAA ARL READY Website (http://www.arl.noaa.gov/ready/hysplit4.html). NOAA Air Resources Laboratory, Silver Spring, MD.

Draxler, R.R. and Rolph, G.D., 2010. HYSPLIT (HYbrid Single-Particle Lagrangian Integrated Trajectory) Model access via NOAA ARL READY Website (http://ready.arl.noaa.gov/HYSPLIT.php). NOAA Air Resources Laboratory, Silver Spring, MD.

Duchon, C.E., and G.R. Essenberg, 2001: Comparative Rainfall Observations from Pit and Above Ground Rain Gauges with and without Wind Shields, *Water Resources Research*, Vol. 37, N. 12, 3253-3263.

Environmental Data Service, 1968: Maximum 12-hour 1000-mb persisting Dew Points Monthly and of Record. *Climatic Atlas of the United States*, Environmental Science Services Administration, U.S. Department of Commerce, Washington D.C., pp. 59-60.

GRASS (Geographic Resources Analysis Support System) GIS is an open source, free software GIS with raster, topological vector, image processing, and graphics production functionality that operates on various platforms. http://grass.itc.it/.

Gou, J. C. Y., Urbonas, Ben, and Stewart, Kevin, 2001. *Rain Catch under Wind and Vegetal Effects*. ASCE, Journal of Hydrologic Engineering, Vol. 6, No. 1

Hansen, E.M., L.C. Schreiner and J.F. Miller, 1982: Application of Probable Maximum Precipitation Estimates – United States East of the 105th Meridian. *Hydrometeorological Report No. 52*, U.S. Department of Commerce, Washington, D.C., 168 pp.

_____, F.K. Schwarz, and J.T Reidel, 1977: Probable Maximum Precipitation Estimates. Colorado River and Great Basin Drainages. *Hydrometeorological Report No. 49*, NWS, NOAA, U.S. Department of Commerce, Silver Spring, MD, 161 pp.

_____, D.D. Fenn, L.C. Schreiner, R.W. Stodt, and J.F. Miller, 1988: Probable Maximum Precipitation Estimates – United States Between the Continental Divide and the 103rd Meridian. *Hydrometeorological Report No. 55A*, U.S. Department of Commerce, Silver Spring, MD, 242 pp.

_____, D.D. Fenn, P. Corrigan, J.L. Vogel, L.C. Schreiner, and R.W. Stodt, 1994: Probable Maximum Precipitation-Pacific Northwest States, *Hydrometeorological Report Number 57*, National Weather Service, National Oceanic and Atmospheric Administration, U. S. Department of Commerce, Silver Spring, MD, 338 pp.

Hershfield, D.M., 1961: Rainfall frequency atlas of the United States for durations from 30 minutes to 24 hours and return periods from 1 to 100 years, *Technical Paper No. 40*, U. S. Weather Bureau, Washington, D.C., 61p.

Kalnay, E., M. Kanamitsu, R. Kistler, W. Collins, D. Deaven, L. Gandin, M. Iredell, S. Saha, G. White, J. Woollen, Y. Zhu, A. Leetmaa, R. Reynolds, M. Chelliah, W. Ebisuzaki, W. Higgins, J. Janowiak, K. Mo, C. Ropelewski, J. Wang, R. Jenne, and D. Joseph, 1996: The NCEP/NCAR 40-Year Reanalysis Project. *Bull. Amer. Meteor. Soc.*, **77**, 437–471.

Kent E.C, Scott D. Woodruff, and David I. Berry, 2007: Metadata from WMO Publication No. 47 and an Assessment of Voluntary Observing Ship Observation Heights in ICOADS. *J. Atmos and Ocean Tech.*, **24(2)**, 214-234.

Martner, B.E, and V. Dubovskiy, 2005: Z-R Relations from Raindrop Disdrometers: Sensitivity to Regression Methods and DSD Data Refinements. 32nd Radar Meteorology Conference, Albuquerque, NM, October, 2005.

Mesinger, F., G. DiMego, E. Kalnay, K. Mitchell, P.C. Shafran, W. Ebisuzaki, D. Jović, J. Woollen, E. Rogers, E.H. Berbery, M.B. Ek, Y. Fan, R. Grumbine, W. Higgins, H. Li, Y. Lin, G. Manikin, D. Parrish, and W. Shi, 2006: North American Regional Reanalysis. *Bull. Amer. Meteor. Soc.*, **87**, 343–360.

Miller, J.F., R.H. Fredrick, and R.J. Tracey, 1973: *NOAA Atlas 2, Precipitation-Frequency Atlas of the Western United States.* U.S. Department of Commerce, National Oceanic and Atmospheric Administration, National Weather Service, Silver Spring, MD.

National Climatic Data Center (NCDC). NCDC TD-3200 and TD-3206 datasets - Cooperative Summary of the Day

National Climatic Data Center (NCDC) Heavy Precipitation Page http://www.ncdc.noaa.gov/oa/climate/severeweather/rainfall.html#maps

National Oceanic and Atmospheric Administration, Forecast Systems Laboratory FSL Hourly/Daily Rain Data, http://precip.fsl.noaa.gov/hourly_precip.html

National Oceanic and Atmospheric Administration Central Library Data Imaging Project *Daily weather maps*, http://docs.lib.noaa.gov/rescue/dwm/data_rescue_daily_weather_maps.html

Neiman, P.J., F.M. Ralph, R.L. Weber, T. Uttal, L.B. Nance, and D.H. Levinson, 2001: Observations of Nonclassical Frontal Propagation and Frontally Forced Gravity Waves Adjacent to Steep Topography. *Mon. Wea. Rev.*, **129**, 2633–2659.

_____, P.J., F.M. Ralph, G.A. Wick, Y.H. Kuo, T.K. Wee, Z. Ma, G.H. Taylor, and M.D. Dettinger, 2008: Diagnosis of an Intense Atmospheric River Impacting the Pacific Northwest: Storm Summary and Offshore Vertical Structure Observed with COSMIC Satellite Retrievals. *Mon. Wea. Rev.*, **136**, 4398–4420.

_____, P.J., F.M. Ralph, G.A. Wick, J.D. Lundquist, and M.D. Dettinger, 2008: Meteorological Characteristics and Overland Precipitation Impacts of Atmospheric Rivers Affecting the West Coast of North America Based on Eight Years of SSM/I Satellite Observations. *J. Hydrometeor.*, **9**, 22–47.

_____, P.J., L.J. Schick, F.M. Ralph, M. Hughes, and G.A. Wick, 2011: Flooding in Western Washington: The Connection to Atmospheric River. Presented at the 25th Conference of Hydrology at the American Meteorological Society annual meeting, Seattle, WA.

Parzybok, T.W., and E.M. Tomlinson, 2006: A New System for Analyzing Precipitation from Storms, *Hydro Review*, Vol. XXV, No. 3, 58-65.

Ralph, F.M., P.J. Neiman, D.E. Kingsmill, P.O.G. Persson, A.B. White, E.T. Strem, E.D. Andrews, and R.C. Antweiler, 2003: The Impact of a Prominent Rain Shadow on Flooding in

California's Santa Cruz Mountains: A CALJET Case Study and Sensitivity to the ENSO Cycle. *J. Hydrometeor.*, **4**, 1243–1264.

_____, F.M., P.J. Neiman, and G.A. Wick, 2004: Satellite and CALJET Aircraft Observations of Atmospheric Rivers over the Eastern North Pacific Ocean during the Winter of 1997/98. *Mon. Wea. Rev.*, **132**, 1721–1745.

_____, F.M., P.J. Neiman, and R. Rotunno, 2005: Dropsonde Observations in Low-Level Jets over the Northeastern Pacific Ocean from CALJET-1998 and PACJET-2001: Mean Vertical-Profile and Atmospheric-River Characteristics. *Mon. Wea. Rev.*, **133**, 889–910.

_____., F.M., P.J. Neiman, and R. Rotunno, 2005: Dropsonde Observations in Low-Level Jets over the Northeastern Pacific Ocean from CALJET-1998 and PACJET-2001: Mean Vertical-Profile and Atmospheric-River Characteristics. *Mon. Wea. Rev.*, **133**, 889–910.

_____., F.M., P.J. Neiman, G.A. Wick, S.I. Gutman, M.D. Dettinger, D.R. Cayan, and A.B. White, 2006: Flooding on California's Russian River: The role of atmospheric rivers. *Geophys. Res. Lett.*, **33**, L13801.

_____., F. M., P. J. Neiman, G. N. Kiladis, K. Weickmann, and D. W. Reynolds, 2011: A Multiscale Observational Case Study of a Pacific Atmospheric River Exhibiting Tropical–Extratropical Connections and a Mesoscale Frontal Wave. *Mon. Wea. Rev.*, **139**, 1169–1189.

Remote Automated Weather Stations RAWS, http://www.raws.dri.edu/index.html

Reynolds, R.W., T.M. Smith, C. Liu, D.B. Chelton, K.S. Casey, and M.G. Schlax, 2007: Daily High-resolution Blended Analysis for Sea Surface Temperature. *J. Climate.*, **20**, 5473-5496.

Riedel, J.T., and L.C. Schreiner, 1980: Comparison of Generalized Estimates of Probable Maximum Precipitation with Greatest Observed Rainfalls, *NOAA Technical Report NWS 25*, U.S. Department of Commerce, NOAA, Silver Spring, Md, 46 pp.

Rolph, G.D., 2003: Real-time Environmental Applications and Display sYstem (READY) Website http://www.arl.noaa.gov/ready/hysplit4.html. NOAA Air Resources Laboratory, Silver Spring, MD.

Rolph, G.D., 2010. Real-time Environmental Applications and Display sYstem (READY) Website http://ready.arl.noaa.gov. NOAA Air Resources Laboratory, Silver Spring, MD.

Schreiner, L.C., and J.T. Riedel, 1978: Probable Maximum Precipitation Estimates, United States East of the 105th Meridian. *Hydrometeorological Report No. 51*, U.S. Department of Commerce, Silver Spring, MD, 242pp.

Smith, C.D., 1950: The Intense Pacific Coast Storms of October 26-28, 1950, *Monthly Weather Review*, 191-195.

Spatial Climate Analysis Service, Oregon Climate Service, Oregon State University. http://www.ocs.orst.edu/prism/

Tomlinson, E.M., 1993: Probable Maximum Precipitation Study for Michigan and Wisconsin, Electric Power Research Institute, Palo Alto, Ca, TR-101554, V1.

_____, Williams, R.A., and T.W. Parzybok, September 2002: Site-Specific Probable Maximum Precipitation (PMP) Study for the Upper and Middle Dams Drainage Basin, Prepared for FPLE, Lewiston, ME.

_____, Williams, R.A., and T.W. Parzybok, September 2003: Site-Specific Probable Maximum Precipitation (PMP) Study for the Great Sacandaga Lake / Stewarts Bridge Drainage Basin, Prepared for Reliant Energy Corporation, Liverpool, New York.

_____, Williams, R.A., and T.W. Parzybok, September 2003: Site-Specific Probable Maximum Precipitation (PMP) Study for the Cherry Creek Drainage Basin, Prepared for the Colorado Water Conservation Board, Denver, CO.

_____, Kappel W.D., Parzybok, T.W., Hultstrand, D., Muhlestein, G., and B. Rappolt, May 2008: Site-Specific Probable Maximum Precipitation (PMP) Study for the Wanahoo Drainage Basin, Prepared for Olsson Associates, Omaha, Nebraska.

_____, Kappel W.D., Parzybok, T.W., Hultstrand, D., Muhlestein, G., and B. Rappolt, June 2008: Site-Specific Probable Maximum Precipitation (PMP) Study for the Blenheim Gilboa Drainage Basin, Prepared for New York Power Authority, White Plains, NY.

_____, Kappel W.D., and T.W. Parzybok, February 2008: Site-Specific Probable Maximum Precipitation (PMP) Study for the Magma FRS Drainage Basin, Prepared for AMEC, Tucson, Arizona.

_____, Kappel, W.D., and T.W. Parzybok, December 2008: Statewide Probable Maximum Precipitation (PMP) Study for the State of Nebraska.

_____, Kappel, W.D., and T.W. Parzybok, February 2009: Site-Specific Probable Maximum Precipitation (PMP) Study for the Tuxedo Lake Drainage Basin, New York.

_____, Kappel, W.D., and T.W. Parzybok, July 2009: Site-Specific Probable Maximum Precipitation (PMP) Study for the Scoggins Dam Drainage Basin, Oregon.

_____, Kappel, W.D., and T.W. Parzybok, February 2010: Site-Specific Probable Maximum Precipitation (PMP) Study for the Magma FRS Drainage Basin, Arizona.

_____, and W. D. Kappel, October 2009: Revisiting PMPs, *Hydro Review*, Vol. 28, No. 7, 10-17.

U.S. Weather Bureau, 1951: Tables of Precipitable Water and Other Factors for a Saturated Pseudo-Adiabatic Atmosphere. *Technical Paper No. 14*, U.S. Department of Commerce, Weather Bureau, Washington, D.C., 27 pp.

U.S. Weather Bureau, 1963, Rainfall Frequency Atlas of the United States, for Duration of 30 Minutes to 24 Hours and Return Periods of 1 to 100 Years, *Technical Paper Number 40*, US. Department of Commerce, Washington, DC, 65 pp.

Woodruff, S.D., H.F. Diaz, S.J. Worley, R.W. Reynolds, and S.J. Lubker, 2005: Early ship observational data and ICOADS. *Climatic Change*, **73**, 169-194.

World Meteorological Organization, 2009: Manual for Estimation of Probable Maximum Precipitation, *Operational Hydrology Report No 1045*, WMO, Geneva, 259 pp.

Worley, S.J., S.D. Woodruff, R.W. Reynolds, S.J. Lubker, and N. Lott, 2005: ICOADS Release 2.1 data and products. *Int. J. Climatol. (CLIMAR-II Special Issue)*, **25**, 823-842.

Appendix A

Sea Surface Temperatures Climatology Maps

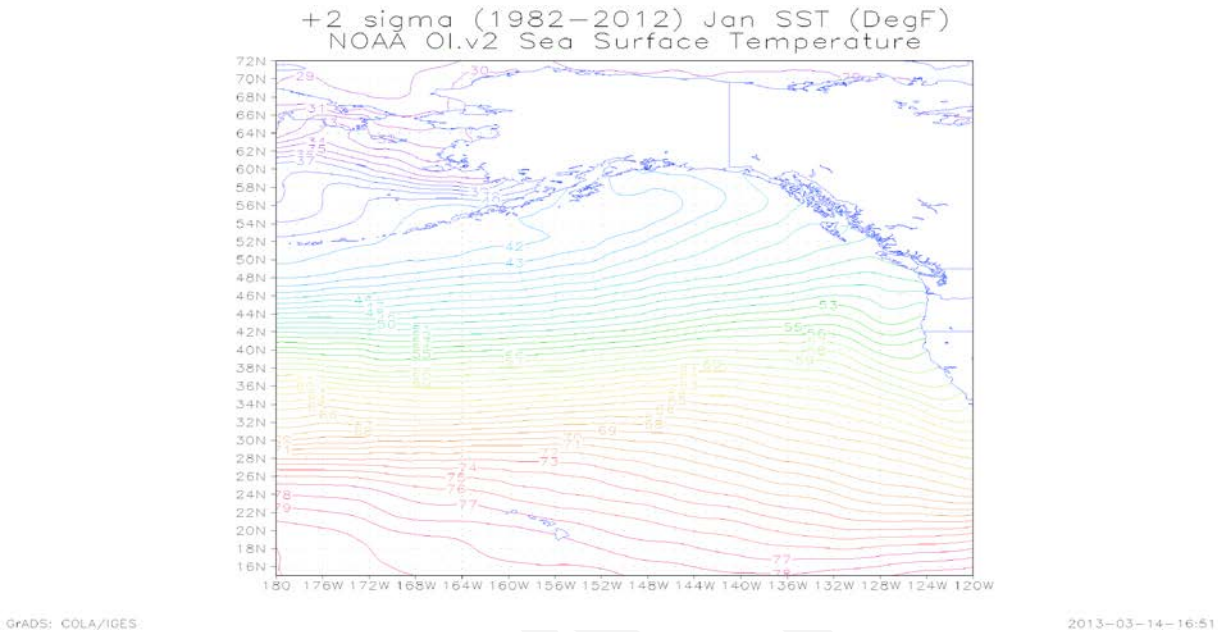
+2 sigma (1982–2012) Jan SST (DegF)
NOAA OI.v2 Sea Surface Temperature
GrADS: COLA/IGES
2013-03-14-16:51

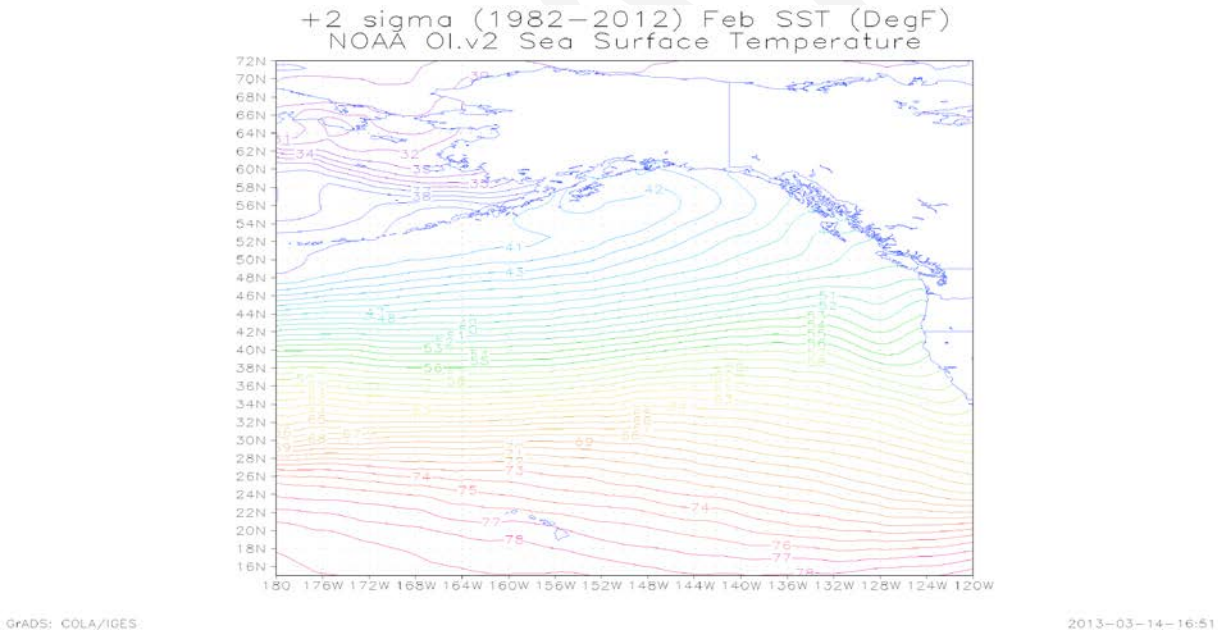
+2 sigma (1982–2012) Feb SST (DegF)
NOAA OI.v2 Sea Surface Temperature
GrADS: COLA/IGES
2013-03-14-16:51

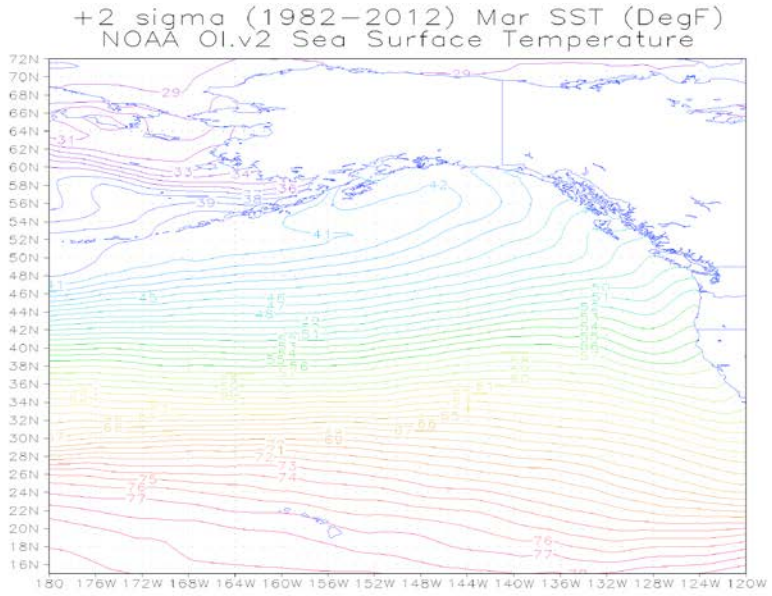
+2 sigma (1982–2012) Mar SST (DegF)
NOAA OI.v2 Sea Surface Temperature
GrADS: COLA/IGES
2013-03-14-16:51

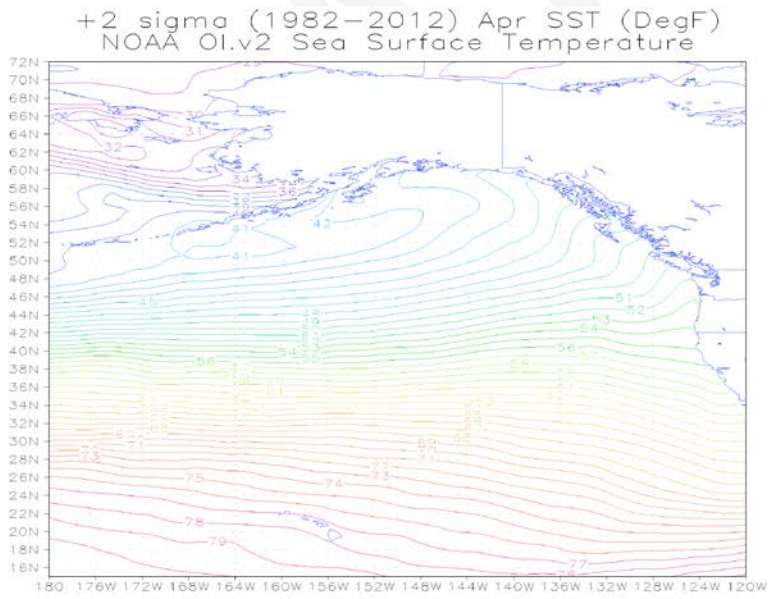
+2 sigma (1982–2012) Apr SST (DegF)
NOAA OI.v2 Sea Surface Temperature
GrADS: COLA/IGES
2013-03-14-16:51

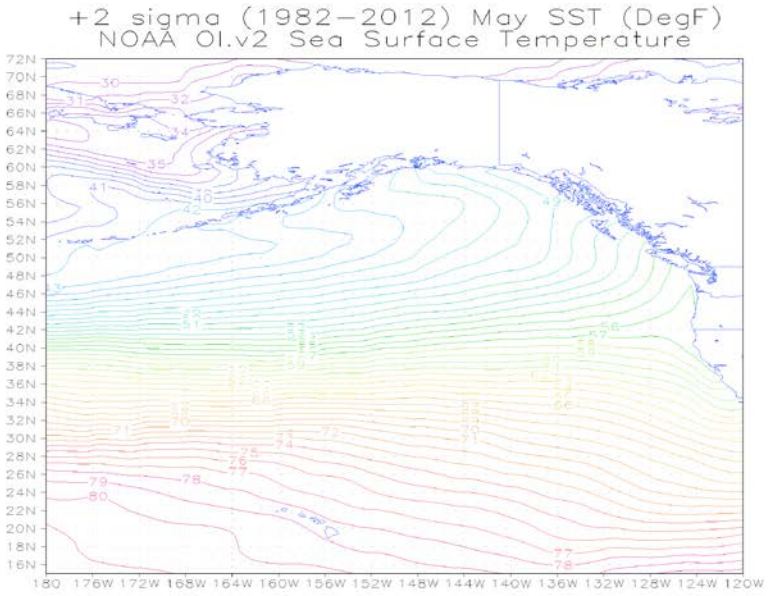
+2 sigma (1982–2012) May SST (DegF)
NOAA OI.v2 Sea Surface Temperature
72N 70N 68N 66N 64N 62N 60N 58N 56N 54N 52N 50N 48N 46N 44N 42N 40N 38N 36N 34N 32N 30N 28N 26N 24N 22N 20N 18N 16N
180 176W 172W 168W 164W 160W 156W 152W 148W 144W 140W 136W 132W 128W 124W 120W
GrADS: COLA/IGES
2013-03-14-16:51

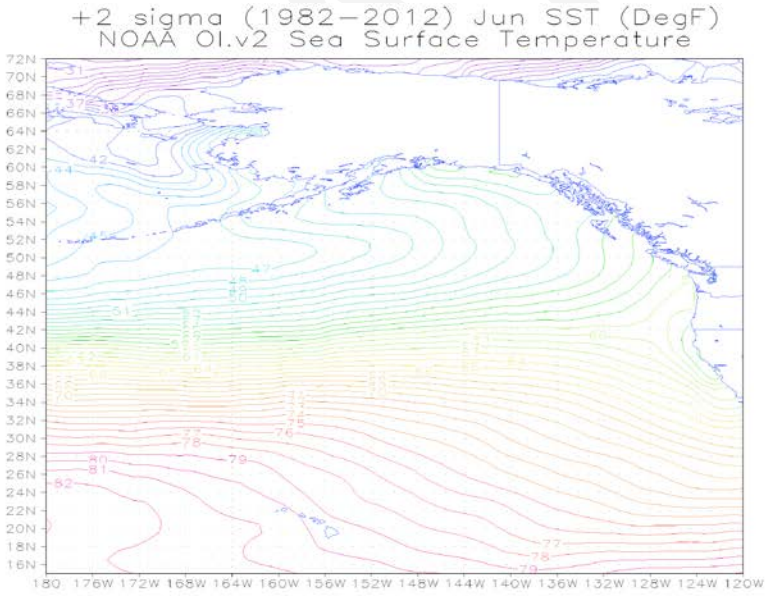
+2 sigma (1982–2012) Jun SST (DegF)
NOAA OI.v2 Sea Surface Temperature
72N 70N 68N 66N 64N 62N 60N 58N 56N 54N 52N 50N 48N 46N 44N 42N 40N 38N 36N 34N 32N 30N 28N 26N 24N 22N 20N 18N 16N
180 176W 172W 168W 164W 160W 156W 152W 148W 144W 140W 136W 132W 128W 124W 120W
GrADS: COLA/IGES
2013-03-14-16:52

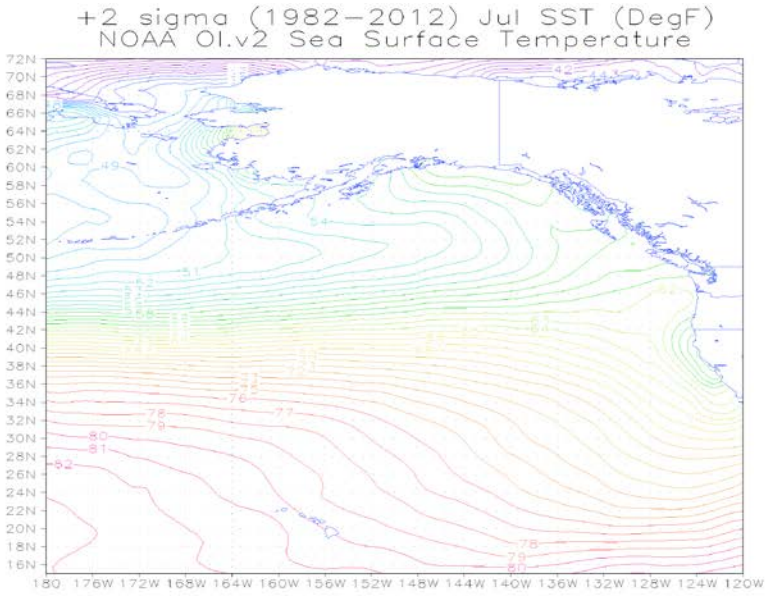
+2 sigma (1982–2012) Jul SST (DegF)
NOAA OI.v2 Sea Surface Temperature
GrADS: COLA/IGES
2013-03-14-16:52

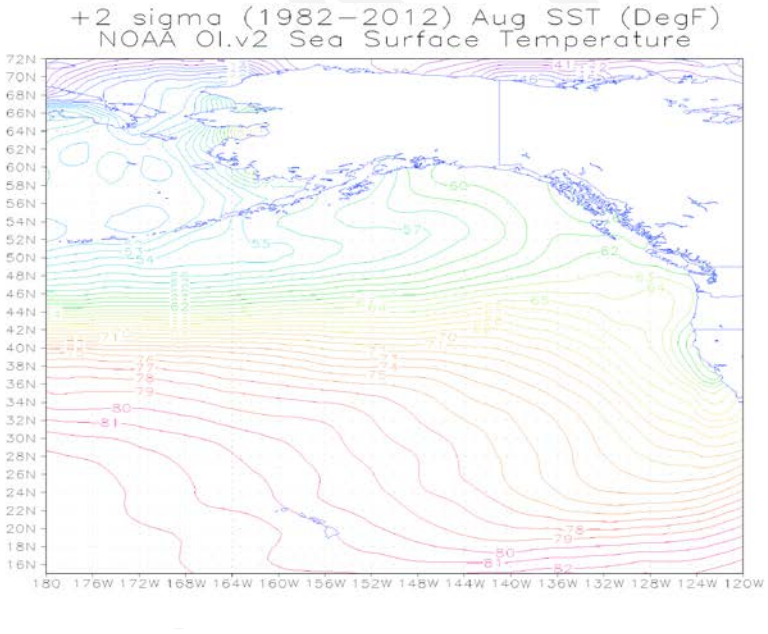
+2 sigma (1982–2012) Aug SST (DegF)
NOAA OI.v2 Sea Surface Temperature
GrADS: COLA/IGES
2013-03-14-16:52

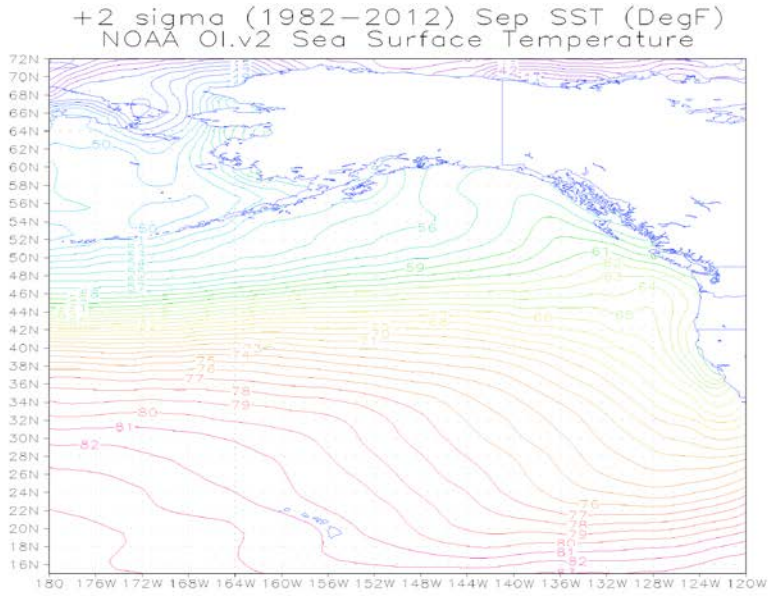
+2 sigma (1982–2012) Sep SST (DegF)
NOAA OI.v2 Sea Surface Temperature
GrADS: COLA/IGES
2013-03-14-16:52

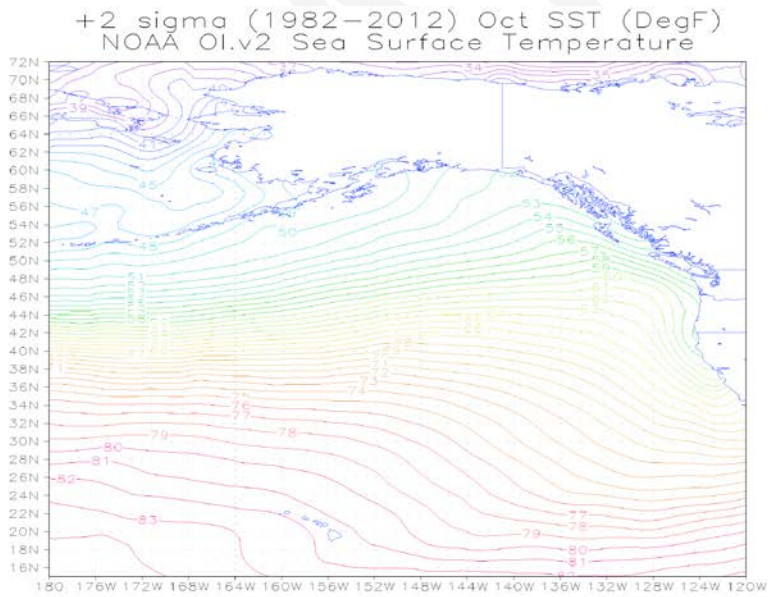
+2 sigma (1982–2012) Oct SST (DegF)
NOAA OI.v2 Sea Surface Temperature
GrADS: COLA/IGES
2013-03-14-16:52

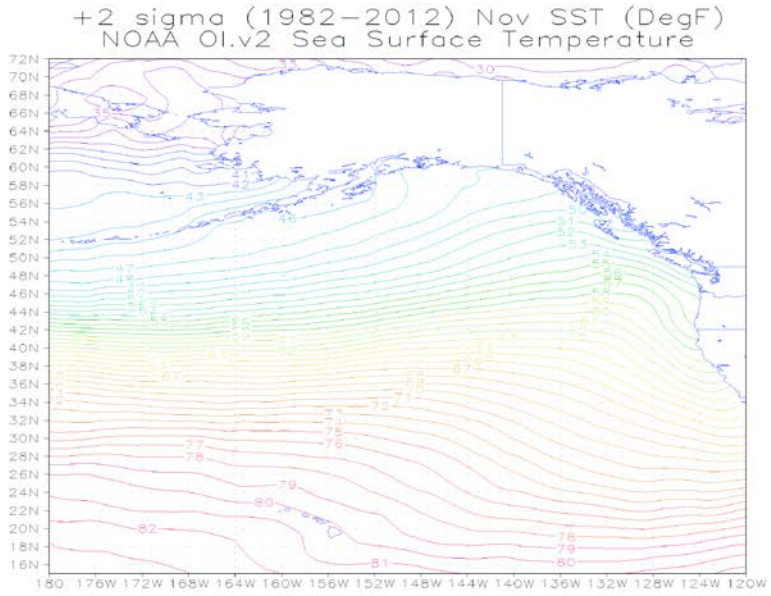
+2 sigma (1982–2012) Nov SST (DegF)
NOAA OI.v2 Sea Surface Temperature
GrADS: COLA/IGES
2013-03-14-16:52

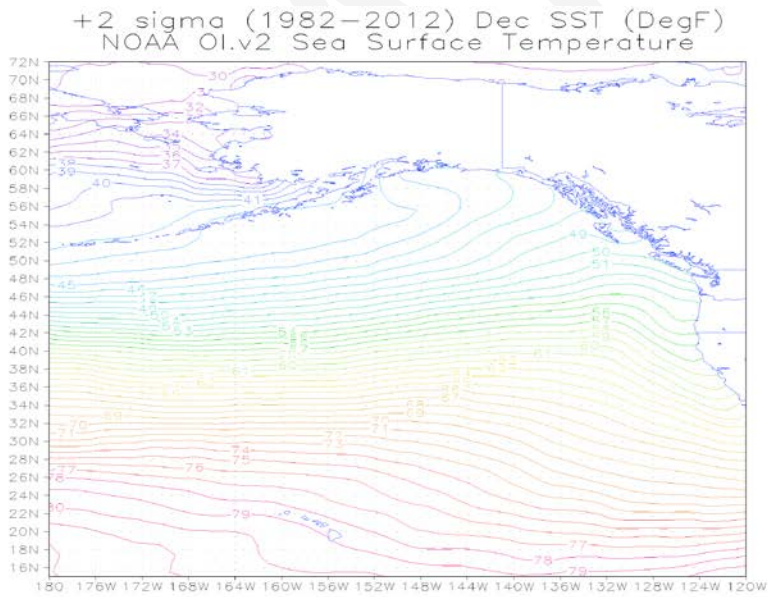
+2 sigma (1982–2012) Dec SST (DegF)
NOAA OI.v2 Sea Surface Temperature
GrADS: COLA/IGES
2013-03-14-16:53

Appendix B

PYTHON Code for ArcGIS PMP Calculation Tool

```
''' ---------------------------------------------------------------------------
Name: PMP_Calc.py
Version: 1.00
ArcGIS Version: ArcGIS Desktop 10.2 SP1 (2013)
Author: Applied Weather Associates
Usage:  The tool is designed to be executed within the ArcMap or ArcCatalog desktop environment.
Required Arguments:
- A basin outline polygon shapefile or feature class
- Directory location path of the "PMP_Evaluation_Tool" folder
- String of durations to analyze.
Description:
   This tool calculates PMP depths for a given drainage basin for the
specified durations.  PMP values are
calculated (in inches) for each grid point (spaced at 90 arc-second intervals)
within (or adjacent to) the drainage basin. A GRID raster layer is created over
the basin from the grid point PMP values.
---------------------------------------------------------------------------'''
#############################################################################
## import Python modules
import sys
import arcpy
from arcpy import env
import arcpy.management as dm
import arcpy.conversion as con
arcpy.env.overwriteOutput = True                                    # Set overwrite option
#############################################################################
## get input parameters
basin = arcpy.GetParameter(0)                                       # get AOI Basin Shapefile
home = arcpy.GetParameterAsText(1)                                  # get location of 'PMP' Project Folder
durInput = arcpy.GetParameter(2)                                    # get durations (string)
dadGDB = home + "\\Input\\DAD_Tables.gdb"                           # location of DAD tables
adjFactGDB = home + "\\Input\\Storm_Adj_Factors.gdb"                 # location of feature datasets containing total adjustment
factors
def pmpAnalysis(aoiBasin, stormType):
   ##########################################################################
   ## Create PMP Point Feature Class from points within AOI basin and add fields
   def createPMPfc():
      global outPath
      env.workspace = outPath + "PMP.gdb"                                   # set environment workspace
      arcpy.AddMessage("\nCreating feature class: PMP_Points...")
      dm.MakeFeatureLayer(home + "\\Input\Non_Storm_Data.gdb\\Vector_Grid\\Vector_Grid_AZ", "vgLayer")    # make a feature
layer of vector grid cells
      dm.SelectLayerByLocation("vgLayer", "INTERSECT", aoiBasin)                # select the vector grid cells that
intersect the aoiBasin polygon
      dm.MakeFeatureLayer(home + "\\Input\Non_Storm_Data.gdb\\Vector_Grid\\Grid_Points_AZ", "gpLayer")    # make a feature
layer of grid points
      dm.SelectLayerByLocation("gpLayer", "HAVE_THEIR_CENTER_IN", "vgLayer")    # select the grid points
within the vector grid selection
      con.FeatureClassToFeatureClass("gpLayer", env.workspace, "PMP_Points")    # save feature layer as
"PMP_Points" feature class
      arcpy.AddMessage("(" + str(dm.GetCount("gpLayer")) + " grid points will be analyzed)")
      # Add PMP Fields
      for dur in durList:
```

```
            arcpy.AddMessage("\n\t...adding field: PMP_" + str(dur))
            dm.AddField("PMP_Points", "PMP_" + dur, "DOUBLE")
        # Add STORM Fields (this string values identifies the driving storm by SPAS ID number)
        for dur in durList:
            arcpy.AddMessage("\n\t...adding field: STORM_" + str(dur))
            dm.AddField("PMP_Points", "STORM_" + dur, "TEXT", "", "", 16)
    def getAOIarea():
        sr = arcpy.Describe(aoiBasin).SpatialReference          # Determine aoiBasin spatial reference system
        srname = sr.name
        srtype = sr.type
        srunitname = sr.linearUnitName                          # Units
        arcpy.AddMessage("\nAOI Basin Spatial Reference:  " + srname + "\nUnit Name: " + srunitname + "\nSpatial Ref. type: " +
srtype)

        aoiArea = 0.0
        rows = arcpy.SearchCursor(aoiBasin)
        for row in rows:
            feat = row.getValue("Shape")
            aoiArea += feat.area
        if srtype == 'Geographic':                              # Must have a surface projection
            arcpy.AddMessage("\nThe basin shapefile's spatial reference '" + srtype + "' is not supported.  Please use a 'Projected'
shapefile or feature class.\n")
            raise SystemExit
        elif srtype == 'Projected':
            if srunitname == "Meter":
                aoiArea = aoiArea * 0.000000386102              # Converts square meters to square miles
            elif srunitname == "Foot" or "Foot_US":
                aoiArea = aoiArea * 0.00000003587               # Converts square feet to square miles
            else:
                arcpy.AddMessage("\nThe basin shapefile's unit type '" + srunitname + "' is not supported.")
                sys.exit("Invalid linear units")                # Units must be meters or feet

        aoiArea = round(aoiArea, 3)
        arcpy.AddMessage("\nArea of interest: " + str(aoiArea) + " square miles.")

        # aoiArea = 100     ## Enable a constant area size
        arcpy.AddMessage("\n***Area used for PMP analysis: " + str(aoiArea) + " sqmi***")
        return aoiArea
    ###########################################################################
    ##  Define dadLookup() function:
    ##  The dadLookup() function determines the DAD value for the current storm
    ##  and duration according to the basin area size.  The DAD depth is interpolated
    ##  linearly between the two nearest areal values within the DAD table.
    def dadLookup(stormLayer, duration, area):              # dadLookup() accepts the current storm layer name (string), the current
duration (string), and AOI area size (float)
        #arcpy.AddMessage("\t\tfunction dadLookup() called.")
        durField = "H_" + duration                          # defines the name of the duration field (eg., "H_06" for 6-hour)
        dadTable = dadGDB + "\\" + stormLayer
        rows = arcpy.SearchCursor(dadTable)

        try:
            row = rows.next()                               # Sets DAD area x1 for basins that are smaller than the smallest DAD area.
            x1 = row.AREASQMI
            y1 = row.getValue(durField)
```

```
        xFlag = "FALSE"                         # Sets DAD area x2 for basins that are larger than the largest DAD area.
    except RuntimeError:                        # return if duration does not exist in DAD table
        return

    #arcpy.AddMessage("\nInitial x1 = " + str(x1) + "\ny1 = " + str(y1))

    row = rows.next()
    i = 0
    while row:                                  # iterates through the DAD table - assiging the bounding values directly above and
below the basin area size
        i += 1
        if row.AREASQMI < area:
            x1 = row.AREASQMI
            y1 = row.getValue(durField)
        else:
            xFlag = "TRUE"
            x2 = row.AREASQMI
            y2 = row.getValue(durField)
            #arcpy.AddMessage("\nLoop " + str(i)+ "\nx1 = " + str(x1) + "\ny1 = " + str(y1) + "\nx2 = " + str(x2))
            break

        row = rows.next()
    del row, rows, i
    if xFlag == "FALSE":
        x2 = area                               # If x2 is equal to the basin area, this means that the largest DAD area is smaller than
the basin and the resulting DAD value must be extrapolated.
        #arcpy.AddMessage("x2 = " + str(x2))
        arcpy.AddMessage("\n\tThe basin area size: " + str(area) + " sqmi is greater than the largest DAD area: " + str(x1) + " sqmi.
DAD value is estimated by extrapolation.")    # In this case, y (the DAD depth) is estimated by extrapolating the DAD area to the
basin area size.
        y = x1 / x2 * y1
        return y                                # The extrapolated DAD depth (in inches) is returned.
    # arcpy.AddMessage("\nArea = " + str(area) + "\nx1 = " + str(x1) + "\nx2 = " + str(x2) + "\ny1 = " + str(y1) + "\ny2 = " + str(y2))

    x = area                                    # If the basin area size is within the DAD table area range, the DAD depth is interpolated
    deltax = x2 - x1                            # to determine the DAD value (y) at area (x) based on next lower (x1) and next higher
(x2) areas.
    deltay = y2 - y1
    diffx = x - x1
    y = y1 + diffx * deltay / deltax
    return y                                    # The interpolated DAD depth (in inches) is returned.
################################################################################
##  Define updatePMP() function:
##  This function updates the 'PMP_XX_' and 'STORM_XX' fields of the PMP_Points
##  feature class with the largest value from all analyzed storms stored in the
##  pmpValues list.
def updatePMP(pmpValues, stormID, duration):                                    # Accepts four arguments: pmpValues - largest
adjusted rainfall for current duration (float list); stormID - driver storm ID for each PMP value (text list); and duration (string)
    pmpfield = "PMP_" + duration
    stormfield = "STORM_" + duration
    gridRows = arcpy.UpdateCursor(outPath + "PMP.gdb\\PMP_Points")              # iterates through PMP_Points rows
    i = 0
    for row in gridRows:
```

```
          row.setValue(pmpfield, pmpValues[i])                              # Sets the PMP field value equal to the Max Adj.
Rainfall value (if larger than existing value).
          row.setValue(stormfield, stormID[i])                              # Sets the storm ID field to indicate the driving storm
event
          gridRows.updateRow(row)
          i += 1
      del row, gridRows, pmpfield, stormfield
      arcpy.AddMessage("\n\t" + duration + "-hour PMP values update complete. \n")
      return
   def outputPMP():
      global outPath
      pmpPoints = outPath + "PMP.gdb\\PMP_Points"                 # Location of 'PMP_Points' feature class which will provide
data for output

      arcpy.AddMessage("\nBeginning PMP Raster Creation...")
      for dur in durList:                                          # This code creates a raster GRID from the current PMP point
layer
         durField = "PMP_" + dur
         outLoc = outPath + "GRIDs.gdb\\pmp_" + dur
         arcpy.AddMessage("\n\tInput Path: " + pmpPoints)
         arcpy.AddMessage("\tOutput raster path: " + outPath)
         arcpy.AddMessage("\tField name: " + durField)
         con.FeatureToRaster(pmpPoints, durField, outLoc, "0.025")
         arcpy.AddMessage("\tOutput raster created...")
      del durField
      outFile = open(outPath + "Text_Output\\PMP_Distribution.txt", 'w')
      arcpy.AddMessage("\nPMP Raster Creation complete.")

      ###### This section applies the metadata templates to the output GIS files ######
      pointMetaLoc = home + "\\Input\\Metadata_Templates\\PMP_Points_Metadata_FGDC.xml"                  # Location of
'PMP_Points' feature class metadata template
      rasMetaLoc = home + "\\Input\\Metadata_Templates\\PMP_Raster_Metadata_FGDC.xml"                        # Location
of 'PMP_XX' raster file metadata template
      arcpy.AddMessage("\nAdding metadata to output files...")
      arcpy.AddMessage("\n\tPMP_Points feature class")
      con.MetadataImporter(pointMetaLoc, pmpPoints)                                         # Applies metadata to
'PMP_Points' feature class
      for dur in durList:                                                  # Applies metadata to 'PMP_XX' GRIDs
         targetPath = outPath + "GRIDs.gdb\\pmp_" + dur
         arcpy.AddMessage("\tPMP_" + str(dur) + " feature class")
         con.MetadataImporter(rasMetaLoc, targetPath)
      arcpy.AddMessage("\nOutput metadata import complete.")
   ################################################################################
   ##  This portion of the code iterates through each storm feature class in the
   ##  'Storm_Adj_Factors' geodatabase (evaluating the feature class only within
   ##  the Local, Tropical, or general feature dataset).  For each duration,
   ##  at each grid point within the aoi basin, the transpositionality is
   ##  confirmed.  Then the DAD precip depth is retrieved and applied to the
   ##  total adjustement factor to yield the total adjusted rainfall.  This
   ##  value is then sent to the updatePMP() function to update the 'PMP_Points'
   ##  feature class.
##~~~~~~~~~~~~~~~~~~~~~~~~~~~~~~~~~~~~~~~~~~~~~~~~~~~~~~~~~~~~~~~~~~~~~~~~~~~~~~~~~~~~~~~~~~~~~~~~~~~~~~~~~~~
~~~~~~~~~~~~~~~~~~~~~~~~~~~~~~~~~~~~~~~~~~~~~~~~~~~~~~~~~~~~~~~~~~~~~##
   desc = arcpy.Describe(basin)                                    # Check to ensure AOI input shape is a Polygon. If not - exit.
```

```
    basinShape = desc.shapeType
    if desc.shapeType == "Polygon":
        arcpy.AddMessage("\nBasin shape type: " + desc.shapeType)
    else:
        arcpy.AddMessage("\nBasin shape type: " + desc.shapeType)
        arcpy.AddMessage("\nError: Input shapefile must be a polygon!\n")
        sys.exit()

    createPMPfc()                                          # Call the createPMPfc() function to create the PMP_Points feature
class.
    env.workspace = adjFactGDB                            # the workspace environment is set to the 'Storm_Adj_Factors'
file geodatabase
    aoiSQMI = round(getAOIarea(),2)                        # Calls the getAOIarea() function to assign area of AOI
shapefile to 'aoiSQMI'

    for dur in durList:
        stormList = arcpy.ListFeatureClasses("", "Point", stormType)          # List all the total adjustment factor feature classes
within the storm type feature dataset.
        arcpy.AddMessage("\n**********************************************************************\nEvaluating " + dur + "-hour duration...")
        pmpList = []
        driverList = []
        gridRows = arcpy.SearchCursor(outPath + "PMP.gdb\\PMP_Points")
        try:
            for row in gridRows:
                pmpList.append(0.0)                        # creates pmpList of empty float values for each grid point to
store final PMP values
                driverList.append("STORM")                 # creates driverList of empty text values for each grid point to
store final Driver Storm IDs
            del row, gridRows
        except UnboundLocalError:
            arcpy.AddMessage("\n***Error: No data present within basin/AOI area.***\n")
            sys.exit()
        for storm in stormList:
            arcpy.AddMessage("\n\tEvaluating storm: " + storm + "...")
            dm.MakeFeatureLayer(storm, "stormLayer")                  # creates a feature layer for the current storm
            dm.SelectLayerByLocation("stormLayer", "HAVE_THEIR_CENTER_IN", "vgLayer")   # examines only the grid points that lie
within the AOI
            gridRows = arcpy.SearchCursor("stormLayer")
            pmpField = "PMP_" + dur
            i = 0
            try:
                dadPrecip = round(dadLookup(storm, dur, aoiSQMI),3)
                arcpy.AddMessage("\t\t" + dur + "-hour DAD value:  " + str(dadPrecip) + chr(34))
            except TypeError:                              # In no duration exists in the DAD table - move to the next storm
                arcpy.AddMessage("\t***Duration '" + str(dur) + "-hour' is not present for " + str(storm) + ".***\n")
                continue
            arcpy.AddMessage("\t\tComparing " + storm + " adjusted rainfall values against current driver values...\n")
            for row in gridRows:
                if row.TRANS == 1:                         # Only continue if grid point is transpositionable ('1' is transpostionable, '0'
is not).
                    try:                                   # get total adj. factor if duration exists
                        maxAdjRain = round(dadPrecip * row.TAF,2)
                        if maxAdjRain > pmpList[i]:
                            pmpList[i] = maxAdjRain
```

```
                    driverList[i] = storm
                except RuntimeError:
                    arcpy.AddMessage("\t\t   *Warning* PMP value failed to set for row " + str(row.CNT))
                    break
            i += 1
        del row
    del storm, stormList, gridRows, dadPrecip
    updatePMP(pmpList, driverList, dur)           # calls function to update "PMP Points" feature class
del dur, pmpList

arcpy.AddMessage("\n'PMP_Points' Feature Class 'PMP_XX' fields update complete for all '" + stormType + "' storms.")

outputPMP()                    # calls outputPMP() function

##~~~~~~~~~~~~~~~~~~~~~~~~~~~~~~~~~~~~~~~~~~~~~~~~~~~~~~~~~~~~~~~~~~~~~~~~~~~~~~~~~~~~~~~~~~~~~~~~~~~~~~~~~~~~~~~~~
~~~~~~~~~~~~~~~~~~~~~~~~~~~~~~~~~~~~~~~~~~~~~~~~~~~~~~~~~~~~~~~~~~~~~~~~##
type = "General"
durList = durInput
outPath = home + "\\Output\\General\\"
arcpy.AddMessage("\nRunning PMP analysis for storm type: " + type)
pmpAnalysis(basin, type)         # Calls the pmpAnalysis() function to calculate the General storm PMP
arcpy.AddMessage("\nGeneral storm analysis
complete...\n*********************************************************************************************************")
```

Appendix C

Short List Storm Analysis Data Used for PMP Development

(Separate Binding)

Appendix D

Storm Precipitation Analysis System (SPAS) Program Description

INTRODUCTION

The Storm Precipitation Analysis System (SPAS) is grounded on years of scientific research with a demonstrated reliability in hundreds of post-storm precipitation analyses. It has evolved into a trusted hydrometeorological tool that provides accurate precipitation data at a high spatial and temporal resolution for use in a variety of sensitive hydrologic applications (Faulkner et al 2004, Tomlinson et al 2003-2012). Applied Weather Associates, LLC and METSTAT, Inc. initially developed SPAS in 2002 for use in producing Depth-Area-Duration values for Probable Maximum Precipitation (PMP) analyses. SPAS utilizes precipitation gauge data, "basemaps" and radar data (when available) to produce gridded precipitation at time intervals as short as 5-minutes, at spatial scales as fine as 1 km^2 and in a variety of customizable formats. To date (February 2014) SPAS has been used to analyze over 330 storm centers across all types of terrain, among highly varied meteorological settings and some occurring over 100-years ago.

SPAS output has many applications including, but not limited to: hydrologic model calibration/validation, flood event reconstruction, storm water runoff analysis, forensic cases and PMP studies. Detailed SPAS-computed precipitation data allow hydrologists to accurately model runoff from basins, particularly when the precipitation is unevenly distributed over the drainage basin or when rain gauge data are limited or not available. The increased spatial and temporal accuracy of precipitation estimates has eliminated the need for commonly made assumptions about precipitation characteristics (such as uniform precipitation over a watershed), thereby greatly improving the precision and reliability of hydrologic analyses.

To instill consistency in SPAS analyses, many of the core methods have remained consistent from the beginning. However, SPAS is constantly evolving and improving through new scientific advancements and as new data and improvements are incorporated. This write-up describes the current inter-workings of SPAS, but the reader should realize SPAS can be customized on a case-by-case basis to account for special circumstances; these adaptations are documented and included in the deliverables. The over arching goal of SPAS is to combine the strengths of rain gauge data and radar data (when available) to provide sound, reliable and accurate spatial precipitation data.

Hourly precipitation observations are generally limited to a small number of locations, with many basins lacking observational precipitation data entirely. However, Next Generation Radar (NEXRAD) data provide valuable spatial and temporal information over data-sparse basins, which have historically lacked reliability for determining precipitation rates and reliable quantitative precipitation estimates (QPE). The improved reliability in SPAS is made possible by hourly calibration of the NEXRAD radar-precipitation relationship, combined with local hourly bias adjustments to force consistency between the final result and "ground truth" precipitation measurements. If NEXRAD radar data are available (generally for storm events since the mid-1990's), precipitation accumulation at temporal scales as frequent as 5-minutes can be analyzed. If

no NEXRAD data are available, then precipitation data are analyzed in hourly increments. A summary of the general SPAS processes are shown in flow chart in Figure D.1.

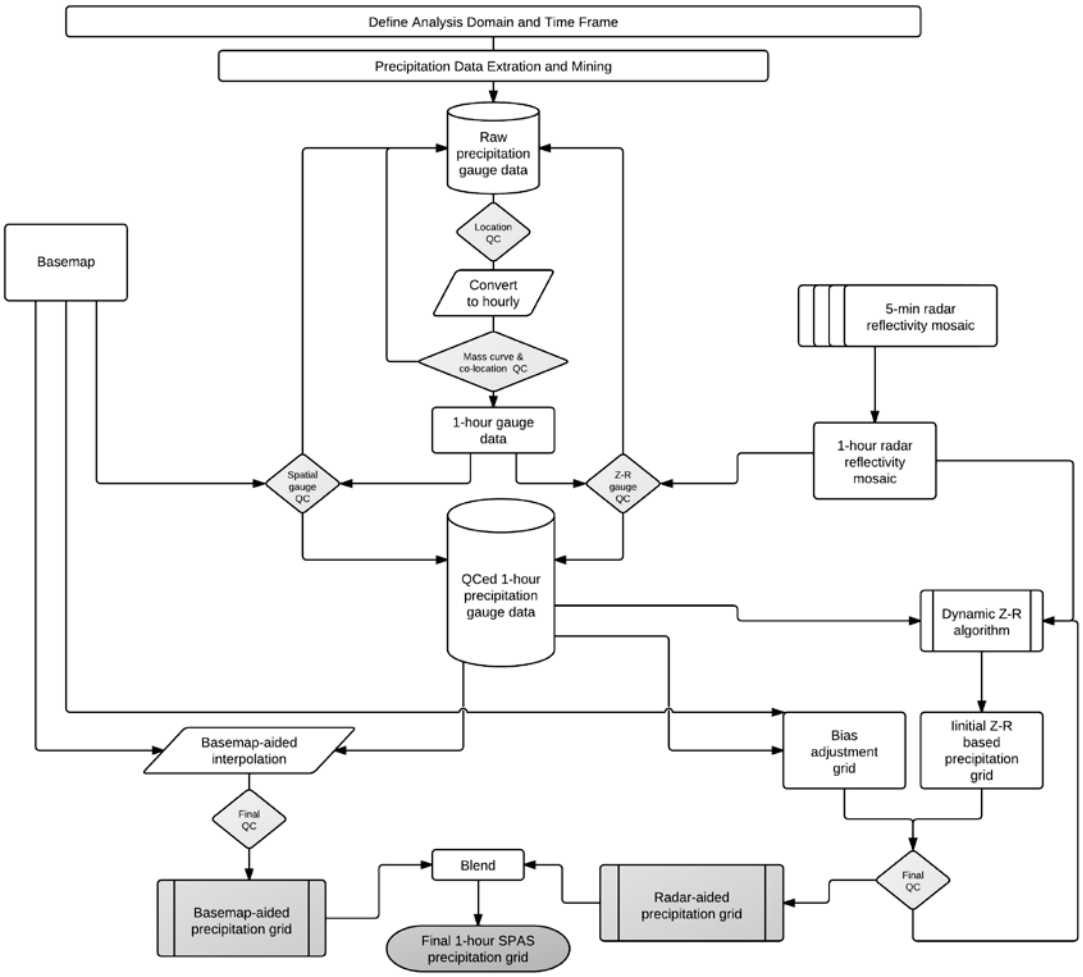

Figure D.1. SPAS flow chart.

SETUP

Prior to a SPAS analysis, careful definition of the storm analysis domain and time frame to be analyzed is established. Several considerations are made to ensure the domain (longitude-latitude box) and time frame are sufficient for the given application.

SPAS Analysis Domain

For PMP applications it is important to establish an analysis domain that completely encompasses a storm center, meanwhile hydrologic modeling applications are more concerned about a specific

basin, watershed or catchment. If radar data are available, then it is also important to establish an area large enough to encompass enough stations (minimum of ~30) to adequately derive reliable radar-precipitation intensity relationships (discussed later). The domain is defined by evaluating existing documentation on the storm as well as plotting and evaluating initial precipitation gauge data on a map. The analysis domain is defined to include as many hourly recording gauges as possible given their importance in timing. The domain must include enough of a buffer to accurately model the nested domain of interest. The domain is defined as a longitude-latitude (upper left and lower right corner) rectangular region.

SPAS Analysis Time Frame

Ideally, the analysis time frame, also referred to as the Storm Precipitation Period (SPP), will extend from a dry period through the target wet period then back into another dry period. This is to ensure that total storm precipitation amounts can be confidently associated with the storm in question and not contaminated by adjacent wet periods. If this is not possible, a reasonable time period is selected that is bounded by relatively lighter precipitation. The time frame of the hourly data must be sufficient to capture the full range of daily gauge observational periods for the daily observations to be disaggregated into estimated incremental hourly values (discussed later). For example, if a daily gauge takes observations at 8:00 AM, then the hourly data must be available from 8:00 AM the day prior. Given the configuration of SPAS, the minimum SPP is 72 hours and aligns midnight to midnight.

The core precipitation period (CPP) is a sub-set of the SPP and represents the time period with the most precipitation and the greatest number of reporting gauges. The CPP represents the time period of interest and where our confidence in the results is highest.

DATA

The foundation of a SPAS analysis is the “ground truth” precipitation measurements. In fact, the level of effort involved in “data mining” and quality control represent over half of the total level of effort needed to conduct a complete storm analysis. SPAS operates with three primary data sets: precipitation gauge data, a “basemap” and, if available, radar data. Table D.1 conveys the variety of precipitation gauges usable by SPAS. For each gauge, the following elements are gathered, entered and archived into SPAS database:

- Station ID
- Station name
- Station type (H=hourly, D=Daily, S=Supplemental, etc.)
- Longitude in decimal degrees
- Latitude in decimal degrees
- Elevation in feet above MSL

- Observed precipitation
- Observation times
- Source
- If unofficial, the measurement equipment and/or method is also noted.

Based on the SPP and analysis domain, hourly and daily precipitation gauge data are extracted from our in-house database as well as the Meteorological Assimilation Data Ingest System (MADIS). Our in-house database contains data dating back to the late 1800s, while the MADIS system (described below) contains archived data back to 2002.

Hourly Precipitation Data

Our hourly precipitation database is largely comprised of data from NCDC TD-3240, but also precipitation data from other mesnonets and meteorological networks (e.g. ALERT, Flood Control Districts, etc.) that we have collected and archived as part of previous studies. Meanwhile, MADIS provides data from a large number of networks across the U.S., including NOAA's HADS (Hydrometeorological Automated Data System), numerous mesonets, the Citizen Weather Observers Program (CWOP), departments of transportation, etc. (see http://madis.noaa.gov/mesonet_providers.html for a list of providers). Although our automatic data extraction is fast, cost-effective and efficient, it never captures all of the available precipitation data for a storm event. For this reason, a thorough "data mining" effort is undertaken to acquire all available data from sources such as U.S. Geological Survey (USGS), Remote Automated Weather Stations (RAWS), Community Collaborative Rain, Hail & Snow Network (CoCoRaHS), National Atmospheric Deposition Program (NADP), Clean Air Status and Trends Network (CASTNET), local observer networks, Climate Reference Network (CRN), Global Summary of the Day (GSD) and Soil Climate Analysis Network (SCAN). Unofficial hourly precipitation are gathered to give guidance on either timing or magnitude in areas otherwise void of precipitation data. The WeatherUnderground and MesoWest, two of the largest weather databases on the Internet, contain a good deal of official data, but also includes data from unofficial gauges.

Table D.1 Different precipitation gauge types used by SPAS.

Precipitation Gauge Type	Description
Hourly	Hourly gauges with complete, or nearly complete, incremental hourly precipitation data.
Hourly estimated	Hourly gauges with some estimated hourly values, but otherwise reliable.
Hourly pseudo	Hourly gauges with reliable temporal precipitation data, but the magnitude is questionable in relation to co-located daily or supplemental gauge.
Daily	Daily gauge with complete data and known observation times.
Daily estimated	Daily gauges with some or all estimated data.
Supplemental	Gauges with unknown or irregular observation times, but reliable total storm precipitation data. (E.g. public reports, storms reports, "Bucket surveys", etc.)
Supplemental estimated	Gauges with estimated total storm precipitation values based on other information (e.g. newspaper articles, stream flow discharge, inferences from nearby gauges, pre-existing total storm isohyetal maps, etc.)

Daily Precipitation Data

Our daily database is largely based on NCDC's TD-3206 (pre-1948) and TD-3200 (1948 through present) as well as SNOTEL data from NRCS. Since the late 1990s, the CoCoRaHS network of more than 15,000 observers in the U.S. has become a very important daily precipitation source. Other daily data are gathered from similar, but smaller gauge networks, for instance the High Spatial Density Precipitation Network in Minnesota.

As part of the daily data extraction process, the time of observation accompanies each measured precipitation value. Accurate observation times are necessary for SPAS to disaggregate the daily precipitation into estimated incremental values (discussed later). Knowing the observation time also allows SPAS to maintain precipitation amounts within given time bounds, thereby retaining known precipitation intensities. Given the importance of observation times, efforts are taken to insure the observation times are accurate. Hardcopy reports of "Climatological Data," scanned observational forms (available on-line from the NCDC) and/or gauge metadata forms have proven to be valuable and accurate resources for validating observation times. Furthermore, erroneous observation times are identified in the mass-curve quality-control procedure (discussed later) and can be corrected at that point in the process.

Supplemental Precipitation Gauge Data

For gauges with unknown or irregular observation times, the gauge is considered a "supplemental" gauge. A supplemental gauge can either be added to the storm database with a storm total and the associated SPP as the temporal bounds or as a gauge with the known, but irregular observation times and associated precipitation amounts. For instance, if all that is known is 3 inches fell between 0800-0900, then that information can be entered. Gauges or reports with nothing more than a storm total are often abundant, but to use them, it is important the precipitation is only from

the storm period in question. Therefore, it is ideal to have the analysis time frame bounded by dry periods.

Perhaps the most important source of data, if available, is from "bucket surveys," which provide comprehensive lists of precipitation measurements collected during a post-storm field exercise. Although some bucket survey amounts are not from conventional precipitation gauges, they provide important information, especially in areas lacking data. Particularly for PMP-storm analysis applications, it is customary to accept extreme, but valid non-standard precipitation values (such a bottles and other open containers that catch rainfall) in order to capture the highest precipitation values.

Basemap

"Basemaps" are independent grids of spatially distributed weather or climate variables that are used to govern the spatial patterns of the hourly precipitation. The basemap also governs the spatial resolution of the final SPAS grids, unless radar data are available/used to govern the spatial resolution. Note that a base map is not required as the hourly precipitation patterns can be based on station characteristics and an inverse distance weighting technique (discussed later). Basemaps in complex terrain are often based on the PRISM mean monthly precipitation (Figure D.2a) or Hydrometeorological Design Studies Center precipitation frequency grids (Figure D.2b) given they resolve orographic enhancement areas and micro-climates at a spatial resolution of 30-seconds (about 800 m). Basemaps of this nature in flat terrain are not as effective given the small terrain forced precipitation gradients. Therefore, basemaps for SPAS analyses in flat terrain are often developed from pre-existing (hand-drawn) isohyetal patterns (Figure D.2c), composite radar imagery or a blend of both.

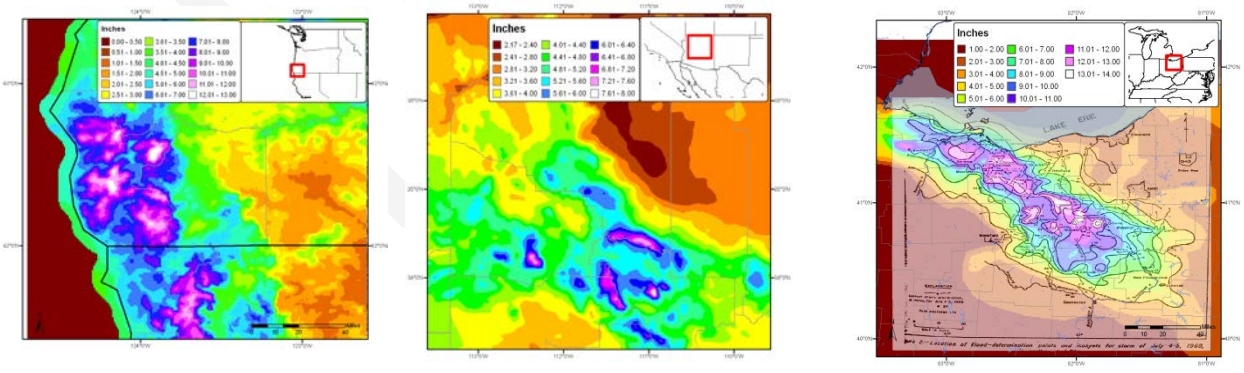

a) **b)** **c)**

Figure D.2 Sample SPAS "basemaps:" (a) A pre-existing (USGS) isohyetal pattern across flat terrain (SPAS #1209), (b) PRISM mean monthly (October) precipitation (SPAS #1192) and (c) A 100-year 24-hour precipitation grid from NOAA Atlas 14 (SPAS #1138).

Radar Data

For storms occurring since approximately the mid-1990s, weather radar data are available to supplement the SPAS analysis. A fundamental requirement for high quality radar-estimated precipitation is a high quality radar mosaic, which is a seamless collection of concurrent weather radar data from individual radar sites, however in some cases a single radar is sufficient (i.e. for a small area size storm event such as a thunderstorm). Weather radar data have been in use by meteorologists since the 1960s to estimate precipitation depths, but it was not until the early 1990s that new, more accurate NEXRAD Doppler radar (WSR88D) was placed into service across the United States. Currently, efforts are underway to convert the WSR88D radars to dual polarization (DualPol) radar. Today, NEXRAD radar coverage of the contiguous United States is comprised of 159 operational sites and there are 30 in Canada. Each U.S. radar covers an approximate 285 mile (460 km) radial extent and while Canadian radars have approximately 256 km (138 nautical miles) radial extent over which their radar can detect precipitation. (see Figure E.3) The primary vendor of NEXRAD weather radar data for SPAS is Weather Decision Technologies, Inc. (WDT), who accesses, mosaics, archives and quality-controls NEXRAD radar data from NOAA and Environment Canada. SPAS utilizes Level II NEXRAD radar reflectivity data in units of dBZ, available every 5-minutes in the U.S. and 10-minutes in Canada.

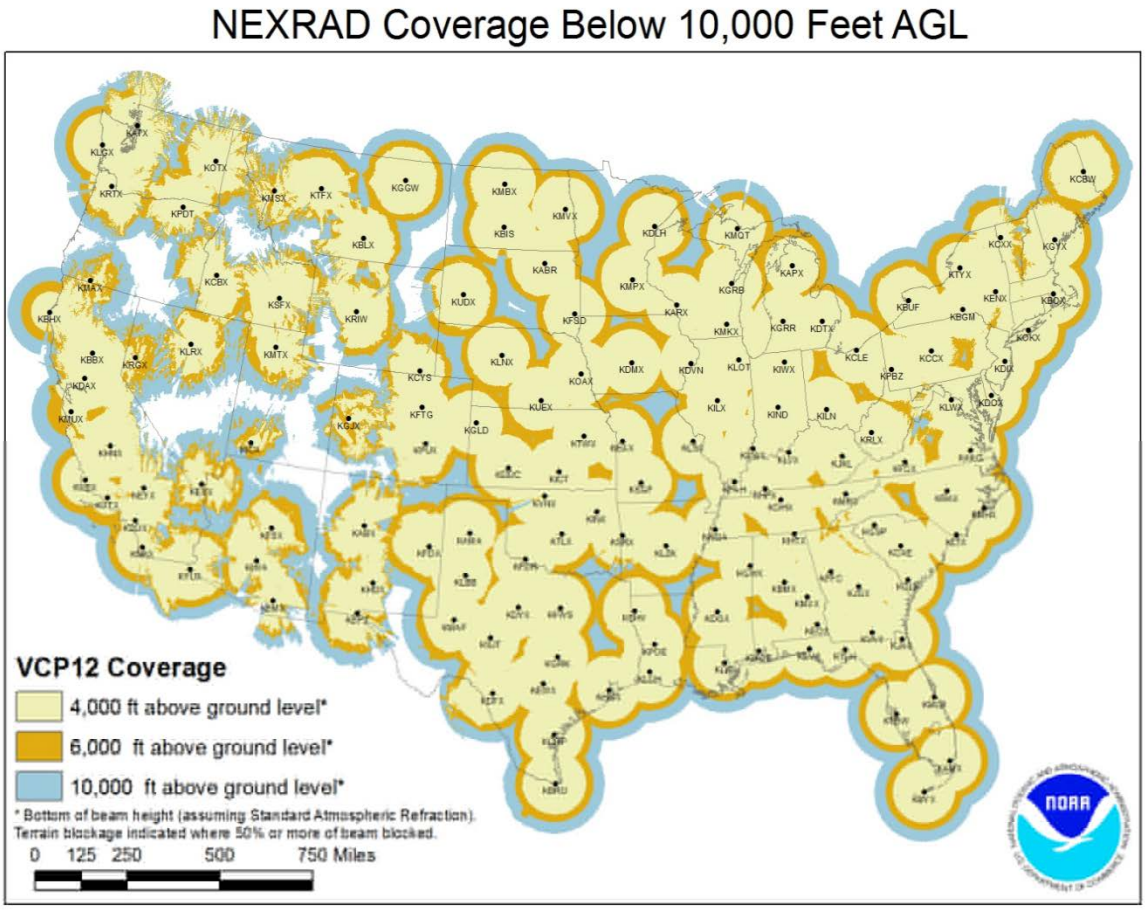

Figure D.3. U.S. radar locations and their radial extents of coverage below 10,000 feet above ground level (AGL). Each U.S. radar covers an approximate 285 mile radial extent over which the radar can detect precipitation.

The WDT and National Severe Storms Lab (NSSL) Radar Data Quality Control Algorithm (RDQC) removes non-precipitation artifacts from base Level–II radar data and remaps the data from polar coordinates to a Cartesian (latitude/longitude) grid. Non-precipitation artifacts include ground clutter, bright banding, sea clutter, anomalous propagation, sun strobes, clear air returns, chaff, biological targets, electronic interference and hardware test patterns. The RDQC algorithm uses sophisticated data processing and a Quality Control Neural Network (QCNN) to delineate the precipitation echoes caused by radar artifacts (Lakshmanan and Valente 2004). Beam blockages due to terrain are mitigated by using 30 meter DEM data to compute and then discard data from a radar beam that clears the ground by less than 50 meters and incurs more than 50% power blockage. A clear-air echo removal scheme is applied to radars in clear-air mode when there is no precipitation reported from observation gauges within the vicinity of the radar. In areas of radar coverage overlap, a distance weighting scheme is applied to assign reflectivity to each grid cell, for multiple vertical levels. This scheme is applied to data from the nearest radar that is unblocked by terrain.

Once the data from individual radars have passed through the RDQC, they are merged to create a seamless mosaic for the United States and southern Canada as shown in Figure D.4. A multi-sensor quality control can be applied by post-processing the mosaic to remove any remaining "false echoes". This technique uses observations of infra-red cloud top temperatures by GOES satellite and surface temperature to create a precipitation/no-precipitation mask. Figure 4 shows the impact of WDT's quality control measures. Upon completing all QC, WDT converts the radar data from its native polar coordinate projection (1 degree x 1.0 km) into a longitude-latitude Cartesian grid (based on the WGS84 datum), at a spatial resolution of ~1/3rdmi^2 for processing in SPAS.

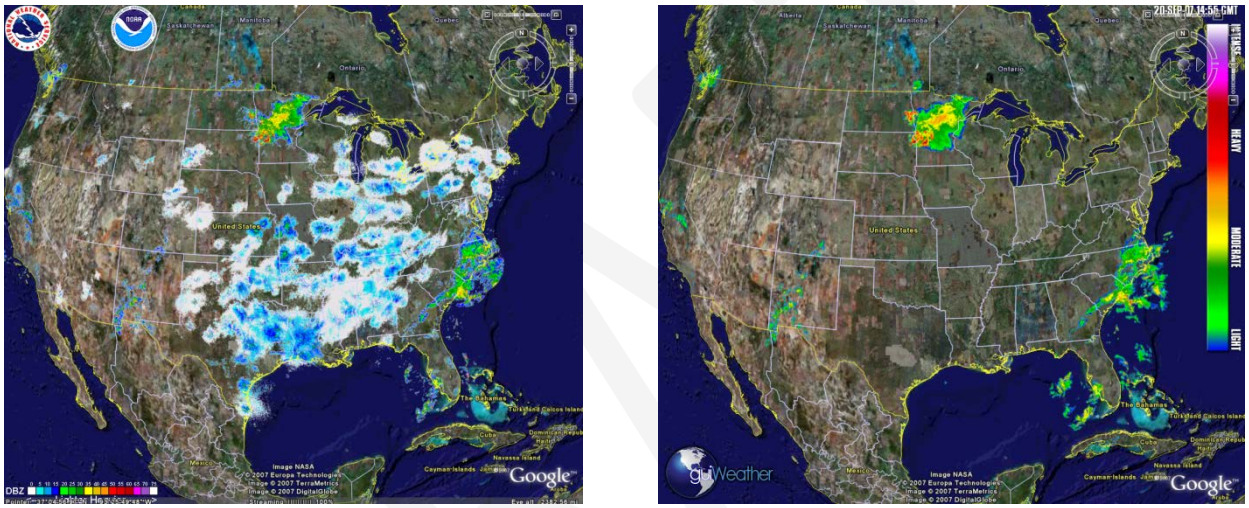

a) **b)**

Figure D.4. (a) Level-II radar mosaic of CONUS radar with no quality control, (b) WDT quality controlled Level-II radar mosaic.

SPAS conducts further QC on the radar mosaic by infilling areas contaminated by beam blockages. Beam blocked areas are objectively determined by evaluating total storm reflectivity grid which naturally amplifies areas of the SPAS analysis domain suffering from beam blockage as shown in Figure D.5.

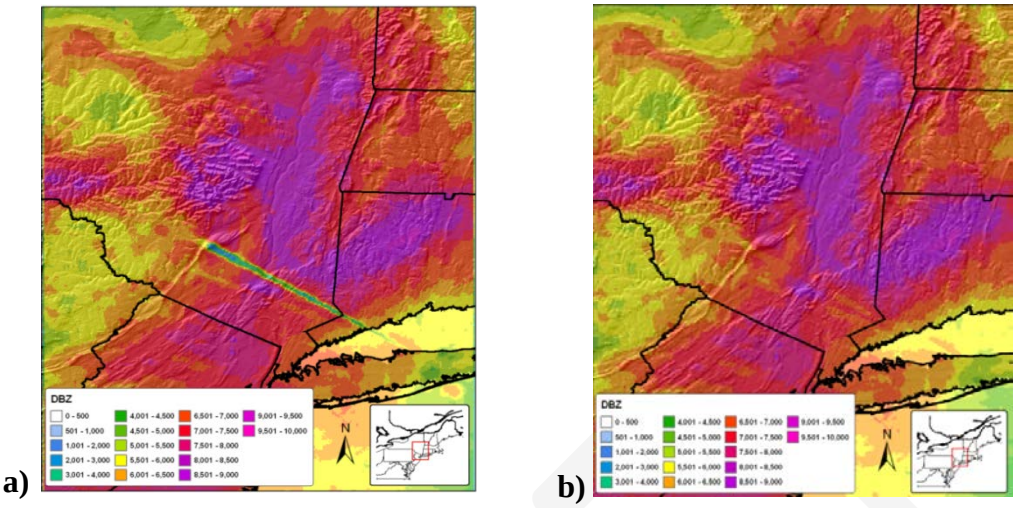

Figure D.5. Illustration of SPAS-beam blockage infilling where (a) is raw, blocked radar and (b) is filled for a 42-hour storm event.

METHODOLOGY

Daily and Supplemental Precipitation to Hourly

To obtain one hour temporal resolutions and utilize all gauge data, it is necessary to disaggregate the daily and supplemental precipitation observations into estimated hourly amounts. This process has traditionally been accomplished by distributing (temporally) the precipitation at each daily/supplemental gauge in accordance to a single nearby hourly gauge (Thiessen polygon approach). However, this may introduce biases and not correctly represent hourly precipitation at daily/supplemental gauges situated in-between hourly gauges. Instead, SPAS uses a spatial approach by which the estimated hourly precipitation at each daily and supplemental gauge is governed by a distance weighted algorithm of all nearby true hourly gauges.

To disaggregate (i.e. distribute) daily/supplemental gauge data into estimate hourly values, the true hourly gauge data are first evaluated and quality controlled using synoptic maps, nearby gauges, orographic effects, gauge history and other documentation on the storm. Any problems with the hourly data are resolved, and when possible/necessary accumulated hourly values are distributed. If an hourly value is missing, the analyst can choose to either estimate it or leave it missing for SPAS to estimate later based on nearby hourly gauges. At this point in the process, pseudo (hourly) gauges can be added to represent precipitation timing in topographically complex locations, areas with limited/no hourly data or to capture localized convention. To adequately capture the temporal variations of the precipitation, a pseudo hourly gauge is sometimes necessary. A pseudo gauge is created by distributing the precipitation at a co-located daily gauge or by creating a completely new pseudo gauge from other information such as inferences from COOP observation forms, METAR visibility data (if hourly precipitation are not already available), lightning data, satellite data, or

radar data. Often radar data are the best/only choice for creating pseudo hourly gauges, but this is done cautiously given the potential differences (over-shooting of the radar beam equating to erroneous precipitation) between radar data and precipitation. In any case, the pseudo hourly gauge is flagged so SPAS only uses it for timing and not magnitude. Care is taken to ensure hourly pseudo gauges represent justifiably important physical and meteorological characteristics before being incorporated into the SPAS database. Although pseudo gauges provide a very important role, their use is kept to a minimum. The importance of insuring the reliability of every hourly gauge cannot be over emphasized. All of the final hourly gauge data, including pseudos, are included in the hourly SPAS precipitation database.

Using the hourly SPAS precipitation database, each hourly precipitation value is converted into a percentage that represents the incremental hourly precipitation divided by the total SPP precipitation. The GIS-ready x-y-z file is constructed for each hour and it includes the latitude (x), longitude(y) and the percent of precipitation (z) for a particular hour. Using the GRASS GIS, an inverse-distance-weighting squared (IDW) interpolation technique is applied to each of the hourly files. The result is a continuous grid with percentage values for the entire analysis domain, keeping the grid cells on which the hourly gauge resides faithful to the observed/actual percentage. Since the percentages typically have a high degree of spatial autocorrelation, the spatial interpolation has skill in determining the percentages between gauges, especially since the percentages are somewhat independent of the precipitation magnitude. The end result is a GIS grid for each hour that represents the percentage of the SPP precipitation that fell during that hour.

After the hourly percentage grids are generated and QCed for the entire SPP, a program is executed that converts the daily/supplemental gauge data into incremental hourly data. The timing at each of the daily/supplemental gauges is based on (1) the daily/supplemental gauge observation time, (2) daily/supplemental precipitation amount and (3) the series of interpolated hourly percentages extracted from grids (described above).

This procedure is detailed in Figure D.6 below. In this example, a supplemental gauge reported 1.40" of precipitation during the storm event and is located equal distance from the three surrounding hourly recording gauges. The procedure steps are:

Step 1. For each hour, extract the percent of SPP from the hourly gauge-based percentage at the location of the daily/supplemental gauge. In this example, assume these values are the average of all the hourly gauges.

Step 2. Multiply the individual hourly percentages by the total storm precipitation at the daily/supplemental gauge to arrive at estimated hourly precipitation at the daily/supplemental gauge. To make the daily/supplemental accumulated precipitation data faithful to the daily/supplemental observations, it is sometimes

necessary to adjust the hourly percentages so they add up to 100% and account for 100% of the daily observed precipitation.

	Hour						
Precipitation	**1**	**2**	**3**	**4**	**5**	**6**	**Total**
Hourly station 1	0.02	0.12	0.42	0.50	0.10	0.00	1.16
Hourly station 2	0.01	0.15	0.48	0.62	0.05	0.01	1.32
Hourly station 3	0.00	0.18	0.38	0.55	0.20	0.05	1.36
	Hour						
Percent of total storm precip.	**1**	**2**	**3**	**4**	**5**	**6**	**Total**
Hourly station 1	2%	10%	36%	43%	9%	0%	100%
Hourly station 2	1%	11%	36%	47%	4%	1%	100%
Hourly station 3	0%	13%	28%	40%	15%	4%	100%
Average	*1%*	*12%*	*34%*	*44%*	*9%*	*1%*	*100%*
Storm total precipitation at daily gauge				1.40			
	Hour						
Precipitation (estimated)	**1**	**2**	**3**	**4**	**5**	**6**	**Total**
Daily station	0.01	0.16	0.47	0.61	0.13	0.02	1.40

Figure D.6 Example of disaggregation of daily precipitation into estimated hourly precipitation based on three (3) surrounding hourly recording gauges.

In cases where the hourly grids do not indicate any precipitation falling during the daily/supplemental gauge observational period, yet the daily/supplemental gauge reported precipitation, the daily/supplemental total precipitation is evenly distributed throughout the hours that make up the observational period; although this does not happen very often, this solution is consistent with NWS procedures. However, the SPAS analyst is notified of these cases in a comprehensive log file, and in most cases they are resolvable, sometimes with a pseudo hourly gauge.

GAUGE QUALITY CONTROL

Exhaustive quality control measures are taken throughout the SPAS analysis. Below are a few of the most significant QC measures taken.

Mass Curve Check

A mass curve-based QC-methodology is used to ensure the timing of precipitation at all gauges is consistent with nearby gauges. SPAS groups each gauge with the nearest four gauges (regardless of type) into a single file. These files are subsequently used in software for graphing and evaluation. Unusual characteristics in the mass curve are investigated and the gauge data corrected, if possible and warranted. See Figure E.7 for an example.

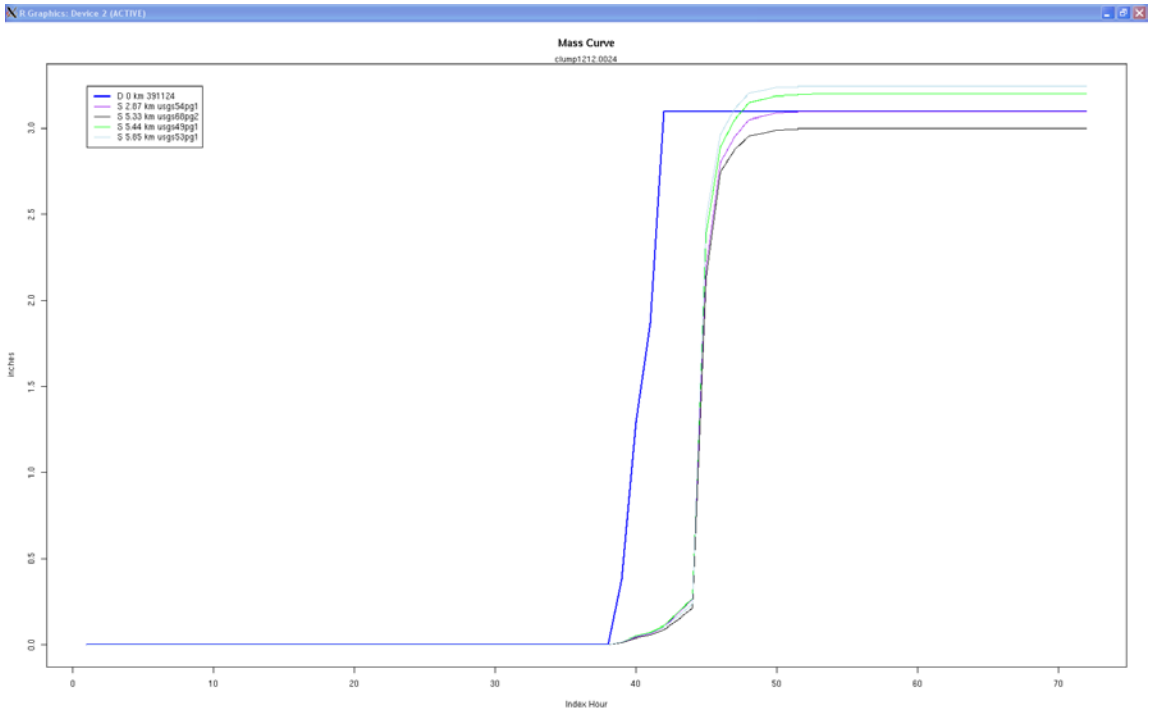

Figure D.7 Sample mass curve plot depicting a precipitation gauge with an erroneous observation time (blue line). X-axis is the SPAS index hour and the y-axis is inches. The statistics in the upper left denote gauge type, distance from target gauge (in km), and gauge ID. In this example, the center gauge (blue line) was found to have an observation error/shift of 1 day.

Gauge Mis-location Check

Although the gauge elevation is not explicitly used in SPAS, it is however used as a means of QCing gauge location. Gauge elevations are compared to a high-resolution 15-second DEM to identify gauges with large differences, which may indicate erroneous longitude and/or latitude values.

Co-located Gauge QC

Care is also taken to establish the most accurate precipitation depths at all co-located gauges. In general, where a co-located gauge pair exists, the highest precipitation is accepted (if deemed accurate). If the hourly gauge reports higher precipitation, then the co-located daily (or supplemental) is removed from the analysis since it would not add anything to the analysis. Often daily (or supplemental) gauges report greater precipitation than a co-located hourly station since hourly tipping bucket gauges tend to suffer from gauge under-catch, particularly during extreme events, due to loss of precipitation during tips. In these cases the daily/supplemental is retained for the magnitude and the hourly used as a pseudo hourly gauge for timing. Large discrepancies between any co-located gauges are investigated and resolved since SPAS can only utilize a single gauge magnitude at each co-located site.

SPATIAL INTERPOLATION

At this point the QCed observed hourly and disaggregated daily/supplemental hourly precipitation data are spatially interpolated into hourly precipitation grids. SPAS has three options for conducting the hourly precipitation interpolation, depending on the terrain and availability of radar data, thereby allowing SPAS to be optimized for any particular storm type or location. Figure D.8 depicts the results of each spatial interpolation methodology based on the same precipitation gauge data.

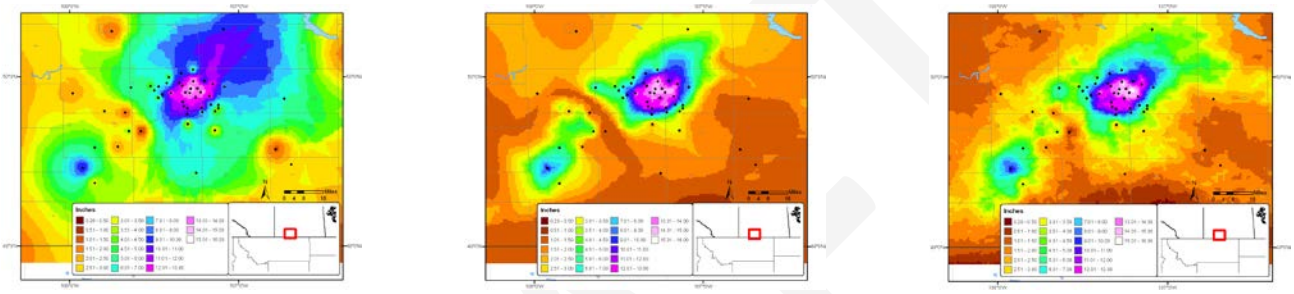

Figure D.8. Depictions of total storm precipitation based on the three SPAS interpolation methodologies for a storm (SPAS #1177, Vanguard, Canada) across flat terrain: (a) no basemap, (b) basemap-aided and (3) radar.

Basic Approach

The basic approach interpolates the hourly precipitation point values to a grid using an inverse distance weighting squared GIS algorithm. This is sometimes the best choice for convective storms over flat terrain when radar data are not available, yet high gauge density instills reliable precipitation patterns. This approach is rarely used.

Basemap Approach

Another option includes use of a "basemap", also known as a climatologically-aided interpolation (Hunter 2005). As noted before, the spatial patterns of the basemap govern the interpolation between points of hourly precipitation estimates, while the actual hourly precipitation values govern the magnitude. This approach to interpolating point data across complex terrain is widely used. In fact, it was used extensively by the NWS during their storm analysis era from the 1940s through the 1970s (USACE 1973, Hansen et al. 1988, Corrigan et al. 1999).

In application, the hourly precipitation gauge values are first normalized by the corresponding grid cell value of the basemap before being interpolated. The normalization allows information and knowledge from the basemap to be transferred to the spatial distribution of the hourly precipitation. Using an IDW squared algorithm, the normalized hourly precipitation values are interpolated to a grid. The resulting grid is then multiplied by the basemap grid to produce the hourly precipitation grid. This is repeated each hour of the storm.

Radar Approach

The coupling of SPAS with NEXRAD provides the most accurate method of spatially and temporally distributing precipitation. To increase the accuracy of the results however, quality-controlled precipitation observations are used for calibrating the radar reflectivity to rain rate relationship (Z-R relationship) each hour instead of assuming a default Z-R relationship. Also, spatial variability in the Z-R relationship is accounted for through local bias corrections (described later). The radar approach involves several steps, each briefly described below. The radar approach cannot operate alone – either the basic or basemap approach must be completed before radar data can be incorporated.

Z-R Relationship

SPAS derives high quality precipitation estimates by relating quality controlled level–II NEXRAD radar reflectivity radar data with quality-controlled precipitation gauge data to calibrate the Z-R (radar reflectivity, Z, and precipitation, R) relationship. Optimizing the Z-R relationship is essential for capturing temporal changes in the Z-R. Most current radar-derived precipitation techniques rely on a constant relationship between radar reflectivity and precipitation rate for a given storm type (e.g. tropical, convective), vertical structure of reflectivity and/or reflectivity magnitudes. This non-linear relationship is described by the Z-R equation below:

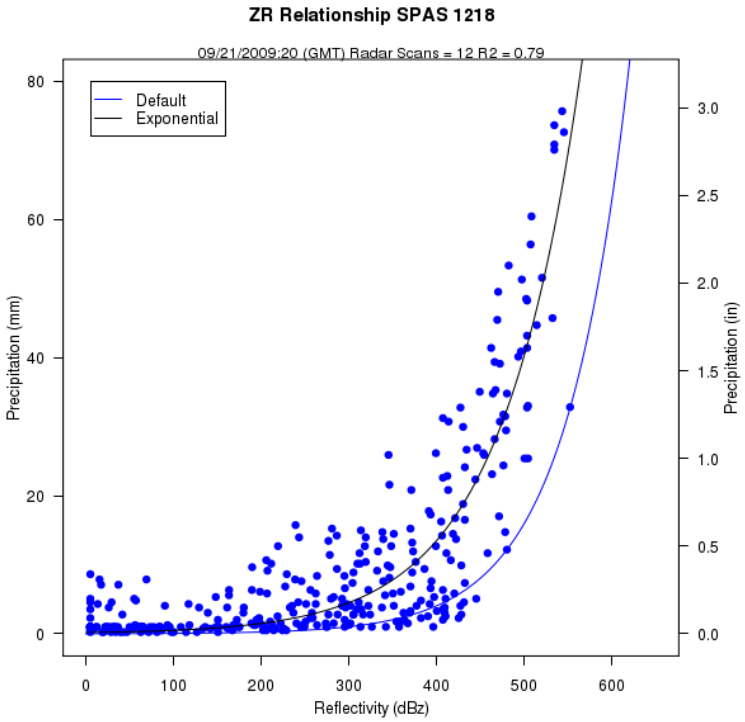

$$Z = A R^{b} \quad (1)$$

Figure D.9. Example SPAS (denoted as "Exponential") vs. default Z-R relationship (SPAS #1218, Georgia September 2009).

Where Z is the radar reflectivity (measured in units of dBZ), R is the precipitation (precipitation) rate (millimeters per hour), A is the "multiplicative coefficient" and b is the "power coefficient". Both A and b are directly related to the rain drop size distribution (DSD) and rain drop number distribution (DND) within a cloud (Martner and Dubovskiy 2005). The variability in the results of Z versus R is a direct result of differing DSD, DND and air mass characteristics (Dickens 2003). The DSD and DND are determined by complex interactions of microphysical processes that fluctuate regionally, seasonally, daily, hourly, and even within the same cloud. For these reasons, SPAS calculates an optimized Z-R relationship across the analysis domain each hour, based on observed precipitation rates and radar reflectivity (see Figure D.9).

The National Weather Service (NWS) utilizes different default Z-R algorithms, depending on the type of precipitation event, to estimate precipitation from NEXRAD radar reflectivity data across the United States (see Figure D.10) (Baeck and Smith 1998 and Hunter 1999). A default Z-R relationship of $Z = 300R^{1.4}$ is the primary algorithm used throughout the continental U.S. However, it is widely known that this, compared to unadjusted radar-aided estimates of precipitation, suffers from deficiencies that may lead to significant over or under-estimation of precipitation.

RELATIONSHIP	Optimum for:	Also recommended for:
Marshall-Palmer ($z=200R^{1.6}$)	General stratiform precipitation	
East-Cool Stratiform ($z=130R^{2.0}$)	Winter stratiform precipitation - east of continental divide	Orographic rain - East
West-Cool Stratiform ($z=75R^{2.0}$)	Winter stratiform precipitation - west of continental divide	Orographic rain - West
WSR-88D Convective ($z=300R^{1.4}$)	Summer deep convection	Other non-tropical convection
Rosenfeld Tropical ($z=250R^{1.2}$)	Tropical convective systems	

Figure D.10. Commonly used Z-R algorithms used by the NWS.

Instead of adopting a standard Z-R, SPAS utilizes a least squares fit procedure for optimizing the Z-R relationship each hour of the SPP. The process begins by determining if sufficient (minimum 12) observed hourly precipitation and radar data pairs are available to compute a reliable Z-R. If insufficient (<12) gauge pairs are available, then SPAS adopts the previous hour Z-R relationship, if available, or applies a user-defined default Z-R algorithm from Figure 9. If sufficient data are available, the one hour sum of NEXRAD reflectivity (Z) is related to the 1-hour precipitation at each gauge. A least-squares-fit exponential function using the data points is computed. The resulting best-fit, one hour-based Z-R is subjected to several tests to determine if the Z-R relationship and its resulting precipitation rates are within a certain tolerance based on the R-squared fit measure and difference between the derived and default Z-R precipitation results.

Experience has shown the actual Z-R versus the default Z-R can be significantly different (Figure D.11). These Z-R relationship vary by storm type and location. A standard output of all SPAS analyses utilizing NEXRAD includes a file with each hour's adjusted Z-R relationship as calculated through the SPAS program.

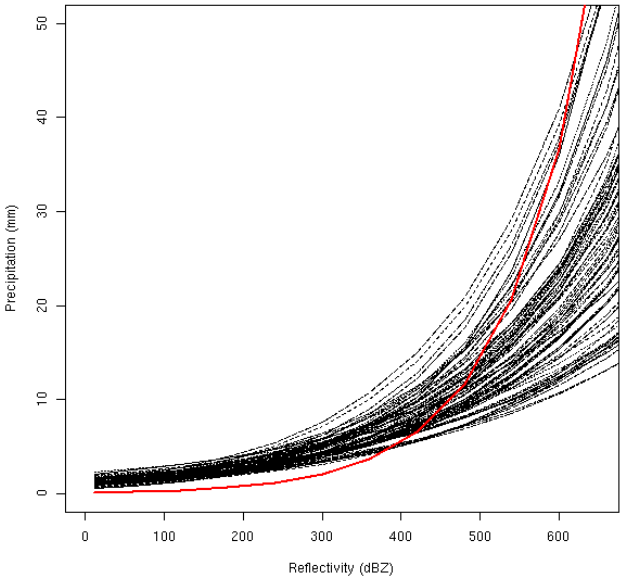

Figure D.11. Comparison of the SPAS optimized hourly Z-R relationships (black lines) versus a default Z=75R2.0 Z-R relationship (red line) for a period of 99 hours for a storm over southern California.

Radar-aided Hourly Precipitation Grids

Once a mathematically optimized hourly Z-R relationship is determined, it is applied to the total hourly Z grid to compute an initial precipitation rate (inches/hour) at each grid cell. To account for spatial differences in the Z-R relationship, SPAS computes residuals, the difference between the initial precipitation analysis (via the Z-R equation) and the actual "ground truth" precipitation (observed – initial analysis), at each gauge. The point residuals, also referred to as local biases, are normalized and interpolated to a residual grid using an inverse distance squared weighting algorithm. A radar-based hourly precipitation grid is created by adding the residual grid to the initial grid; this allows the precipitation at the grid cells for which gauges are "on" to be true and faithful to the gauge measurement. The pre-final radar-aided precipitation grid is subject to some final, visual QC checks to ensure the precipitation patterns are consistent with the terrain; these checks are particularly important in areas of complex terrain where even QCed radar data can be unreliable. The next incremental improvement with SPAS program will come as the NEXRAD radar sites are upgraded to dual-polarimetric capability.

Radar- and Basemap-Aided Hourly Precipitation Grids

At this stage of the radar approach, a radar- and basemap-aided hourly precipitation grid exists for each hour. At locations with precipitation gauges, the grids are equal, however elsewhere the grids can vary for a number of reasons. For instance, the basemap-aided hourly precipitation grid may depict heavy precipitation in an area of complex terrain, blocked by the radar, whereas the radar-aided hourly precipitation grid may suggest little, if any, precipitation fell in the same area. Similarly, the radar-aided hourly precipitation grid may depict an area of heavy precipitation in flat terrain that the basemap-approach missed since the area of heavy precipitation occurred in an area without gauges. SPAS uses an algorithm to compute the hourly precipitation at each pixel given the two results. Areas that are completely blocked from a radar signal are accounted for with the basemap-aided results (discussed earlier). Precipitation in areas with orographically effective terrain and reliable radar data are governed by a blend of the basemap- and radar-aided precipitation. Elsewhere, the radar-aided precipitation is used exclusively. This blended approach has proven effective for resolving precipitation in complex terrain, yet retaining accurate radar-aided precipitation across areas where radar data are reliable. Figure D.12 illustrates the evolution of final precipitation from radar reflectivity in an area of complex terrain in southern California.

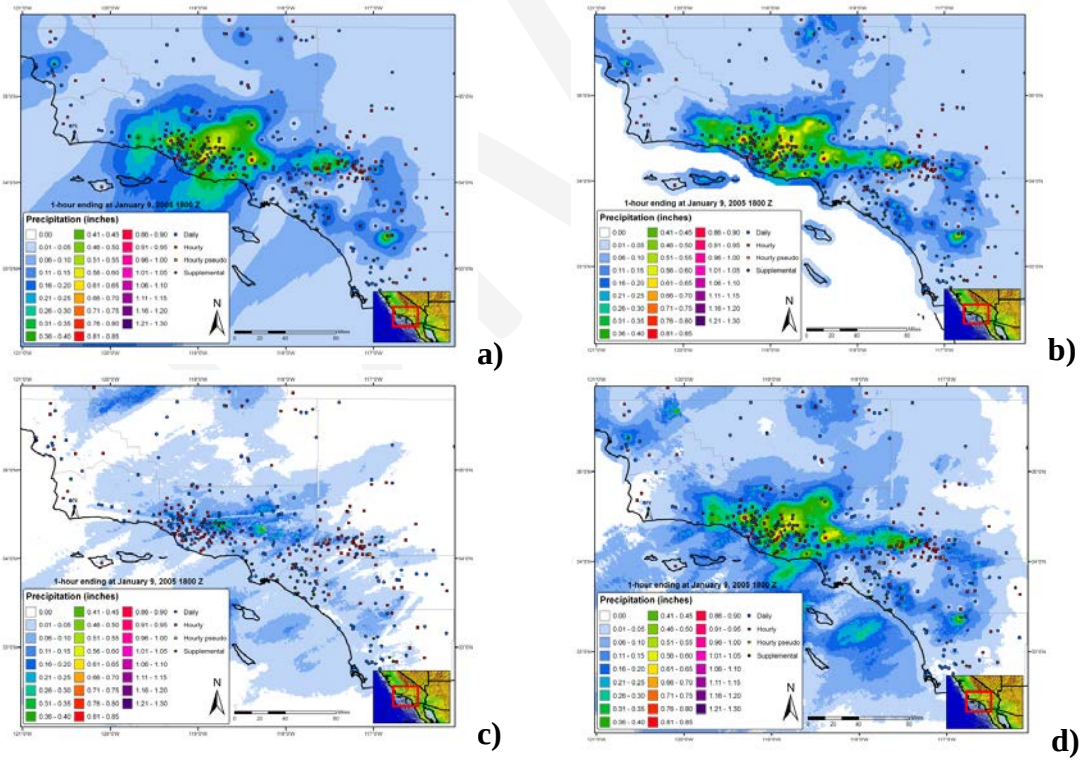

Figure D.12. A series of maps depicting 1-hour of precipitation utilizing (a) inverse distance weighting of gauge precipitation, (b) gauge data together with a climatologically-aided interpolation scheme, (c) default Z-R radar-estimated interpolation (no gauge correction) and (d) SPAS precipitation for a January 2005 storm in southern California, USA.

SPAS versus Gauge Precipitation

Performance measures are computed and evaluated each hour to detect errors and inconsistencies in the analysis. The measures include: hourly Z-R coefficients, observed hourly maximum precipitation, maximum gridded precipitation, hourly bias, hourly mean absolute error (MAE), root mean square error (RMSE), and hourly coefficient of determination (r^2).

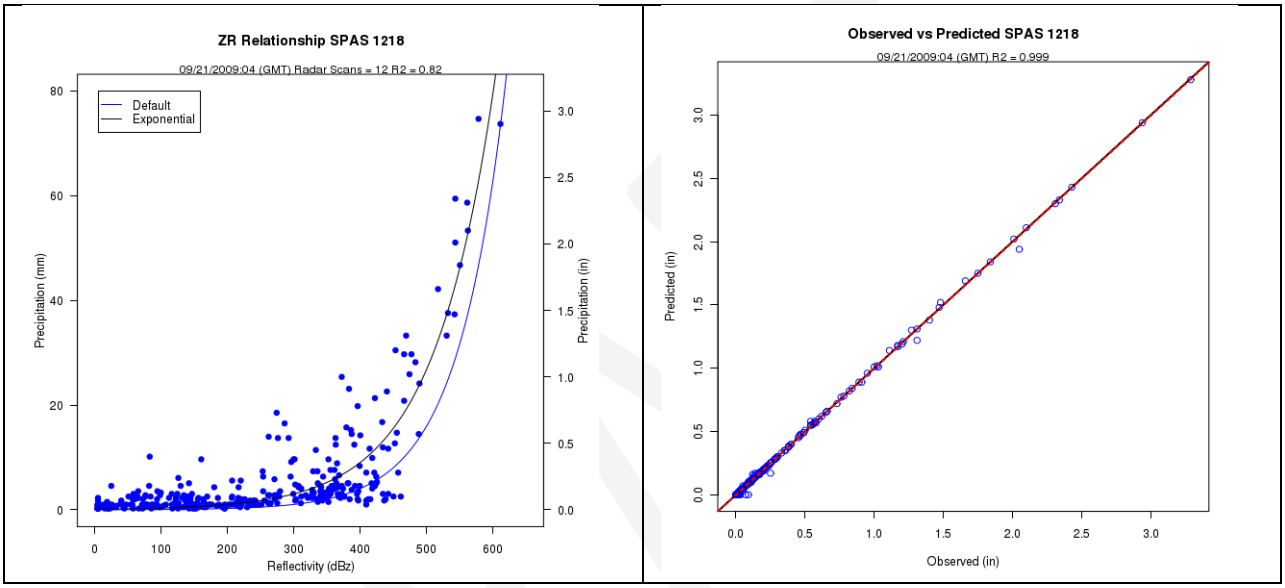

Figure D.13. Z-R plot (a), where the blue line is the SPAS derived Z-R and the black line is the default Z-R, and the (b) associated observed versus SPAS scatter plot at gauge locations.

Comparing SPAS-calculated precipitation (R_{spas}) to observed point precipitation depths at the gauge locations provides an objective measure of the consistency, accuracy and bias. Generally speaking SPAS is usually within 5% of the observed precipitation (see Figure D.13). Less-than-perfect correlations between SPAS precipitation depths and observed precipitation at gauged locations could be the result of any number of issues, including:

- **Point versus area:** A rain gauge observation represents a much smaller area than the area sampled by the radar. The area that the radar is sampling is approximately 1 km^2, whereas a standard rain gauge has an opening 8 inches in diameter, hence it only samples approximately $8.0x10^{-9}$ km^2. Furthermore, the radar data represents an average reflectivity (Z) over the grid cell, when in fact the reflectivity can vary across the 1 km^2 grid cell. Therefore, comparing a grid cell radar derived precipitation value to a gauge (point) precipitation depth measured may vary.

- **Precipitation gauge under-catch:** Although we consider gauge data "ground truth," we recognize gauges themselves suffer from inaccuracies. Precipitation gauges, shielded and unshielded, inherently underestimate total precipitation due to local airflow, wind under-catch, wetting, and evaporation. The wind under-catch errors are usually around 5% but can be as large as 40% in high winds (Guo et al 2001, Duchon and Essenberg 2001, Ciach 2003, Tokay et al 2010). Tipping buckets miss a small amount of precipitation during each tip of the bucket due to the bucket travel and tip time. As precipitation intensities increase, the volumetric loss of precipitation due to tipping tends to increase. Smaller tipping buckets can have higher volumetric losses due to higher tip frequencies, but on the other hand capture higher precision timing.

- **Radar Calibration:** NEXRAD radars calibrate reflectivity every volume scan, using an internally generated test. The test determines changes in internal variables such as beam power and path loss of the receiver signal processor since the last off-line calibration. If this value becomes large, it is likely that there is a radar calibration error that will translate into less reliable precipitation estimates. The calibration test is supposed to maintain a reflectivity precision of 1 dBZ. A 1 dBZ error can result in an error of up to 17% in R_{spas} using the default Z-R relationship $Z=300R^{1.4}$. Higher calibration errors will result in higher R_{spas} errors. However, by performing correlations each hour, the calibration issue is minimized in SPAS.

- **Attenuation:** Attenuation is the reduction in power of the radar beams' energy as it travels from the antenna to the target and back. It is caused by the absorption and the scattering of power from the beam by precipitation. Attenuation can result in errors in Z as large as 1 dBZ especially when the radar beam is sampling a large area of heavy precipitation. In some cases, storm precipitation is so intense (>12 inches/hour) that individual storm cells become "opaque" and the radar beam is totally attenuated. Armed with sufficient gauge data however, SPAS will overcome attenuation issues.

- **Range effects:** The curvature of the Earth and radar beam refraction result in the radar beam becoming more elevated above the surface with increasing range. With the increased elevation of the radar beam comes a decrease in Z values due to the radar beam not sampling the main precipitation portion of the cloud (i.e. "over topping" the precipitation and/or cloud altogether). Additionally, as the radar beam gets further from the radar, it naturally samples a larger and larger area, therefore amplifying point versus area differences (described above).

- **Radar Beam Occultation/Ground Clutter:** Radar occultation (beam blockage) results when the radar beam's energy intersects terrain features as depicted in Figure D.14. The result is an increase in radar reflectivity values that can result in higher than normal

precipitation estimates. The WDT processing algorithms account for these issues, but SPAS uses GIS spatial interpolation functions to infill areas suffering from poor or no radar coverage.

- **Anomalous Propagation (AP)** - AP is false reflectivity echoes produced by unusual rates of refraction in the atmosphere. WDT algorithms remove most of the AP and false echoes, however in extreme cases the air near the ground may be so cold and dense that a radar beam that starts out moving upward is bent all the way down to the ground. This produces erroneously strong echoes at large distances from the radar. Again, equipped with sufficient gauge data, the SPAS bias corrections will overcome AP issues.

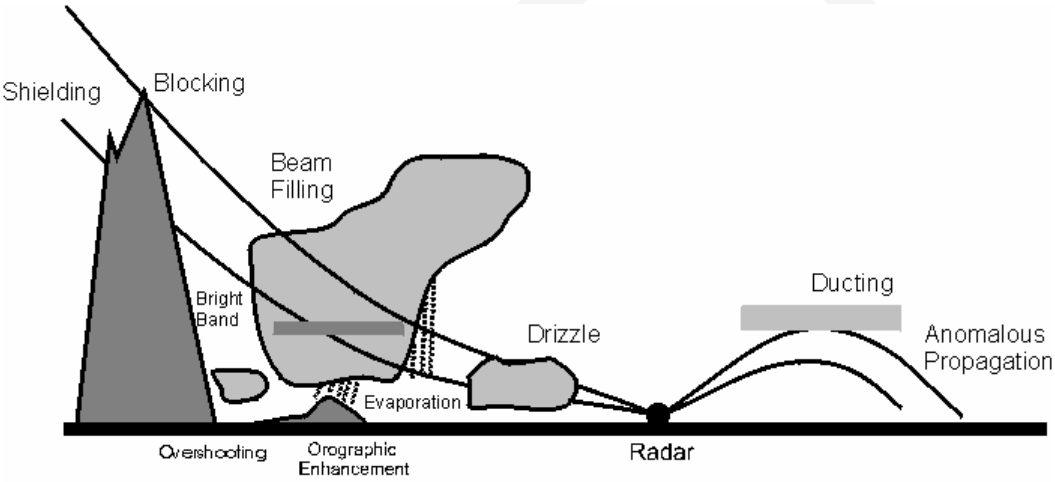

Figure D.14 Depiction of radar artifacts. (Source: Wikipedia)

SPAS is designed to overcome many of these short-comings by carefully using radar data for defining the spatial patterns and relative magnitudes of precipitation, but allowing measured precipitation values ("ground truth") at gauges to govern the magnitude. When absolutely necessary, the observed precipitation values at gauges are nudged up (or down) to force SPAS results to be consistent with observed gauge values. Nudging gauge precipitation values helps to promote better consistency between the gauge value and the gridcell value, even though these two values sometimes should not be the same since they are sampling different area sizes. For reasons discussed in the "SPAS versus Gauge Precipitation" section, the gauge value and gridcell value can vary. Plus, SPAS is designed to toss observed individual hourly values that are grossly inconsistent with radar data, hence driving a difference between the gauge and gridcell. In general, when the gauge and gridcell value differ by more than 15% and/or 0.50 inches, and the gauge data have been validated, then it is justified to artificially increase or decrease slightly the observed gauge value to "force" SPAS to derive a gridcell value equal to the observed value. Sometimes simply shifting the gauge location to an adjacent gridcell resolves the problems. Regardless, a large gauge versus

gridcell difference is a "red flag" and sometimes the result of an erroneous gauge value or a mis-located gauge, but in some cases the difference can only be resolved by altering the precipitation value.

Before results are finalized, a precipitation intensity check is conducted to ensure the spatial patterns and magnitudes of the maximum storm intensities at 1-, 6-, 12-, etc. hours are consistent with surrounding gauges and published reports. Any erroneous data are corrected and SPAS re-run. Considering all of the QA/QC checks in SPAS, it typically requires 5-15 basemap SPAS runs and, if radar data are available, another 5-15 radar-aided runs, to arrive at the final output.

Test Cases

To check the accuracy of the DAD software, three test cases were evaluated.

"Pyramidville" Storm

The first test was that of a theoretical storm with a pyramid shaped isohyetal pattern. This case was called the Pyramidville storm. It contained 361 hourly stations, each occupying a single grid cell. The configuration of the Pyramidville storm (see Figure D.15) allowed for uncomplicated and accurate calculation of the analytical DA truth independent of the DAD software. The main motivation of this case was to verify that the DAD software was properly computing the area sizes and average depths.

1. Storm center: 39°N 104°W
2. Duration: 10-hours
3. Maximum grid cell precipitation: 1.00"
4. Grid cell resolution: 0.06 sq.-miles (361 total cells)
5. Total storm size: 23.11 sq-miles
6. Distribution of precipitation:
   Hour 1: Storm drops 0.10" at center (area 0.06 sq-miles)
   Hour 2: Storm drops 0.10" over center grid cell AND over one cell width around hour 1 center
   Hours 3-10:
   1. Storm drops 0.10" per hour at previously wet area, plus one cell width around previously wet area
   2. Area analyzed at every 0.10"
   3. Analysis resolution: 15-sec (~.25 square miles)

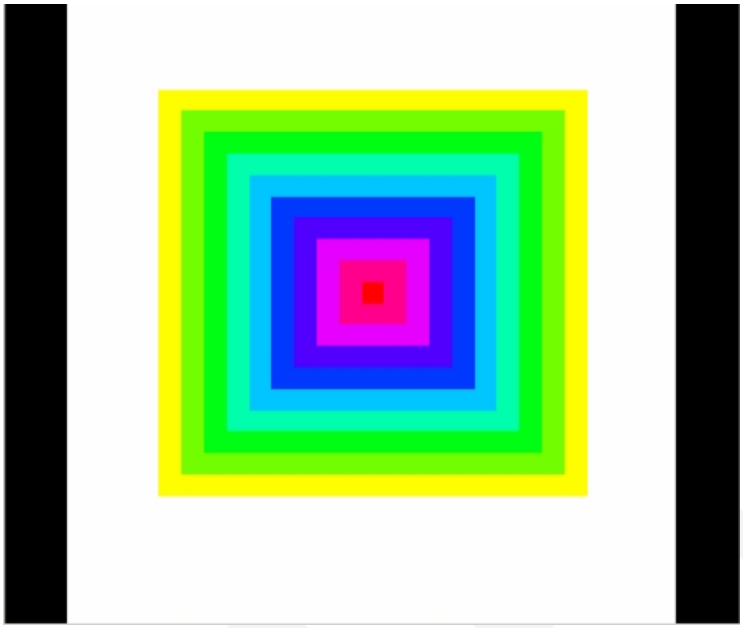

Figure D.15 "Pyramidville" Total precipitation. Center = 1.00", Outside edge = 0.10".

The analytical truth was calculated independent of the DAD software, and then compared to the DAD output. The DAD software results were equal to the truth, thus demonstrating that the DA estimates were properly calculated (Figure D.16).

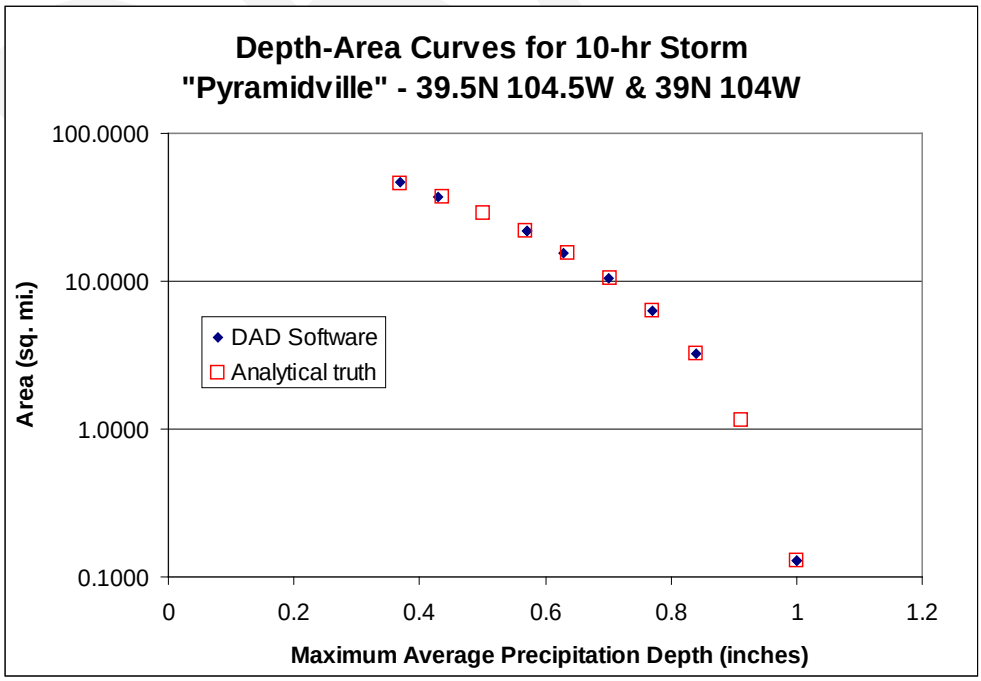

Figure D.16 10-hour DA results for "Pyramidville"; truth vs. output from DAD software.

The Pyramidville storm was then changed such that the mass curve and spatial interpolation methods would be stressed. Test cases included:

- Two-centers, each center with 361 hourly stations
- A single center with 36 hourly stations, 0 daily stations
- A single center with 3 hourly stations and 33 daily stations

As expected, results began shifting from the 'truth,' but minimally and within the expected uncertainty.

Ritter, Iowa Storm, June 7, 1953

Ritter, Iowa was chosen as a test case for a number of reasons. The NWS had completed a storm analysis, with available DAD values for comparison. The storm occurred over relatively flat terrain, so orographics were not an issue. An extensive "bucket survey" provided a great number of additional observations from this event. Of the hundreds of additional reports, about 30 of the most accurate reports were included in the DAD analysis.

The DAD software results are very similar to the NWS DAD values (Table D.2).

Table D.2. The percent difference [(AWA-NWS)/NWS] between the AWA DA results and those published by the NWS for the 1953 Ritter, Iowa storm.

% Difference

	Duration (hours)				
Area (sq.mi.)		6	12	24	total
10		-15%	-7%	2%	2%
100		-7%	-6%	1%	1%
200		2%	0%	9%	9%
1000		-6%	-7%	4%	4%
5000		-13%	-8%	2%	2%
10000		-14%	-6%	0%	0%

Westfield, Massachusetts Storm, August 8, 1955

Westfield, Massachusetts was also chosen as a test case for a number of reasons. It is a probable maximum precipitation (PMP) driver for the northeastern United States. Also, the Westfield storm was analyzed by the NWS and the DAD values are available for comparison. Although this case proved to be more challenging than any of the others, the final results are very similar to those published by the NWS (Table D.3).

Table D.3. The percent difference [(AWA-NWS)/NWS] between the AWA DA results and those published by the NWS for the 1955 Westfield, Massachusetts storm.

% Difference

	Duration (hours)						
Area (sq. mi.)	6	12	24	36	48	60	total
10	2%	3%	0%	1%	-1%	0%	2%
100	-5%	2%	4%	-2%	-6%	-4%	-3%
200	-6%	1%	1%	-4%	-7%	-5%	-5%
1000	-4%	-2%	1%	-6%	-7%	-6%	-3%
5000	3%	2%	-3%	-3%	-5%	-5%	0%
10000	4%	9%	-5%	-4%	-7%	-5%	1%
20000	7%	12%	-6%	-3%	-4%	-3%	3%

The primary components of SPAS are: storm search, data extraction, quality control (QC), conversion of daily precipitation data into estimated hourly data, hourly and total storm precipitation grids/maps and a complete storm-centered DAD analysis.

OUTPUT

Armed with accurate, high-resolution precipitation grids, a variety of customized output can be created (see Figures D.17A-D). Among the most useful outputs are sub-hourly precipitation grids for input into hydrologic models. Sub-hourly (i.e. 5-minute) precipitation grids are created by applying the appropriate optimized hourly Z-R (scaled down to be applicable for instantaneous Z) to each of the individual 5-minute radar scans; 5-minutes is often the native scan rate of the radar in the US. Once the scaled Z-R is applied to each radar scan, the resulting precipitation is summed up. The proportion of each 5-minute precipitation to the total 1-hour radar-aided precipitation is calculated. Each 5-minute proportion (%) is then applied to the quality controlled, bias corrected 1-hour total precipitation (created above) to arrive at the final 5-minute precipitation for each scan. This technique ensures the sum of 5-minute precipitation equals that of the quality controlled, bias corrected 1-hour total precipitation derived initially.

Depth-area-duration (DAD) tables/plots, shown in Figure D.17d, are computed using a highly-computational extension to SPAS. DADs provide an objective three dimensional (magnitude, area size, and duration) perspective of a storms' precipitation. SPAS DADs are computed using the procedures outlined by the NWS Technical Paper 1 (1946).

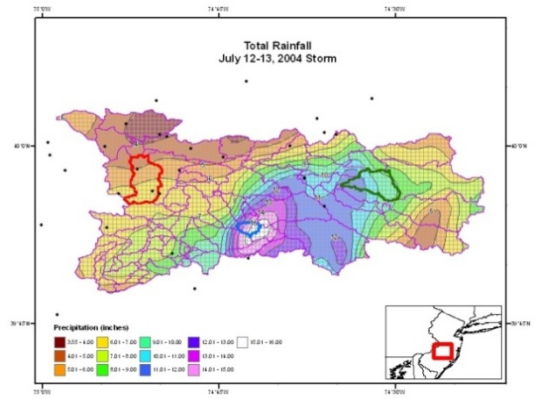

a)

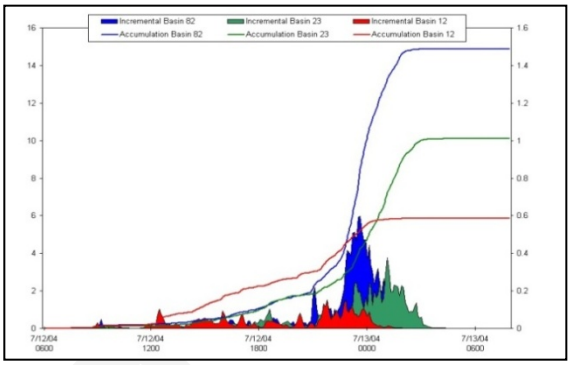

b)

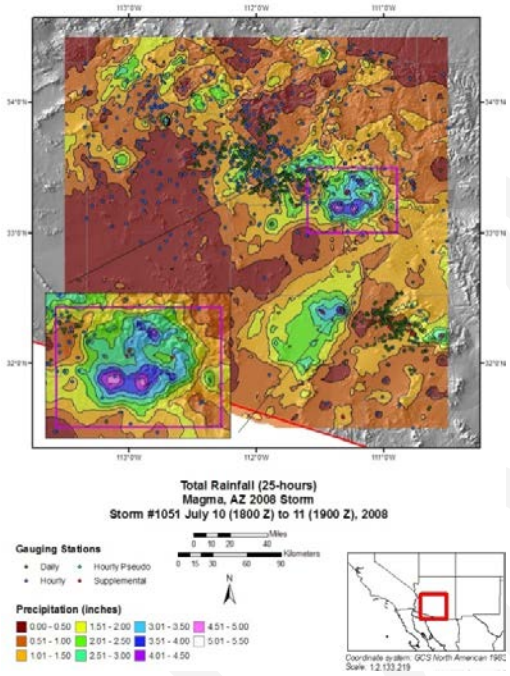

c)

Storm 1048 - Hokah, MN August 18 - August 21, 2007

MAXIMUM AVERAGE DEPTH OF PRECIPITATION (INCHES)

Area (mi²)	Duration (hours)									
	1	3	6	12	18	24	36	48	72	Total
0.24	2.45	4.77	7.85	11.89	14.88	17.31	17.55	18.19	18.26	18.26
1	2.12	4.53	7.56	11.64	14.59	17.05	17.31	17.95	18.02	18.02
10	2.12	4.53	7.49	11.10	13.88	15.96	16.31	17.03	17.15	17.17
25	2.12	4.53	6.92	10.42	12.86	14.89	15.34	16.23	16.45	16.46
50	2.11	4.40	6.64	9.65	12.13	14.05	14.46	15.49	15.79	15.79
100	2.09	4.10	6.33	9.37	11.52	13.27	13.93	14.76	15.14	15.14
200	2.03	3.79	6.00	8.87	10.96	12.62	13.37	14.22	14.52	14.52
300	1.95	3.61	5.74	8.55	10.64	12.06	12.99	13.74	14.04	14.04
500	1.79	3.35	5.47	8.13	10.11	11.60	12.27	13.01	13.29	13.30
1,000	1.53	2.99	4.95	7.33	9.17	10.51	11.13	11.84	12.07	12.07
2,000	0.95	2.55	4.36	6.18	8.09	9.30	9.85	10.54	10.75	10.76
5,000	0.87	2.02	3.45	5.19	6.53	7.61	8.18	8.79	8.96	8.98
10,000	0.83	1.54	2.89	4.02	5.39	6.09	6.78	7.31	7.53	7.55
20,000	0.41	0.95	1.84	3.02	3.97	4.53	5.13	5.63	5.87	5.90

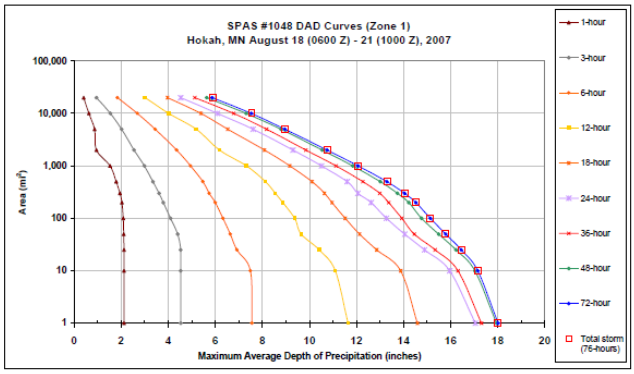

d)

Figure D.17. Various examples of SPAS output, including (a) total storm map and its associated (b) basin average precipitation time series, (c) total storm precipitation map, (d) depth-area-duration (DAD) table and plot.

SUMMARY

Grounded on years of scientific research with a demonstrated reliability in post-storm analyses, SPAS is a hydro-meteorological tool that provides accurate precipitation analyses for a variety of applications. SPAS has the ability to compute precise and accurate results by using sophisticated timing algorithms, "basemaps", a variety of precipitation data and most importantly NEXRAD weather radar data (if available). The approach taken by SPAS relies on hourly, daily and

supplemental precipitation gauge observations to provide quantification of the precipitation amounts while relying on basemaps and NEXRAD data (if available) to provide the spatial distribution of precipitation between precipitation gauge sites. By determining the most appropriate coefficients for the Z-R equation on an hourly basis, the approach anchors the precipitation amounts to accepted precipitation gauge data while using the NEXRAD data to distribute precipitation between precipitation gauges for each hour of the storm. Hourly Z-R coefficient computations address changes in the cloud microphysics and storm characteristics as the storm evolves. Areas suffering from limited or no radar coverage are estimated using the spatial patterns and magnitudes of the independently created basemap precipitation grids. Although largely automated, SPAS is flexible enough to allow hydro-meteorologists to make important adjustments and adapt to any storm situation.

REFERENCES

Baeck M.L., Smith J.A., 1998: "Precipitation Estimation by the WSR-88D for Heavy Precipitation Events", *Weather and Forecasting*: Vol. 13, No. 2, pp. 416–436.

Ciach, G.J., 2003: Local Random Errors in Tipping-Bucket Rain Gauge Measurements. *J. Atmos. Oceanic Technol.*, **20**, 752–759.

Corps of Engineers, U.S. Army, 1945-1973: Storm Rainfall in the United States, Depth-Area-Duration Data. Office of Chief of Engineers, Washington, D.C.

Corrigan, P., Fenn, D.D., Kluck, D.R., and J.L. Vogel, 1999: Probable Maximum Precipitation Estimates for California. *Hydrometeorological Report No. 59*, U.S. National Weather Service, National Oceanic and Atmospheric Administration, U.S. Department of Commerce, Silver Spring, MD, 392 pp.

Dickens, J., 2003: "On the Retrieval of Drop Size Distribution by Vertically Pointing Radar", American Meteorological Society 32nd Radar Meteorology Conference, Albuquerque, NM, October 2005.

Duchon, C.E., and G.R. Essenberg, 2001: Comparative Precipitation Observations from Pit and Above Ground Rain Gauges with and without Wind Shields, *Water Resources Research*, Vol. 37, N. 12, 3253-3263.

Faulkner, E., T. Hampton, R.M. Rudolph, and Tomlinson, E.M., 2004: Technological Updates for PMP and PMF – Can They Provide Value for Dam Safety Improvements? Association of State Dam Safety Officials Annual Conference, Phoenix, Arizona, September 26-30, 2004.

Guo, J. C. Y., Urbonas, B., and Stewart, K., 2001: Rain Catch under Wind and Vegetal Effects. ASCE, *Journal of Hydrologic Engineering*, Vol. 6, No. 1.

Hansen, E.M., Fenn, D.D., Schreiner, L.C., Stodt, R.W., and J.F., Miller, 1988: Probable Maximum Precipitation Estimates, United States between the Continental Divide and the 103rd Meridian, *Hydrometeorological Report Number 55A*, National weather Service, National Oceanic and Atmospheric Association, U.S. Dept of Commerce, Silver Spring, MD, 242 pp.

Hunter, R.D. and R.K. Meentemeyer, 2005: Climatologically Aided Mapping of Daily Precipitation and Temperature, *Journal of Applied Meteorology*, October 2005, Vol. 44, pp. 1501-1510.

Hunter, S.M., 1999: Determining WSR-88D Precipitation Algorithm Performance Using The Stage III Precipitation Processing System, Next Generation Weather Radar Program, WSR-88D Operational Support Facility, Norman, OK.

Lakshmanan, V. and M. Valente, 2004: Quality control of radar reflectivity data using satellite data and surface observations, 20th Int'l Conf. on Inter. Inf. Proc. Sys. (IIPS) for Meteor., Ocean., and Hydr., Amer. Meteor. Soc., Seattle, CD-ROM, 12.2.

Martner, B.E, and V. Dubovskiy, 2005: Z-R Relations from Raindrop Disdrometers: Sensitivity To Regression Methods And DSD Data Refinements, 32nd Radar Meteorology Conference, Albuquerque, NM, October, 2005

Tokay, A., P.G. Bashor, and V.L. McDowell, 2010: Comparison of Rain Gauge Measurements in the Mid-Atlantic Region. *J. Hydrometeor.*, **11**, 553-565.

Tomlinson, E.M., W.D. Kappel, T.W. Parzybok, B. Rappolt, 2006: Use of NEXRAD Weather Radar Data with the Storm Precipitation Analysis System (SPAS) to Provide High Spatial Resolution Hourly Precipitation Analyses for Runoff Model Calibration and Validation, ASDSO Annual Conference, Boston, MA.

Tomlinson, E.M., and T.W. Parzybok, 2004: Storm Precipitation Analysis System (SPAS), proceedings of Association of Dam Safety Officials Annual Conference, Technical Session II, Phoenix, Arizona.

Tomlinson, E.M., R.A. Williams, and T.W. Parzybok, September 2003: Site-Specific Probable Maximum Precipitation (PMP) Study for the Great Sacandaga Lake / Stewarts Bridge Drainage Basin, Prepared for Reliant Energy Corporation, Liverpool, New York.

Tomlinson, E.M., R.A. Williams, and T.W. Parzybok, September 2003: Site-Specific Probable Maximum Precipitation (PMP) Study for the Cherry Creek Drainage Basin, Prepared for the Colorado Water Conservation Board, Denver, CO.

Tomlinson, E.M., Kappel W.D., Parzybok, T.W., Hultstrand, D., Muhlestein, G., and B. Rappolt, May 2008: Site-Specific Probable Maximum Precipitation (PMP) Study for the Wanahoo Drainage Basin, Prepared for Olsson Associates, Omaha, Nebraska.

Tomlinson, E.M., Kappel W.D., Parzybok, T.W., Hultstrand, D., Muhlestein, G., and B. Rappolt, June 2008: Site-Specific Probable Maximum Precipitation (PMP) Study for the Blenheim Gilboa Drainage Basin, Prepared for New York Power Authority, White Plains, NY.

Tomlinson, E.M., Kappel W.D., and T.W. Parzybok, February 2008: Site-Specific Probable Maximum Precipitation (PMP) Study for the Magma FRS Drainage Basin, Prepared for AMEC, Tucson, Arizona.

Tomlinson, E.M., Kappel W.D., Parzybok, T.W., Hultstrand, D., Muhlestein, G., and P. Sutter, December 2008: Statewide Probable Maximum Precipitation (PMP) Study for the state of Nebraska, Prepared for Nebraska Dam Safety, Omaha, Nebraska.

Tomlinson, E.M., Kappel, W.D., and Tye W. Parzybok, July 2009: Site-Specific Probable Maximum Precipitation (PMP) Study for the Scoggins Dam Drainage Basin, Oregon.

Tomlinson, E.M., Kappel, W.D., and Tye W. Parzybok, February 2009: Site-Specific Probable Maximum Precipitation (PMP) Study for the Tuxedo Lake Drainage Basin, New York.

Tomlinson, E.M., Kappel, W.D., and Tye W. Parzybok, February 2010: Site-Specific Probable Maximum Precipitation (PMP) Study for the Magma FRS Drainage Basin, Arizona.

Tomlinson, E.M., Kappel W.D., Parzybok, T.W., Hultstrand, D.M., Muhlestein, G.A., March 2011: Site-Specific Probable Maximum Precipitation Study for the Tarrant Regional Water District, Prepared for Tarrant Regional Water District, Fort Worth, Texas.

Tomlinson, E.M., Kappel, W.D., Hultstrand, D.M., Muhlestein, G.A., and T. W. Parzybok, November 2011: Site-Specific Probable Maximum Precipitation (PMP) Study for the Lewis River basin, Washington State.

Tomlinson, E.M., Kappel, W.D., Hultstrand, D.M., Muhlestein, G.A., and T. W. Parzybok, December 2011: Site-Specific Probable Maximum Precipitation (PMP) Study for the Brassua Dam basin, Maine.

U.S. Weather Bureau, 1946: Manual for Depth-Area-Duration analysis of storm precipitation. *Cooperative Studies Technical Paper No. 1*, U.S. Department of Commerce, Weather Bureau, Washington, D.C., 73pp.